City Research Online

City, University of London Institutional Repository

The evolution of multiplayer cooperation and complex social behaviour in structured and mobile populations

Diogo Luís Neves dos Santos Pires

City, University of London

Department of Mathematics

November 2024

Contents

List of Figures

List of Tables

Acknowledgements

First and foremost, I would like to express my gratitude to Mark Broom for his mentorship throughout my PhD journey. His sharp vision as a scientist and mathematician was key in shaping this thesis, and his committed support and availability were a constant source of reassurance. I am especially thankful for the numerous opportunities he offered and for the freedom he granted me to explore diverse research directions, always encouraging me to forge my own path.

Throughout this journey, I am deeply grateful to have been surrounded by so many close friends with whom to share a passion for both life and research. My heartfelt thanks go to Christo, Elli, Hanka, Carlos, Terrucha, Miche, Fabio, Beth,

Alex, Gosia, and Marta, though the list could go on endlessly. I am excited to see where the next steps will take each and every one of you.

I am especially thankful to these and many other friends who, throughout this thesis, formed an incredibly caring and supportive network. A special thanks goes to Joana, Ana, André, and Carolina, who over three years ago made me feel instantly at home in London. I am also grateful to the friends I've had the pleasure of living with, Adi and Lucille, and to those in Southeast London, where I spent so many weekends, Francisca, Paloma, Ricardo and Natacha. To my lifelong friend, Bea, thank you for your contagious enthusiasm for life and your constant presence in mine. I am also immensely thankful to the people who shared so much of their lives with me during my research visits: Cris, Guille, André, Veni, Simon, Jada, Hunter, Shari, and Jasmin. Finally, my gratitude goes to all my friends back in Lisboa, Viana, and Porto, as well as those who, like me, have moved to new places. It's truly a privilege to have so many places to call home. This thesis is as much yours as it is mine.

Um abraço especial à minha família, em particular aos meus pais, Luísa e Luís, e ao meu irmão, João. Obrigado por me terem proporcionado tantas oportunidades na vida e por me terem motivado desde sempre a questionar o mundo à minha volta. Espero um dia poder retribuir-vos tudo o que me deram.

Declaration

I hereby confirm that the research work included within this thesis, entitled "The evolution of multiplayer cooperation and complex social behaviour in structured and mobile populations", in fulfilment of the requirements for the award of the degree of Doctor of Philosophy and submitted to the Department of Mathematics at City, University of London is my own work carried out during the period 07/2021–11/2024 under the supervision of Professor Mark Broom, or that where it has been carried out in collaboration with others that this is duly acknowledged below.

I confirm that this thesis has not been previously submitted for the award of a degree by this or any other university.

Signature: Diogo L. Pires

Date: February 21, 2025

Contributions

The academic contributions made during the time this research was carried out are listed below:

Published Papers

- Morison, C., Fic, M., Marcou, T., Mohamadichamgavi, J., Antón, J. R., Sayyar, G., Stein, A., Bastian, F., Krakovská, H., Krishnan, N., **Pires, D. L.**, Satouri, M., Thomsen, F.J., Tjikundi, K. & Ali, W. (2025), 'Public Goods Games in Disease Evolution and Spread', *Dynamic Games and Applications.*

- **Pires, D. L.** & Broom, M. (2024), 'The rules of multiplayer cooperation in networks of communities', *PLoS Computational Biology*, **20**(8), e1012388.

- **Pires, D. L.**, Erovenko, I. V. & Broom, M. (2023), 'Network topology and movement cost, not updating mechanism, determine the evolution of cooperation in mobile structured populations', *PLoS ONE*, **18**(8), e0289366.

- **Pires, D. L.** & Broom, M. (2022), 'More can be better: An analysis of single-mutant fixation probability functions under 2×2 games', *Proceedings of the Royal Society A: Mathematical, Physical and Engineering Sciences*, **478**, 20220577.

Preprints

- Cassells, D., Costantini, L., Ashery, A. F., Gadge, S., **Pires, D. L.**, Sánchez-Cortés, M. Á., Santoro, A. & Omodei, E. (2024), 'A 72h exploration of the co-evolution of food insecurity and international migration', *arXiv preprint arXiv:2407.03117.*

Working papers

- **Pires, D. L.**, Castagno, P., Mancuso, V. & Ajmone Marsan, M., 'Self-organisation of common good usage and an application to Internet services', submitted to PNAS.

- **Pires, D. L.** & Broom, M., 'Multiplayer social dilemmas in completely mixed populations and networks of mixing communities', in prep.

- **Pires, D.L.** & Hanel R., 'Skill transmission dynamics and the emergence of new skills', in prep.

Abstract

The self-organisation of social behaviour is observed across populations of varying complexity. Evolutionary game theory models such systems by describing interactions between individuals as evolutionary games. This thesis leverages a wide range of tools from evolutionary game theory to develop models of population dynamics and advance our understanding of the evolution of social behaviour, spanning from simple to complex social interactions and their applications.

We start by analysing fixation processes on finite, well-mixed populations. We show that new strategies have higher probability of fixation in larger populations for half of all pairwise games, including the widely studied Prisoner's Dilemma, Hawk-Dove and Stag Hunt games.

Next, we consider multiplayer social dilemmas on networks to examine the evolution of cooperation under various assumptions about population structure and individual mobility. We find that limited movement leading to community organisation strongly promotes the evolution of cooperation in public goods dilemmas. In particular, large networks of small communities prove highly effective. Comparisons with completely mixed populations show that increased community mixing often hampers cooperation. We also observe the robust co-evolution of cooperation and high-mobility strategies under conditional movement. In regular networks, cooperators are able to find each other while evading defectors for extended periods.

These two mechanisms for the evolution of cooperation differ fundamentally: community structure relies on the viscosity of the evolutionary process on the network, whereas conditional movement depends on the evolution of mobile assortative behaviour. This distinction is supported by a detailed analysis of six different evolutionary dynamics.

Further, we develop two new dynamic models for infinite populations, adapting evolutionary game theory concepts to study other systems. The first examines the

Win-Stay, Lose-Shift strategy in common goods usage. We propose its implementation by mobile users accessing Internet services, supported by its good performance in realistic stochastic simulations. This theory extends to the distribution over grazing and foraging land and may be used to propose solutions to operators of public transport or alternative technological common goods. The second model explores productive interaction and the transmission-selection of skills. Advances in economic complexity and evolutionary economic geography show us the impact of a skilled workforce on industrial development and its geographic organisation. We use this as motivation to study the evolution and co-existence skills and their synergistic production within social systems.

Chapter 1

Introduction

The self-organisation of social behaviour is observed across populations of all levels of complexity, from microorganisms to human societies. Due to its pervasiveness in all its diverse forms in both social and biological systems, understanding its evolutionary origins is crucial. Evolutionary game theory has been instrumental in this area, leading to the development of mathematical and computational models, as well as experiments, that shed a light on the evolutionary origins of social behaviour. Although originally developed to model the natural selection of genetically determined traits and behaviour, it has been adapted and extensively employed to study cultural evolution, helping us understand the emergence and spread of behaviour within social systems. Evolutionary game theory has thus been applied to explain the evolution of cooperative behaviour, signalling systems and language, coordinated action, territoriality, reciprocal altruism, social norms, and more.

This thesis leverages these developments to advance theories on the evolution of social behaviour, spanning from simple to complex social interactions. In this context, complexity emerges from the interplay between different dimensions of social behaviour, such as cooperation under social dilemmas, multiplayer interactions, community and network structure, and individual mobility. In this introductory chapter, we begin by presenting an introduction to evolutionary game theory along with the basics of the most impactful and relevant models to the work developed in this thesis. We will introduce social dilemmas, both in pairwise interactions and in groups, describing the decisions individuals often face between socially and individually advantageous actions, which can be framed as a choice between cooperation and defection. There are several mechanisms that explain why cooperative behaviour is

adopted by individuals and we set out some of the ways in which these have been modelled. Moreover, we introduce recent advances in evolutionary game theory in the context of structured and mobile populations, which will be used in the following chapters. Finally, we will outline the work done in the remaining chapters of this thesis.

1.1 Evolutionary game theory

1.1.1 Introduction to game theory

Game theory provides a framework to study decision making in the context of strategic interactions. Strategic interactions are those where the outcome of the decisions of one individual depends not only on their own decisions, but also on those of others. These settings can be formalised as a game. This theory was originally developed by John von Neumann, whose first publication on the topic goes as far back as von Neumann (1928) with the translated title from German as "On the theory of games of strategy". His work on the development of game theory eventually led him to co-author with Oskar Morgenstern their acclaimed book on the "Theory of Games and Economic Behavior" (von Neumann & Morgenstern 1944).

In game theory, a game is defined by the *players* partaking in the interactions. In other words, those whose decisions may affect the outcome experienced by others. Secondly, each player has a set of actions available to them every time they have to make a decision in a game. A *strategy* for a game is defined as a complete contingent plan determining which action to take at every decision point. If a player chooses one of the strategies available in their *strategy space* deterministically, we call that a *pure strategy*. If they choose it following a defined probability distribution, we call it a *mixed strategy*. Finally, each combination of strategies of all involved players will have an *outcome*, which can be quantified by the *payoff* received by each player.

We consider games with a finite number of players, each with a finite number of pure strategies available to them, and that they make their decisions simultaneously. In these cases, the game can be directly represented in its *normal form*. In the particular case of a 2-player game, typically referred to as pairwise game, the normal form representation corresponds to a payoff matrix, leading to the coining of such games as *matrix games*.

Moreover, if all players have the same strategy space, and the payoffs received

depend only on the strategies used and not on who is using them, we may call this a *symmetric game.* In this thesis, we will mainly focus on such games, both pairwise and multiplayer (more than 2) symmetric games. For now, let us consider the payoff matrix M of a general 2×2 symmetric game:

	A	B
A	a	b
B	c	d

Table 1.1: Payoff matrix of a 2×2 symmetric game.

We call A and B the strategies at their disposal. After each encounter, the focal individual receives a payoff defined by this payoff matrix. Individuals using A receive a and b respectively against individuals using A and B; while individuals using B receive c and d respectively against individuals using A and B.

In this context, we define a mixed strategy as $\mathbf{p} = [p_1, 1 - p_1]$, where p_1 is the the probability of choosing pure strategy A, and $1 - p_1$ the probability of choosing strategy B. The expected payoff received by a player using strategy $\mathbf{p}$ against a player using strategy $\mathbf{q} = [q_1, 1 - q_1]$ can be calculated as $\mathrm{E}[\mathbf{p,q}] = \mathbf{p}M\mathbf{q^T}$.

Classical game theory provides tools to analyse such strategic settings, usually under the assumption that all individuals behave rationally. The most impactful of such concepts is that of a *Nash equilibrium*, originally proposed by John Nash in Nash (1951). The Nash equilibrium is defined as a strategy profile, i.e. a combination of strategies of different individuals, which are mutually best responses to each other. In other words, if all individuals are choosing their respective strategy from that strategy profile, then none of them has an incentive to deviate from it.

This concept has been key in the context of economics and political sciences, where the assumption of rationality may be valid. However, this assumption makes it limited not only in its application to such disciplines, but especially in its application to the study of complex social behaviour in social and biological sciences, where a large number of individuals and a spectrum of cognitive and rational capacities are present. Evolutionary game theory has proved to be useful to approach such settings.

1.1.2 Evolutionary game theory and evolutionarily stable strategies

Evolutionary game theory proposes an extension of some of the essential aspects that define a game to study the evolution of behaviour in populations. In this context, instead of a theory or rational decision-making in strategic environments, we consider a *population* of individuals who are not necessarily rational. Similarly to classical game theory, when individuals in this population interact, the resulting strategy profile leads to an outcome with payoffs for all individuals involved in the game. Each individual has an associated strategy, which might not be the result of their conscious choice. This theory was originally developed in the context of evolutionary biology, where strategies are often referred to as types. These are typically referred to as evolutionary games, simply meaning that they are symmetric, i.e. the outcomes depend only on the strategies used and not on the particular set of individuals picked to play. For a given composition of the population the *fitness* of an individual is supposed to be the average payoff received in their interactions in the population. Based on the ideas of natural selection, fitter strategies would be selected and therefore evolve in the population.

In 1973, John Maynard Smith and George Robert Price published their pioneering work on evolutionary game theory (Maynard Smith & Price 1973), where they introduced this setup and the concept of an *evolutionarily stable strategy* (ESS) as one which when adopted by a population resists invasion by any other possible strategy. This formalised evolutionary games, inspired by the solution concept of unbeatable strategy as introduced by Hamilton (1967) for the evolution of the sex ratio. Shortly after that, the concept of ESS was further developed by Maynard Smith (1974), and eventually led to the publication of the book "Evolution and the Theory of Games" (Maynard Smith 1982), which was key in establishing evolutionary game theory as a powerful tool to study the evolution of behaviour.

In symmetric matrix games, a mixed strategy $\mathbf{p}$ is said to be an ESS if and only if, for all possible $\mathbf{q} \neq \mathbf{p}$, we have:

1. $E[\mathbf{p},\mathbf{p}] \geq E[\mathbf{q},\mathbf{p}]$, and

2. If $E[\mathbf{p},\mathbf{p}] = E[\mathbf{q},\mathbf{p}]$, then $E[\mathbf{p},\mathbf{q}] > E[\mathbf{q},\mathbf{q}]$.

In such games, condition 1 is equivalent to the Nash equilibrium condition. However, condition 2 adds an extra restriction, thus meaning that not all Nash equilibria of

symmetric matrix games played by populations are necessarily ESSs. Conditions 1 and 2 are thus respectively referred to as the equilibrium and stability conditions of a strategy.

The concept of an ESS has been extensively employed to understand the stability of a spectrum of social behaviour by considering evolutionary games as described above. This includes the study of aggressive territorial behaviour (Maynard Smith & Price 1973, Maynard Smith 1974, 1982, Broom & Rychtář 2013), coordination of social norms (Skyrms 2004, 1996) signalling and language (Maynard Smith 1991, Maynard Smith & Harper 2003, Skyrms 2010), and, the one most relevant to us, cooperation (Axelrod & Hamilton 1981, Axelrod 1984, Poundstone 1992).

Moreover, there are contexts where the concept of ESS can be useful, even though individuals do not hold direct pairwise interactions. Alternatively, these are sometimes modelled as individuals playing the field games (Broom & Rychtář 2013), in which case the fitness of an individual depends both on their strategy and (nonlinearly) on the field strategy, i.e. the aggregation of all strategies played by the population. This is useful when thinking about the evolution of the sex ratio, and is present in the original solution proposed by Hamilton (1967), which was key to the later development of the ESS. In this case, it was shown that the sex ratio $1 : 1$ is an ESS of the system.

Another context where these alternative games are important was in understanding food competition in territorial patches. The ideal free distribution (IFD) theory, originally developed by Fretwell & Lucas (1969) in the context of animal territorial behaviour, predicts that individuals will distribute themselves across different resource patches to maximise their own benefit, assuming perfect knowledge and no movement costs. As a result, individuals spread in a way that equalises availability or quality across all used resources. The fact that the IFD strategy constitutes an ESS was later proven by Cressman & Křivan (2006) considering a playing the field game.

Even though the concept of an ESS proved to be useful, it reflected only a static analysis of the stability of strategies in these evolutionary systems. As such, it does not provide information as to whether the system would dynamically evolve to such states or not.

1.1.3 Replicator equation and population dynamics

The first model to describe the population dynamics of evolutionary games was the replicator equation (Taylor & Jonker 1978, Hofbauer & Sigmund 1998). The replicator equation defines changes in the frequency x_i of each strategy i in the population as follows:

$$\frac{dx_i}{dt} = x_i \left(F_i - \bar{F} \right), \tag{1.1}$$

where F_i is the fitness of strategy i and $\bar{F}$ is the average fitness of the population.

This set of equations tracks the composition of the population and its dynamical change over time. Any strategy with a fitness higher than the average fitness of the population will tend to increase its frequency, whereas any strategy with a fitness below the average will decrease its frequency. From the point of view of natural selection, this is a direct outcome of the definition of fitness as reproductive success.

It was originally shown by Taylor & Jonker (1978) that if a given strategy is an ESS, then it is necessarily an equilibrium state of the replicator equation which is strictly stable. Furthermore, Zeeman (1980) shows that all ESSs are attractors of the replicator dynamics, thus meaning that they have a set of initial population composition that will converge to it. The stability properties of the equation have been analysed in Bomze (1986) and Cressman (1990), and later summarized in Hofbauer & Sigmund (1998).

Other sets of differential equations have been proposed with the aim of describing alternative dynamics of how the frequency of strategies may change in a population. The replicator-mutator equation was introduced by Page & Nowak (2002) incorporating the effect of mutations onto the replicator equation. In an attempt to describe cultural evolution, the imitation dynamics were developed in Helbing (1992), under which individuals selectively adopt the strategies of those with whom they meet. Moreover, Matsui (1992) introduces the best response dynamics, under which individuals adopt the rational best response to the strategies played in the population.

Similarly, in chapter 7, we will develop an alternative population dynamics model of interactions between skills and their transmission-selection. In that model, we will combine aspects of evolutionary games and the replicator equation with aspects of epidemiological modelling.

1.1.4 Evolutionary games on finite populations

The conceptualisation of evolutionary dynamics of different behavioural types in populations was later extended to finite populations. This was done resorting to the (fixed fitness) Moran process introduced in Moran (1958). This stochastic process describes the evolution of a population of size N where there is competition between two alleles A and B with respective fitness r and 1. At each time step one of the individuals of the population is randomly chosen to reproduce proportional to their fitness and another one is uniformly at random chosen to die.

This process was extended in Nowak et al. (2004) by incorporating frequency-dependent fitness into the original birth-death process, thus allowing for the study of evolutionary games on finite populations. This model is often referred to as the frequency-dependent Moran process (Nowak et al. 2004, Taylor et al. 2004), which we will define in detail in chapter 2. In contrast to the replicator equation, the Moran process with frequency-dependent fitness did not assume populations to be infinite nor that selection acted deterministically. However, it still proved to be extensively mathematically tractable and permitted the incorporation of new features of real populations which could be later simulated through agent-based models.

These models introduced a new concept of evolutionary stability. An evolutionarily stable strategy in a finite population of size N (ESS_N) is defined as a strategy which when adopted by a population of that size, selection opposes the invasion and fixation by any other strategy (Schaffer 1988, Nowak et al. 2004). These two requirements respectively provide equilibrium and stability conditions of a given strategy (Broom & Rychtář 2013). Let us think of a strategy A. Selection is said to oppose invasion when no single mutant B holds a higher fitness than the residents of an otherwise pure population using strategy A. Selection is said to oppose fixation when no single mutant using strategy B is able to fixate in the population with a fixation probability, denoted ρ^B, larger than the one obtained under neutral selection, denoted $\rho^{neutral} = 1/N$ (see Taylor et al. (2004)).

Similarly to the limitations of the original ESS, simply concluding that a strategy A is stable, i.e. $\rho^B < \rho^{neutral}$ for all alternative strategies B, is not enough to determine whether it will evolve. Here we use the definition that a strategy A evolves if $\rho^A > \rho^{neutral} > \rho^B$ for all alternative strategies B. This originates in the following classification of evolutionary outcomes for games with 2 strategies A and

B inspired from (Taylor et al. 2004):

- Selection favours A if $\rho^A > \rho^{neutral} > \rho^B$;

- Selection favours B if $\rho^B > \rho^{neutral} > \rho^A$;

- Selection favours instability if $\rho^A > \rho^{neutral}$ and $\rho^B > \rho^{neutral}$;

- Selection favours bi-stability if $\rho^A < \rho^{neutral}$ and $\rho^B < \rho^{neutral}$.

As the definition of an ESS_N suggests, the stability of a strategy depends not only on the game played but on the population size as well (Taylor et al. 2004). It was also shown that of the 16 possible combinations of selection favouring or opposing the invasion and fixation of strategists B by strategists A and vice-versa, only 8 of those are possible evolutionary scenarios under the frequency-dependent Moran process (Taylor et al. 2004). For strong selection, however, the evolutionary outcomes were shown to correspond to the classical infinite population ones, first under the frequency-dependent Moran process (Della Rossa et al. 2017), and then under general fitness mappings (Huang et al. 2018).

Meanwhile, the literature on evolutionary games on finite populations grew substantially. This literature often focused on analysing fixation probabilities, given their role on determining the evolutionary outcome of a system. Therefore, studying fixation probabilities and their relation with other aspects of populations and games became important to understand the evolution of social behaviour.

As such, fixation probabilities have been studied as functions of the initial number of mutants (de Souza et al. 2019), and it has been proved that each of the 8 possible evolutionary scenarios has associated to it one (and only one) of three function shapes. In (Traulsen et al. 2006, 2007), they were studied in relation to the initial number of mutants and intensity of selection under the pairwise comparison process. They have also been extensively studied in the context of structured populations (Broom et al. 2010, Hadjichrysanthou et al. 2011).

Fixation probabilities describe the likelihood of changing from one pure state to another after one mutation occurs, conditional on mutations being rare enough. Following (Fudenberg et al. 2006), under games with two or more strategies they can be used to construct a simplified Markov chain between pure states, and allow the computation of the long-term stationary distribution over them (Hauert et al. 2007, Van Segbroeck et al. 2009, Santos et al. 2011, Wagner 2020). The validity of these

approximations under rare mutations has been analysed analytically in Wu et al. (2012) and through comparison with simulations (Hauert et al. 2007, Van Segbroeck et al. 2009). The concerns raised over the existence of mixed stable states leading to quasi-stationary distributions (Nasell 1999*b,a*, Zhou et al. 2010) have been tackled in this context by considering higher-order approximations including those states as configurations of interest (Vasconcelos et al. 2017).

The dependence of fixation probabilities on population size has been analysed, for instance through the calculation of their asymptotic limits. This was initially done by Antal & Scheuring (2006), who obtained quantitative limits for some cases, but only qualitative ones in others, whose error was later estimated by de Souza et al. (2019). These results were later expanded for two different limit orders of weak selection by Sample & Allen (2017), who also corrected some borderline cases under arbitrary values of intensity of selection.

In chapter 2, we further develop the understanding of the relation between fixation probabilities and population size for symmetric pairwise games, by providing a systematic analysis of the different effects that can be observed in all possible games. This chapter is based on the work published in Pires & Broom (2022).

1.2 Evolution of cooperation

Social individuals regularly face situations of conflict of interests. Some of these situations are described as social dilemmas when there is a conflict between the individual and the social interests. This is often framed as a choice one has to make between defection and cooperation. A classic example of this is offered by the use of pairwise Prisoner's Dilemma. A later formulation of the dilemma, called the donation game proposed that players may choose to cooperate and thus pay a cost K to give a reward V to the other player, whereas defectors do not. Other formulations of the donation game use parameters b and c for the reward and cost, respectively. However, we will use V and K for consistency with the multiplayer social dilemmas introduced later in this chapter. This game would lead to the following 2×2 payoff matrix:

	C	D
C	$V - K$	$-K$
D	V	0

Table 1.2: Payoff matrix of the 2×2 donation game.

The justifiable assumption that $V > K > 0$ leads to the ordering of payoffs which characterises the Prisoner's Dilemma: $V > V - K > 0 > -K$. In each interaction, individuals benefit from defecting regardless of who their opponent is ($V > V - K$ and $0 > -K$), making defection not only an ESS, but a dominant strategy of the game, i.e. a strategy that always provides a player with the highest payoff, regardless of what the other player does. However, all individuals do better in a population of cooperators than in a population of defectors ($V - K > 0$). This encapsulates the conflict between individual and social interest.

Several mechanisms have been proposed in order to explain the evolution of cooperation, five of which are summarised in Nowak (2006) and succinctly described here. 1. Kin selection is based on the idea that genetic relatedness among individuals links the evolutionary fate of cooperators, allowing them to derive an indirect evolutionary benefit from the success of their relatives. 2. Direct reciprocity suggests that individuals may condition their behaviour on past interactions, cooperating with those who have cooperated before. 3. Indirect reciprocity extends this principle by incorporating reputation: an individual's behaviour, as observed by third parties, influences how others interact with them. 4. Network reciprocity posits that structured interactions create clusters of cooperators who reinforce one another's success, making cooperation more viable. 5. Group selection proposes that competition between groups, rather than just between individuals, can favour cooperation if cooperative groups outperform others.

Since then, the literature on the evolution of cooperation has expanded significantly, leading to a deeper understanding of these mechanisms and their interplay. In the next two sections, we focus on two of these mechanisms and how they have been modelled.

1.2.1 Iterated games and conditional strategies

Direct reciprocity was originally proposed by Trivers (1971) as a mechanism to explain altruism between unrelated individuals. In theory, this mechanism would allow

individuals to reciprocate altruistic actions when they face repeated encounters. In this context, we will depart from the simultaneous one-move games we have considered so far under which cooperation is not evolutionarily stable, and enter the realm of iterated games. In such games, individuals may act conditionally based on the information they have on the actions of others.

The iterated Prisoner's Dilemma was popularised by Robert Axelrod in his book on "The evolution of cooperation" (Axelrod 1984), where he expanded on the work done together with William D. Hamilton in Axelrod & Hamilton (1981). In their work, they ran two series of tournaments where conditional strategies for the iterated Prisoner's Dilemma were tested against each other. The Tit-for-tat is a remarkably simple strategy, where individuals always start a new interaction by choosing cooperation, and then simply repeat the last action of the other individual, i.e. cooperate if the other cooperated, and defect if the other defected. This strategy won both tournaments, thus proving itself to be robust. Additionally, it was proved that it is an ESS of the iterated Prisoner's Dilemma. Its success was attributed to three factors: its willingness to cooperate, its retaliation against defection, while being quickly forgiving after a single retaliation.

In later work, tit-for-tat was shown to perform less well when facing errors in noisy repeated games, due to the successive series of retaliations that one single error would lead to in a repeated encounter (Fundenberg & Maskin 1990). This led to the proposition of variations of the original strategy, such as the generous tit-for-tat, under which the individuals still cooperated with a small probability if their opponent defected (Nowak & Sigmund 1992).

However, another strategy introduced as Pavlov (Kraines & Kraines 1989) and eventually renamed Win-Stay Lose-Shift (WSLS) was soon after shown to overthrow tit-for-tat and its variations (Nowak & Sigmund 1993, Kraines & Kraines 2000). In this strategy, individuals use the same action if they have had a successful payoff, or shift to an alternative option if it was unsuccessful. Successful payoffs are received every time the other individual cooperates and unsuccessful ones every time the other individual defects. The WSLS strategy corrects occasional mistakes much more quickly than tit-for-tat and it is able to exploit unconditional cooperators, thus explaining its general success. Nonetheless, similarly to tit-for-tat, the WSLS strategy only requires the knowledge of the previous immediate outcome.

As such, the simple principle behind this strategy is much more general than

the application to iterated games elaborated here. Its origins can be traced back to the original ideas of Robbins (Robbins 1952) which motivated the development of multi-armed bandit methods. These are algorithms that balance exploration and exploitation to optimise decision-making in uncertain environments by adaptively selecting actions based on observed rewards. Moreover, the principle is also present in iterated interactions under which individuals have the possibility to move, where walking away from defectors leads to the success of cooperation (Aktipis 2004). In chapter 5, we make use of this principle to study the co-evolution of conditional movement and cooperation in a spatial social dilemma. Finally, in chapter 6, we extend this principle to the choice and usage of common goods when there are multiple available options and study the resulting dynamics.

1.2.2 Evolutionary games on graphs

Another assumption that was previously used when concluding that defection is an ESS of the Prisoner's Dilemma was that the population was well-mixed, i.e. everyone interacts with the same frequency with everyone else in the population and individual fitness is thus calculated from an arithmetic average of the payoffs obtained. This assumption is often used within evolutionary game theory. However, real populations are often observed to be structured in the sense that the interactions between individuals are not random and distinct connections may form (Amaral et al. 2000, Dorogovtsev & Mendes 2003, Proulx et al. 2005, May 2006). At the same time, this feature has long been known to affect the outcome of evolutionary processes (Kimura & Weiss 1964, Levins 1969, Nowak & May 1992). As a consequence, structure was incorporated into evolutionary models of finite populations by considering individuals, originally with fixed fitness, to be represented by nodes of an evolutionary graph (Lieberman et al. 2005). This framework, coined as evolutionary graph theory, adapted the previous birth-death process to structured populations by choosing an individual from the population to reproduce randomly proportional to their fitness and, thereafter, choosing uniformly at random one of their neighbours to die and be replaced by the offspring of the first.

This framework was soon after adapted considering evolutionary games on graphs. In this case, the graph also represents a social interaction network, which determines which individuals interact with each other. Therefore, the fitness of individuals on the graph is obtained through an average of the payoffs they get playing pairwise

games with their neighbours. Population structure was found to sustain the evolution of cooperation in large regular graphs when the benefit-to-cost ratio of cooperation (V/K) exceeds the number of neighbours of each individual (Ohtsuki et al. 2006). This success was associated with the viscosity of the evolutionary process on the graph, i.e. the fact that individuals transmit their behaviour locally to their neighbours. This makes cooperators to be more often surrounded by cooperators in comparison to defectors, giving them an evolutionary advantage. The simplicity of the rule consolidated population structure as one fundamental mechanism for the evolution of cooperation (Nowak 2006).

However, the positive result wasn't obtained for the birth-death process described before, but for the alternative death-birth process. In the death-birth process, one individual from the population is uniformly at random chosen to die, and one of their neighbours is randomly chosen proportional to their fitness to reproduce and replace the first with their offspring. This was one of the first instances where the chosen evolutionary dynamics was observed to affect the qualitative results obtained under evolutionary games. Nonetheless, the qualitative differences have been shown to vanish under a generalisation of the dynamics (Zukewich et al. 2013).

Since then, some topological features of social interaction networks have been shown to have a strong positive impact on the evolution of cooperation in the pairwise Prisoner's Dilemma. These included low average degree (Ohtsuki et al. 2006), scale-free properties (Santos & Pacheco 2005, Santos, Rodrigues & Pacheco 2006), particularly with high clustering (Assenza et al. 2008), high degree heterogeneity (Santos, Pacheco & Lenaerts 2006), and strong pair ties (Allen et al. 2017). However, the extension of these population structure models to multiplayer interactions is not trivial and considering only lower-order networks with dyadic interactions is often insufficient to represent them (Perc et al. 2013). In this thesis, we will focus on a framework of multiplayer social dilemmas on networks, which will be used to develop the work of chapters 3, 4, and 5.

1.3 Multiplayer social dilemmas on networks

1.3.1 Multiplayer social dilemmas

Many collective action problems that individuals face require accounting for multiplayer interactions (Hamburger 1973, Fox & Guyer 1978, Pacheco et al. 2009, Souza

et al. 2009, Santos et al. 2015, Broom et al. 2019). Similarly to pairwise social dilemmas, multiplayer social dilemmas can be characterised by the conflict between choosing cooperation as a socially optimal strategy and defection as an individually optimal strategy (Broom et al. 2019). As defined before, symmetric games are those under which the outcomes depend only on the used strategies and not on the set of individuals playing the game. Therefore, under symmetric multiplayer social dilemmas with two strategies, the payoff received by a given player depends only on their strategy and on the number of other cooperators and defectors in their group. A panoply of these dilemmas has been previously considered in the literature, some of which are categorised by Broom et al. (2019). We present those dilemmas in chapter 3, where we first study them, and a subset of them is further explored in chapters 4 and 5. An alternative social dilemma is then introduced in chapter 6.

Public goods dilemmas are defined as those under which cooperation involves the production of a reward V at an individual cost K, which is then consumed by individuals within the group. These dilemmas have wide variations in the literature, namely to which extent the public goods are non-rivalrous or non-excludable, whether costs are shared or independent, and even the shape of the production function. On the other hand, commons dilemmas typically represent scenarios with pre-existing resources, where cooperation can involve the sustainable consumption of the resource V and defection involves an aggressive attempt to monopolise them with cost K. A different dilemma relating to common goods is introduced in chapter 6, where instead of choosing between shared or monopolised consumption, individuals choose which of a selection of available common goods they will use. This will lead to a setting equivalent to the one studied in the IFD mentioned before.

However, considering structured populations interacting in the simplest two-strategy symmetric multiplayer social dilemmas may be done in several different ways. In the first accounts of evolutionary multiplayer games on networks, each individual in an evolutionary graph is determined to interact in a group with all their neighbours simultaneously, as well as to partake in the groups assembling in their neighbours (Santos et al. 2008). This means that there is a higher-order interaction network emerging from the underlying evolutionary graph, whose topological features may not be fully clear based on the simple understanding of the original graph. It thus became necessary to develop a more transparent way to describe higher-order interactions in structured populations interacting via multiplayer

games. This followed the general trend observed not only in evolutionary games, but in other dynamical processes, such as diffusion, synchronization, spreading, and social dynamics, as reviewed in Battiston et al. (2020).

Alternative formulations to multiplayer games on networks have since been developed. Evolutionary set theory originally proposed that each individual may be part of several interaction sets which can change dynamically (Tarnita et al. 2009). In parallel, higher-order interactions have been represented by bipartite graphs with a set of nodes for the individuals and another set of nodes denoting potentially interacting groups (Gómez-Gardeñes, Romance, Criado, Vilone & Sánchez 2011, Gómez-Gardeñes, Vilone & Sánchez 2011, Peña & Rochat 2012). These have shown that accounting for interacting groups in a different way may lead to fundamentally different results, even when the corresponding evolutionary graph is the same, as it is summarised in Perc et al. (2013). More recently, evolutionary dynamics on hypergraphs have been proposed, where each hyperlink represents an interacting group and selection occurs within them (Alvarez-Rodriguez et al. 2021). Models of hypergraphs have since been use to explain radical behaviour in group decision processes (Civilini et al. 2021), as well as explosive cooperation in multiplayer versions of the prisoner's dilemma (Civilini et al. 2024). See Majhi et al. (2022) for a recent more general review of dynamics on higher-order networks. In this work we will focus on the general and flexible framework introduced in Broom & Rychtář (2012), where higher-order interactions in the form of multiplayer games emerge from encounters of individuals on networks.

1.3.2 The Broom-Rychtář framework

In this thesis, particularly in chapters 3 to 5, we will extensively use the framework introduced in its general form in Broom & Rychtář (2012), which offered a mathematically tractable approach to address multiplayer social dilemmas on networks. A population of individuals is considered to be distributed over a spatial network. Individuals may follow a given movement model. Interacting groups of individuals emerge from their simultaneous presence on the same node of the network. Evolutionary dynamics such as the original birth-death, death-birth or link dynamics (Masuda 2009, Pattni et al. 2017), are adapted to operate under the classical assumption from evolutionary pairwise games on graphs that two individuals replace each other depending on the frequency of their interactions, in this case within the

same group. This way, the evolutionary graph emerges from the observed interactions of individuals, and not the other way around, providing a more transparent framework to describe higher-order interactions.

In the original paper where the framework is proposed (Broom & Rychtář 2012), movement models are described as history-independent if the population distribution is independent of the history of the movement process, and as row-independent if the players move independently of each other. Various movement models have been explored so far under this framework, an overview of which is provided in Broom et al. (2021). These have included completely independent movement (Broom & Rychtář 2012, Bruni et al. 2014, Broom et al. 2015, Pattni et al. 2017, Schimit et al. 2019, 2022, Pires & Broom 2024), movement contingent on previous interactions (history-dependent) (Pattni et al. 2018, Erovenko et al. 2019, Pires et al. 2023, Erovenko & Broom 2024), and coordinated movement between individuals (row-dependent) (Broom et al. 2020, Haq et al. 2024).

The territorial raider model was originally proposed as a model of completely independent movement (Broom & Rychtář 2012, Bruni et al. 2014). This model is adapted in Broom et al. (2015) to describe the local independent movement of individuals around their home nodes, governed by one single parameter, the individuals' home fidelity (h). In the meantime, the model has been used to explore small networks (Broom et al. 2015) and intermediate-sized complex networks with diverse structural properties (Schimit et al. 2019, 2022). Furthermore, the territorial raider model was extended in Pattni et al. (2017) to include subpopulations of individuals with the same home node, and therefore equivalent position distributions.

In chapter 3, we will formally introduce this model and derive the dynamics obtained in the limit of large home fidelity ($h \rightarrow \infty$), under which strictly defined communities emerge. We use that limit to explore community structured networks and show that these provide a path for the evolution of cooperation under the general social dilemmas presented in Broom et al. (2019). The work presented in that chapter is based on Pires & Broom (2024). In chapter 4, we explore the opposite limit of low home fidelity ($h = 1$) under complete territorial networks, showing that this reflects what is defined in Broom & Rychtář (2012) as a completely mixed population. We further use this as a term of comparison for the results obtained under complete, star and circle networks with mixing communities in a subset of the general multiplayer social dilemmas previously analysed.

Furthermore, a Markov movement model is a particular type of history-dependent model, where the distribution of the population on the following time step depends only on its most recent distribution (Broom & Rychtář 2012). A particular Markov model is proposed in Pattni et al. (2018), under which individuals move conditional on their satisfaction with their current group composition. Several results have been achieved in this context for complete networks in Pattni et al. (2018), and in comparison with star and circle networks in Erovenko et al. (2019) and with random networks in Erovenko & Broom (2024).

In chapter, 5 we will formally define this model and expand these results by considering a set of alternative evolutionary dynamics which were introduced in Pattni et al. (2017) for the general framework. We show that the co-evolution of cooperation and assortative movement between cooperators occurs under all considered evolutionary dynamics, with no major qualitative differences observed. The evolution of cooperation is largely determined by the topology of the spatial network and the movement costs. This shows that this mechanism for the evolution of cooperation is different to the one previously observed in static networks and independent movement models, where the dynamics chosen are highly impactful. These results will be analysed in comparison with such models. The work presented in this chapter is based on Pires et al. (2023).

1.4 Outline

In this section we provide an outline of the work presented in the following chapters of this thesis. Some of this information is mentioned throughout the introduction, and condensed here to facilitate the task of finding it to the reader.

In chapter 2, we define the frequency-dependent Moran process and how to get the fixation probability of a single mutant on well-mixed populations where individuals play pairwise, 2-strategy games. We present fixation probabilities as functions of population size and categorise the possible shapes they can have for each of the 24 possible orderings of the entries of the payoff matrix. We prove that in nine orderings these functions are monotonically decreasing, similarly to what occurs under fixed fitness. However, in 12 orderings, which included well-known games such as the Hawk-Dove game, the Prisoner's Dilemma, and the Stag Hunt game, we observed that increasing population size may lead to the increase of the fixation probability

of a single mutant for low, high and intermediate population sizes. This establishes that evolutionary games on finite populations reveal counter-intuitive effects for the simplest possible models, which would be overlooked in infinite population models. This chapter is based on the work published in Pires & Broom (2022) resulting from joint work with Professor Mark Broom.

In chapter 3, we formally introduce the territorial raider model with communities populating each node. We will derive the dynamics obtained in the limit of large home fidelity ($h \to \infty$), under which strictly defined communities emerge. We introduce the general social dilemmas presented in Broom et al. (2019) and show that community structured networks provide a path for the evolution of cooperation under all of them. We obtain analytical rules for the evolution of cooperation under weak selection for all these dilemmas and the six different evolutionary dynamics adapted to this framework in Pattni et al. (2017). In particular, populations organising into larger networks of local smaller sized communities systematically facilitated the evolution of cooperation in public goods dilemmas. The work presented in this chapter is published in Pires & Broom (2024), which resulted from joint work with Mark Broom.

In chapter 4, we further explore the territorial raider model, focusing on the opposite limit of low home fidelity ($h = 1$) under complete territorial networks. We argue that this scenario reflects what is defined in Broom & Rychtář (2012) as the completely mixed population for multiplayer games. This is a particular type of well-mixed population, since in multiplayer games, contrary to pairwise games, being well-mixed does not specify a unique population. We further apply the general results obtained under the completely mixed population to five of the multiplayer social dilemmas introduced in chapter 3. We use these results as a term of comparison for the one obtained under large home fidelity in chapter 3, and new results obtained for complete, star and circle networks with mixing communities. This chapter is the result of a working paper done together with Mark Broom.

In chapter 5, we formally define a Markov movement model under which individuals move contingent on their satisfaction with their current group composition. This will then be used to assess the co-evolution of cooperation with strategic mobility under complete, circle and star networks. We show that evolution of cooperation is largely determined by the network topology and the movement costs. Once again, we consider six different evolutionary dynamics and show that there are no signif-

icant qualitative differences in the evolutionary outcomes observed between them. This is set in contrast to what is observed in other models, such as pairwise games on static social interaction networks and the territorial model in chapters 3 and 4, where only a subset of the dynamics allow cooperation to evolve. The work presented in this chapter is based on the work published in Pires et al. (2023), which results from a collaboration with Professor Igor Erovenko and Mark Broom. This collaboration highly benefited from a secondment hosted by Igor Erovenko from February to May 2022, at the University of North Carolina in Greensboro, USA.

In chapter 6, we explore the self-organisation of common good usage and consumption when individuals have to choose between several available options with limited information. We extend the WSLS strategy introduced above to such systems: since the quality of each common good decreases with the number of current users, WSLS allows them to use a particular common good until its usage fails or quality falls below a threshold, at which point they shift to a different option. We show that the dynamics derived from a population of individuals using such a simple strategy leads to a distributed, although not optimal, equilibrium. However, hybrid systems where some individuals can store information about their previous experience and adapt their tolerance to failure may achieve an equilibrium with equalised quality akin to the ideal free distribution. The application of the results to the server selection problem faced in Internet services shows the potential of adapting game-theoretic concepts to real world problems. The usage of this strategy and the validity of the concepts can be extended to understand other systems such as population distribution on grazing or foraging land or propose solutions to operators of systems of public transport or other technological commons. The work presented in this chapter is based on a working paper done in collaboration with Dr Paolo Castagno, Professor Marco Ajmone Marsan, and Professor Vincenzo Mancuso. This collaboration was initiated during a research secondment hosted by Marco Ajmone Marsan and Vincenzo Mancuso in January and February 2024 in the Opportunistic Architectures Lab, at the IMDEA Networks Institute in Madrid, Spain.

In chapter 7, we introduce a population dynamics model of productive interaction between skills and their transmission, incorporating elements of both epidemic and evolutionary game-theoretic modelling. We consider individuals to form a well-mixed population interacting through a pairwise game, where skills are transmitted through contact, i.e. productive interactions, with a fitness-dependent transmission

rate. We show that skills may be individually sustainable depending on their loss rate when they originally appear in an unskilled population and on their intra-specific skill synergy which measures the supra-linear productive complementary of a given skill. The evolution of a new skill against a previous skill equilibrium is dependent on its synergistic coefficient with the average equilibrium skill. We also derive conditions for the stable co-existence of two skills. The work presented in this chapter is based on a working paper done in collaboration with Professor Rudolf Hanel. This collaboration was initiated during a research secondment from April to July 2023, hosted by Rudolf Hanel at the Complexity Science Hub and the Medical University of Vienna, Austria.

Chapter 2

Fixation probability functions under general pairwise games[1]

2.1 Introduction

Evolutionary games on finite populations provide new tools and concepts useful to study the dynamics of evolution. As introduced in chapter 1, a strategy is only stable in a finite population if selection opposes the successful fixation of other mutant strategies on it. Hence, fixation processes and, in the particular, fixation probabilities became a central part of understanding the self-organisation of collective behaviour.

In chapter 1, we review how fixation probabilities can be useful in understanding evolutionary games on finite populations and how they have been explored so far. Taking into consideration the central importance they gained in the context of evolutionary theory, this chapter analyses them systematically as functions of population size under the simplest 2×2 games. As such, in section 2.2, we start by defining the frequency-dependent Moran process and deriving the closed-form expression of the fixation probability of a single mutant strategy in a population playing 2×2 games. In section 2.3, we classify the games based on the 24 possible orderings of their payoff matrix' entries, starting with a summary of the function shapes analysed in the following sections and observed under each one of the games.

In section 2.3.1, we prove that nine of the games always lead to monotonically decreasing fixation probability functions. We tested the remaining orderings and

---

[1]This chapter is based on the work published in Pires & Broom (2022), which results from a collaboration with Professor Mark Broom.

concluded that three additional orderings may not have any non-monotonically decreasing functions. These included the fixation of 6 dominated strategies, i.e. strategies that always provide a player with the lowest payoff, regardless of what the other player does, one dominating strategy, and five strategies from coordination games.

However, increasing population size may not only change whether mutants fixate below or above neutrality (Nowak et al. 2004, Taylor et al. 2004), but can correspond to actual increases of single mutant fixation probabilities. We observed diverse fixation functions with increasing regions under the twelve remaining orderings. These included all six strategies from anti-coordination games such as the Hawk-Dove/Snowdrift game (Maynard Smith & Price 1973, Broom & Rychtář 2013, Hauert & Doebeli 2004, Doebeli & Hauert 2005), the fixation of five dominating strategies such as defectors in the Prisoner's Dilemma (Axelrod 1984, Poundstone 1992), and the fixation of stag hunters in the Stag Hunt game (Skyrms 2001, 2004) (the only exception in coordination games).

In section 2.3.2, fixation functions that increased from a global minimum to a positive asymptotic value were explored and found to be pervasive. In some anti-coordination games (e.g. fixation of Doves) this shape was found every time the payoff matrix led to a positive asymptotic value. These functions seem to have passed mostly unnoticed in the past with the exception of Broom et al. (2010), where it was briefly noted that they could be observed under the Hawk-Dove game. We propose that they may have been hidden by the weak selection limit (Nowak et al. 2004, Traulsen et al. 2006, 2007, Wild & Traulsen 2007), especially if this limit was considered to be dominant over the large population one (Sample & Allen 2017).

In section 2.3.3, we show that it should be possible to see fixation increasing for the smallest populations $N = 2$ under 6 different orderings: three dominating, two anti-coordination, and one coordination game (Stag Hunt) strategy ordering. We find three different ways this can happen – functions might increase monotonically, or they increase up to a global maximum and then decrease to a positive asymptotic value or to zero.

Finally, in section 2.3.4, we explore fixation functions with two extremes: decreasing for small populations, increasing for intermediate population sizes, and decreasing again for larger populations. These were observed both with positive and zero asymptotic values. The first were observed under the fixation of two dom-

inating strategies, and the second under anti-coordination and Stag Hunt games. These were all observed for transitions between functions with one global extreme and other function shapes.

2.2 Fixation probability in well-mixed populations under pairwise games

Let us consider a well-mixed population of individuals who interact pairwise according to a general 2×2 symmetric game, and call A and B the strategies at their disposal. After each encounter, they receive a payoff defined by the 2×2 payoff matrix introduced in table 1.1 with payoffs a, b, c, and d. We consider all payoff matrix entries to be strictly positive.

Each individual in a well-mixed population interacts on average with the same frequency with all others. In this context, their fitness is simply the average of the payoffs received over the encounters they have with other individuals in the population. Considering a population with N individuals, where i individuals are using strategy A and $N - i$ using B, the fitness of individuals using A and B are, respectively, the following:

$$f_i^N = \frac{a(i-1) + b(N-i)}{N-1},$$ (2.1)

$$g_i^N = \frac{ci + d(N-i-1)}{N-1}.$$ (2.2)

However, selection may depend on factors beyond the studied game, which on average should represent equal contributions to each individual's fitness, irrespective of their strategy. To account for this, we use the fitness formulation proposed in Nowak et al. (2004), which includes a parameter representing the intensity of selection $w \in [0, 1]$:

$$f_i^N = 1 - w + w\frac{a(i-1) + b(N-i)}{N-1},$$ (2.3)

$$g_i^N = 1 - w + w\frac{ci + d(N-i-1)}{N-1}.$$ (2.4)

Changing w is equivalent to performing a transformation of the original payoff matrix. However, as this transformation does not change the original game ordering,

we will set $w = 1$ for most of our analysis (leading back to equations 2.1 and 2.2), except when intending to study the explicit effects of intensity of selection.

Selection may act in different ways on the evolutionary process, and hence the fitness of each individual may be considered on the first (birth) event (Nowak et al. 2004, Taylor et al. 2004), on the second (death) event (Ohtsuki et al. 2006), on simultaneous events (Pattni et al. 2017), or to depend exponentially on both individuals' payoffs (Traulsen et al. 2006). Here we are focusing on the birth-death process with selection in the birth event, which is typically described as the frequency-dependent Moran process (Nowak et al. 2004, Taylor et al. 2004). This is a process under which it has been suggested that cooperators perform generally worse (Ohtsuki et al. 2006, Pattni et al. 2015) when compared to the results obtained under the others.

During each step of this process, one individual in the population gives birth proportionally to their fitness and another one dies randomly in the population. Taking this into consideration, for each evolutionary step, the probabilities of having the number of individuals i using strategy A increasing by one $\left(P_{i+}^{N}\right)$, decreasing by one $\left(P_{i-}^{N}\right)$, or remaining the same $\left(P_{i=}^{N}\right)$ are the following:

$$P_{i+}^{N} = \frac{i f_i^N}{i f_i^N + (N-i) g_i^N} \frac{N-i}{N}, \tag{2.5}$$

$$P_{i-}^{N} = \frac{(N-i) g_i^N}{i f_i^N + (N-i) g_i^N} \frac{i}{N}, \tag{2.6}$$

$$P_{i=}^{N} = 1 - P_{i+}^{N} - P_{i-}^{N}. \tag{2.7}$$

In the first expression above, we take the product of the probability of choosing an individual using strategy A for birth proportional to their fitness (left) with the probability of choosing an individual using strategy B for death uniformly (right). In the second expression we calculate the probability of the opposite choice. Finally, in the third expression, we consider the probability that the two individuals chosen for birth and death use the same strategy, which is complementary to the union of the two previous events.

All the other transitions are impossible by definition of the dynamics. This stochastic process is defined as a Markov chain, under which there are two absorbing states: $i = 0$ and $i = N$. If the population falls into one of these, it will stay there for the remaining evolutionary time.

To compute the probability of one single mutant A fixating in the population,

i.e. seeing the system transitioning from $i = 1$ to $i = N$, we have to consider a recursive relation based on equations 2.5, 2.6 and 2.7. Following Karlin & Taylor (1975), this relation leads to a closed-form expression for the fixation probability

$$\rho_N = \frac{1}{1 + \sum_{j=1}^{N-1} \prod_{k=1}^{j} \gamma_k^N}, \qquad (2.8)$$

where γ_k^N is defined as

$$\gamma_k^N = \frac{P_{k-}^N}{P_{k+}^N}. \qquad (2.9)$$

Applying equations 2.5 and 2.6, the term γ_k^N reduces to the relative fitness of residents in a population with k mutants and N total individuals. It will prove useful to express it as an explicit function of the number of mutants k and the population size N when $w = 1$:

$$\gamma_k^N = \frac{g_k^N}{f_k^N} = \frac{ck + d(N - k - 1)}{a(k - 1) + b(N - k)}. \qquad (2.10)$$

2.3 Fixation probability functions

General 2×2 matrix games are often defined by the ordering of the four payoff matrix entries from table 1.1 (see e.g. Broom & Rychtář (2013), Traulsen et al. (2007)). Even though there are 24 possible orderings, pairs of orderings having b and c swapped as well as a and d correspond to the same game with the definition of strategies A and B swapped. Therefore, there are a total of 12 independent 2×2 games, each with a pair of complementary orderings. These pairs are shown together in table 2.1 and delimited by horizontal lines. Strategy A in each ordering is considered the mutant and B is considered the resident.

In infinite populations, equilibria under these games are limited to three scenarios (Maynard Smith & Price 1973, Taylor & Jonker 1978, Hofbauer & Sigmund 1998, Traulsen & Hauert 2009). They either have one pure evolutionarily stable strategy (ESS), one mixed ESS, or two pure ESS. These are respectively named games of dominance, anti-coordination, and coordination, and they relate to distinct invasion scenarios in finite populations (Taylor et al. 2004). The correspondence between these games and the ordering of their payoffs is set in the first two columns of table 2.1. For each pair of dominance games on the table, the first ordering corresponds to having mutant A invading B, while the second corresponds to B invading A. All

other pairs of complementary game orderings did not follow any particular order.

However, under finite populations, evolutionary outcomes are defined not only by whether selection favours or opposes invasion, but also by whether it does so with fixation (Taylor et al. 2004). In the following sections, we will explore some of the possible ways in which fixation probabilities may depend on population size in 2×2 games. We found that there are at least 8 shapes that single mutant fixation probability functions ρ_N can take:

1. Always decreasing to a positive value (DP);

2. Always decreasing to 0 (D0);

3. Decreasing until they get to a minimum and then increasing up to a positive value (DUP);

4. Always increasing up to a positive value (UP);

5. Increasing up to a maximum and then decreasing to a positive value (UDP);

6. Increasing up to a maximum and then decreasing to 0 (UD0);

7. Decreasing to a minimum, then increasing up to a maximum, and finally decreasing to a positive value (DUDP);

8. Decreasing to a minimum, then increasing up to a maximum, and finally decreasing to 0 (DUD0).

We observed a higher diversity of fixation functions with increasing regions mainly under anti-coordination games (e.g. Hawk-Dove/Snowdrift game), the fixation of dominating strategies (e.g. defectors in the Prisoner's Dilemma), and the fixation of stag hunters under the game with the same name (the only exception in coordination games). In table 2.1, we have represented both the fixation function shapes observed under each game, and how the analytical results reflected on them. In section 2.3.1, we prove that some orderings always have decreasing fixation probability functions, and then explore these functions (shapes 1 and 2). In section 2.3.2, we explore functions with one global minimum (shape 3), state these are pervasive across dominance and anti-coordination games and suggest that these might have been concealed by the weak selection limit. In section 2.3.3, we obtain the conditions under which it is possible to see fixation probability functions increasing for very

Type of Game	Game	Ordering	Shapes of fixation functions ρ_N found having positive asymptotic value	null asymptotic value	Always decreasing ρ_N	Possibility of $\rho_3 > \rho_2$
	PD (D)	$b > d > a > c$	DP DUP	D0	No	
	PD (C)	$c > a > d > b$		D0	Tested	
Dominance Games (one pure ESS)		$a > c > b > d$ $d > b > c > a$	DP DUP UP UDP DUDP	D0	No Tested	Yes
		$a > b > c > d$ $d > c > b > a$	DP DUP UP UDP DUDP	D0	No Proven (T1+T2)	Yes
		$a > b > d > c$ $d > c > a > b$	DP	D0	Proven (T1) Proven (T1)	
		$b > a > d > c$ $c > d > a > b$	DP DUP	D0	No Tested	
		$b > a > c > d$ $c > d > b > a$	DP DUP UP	D0	No Proven (T2)	Yes
Anti-Coordination Games (one mixed ESS)	HD (D)	$c > a > b > d$	DUP	D0 DUD0	No	
	HD (H)	$b > d > c > a$	DP DUP	D0 DUD0	No	
		$b > c > a > d$ $c > b > d > a$	DUP UP	D0 DUD0	No No	Yes
		$b > c > d > a$ $c > b > a > d$	DUP UP	D0 DUD0	No No	Yes
Coordination Games (two pure ESS)	SH (S)	$a > c > d > b$	DUP	D0 UD0 DUD0	No	Yes
	SH (H)	$d > b > a > c$		D0	Proven (T1)	
		$a > d > b > c$ $d > a > c > b$		D0	Proven (T1) Proven (T1)	
		$a > d > c > b$ $d > a > b > c$		D0	Proven (T1) Proven (T1)	

Table 2.1: Summary of results for general 2×2 games. General 2×2 games can be defined by the ordering of the payoff matrix's entries. There is a total of 24 orderings, corresponding to 12 independent 2×2 games with distinguishable strategies. Pairs of orderings of the same game are enclosed between horizontal lines. We split games into three types – dominance, anti-coordination and coordination games – depending on the type of equilibria observed under them. Orderings corresponding to known games are signalled – Prisoner's Dilemma (PD), Hawk-Dove or Snowdrift (HD), Stag Hunt (SH) – and the strategy considered to be mutant A indicated in parenthesis. The first/second ordering of each pair of dominance games corresponds to the fixation of the dominating/dominated strategy. Under the other two types of games, pairs did not follow any particular ordering. The shapes of fixation functions ρ_N found under each of the orderings were listed, separated by the ones having positive and null asymptotic values. The last two columns summarise the analytical results of sections 2.3.1 and 2.3.3 respectively. Some game orderings were "Proven" to always have decreasing fixation functions ρ_N, either by Theorem 1 (T1) or by Theorem 2 (T2). One of the orderings resulted from a joint proof (T1+T2) for its two subsets: $bc \leq ad$ by T1 and $bc \geq ad$ by T2. We did not include the results for incomplete orderings. Other orderings seemed to always have these functions after being "Tested" systematically. Finally, other orderings were found to at least sometimes hold non-decreasing functions, labelled "No" in that column. This can be confirmed by the listing of shapes found under each ordering. Condition $\rho_3 > \rho_2$ was met under the signalled orderings when eq. 2.30 was fulfilled.

small populations and explore the functions under which this happens (shapes 4, 5 and 6). Finally, in section 2.3.4, we study the settings under which fixation probabilities are seen to have two extremes – a local minimum and a local maximum – before decreasing either to a positive value (shape 7) or to zero (shape 8) and associate these with transitions from functions with one global extreme (minimum or maximum) to other shapes.

2.3.1 Decreasing fixation probability functions

Under the fixed-fitness Moran process (Moran 1958), increasing the size N of a finite population always leads to a decrease in the probability that a single mutant has of fixating on the whole population. When frequency-dependent fitness is introduced (Nowak et al. 2004), despite this not being necessarily true, it is still observed to happen often. To probe the 2×2 games under which $\rho_{N+1} > \rho_N$ is always true, we obtain Theorems 1 and 2.

Theorem 1. *If the payoff matrix entries of a 2×2 game satisfy $b < a$ and $c \leq d$ or $b \geq a$ and $bc \leq ad$, then the fixation probability ρ_N of a single mutant using A decreases monotonically with N.*

Proof. We try to prove that $\rho_N > \rho_{N+1}$ is always true under some games. We start by comparing the closed-form expressions for the fixation probabilities recalling equation 2.8 and focusing on their denominators:

$$\rho_N > \rho_{N+1} \Leftrightarrow \frac{1}{1 + \sum_{j=1}^{N-1} \prod_{k=1}^{j} \gamma_k^N} > \frac{1}{1 + \sum_{j=1}^{N} \prod_{k=1}^{j} \gamma_k^{N+1}} \Leftrightarrow$$

$$(2.11)$$

$$\Leftrightarrow \sum_{j=1}^{N-1} \prod_{k=1}^{j} \gamma_k^N < \sum_{j=1}^{N} \prod_{k=1}^{j} \gamma_k^{N+1}.$$

Isolating the extra term on the sum on the right hand-side and joining the remaining two sums of $N - 1$ terms, we get the following condition:

$$\rho_N > \rho_{N+1} \Leftrightarrow \sum_{j=1}^{N-1} \left[\prod_{k=1}^{j} \gamma_k^N - \prod_{k=1}^{j} \gamma_k^{N+1} \right] < \prod_{k=1}^{N} \gamma_k^{N+1}. \qquad (2.12)$$

The right hand-side product is strictly positive because all values of γ_k^{N+1} are so

as well. Then, if the following more strict condition is fulfilled

$$\sum_{j=1}^{N-1} \left[\prod_{k=1}^{j} \gamma_k^N - \prod_{k=1}^{j} \gamma_k^{N+1} \right] \leq 0, \tag{2.13}$$

we will necessarily have $\rho_N > \rho_{N+1}$.

Any payoff matrix fulfilling $\gamma_k^N \leq \gamma_k^{N+1} \forall k = \{1, ..., N-1\}; N \in \{2, 3, ...\}$, satisfies condition 2.13. Thus, single mutant fixation probabilities in such games will necessarily be decreasing functions of N. Under the frequency-dependent Moran process, γ_k^N is equivalent to the relative fitness of resident strategy B as it is seen in equation 2.10. Therefore, $\gamma_k^N \leq \gamma_k^{N+1}$ leads to the following condition in that case:

$$\frac{ck + d(N-k-1)}{a(k-1) + b(N-k)} \leq \frac{ck + d(N-k)}{a(k-1) + b(N-k+1)}, \tag{2.14}$$

which after some algebra becomes

$$(bc - ad)k \leq (b-a)d. \tag{2.15}$$

We are interested in the games that satisfy this condition for all values of $k = \{1, ..., N-1\}$ and $N \in \{2, 3, ...\}$, which is equivalent to saying that

$$bc - ad \leq \inf\left(\left\{ \frac{(b-a)d}{k} : k = 1, ..., N-1; N \in \{2, 3, ...\} \right\} \right). \tag{2.16}$$

The value of k for which the infimum occurs depends only on whether $(b-a)d$ is negative or positive.

1. Case $b < a$:

   This case leads to $(b-a)d < 0$, and therefore the infimum on equation 2.16 occurs for the minimum value the k can assume $k = 1$, regardless of the value N. Thus, the condition becomes $bc - ad \leq (b-a)d$, which simplifies to

$$c \leq d. \tag{2.17}$$

2. Case $b \geq a$:

   This case leads to $(b-a)d \geq 0$, and therefore the infimum on equation 2.16 occurs for the largest possible value of k, which will be $k = N - 1$. Since

$(b - a)d$ is non-negative and k unbounded, the infimum is zero. The condition becomes

$$bc \leq ad. \tag{2.18}$$

All games contained in these two cases will necessarily have a fixation probability with a decreasing function on N.

$\square$

Theorem 2. *If the payoff matrix entries of a 2×2 game satisfy $c \geq d \geq b \geq a$, or $bc \geq ad$, $c + d \geq 2b$ and $c < d$, then the fixation probability ρ_N of a single mutant using A decreases monotonically with N.*

Proof. As in the proof of Theorem 1, we start by comparing the closed-form expressions for the fixation probabilities (eq. 2.11). We then follow an alternative path, isolating the first term ($j = 1$) instead of the last one ($j = N$) in the sum with N elements, and obtain the following relation:

$$\rho_N > \rho_{N+1} \Leftrightarrow \sum_{j=1}^{N-1} \left[\prod_{k=1}^{j} \gamma_k^N - \gamma_1^{N+1} \prod_{k=1}^{j} \gamma_{k+1}^{N+1} \right] < \gamma_1^{N+1}. \tag{2.19}$$

Following the same reasoning as in the previous proof, because γ_1^{N+1} is strictly positive, a game meeting the more strict condition

$$\sum_{j=1}^{N-1} \left[\prod_{k=1}^{j} \gamma_k^N - \gamma_1^{N+1} \prod_{k=1}^{j} \gamma_{k+1}^{N+1} \right] \leq 0, \tag{2.20}$$

will necessarily lead to $\rho_N > \rho_{N+1}$.

By the same reasoning used before, this includes all the payoff matrices that meet $\gamma_k^N \leq \gamma_{k+1}^{N+1}$ and $\gamma_1^{N+1} \geq 1 \forall k = \{1, ..., N-1\}; N \in \{2, 3, ...\}$. The second part of the condition had to be added to assure that the constant coefficient on the right hand-side product did not make it smaller than the left hand-side product. Applying the form that γ_k^N assumes under the frequency-dependent Moran process (equation 2.10), having $\gamma_k^N \leq \gamma_{k+1}^{N+1}$ and $\gamma_1^{N+1} \geq 1$ is equivalent to

$$\begin{cases} a(c - d) \leq (bc - ad)(N - k) \\ d - c \leq (d - b)N. \end{cases} \tag{2.21}$$

To fulfill these equations for all $k = \{1, ..., N-1\}$ and $N = \{2, 3, ...\}$, we get the following condition:

$$
\begin{cases}
bc - ad \geq \sup\left(\left\{\dfrac{a(c-d)}{N-k} : k = 1, ..., N-1; N = 2, 3, ...\right\}\right) \\[2mm]
d - b \geq \sup\left(\left\{\dfrac{d-c}{N} : N = 2, 3, ...\right\}\right).
\end{cases}
\tag{2.22}
$$

Parallel to the proof of Theorem 1, the suprema in both equations depend only on the sign of the terms $a(c-d)$ and $d-c$, which are related.

1. Case $c < d$:

   This case leads to $a(c-d) < 0$ and $d-c > 0$. There, the supremum on the top equation in 2.22 is zero, and the one on the bottom equation occurs for $N = 2$. Therefore, condition 2.22 is fulfilled if $bc - ad \geq 0$ and $d - b \geq (d-c)/2$, leading to:

   $$
   bc \geq ad, \quad c + d \geq 2b.
   \tag{2.23}
   $$

2. Case $c \geq d$:

   Under this case, the suprema from equation 2.22 occur for $k = N - 1$ in the top equation, and zero in the bottom one. Therefore, condition 2.22 turns into $bc - ad \geq a(c-d)$ and $d - b \geq 0$, which lead to:

   $$
   b \geq a, \quad d \geq b.
   \tag{2.24}
   $$

Any game meeting these conditions will necessarily have a fixation probability with a decreasing function on N.

$\square$

Under Theorem 1, there are a total of 7 orderings of the payoff matrix values represented in table 2.1 that always satisfy the obtained condition. The first condition includes exclusively 6 complete orderings corresponding to the fixation of strategies from the fourth dominance game listed in table 2.1, and the two last coordination games. The second condition is always satisfied by ordering $d > b > a > c$ corresponding to the fixation of Hare Hunters in the Stag Hunt game, and it is partially met for subsets of other 4 dominance game orderings: $b > d > a > c$, $d > b > c > a$, $d > c > b > a$ and $b > a > d > c$.

Under Theorem 2, the first condition in the union defines exclusively the complete ordering $c > d > b > a$ corresponding to the fixation process of a dominated strategy. The second condition is only satisfied partially under the two orderings $d > b > c > a$ and $d > c > b > a$, both of which are already partially covered by the condition from Theorem 1. Joining Theorems 1 and 2, it can be easily shown that ordering $d > c > b > a$ ends up covered completely by the union of both final conditions, thus always holding decreasing fixation functions.

Additionally, if the dependence of the fixation probability on population size were considered only for large N, the second condition in equation 2.22 would simply lead to $d \geq b$. Together with the conditions from Theorem 1, the large N conditions would further cover the complete ordering $d > b > c > a$ as well.

It is worth noting that both Theorems 1 and 2 were proved by analysing the transition probability ratios γ_k^N (eq. 2.9), which under the frequency-dependent Moran process become the relative fitness of individuals using B (eq. 2.10). It can be seen that increasing population size by one individual impacted fixation probabilities in two ways: 1) added an extra term to the sum, and 2) changed ratios γ_k^N to γ_k^{N+1} in the already existing terms. Contrary to what happens under these orderings, fixation probability functions might not be monotonically decreasing functions of N if the sum of all terms in the denominator of equation 2.8 decreases with N, despite the increase of the number of terms. As will be shown in later sections 2.3.2, 2.3.3, and 2.3.4, this is possible under cases where adding individuals to the population decreases the relative fitness γ_k^N enough to compensate for the extra individuals that one single mutant would have to replace.

Games with decreasing functions

Focusing on the games under which fixation probabilities are decreasing functions of N, these might have either a zero or positive asymptotic limit, depending on the values in the payoff matrix. According to (Antal & Scheuring 2006), dominance games have a mutant strategy holding a positive asymptotic value if $a > c$ and $b > d$, otherwise this value is zero. Looking at the entries in table 2.1 corresponding to these games, we may conclude that the first game ordering for every pair (i.e. the dominating strategy) always holds a positive asymptotic value (DP when decreasing), while the second (i.e. the dominated strategy) always holds a null asymptotic value (D0 when decreasing).

Decreasing fixation probability functions were observed under all dominance game orderings, both for dominating and dominated mutant strategies. Three of the orderings corresponding to the fixation of dominated strategies were proved to only have decreasing functions, and the remaining three were tested for a wide choice of values with no non-decreasing counter-examples found. On the other side, all five dominating mutants which were not proven to hold decreasing fixation functions were found to have examples of fixation probability functions which increased for some value of population size, thus holding alternative shapes.

Regarding anti-coordination games, the borderline condition between having a mutant strategy fixating positively and with null probability asymptotically was obtained in Antal & Scheuring (2006), which depended only on the payoff values. The original expression was then redefined in Sample & Allen (2017) based on I, the definite integral of $\ln(\gamma(\alpha))$ evaluated between 0 and 1, which under $w = 1$ becomes

$$I = \ln \left(\frac{c^{\frac{c}{c-d}} b^{\frac{b}{a-b}}}{d^{\frac{d}{c-d}} a^{\frac{a}{a-b}}} \right). \tag{2.25}$$

The function $\gamma(\alpha)$ is the relative fitness γ_k^N (eq. 2.10) under $N \to \infty$, which depends only on the fraction of mutants $\alpha = k/N$ instead of k and N independently.

They showed that the general borderline condition should be $I = 0$. If the parametrisation of intensity of selection w is considered (see eqs. 2.3 and 2.4), and the weak selection limit taken after the large population limit in exactly this order, condition $I = 0$ should become equivalent to $a + b = c + d$.

We observed that under $I > 0$, i.e. when the asymptotic fixation probability is null, it is always possible to see decreasing fixation functions (D0) under these games. Otherwise, under $I < 0$, i.e. when the mutant strategy fixates positively in the asymptotic limit, the fixation of hawks under the Hawk-Dove game represented the only one of those game orderings which could have strictly decreasing functions for some choices of the payoff matrix. In section 2.3.2, we propose an explanation for why fixation function shapes beyond the decreasing one have not been referred to in most of the previous literature, with the exception of Broom et al. (2010). This is so despite the fact they are always observed under some of these game orderings, such as the one which represents the fixation of mutant doves under the Hawk-Dove game.

Under coordination games, asymptotic fixation values are always null indepen-
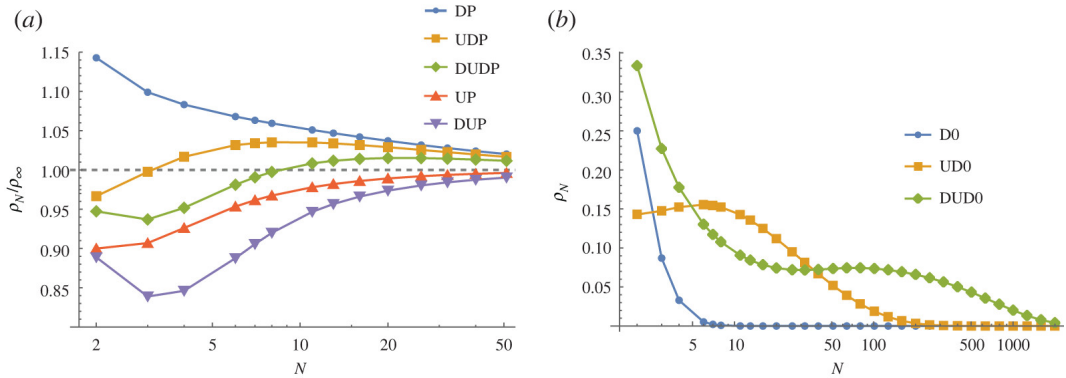
Figure 2.1: Summary of shapes of single mutant fixation probability functions ρ_N under 2×2 games. Figure 2.1a represents curves normalised by their positive asymptotic values ($\rho_\infty = 1 - d/b$) for simplification, and figure 2.1b represents curves with null asymptotic values. Results were obtained for the following payoff values: DP $[80, 6, 1, 1.5]$, UDP $[20, 3, 1.9, 1.1]$, DUDP $[8, 1.8, 2, 0.9]$, UP $[10, 3, 2, 1]$, DUP $[3, 4, 2, 1]$, D0 $[2, 1, 3, 4]$, UD0 $[13, 0.5, 3, 1]$, DUD0 $[3, 2, 4, 1.235]$. These payoff values were chosen to get optimal clarity of figures.

dent of the strategy considered as the mutant, as noted by Antal & Scheuring (2006). Here we add that five of these orderings (two pairs of complementary orderings and the one representing hare hunter fixation under the Stag Hunt game), were proven to always have strictly decreasing fixation probabilities (D0). Regarding the other ordering, which corresponds to stag fixation under the Stag Hunt game, there were striking examples of alternative fixation probability functions which will be mentioned in sections 2.3.3 and 2.3.4.

2.3.2 Fixation probability functions with one minimum

Under some of the explored 2×2 games, there were alternatives to the way the fixation probability of a single mutant depended on population size N. One common pattern found in these functions across anti-coordination games and the fixation of dominating strategies showed an initial plunge for small population sizes until a global minimum of the fixation probability ρ_N was reached. We called N_{min} to the population size under which this happened. This was followed by a steady increase up to a positive asymptotic value which can be computed following Antal & Scheuring (2006).

This type of dependence was not observed under any of the 6 coordination game orderings nor the other 6 orderings referring to the fixation of dominated strategies. It was so because all of these fixation probabilities have null asymptotic values. On the other hand, it was sometimes observed under the fixation of dominating strategies, such as $b > d > a > c$, $a > c > b > d$, $a > b > c > d$, $b > a > d > c$, and

$b > a > c > d$. This included the fixation of defectors under the Prisoner's Dilemma (see for instance $[2, 4, 1.9, 2.1]$). The occurrence of this dependence under this set of games seems to be completely absent from the previous literature.

Nonetheless, it was under anti-coordination games that we found this behaviour to be pervasive. This was present under all but one anti-coordination game orderings. The game ordering found to be an exception ($c > b > d > a$) does not seem to meet $I < 0$, a criterion necessary to have a positive asymptotic value and thus observe this profile of fixation probability. On top of this, as already noted in section 3.2, four out of these five anti-coordination game orderings did not seem to accommodate strictly decreasing functions of population size, so it seems like the fixation probability ρ_N increasing with population size N for populations larger than a value N_{min} seems to be the norm rather than the exception under these games.

Despite being pervasive under these games, which have been thoroughly studied in the past (Maynard Smith & Price 1973, Hauert & Doebeli 2004, Doebeli & Hauert 2005, Broom & Rychtář 2013, 2012, Broom et al. 2015), this effect did not receive much attention, with the exception of Broom et al. (2010). A significant amount of approaches to finite games have considered the weak selection limit (Traulsen et al. 2006, Wild & Traulsen 2007, Sample & Allen 2017) and show that when selection tends to zero fast enough (when compared to the increase of population size), we should expect fixation probability functions to always decrease asymptotically. Motivated by this, we have looked at the impact of decreasing intensity of selection on the fixation probability functions, represented in figure 2.2. For a fixed choice of payoffs $[a, b, c, d]$, decreasing the intensity of selection w pushes the population size from which fixation starts to increase N_{min} to larger values. In fact, they seem to be approximately inversely proportional, $N_{min}(w) \sim 1/w$ (see appendix A).

These results suggest that even if we consider an arbitrarily small value of the intensity of selection (i.e. weak selection limit), we may still see fixation probabilities increase with population size for large enough populations $N > N_{min}(w)$ (i.e. large population limit). This should not contradict the results obtained in Sample & Allen (2017), since in the scenario we are describing the large population limit should dominate over the weak selection one. Additionally, because turning points $N_{min}(w)$ become very large under weak selection, fixation probabilities could become less representative of what happens under anti-coordination games in finite populations. Even though pure states are absorbing ones, when mutations are considered,
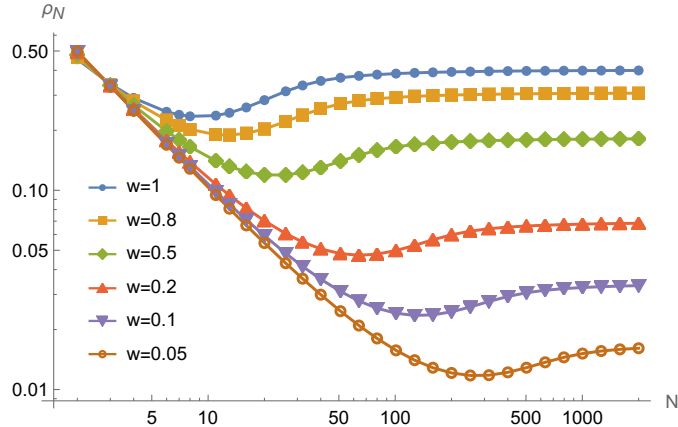
Figure 2.2: Functions of single mutant fixation probability and the effect of weak selection on moving their minimum values (under shape DUP) to higher population sizes N. The fixation probabilities shown were obtained for the fixation of doves under the Hawk-Dove game with $[5.5, 5, 6, 3]$.

the population might spend most of the evolutionary time in particular transient states (Antal & Scheuring 2006, Vasconcelos et al. 2017), which can also be called quasi-stationary states (Zhou et al. 2010, Overton et al. 2022, Nasell 1999b,a). In appendix A, we show that average conditional fixation times increase polynomially with $N_{min}(w)$ as they do with N under neutral fixation, instead of increasing exponentially as is predicted for anti-coordination games under a fixed intensity of selection (Antal & Scheuring 2006). These results highlight why it is essential to beware of the impact of the order in which the weak selection limit $w \to 0$ and the large population limit $N \to \infty$ are considered under evolutionary dynamics, as has been clearly stated in Sample & Allen (2017).

2.3.3 Fixation probability functions increasing under small populations

Under a restricted number of games of all three types (dominance, anti-coordination, coordination), fixation probabilities were observed to increase with population size N for small populations. The particular case where $\rho_3 > \rho_2$ holds is an extreme one where this may happen. However, the condition represented by that is simple enough to allow an analytical approach.

Theorem 3. *If the payoff matrix entries of a 2×2 game satisfy $c > d$ and $a + b > 2c(c + d)/(c - d)$, then $\rho_3 > \rho_2$.*

Proof. The fixation probability values under these population sizes are the following:

$$\rho_2 = \frac{1}{1 + \gamma_1^2}, \tag{2.26}$$

$$\rho_3 = \frac{1}{1 + \gamma_1^3 + \gamma_1^3 \cdot \gamma_2^3}. \tag{2.27}$$

These equations lead to the equivalence

$$\rho_3 > \rho_2 \Leftrightarrow \gamma_1^3 + \gamma_1^3 \cdot \gamma_2^3 < \gamma_1^2 \Leftrightarrow \gamma_1^3 \cdot \left(1 + \gamma_2^3\right) < \gamma_1^2. \tag{2.28}$$

Applying the definition of γ_i^N under the frequency-dependent Moran process (equation 2.10) on equation 2.28, we get the simplified condition

$$a + b > \lambda \text{ and } c > d, \tag{2.29}$$

where we have used λ, defined as

$$\lambda = 2 \ \frac{c\,(c+d)}{c-d}. \tag{2.30}$$

$\square$

This condition is only possible under six of the 24 possible payoff ordering. There are twelve orderings where $c > d$ but only in six of them is possible to have $a + b > \lambda$. These are the ones where $c > d$ and either a or b is the largest entry in the payoff matrix. These orderings are itemised in the last column of table 2.1.

Condition 2.28 highlights the conflict of having one extra individual in a population. One more resident leads to mutants having another individual to replace. Thus the presence of an extra term on the left hand-side of equation 2.28. In order to observe fixation probabilities increasing from population size $N = 2$ to $N = 3$, the relative fitness of residents needs to be much lower for higher proportions of them in the population.

There was a total of three shapes of fixation probability functions found that met $\rho_3 > \rho_2$. Fixation probabilities might increase monotonically up to a positive asymptotic value (UP), they might increase up to a maximum value and then decrease down to a positive value (UDP), or they might increase up to a maximum and then decrease to zero (UD0). These three shapes are represented in the summary

37

presented in figure 2.1.

Three of the orderings that satisfy this condition correspond to the fixation of dominating strategies. This means that the fixation probability's asymptotic value under all of these cases is positive. Under the two orderings $a > c > b > d$ and $a > b > c > d$ both UP and UDP were found depending on the particular parameter choices, while under $b > a > c > d$ only UP was found.

Under the two anti-coordination game orderings which are able to satisfy these conditions, the only shape found from these three was UP. Systematic checks suggest that equation $I > 0$ is either not satisfied at all, or at least at the same time as equation 2.29 under those two orderings. This means that when fixation probabilities increase from $N = 2$ to $N = 3$ under those two orderings, we should only observe functions with positive asymptotic fixation probabilities (i.e. UD0 should never be observed there).

Fixation probability functions with that shape – having one maximum and then tending to zero (UD0) – were found only for the fixation of stag hunters under the Stag Hunt game. This is the case exhibited in figure 2.1b. As suggested by the tests mentioned in the previous paragraphs, there seems to be no other ordering where UD0 could be observed, therefore establishing the particularity of this game and justifying further interest in its study.

2.3.4 Fixation probability functions with two extremes

Under orderings corresponding to games of all three types, fixation probability functions ρ_N were sometimes observed to decrease with population size N for small populations, have an increasing region for intermediate population sizes and finally decrease again under large populations. These increasing regions were necessarily delimited by two local extremes, one minimum and one maximum.

Under anti-coordination games, these regions were observed only when asymptotic values were null (DUD0) and occurred when the choice payoffs led to a positive value of I very close to zero (see equation 2.25). If $I > 0$ then a mutant using A has a null probability of fixation in the limit $N \to \infty$. However, close to the border $I = 0$ and for small enough populations, they may fixate similarly as if they were on the negative side. In the particular case in figure 2.3, $N = 200$ is enough for $I \leq 10^{-3}$. The occurrence of two extremes and the increasing regions to which they lead seemed to be transitional features between having the decreasing D0 (seen un-

der a high enough positive I), and the asymptotically positive DUP (seen under a negative I). Additionally, as we get further closer to $I \to 0^+$, we see the positive values of ρ_N breaking down to zero only for larger and larger population sizes.
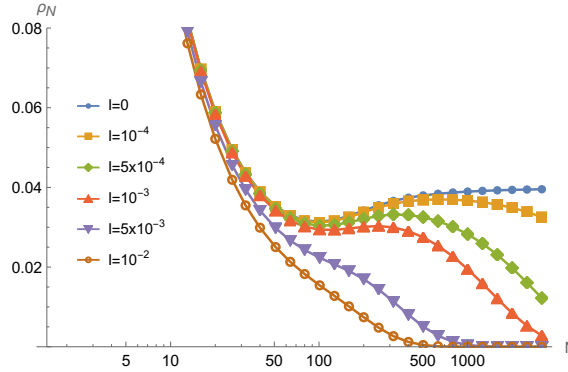
Figure 2.3: Functions of single mutant fixation probability transitioning from having shape DUP ($I = 0$) to D0 ($I = \{5 \times 10^{-3}, 10^{-2}\}$) through DUD0 ($I = \{10^{-4}, 5 \times 10^{-4}, 10^{-3}\}$). Fixation probabilities were obtained for games with payoff parameters $[5.5, 5, 6, d]$ and population size N. The values of d were calculated from each chosen value of I (eq. 2.25). Their choice maintains the game under ordering $c > a > b > d$ – mutant doves under Hawk-Dove game – and reproduces the approach of limit $I \to 0^+$. The approximate values of d are, in order, $d = 4.530$ ($I = 0$), $d = 4.531$, $d = 4.535$, $d = 4.540$, $d = 4.581$, and $d = 4.631$.

This shape was also observed in the context of the fixation of a stag hunters in the Stag Hunt game when function shapes transitioned between D0 and UD0, i.e. between always decreasing and having a global maximum (instead of a global minimum as in the previous case). This is shown in figure 2.4.
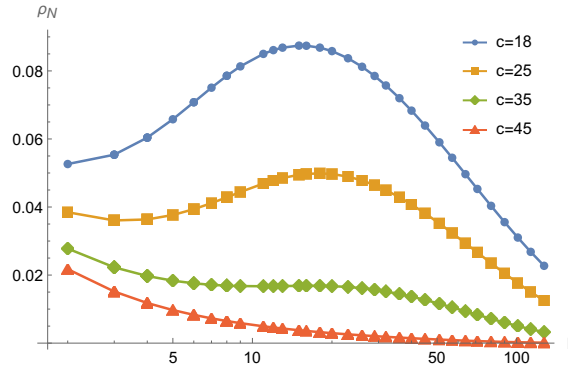
Figure 2.4: Functions of single mutant fixation probability transitioning from having shape UD0 ($c = 18$) to D0 ($c = 45$) through DUD0 ($c = \{25, 35\}$). Fixation probabilities were obtained for games with payoff parameters $[50, 1, c, 2]$ and population size N. The values of c were chosen as to always being under ordering $a > c > d > b$ and allowing condition $\rho_3 > \rho_2$ (eq. 2.29) to be met only for the lowest value $c = 18$.

A parallel fixation probability function having an intermediate population size increasing region between two extremes, but with a positive asymptotic value (DUDP) was observed under the fixation of two dominating strategies. This can be seen both in the summarising figure 2.1a and in figure 2.5. This shape was observed under

orderings $a > c > b > d$ and $a > b > c > d$, and seems to happen as a transition between functions with one global minimum (DUP) and functions which start increasing up to a global maximum and then decrease to a positive value (UDP). Those are the only two orderings that may satisfy $\rho_3 > \rho_2$ by taking the form of UDP.
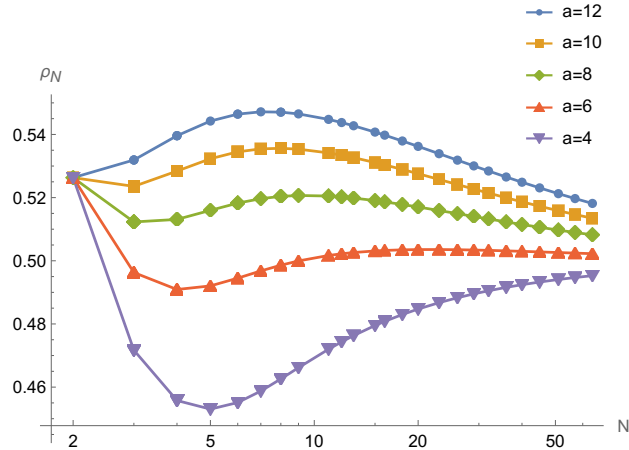
Figure 2.5: Functions of single mutant fixation probability transitioning from having shape UDP ($a = 12$) to DUP ($a = 4$) through DUDP ($a = \{10, 8, 6\}$). Fixation probabilities were obtained for games with payoff parameters $[a, 2, 1.8, 1]$ and population size N. The values of a were chosen as to always being under ordering $a > b > c > d$ and allowing condition $\rho_3 > \rho_2$ (eq. 2.29) to be met only for the highest value $a = 12$.

These results suggest that the shapes DUDP and DUD0 having two extremes delimiting an intermediate population size increasing region occur for transitions between fixation functions with one global extreme, either a maximum or a minimum, and other function shapes. Functions with one global extreme are characterised by having different trends (increasing/decreasing) for small and large population sizes. If incrementally changing the payoff matrix values switches the increasing trend to a decreasing one, an increasing region may emerge under intermediate population sizes.

2.4 Discussion

Understanding fixation processes and the probability of their occurrence is essential to the analysis of evolutionary games on finite populations. In this context, Taylor et al. (2004) observed that even if individuals are interacting via the same game, the size N of the population where they are included could lead to different evolutionarily stable strategies ESS_N as defined by Nowak et al. (2004). This is an

emerging feature of evolutionary processes under frequency-dependent fitness since stability under the fixed fitness Moran process never depends on population size. Here, we provided an extensive analysis of the dependence of single mutant fixation probabilities on population size, focusing on the simplest 2×2 games in well-mixed populations.

We have proved that under nine game orderings, fixation probabilities should be strictly decreasing functions. Under three other game orderings, extensive tests were performed without finding any other form of dependence beyond this one. Altogether, these games included the fixation of all six dominated strategies, one dominating strategy, and almost all strategies under coordination game orderings (five out of six).

However, a lot of interesting dependences on population size N arise in the remaining 12 game orderings, under which single mutant fixation functions were observed to have intervals of population sizes for which they increased with N. As counter-intuitive as this may seem, populations having extra individuals whom a single mutant would have to replace during fixation might actually increase that mutant's chances of fixating.

Under large populations, this happened when the mutant's relative fitness was higher under lower proportions of its type in the population, i.e. when mutants did relatively better among residents than they did between them: $d/b < c/a$. In this limit, the selection dynamics are completely characterised by the two ratios, as was already noted by Taylor et al. (2004). Increasing population size guaranteed that both mutants and residents interacted less frequently with residents in the initial steps of the fixation process, and therefore the increase in the number of resident individuals to be replaced by one mutant was compensated by the higher replacement probabilities.

Surprisingly, fixation functions were observed to increase under cases where mutants did relatively worse among residents than among themselves for large populations. This was observed under 3 game orderings, where fixation probabilities increased for small populations but eventually decreased to infinity. It was also noted by Taylor et al. (2004) that payoffs b and c are the only relevant entries of the payoff matrix under $N = 2$. Thus, under small populations, increasing population size means increasing the maximum frequency of individuals of the same type that are found in the population before fixation occurs (e.g. 0% for $N = 2$, 50% for

$N = 3$, 80% for $N = 6$). Increasing population size thus increases the frequency of interactions between equal types. Having high enough $a > \lambda - b$ and low enough $d < c$ allowed for fixation probabilities to increase for the smallest population sizes, even when $d/b > c/a$.

The confluence of all these effects in the 12 remaining orderings resulted in a high diversity of shapes of single mutant fixation probability functions. From functions with one minimum (DUP), to always increasing functions (UP), initially increasing but asymptotically decreasing ones (UDP and UD0) and functions with two extremes (DUDP and DUD0). We tried to understand under which orderings, and why, these function shapes emerged.

Anti-coordination games, such as the Hawk-Dove (Maynard Smith & Price 1973, Broom & Rychtář 2013) (also called Snowdrift game (Hauert & Doebeli 2004, Doebeli & Hauert 2005)) were shown to hold a wide variety of fixation probability function shapes. One of the most striking observations was the pervasiveness of functions with one minimum, a shape which was already noted in Broom et al. (2010) under the fixation of dove strategy. In some orderings, this was the only shape observed when asymptotic values were positive, even for arbitrarily low values of intensity of selection. While it was shown in Sample & Allen (2017) that fixation probabilities decrease with population size when the weak selection limit is dominant over the large population limit, our results suggest that if the considered limit order is the reverse, weak selection does not necessarily erase these non-decreasing shapes. Additionally, when approaching the limit where fixation functions change from being asymptotically null to having this shape with a global minimum, all anti-coordination game orderings showed functions with two extremes. Finally, two of these orderings also showed monotonically increasing shapes when b was sufficiently large, i.e. when mutants benefited the most from interacting with residents.

The six game orderings associated with the fixation of dominating strategies (Taylor et al. 2004) (also named unbeatable in the literature (Hamilton 1967, Nowak et al. 2004)), such as defectors under the Prisoner's Dilemma (Axelrod 1984, Poundstone 1992), were observed to hold monotonically decreasing functions, with one complete ordering and subsets of some of the remaining being comprehended in the conditions of Theorems 1 and 2. However, they were also shown to have a wide variety of other function shapes. Functions with one global minimum were observed under five out of the six orderings. Under three of these orderings, we observed

monotonically increasing functions. Two of them additionally showed alternative functions keeping an initial increase but decreasing for larger population sizes, and also functions with two extremes when transitioning between those with a global minimum and the previous shape. On the other side, the fixation of dominated strategies, such as Cooperation under the same games, was proved or tested to systematically hold monotonically decreasing functions.

In the context of coordination games, we have proved that under five out of the six possible orderings, fixation functions were always monotonically decreasing. However, the fixation of stag hunters (the reward-dominant strategy under the Stag Hunt game (Skyrms 2001, 2004)) was observed to have exceptional results in this context. If the reward for cooperation a is large enough, we observe initially increasing functions that then tend to zero thus holding a maximum. This shows that there is an optimal population size for the fixation of a single stag hunter in those cases. Functions with two extremes were observed under these games, when transitioning between the monotonically decreasing functions and the ones with a global maximum, leading to fixation probabilities not varying a lot for a wide range of population sizes.

Chapter 3

Evolution of cooperation in multiplayer social dilemmas under community structure[1]

3.1 Introduction

Understanding how individuals organise into social communities is of interest to various research fields due their ubiquitous presence in social systems. This is shown by the study of networks of friendships, academic collaborations, individual interests, online discourse, and political affiliation, among other social interaction systems (Girvan & Newman 2002, Newman 2006, Porter et al. 2009, Newman 2012). Its organisation occurs down to the smallest scale of human societies, which has motivated looking at the small interaction groups in which we partake as a core configuration of our social psychology (Caporael 1997). This has been further supported by experimental studies showing that small groups, and their limit of dyadic interactions, constitute most of our social encounters (Peperkoorn et al. 2020). Animal groups often organise themselves into social communities as well (Krause & Ruxton 2002). Their formation can be motivated by the fragmentation of habitats, and its subsequent impact on ecological networks has led to the study of evolution in metapopulations (Levins 1969, Hanski 1998). Even in the presence of migration fluxes involving roaming great distances, animals may maintain the same community and social ties, either by collectively coordinating their movements (Petit & Bon

---

2010, Couzin et al. 2003), or by coming back to the same territorial patches where they once settled (Ketterson & Nolan Jr 1990, Woodroffe et al. 1997, Woodroffe & Ginsberg 1999).

The organisation of individuals into social communities significantly influences their behaviour with one another, particularly when facing social dilemmas. As described in chapter 1, social dilemmas have been extensively modelled using evolutionary game theory. Incorporating community structure into these models has thus far entailed considering events of two different natures: within-community reproduction and between-community migration. These models are typically referred to as metapopulation dynamics, a classification of which has been performed in Yagoobi et al. (2023). The distinct nature of between-community events has been further emphasised by considering community-level events, such as group reproduction (Akdeniz & van Veelen 2020) or group splitting (Traulsen & Nowak 2006, Traulsen et al. 2008), which involve the replacement of entire groups either by other groups or by single individuals. Others have considered different intensities of selection acting on within- and between-community events (Wang et al. 2011, Hauert & Imhof 2012). Some of these modelling features suggest inspiration from multilevel selection to different degrees, which we intentionally avoid in our current work. Although these approaches lead to the evolution of pairwise cooperation, they may rely on the distinct nature of between-community events to do so, or even on additional mechanisms present such as punishment strategies (Wang et al. 2011).

Furthermore, metapopulation models generally assume that communities are connected to each other in the same way, with few exceptions to this (Akdeniz & van Veelen 2020) as is pointed out in Yagoobi & Traulsen (2021). Nonetheless, as reviewed in chapter 1, the topological features of interaction and spatial networks often have a strong interplay with the evolution of cooperation. However, considering both community and network structure within a mathematically tractable framework poses several problems.

The framework introduced in its general form in Broom & Rychtář (2012) and reviewed in chapter 1 offers a novel approach to multiplayer social dilemmas, where interacting groups of individuals emerge from their simultaneous presence on the nodes of a spatial network. In particular, we propose the use of the territorial raider model to study evolutionary dynamics in network- and community-structured populations with multiplayer interactions. We start by formally defining this model

in section 3.2, which will be used not only in this chapter, but also on chapter 4.

In section 3.3, we introduce the limit of high home fidelity, where communities exhibit asymptotically low mobility. We derive the evolutionary process arising in this limit for the six introduced dynamics and derive exact expressions for single mutant fixation probabilities under any network of communities. The analysis in this section is substantiated by the work in section B.1 of the appendix. In section 3.4, we show that the simple balance between within-community fixation and between community replacements determines whether cooperation evolves. We obtain the contributions under weak selection of the two types of events to fixation probabilities for 10 multiplayer social dilemmas. These findings are complemented by the content in section B.2 of the appendix. In section 3.5, we use this balance to derive the rules of multiplayer cooperation under the general multiplayer social dilemmas. In section 3.6, we analyse in detail one particular game, the Charitable Prisoner's Dilemma, and draw a comparison with some of the results obtained in the widely explored pairwise donation game. Finally, in section 3.7, we connect our findings to the relevant literature on multiplayer social dilemmas, metapopulation dynamics, and mobile structured populations.

3.2 The territorial raider model

The general framework introduced in Broom & Rychtář (2012) has been used to study the interplay between population structure, movement and multiplayer interactions. Here, we focus on the territorial raider model, a model of fully independent movement, which was generalised in Pattni et al. (2017) to account for subpopulations or, as we will refer to them, communities. We start by defining structure and the movement rules of this model. We then revisit the general approach to social dilemmas outlined in Broom et al. (2019), and finish by presenting the set of evolutionary dynamics defined in Pattni et al. (2017).

3.2.1 Network structure and territorial movement

A population is composed of N individuals $I_n = I_1, ..., I_N$. Individuals are positioned on a spatial network with M places $P_m = P_1, ..., P_M$, which has a set of edges connecting them. Even though the terms "graph" and "network" are often used interchangeably in the literature, here and in the following chapters we follow the

same terminology used in Schimit et al. (2019). The term graph will only be used for the underlying evolutionary graph representing the replacement structure between **individuals**, and network will be used to refer to the network of **places**.

Under fully independent movement models, the position of each individual is independent both of where they were previously and of where other individuals will be (Broom & Rychtář 2012). Therefore, the probability that an individual I_n is in place P_m is generally defined by p_{nm}. Under the territorial raider model used in this chapter, each node of the network represents the home of a community of Q individuals. The probability distribution of their positions is defined as the following:

$$
p_{nm} = \begin{cases} h/(h + d_n), & \text{if home of } I_n \text{ is } P_m, \\ 1/(h + d_n), & \text{if home of } I_n \text{ is connected to } P_m \text{ and it is not } P_m, \\ 0, & \text{otherwise,} \end{cases} \quad (3.1)
$$

where h is the home fidelity parameter, and d_n is the degree of the home node of individual I_n. This movement model is governed by a single parameter h yet allows for different movement propensities governed by the opportunities available to each individual, reflecting basic characteristics of local limited mobility present in animal populations based on territorial behaviour (Ketterson & Nolan Jr 1990, Woodroffe et al. 1997, Woodroffe & Ginsberg 1999) as well as human social systems. Alternative models could be used, some of which would lead to exactly the same results, as it is briefly discussed in the next section. We use the version of the territorial raider model under which each node of the network is home to a community of Q individuals, and thus M denotes the number of communities and $N = MQ$. The probability distribution of positions under the territorial raider model is represented in figure 3.1. Communities have been referred to in previous models as subpopulations (Pattni et al. 2017) or demes (Hauert & Imhof 2012). The below definitions are valid for any distribution p_{nm} of a fully independent movement model.

A group of individuals $\mathcal{G}$ has probability $\chi(m, \mathcal{G})$ of meeting in node P_m, which is given by:

$$
\chi(m, \mathcal{G}) = \prod_{i \in \mathcal{G}} p_{im} \prod_{j \notin \mathcal{G}} (1 - p_{jm}). \quad (3.2)
$$

The fitness of each individual I_n is obtained through the weighted average of the payoffs $R_{n,m,\mathcal{G}}$ received in each place P_m and each group composition $\mathcal{G}$ they can be in. We further introduce w, the intensity of selection as defined in Nowak et al.
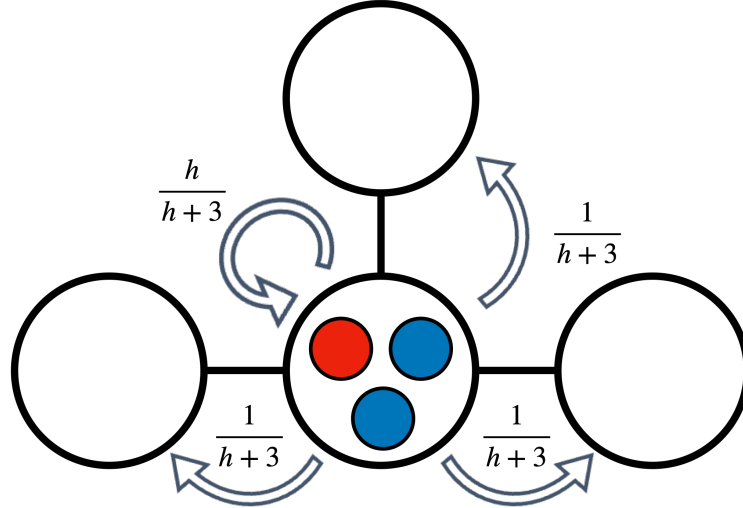
Figure 3.1: Representation of a small community network under the territorial raider model. At each time step, individuals initiate their movement from their home node, and can either remain there or move to any of the adjacent nodes, returning to their home node prior to the next time step. In this figure, we represent the resulting probability distribution for the community in the centre of the network.

(2004), which measures the extension to which the outcomes of the game contribute to the fitness of individuals:

$$F_n = 1 - w + w \sum_m \sum_{\mathcal{G}:n\in\mathcal{G}} \chi(m,\mathcal{G}) R_{n,m,\mathcal{G}}. \tag{3.3}$$

We bring attention to an alternative notation used in the literature, where a background payoff defined as R is introduced. This alternative notation has been used in movement models (Broom et al. 2015, Pattni et al. 2017, Erovenko et al. 2019, Pires et al. 2023) and it will be used in chapter 5. The background payoff is typically included within the effective reward received in each interaction, which we denote $R'_{n,m,\mathcal{G}} = R_{n,m,\mathcal{G}} + R$. This leads to the following adjustments to the fitness of individuals:

$$F'_n = \sum_m \sum_{\mathcal{G}:n\in\mathcal{G}} \chi(m,\mathcal{G}) R'_{n,m,\mathcal{G}}. \tag{3.4}$$

In the present and the following chapter (chapters 3 and 4), we will use intensity of selection w, as this is revealed to be more practical when inspecting the weak selection limit. Nonetheless, the second approach leads to a simple rescaling of the fitness $F' = \frac{1}{w}F$ when $R = \frac{1-w}{w}$, which has no impact on the evolutionary dynamics introduced later. In chapter 5, we used the second notation with a rescaling of the parameters that would be equivalent to using the first notation setting the intensity of selection $w = 0.5$.

3.2.2 Multiplayer social dilemmas

We consider the multiplayer social dilemmas studied in Broom et al. (2019). Individuals have two strategies available to them: to cooperate (C) or to defect (D). In these dilemmas, payoffs can be represented as $R_{n,m,\mathcal{G}} \equiv R_{c,d}^C (\equiv R_{c,d}^D)$ when the focal individual I_n is a cooperator (defector), as they are determined by the type of the focal individual and the number of cooperators c, and defectors d in their current group. We present the payoffs received under each social dilemma in table 3.1, where V represents the value of the reward shared, and K the cost paid by individuals in the group. In public goods dilemmas, cooperation involves the production of a reward V at a cost K, which is consumed by individuals within the group. In contrast, commons dilemmas typically represent scenarios with pre-existing resources, where cooperation can involve, among other things, the sustainable consumption of the resources. In the HD dilemma, the only commons dilemma we study here, cooperators evenly share the reward V, while defectors attempt to consume it entirely,

Multiplayer Game	$R_{c,d}^C$	$R_{c,d}^D$
Charitable Prisoner's Dilemma (CPD) (Broom et al. 2015)	$\begin{cases} \frac{c-1}{c+d-1}V - K & c > 1 \\ -K & c = 1 \end{cases}$	$\begin{cases} \frac{c}{c+d-1}V & c > 0 \\ 0 & c = 0 \end{cases}$
Prisoner's Dilemma (PD) (Hamburger 1973)	$\frac{c}{c+d}V - K$	$\frac{c}{c+d}V$
Prisoner's Dilemma with Variable production function (PDV) (Archetti & Scheuring 2012)	$\frac{V}{c+d}\sum_{n=0}^{c-1}\omega^n - K, w > 0$	$\frac{V}{c+d}\sum_{n=0}^{c-1}\omega^n, w > 0$
Volunteer's Dilemma (VD) (Diekmann 1985)	$V - K$	$\begin{cases} V & c > 0 \\ 0 & c = 0 \end{cases}$
Snowdrift (S) (Archetti & Scheuring 2012)	$V - \frac{K}{c}$	$\begin{cases} V & c > 0 \\ 0 & c = 0 \end{cases}$
Threshold Volunteer's Dilemma (TVD) (Archetti & Scheuring 2012)	$\begin{cases} V - K & c \geq L \\ -K & c < L \end{cases}$	$\begin{cases} V & c \geq L \\ 0 & c < L \end{cases}$
Stag Hunt (SH) (Pacheco et al. 2009)	$\begin{cases} \frac{c}{c+d}V - K & c \geq L \\ -K & c < L \end{cases}$	$\begin{cases} \frac{c}{c+d}V & c \geq L \\ 0 & c < L \end{cases}$
Fixed Stag Hunt (FSH) (Pacheco et al. 2009)	$\begin{cases} \frac{V}{c+d} - K & c \geq L \\ -K & c < L \end{cases}$	$\begin{cases} \frac{V}{c+d} & c \geq L \\ 0 & c < L \end{cases}$
Threshold Snowdrift (TS) (Souza et al. 2009)	$\begin{cases} V - \frac{K}{c} & c \geq L \\ -\frac{K}{L} & c < L \end{cases}$	$\begin{cases} V & c \geq L \\ 0 & c < L \end{cases}$
Hawk–Dove (HD) (Broom & Rychtář 2012)	$\begin{cases} \frac{V}{c} & d = 0 \\ 0 & d > 0 \end{cases}$	$\frac{V - (d-1)K}{d}$

Table 3.1: Payoffs obtained by a focal cooperator $R_{c,d}^C$ or a focal defector $R_{c,d}^D$ in a group with c cooperators and d defectors playing general social dilemmas. Social dilemmas are referred to in the text by the acronyms introduced in this table.

either winning it occasionally or losing it to other defectors while incurring a cost K.

3.2.3 Evolutionary dynamics

We follow an approach grounded on evolutionary graph theory (Lieberman et al. 2005). The population has a corresponding evolutionary graph represented by the adjacency matrix $\mathbf{W} = (w_{ij})$, with w_{ij} denoting the replacement weights which determine the likelihood of individual I_i replacing I_j in an evolutionary step. In contrast with the original formulation of evolutionary pairwise games on graphs, the interaction structure between individuals is an emerging feature of the model. We follow the procedure used in Pattni et al. (2017), under which replacement weights are determined by the fraction of time any two individuals spend interacting within the network. They spend their time equally with each of the other individuals in their groups, and time spent alone contributes to their self-replacement weights. This leads to the following definition:

$$w_{ij} = \begin{cases} \displaystyle\sum_m \sum_{\mathcal{G}:i,j\in\mathcal{G}} \frac{\chi(m,\mathcal{G})}{|\mathcal{G}|-1}, & i \neq j, \\ \displaystyle\sum_m \chi(m,\{i\}), & i = j. \end{cases} \tag{3.5}$$

Let us consider that the population goes through an evolutionary process operating on the strategies C and D used by each individual. This is modelled in discrete evolutionary steps, during which individuals may update their strategies. The probability that, at a given step, the strategy of an individual I_i replaces that of I_j is denoted by the replacement probability τ_{ij}. This probability may depend in different ways on the fitness of individuals, thereby incorporating selection into the process, and on the replacement weights, thereby capturing their interaction structure. We recall the dynamics outlined in Pattni et al. (2017), and their respective replacement probabilities τ_{ij} are summarised in table 3.2. The evolutionary dynamics are classified as birth-death (BD) if an individual is first selected for birth and then another one for death; death-birth (DB) if the reverse order of events is considered; and link (L) if an edge of the evolutionary graph is directly chosen. Under each of these, selection can act either on the birth (B) or the death (D) event. The combination of these two factors leads to 6 different evolutionary dynamics which are referred to

by the letters used for their dynamics followed by the letter referring to which of the events selection acts on, e.g. BDB means that we chose birth-death dynamics with selection acting during birth, while LD means that we choose a link with selection acting on the death end. These codes are used in table 3.2 where we present the resulting birth and death, or replacement probabilities.

Evolutionary dynamics and replacement probabilities			
BDB	$b_i = \dfrac{F_i}{\sum_n F_n}, d_{ij} = \dfrac{w_{ij}}{\sum_n w_{in}}$	DBD	$d_j = \dfrac{F_j^{-1}}{\sum_n F_n^{-1}}, b_{ij} = \dfrac{w_{ij}}{\sum_n w_{nj}}$
DBB	$d_j = 1/N, b_{ij} = \dfrac{w_{ij}F_i}{\sum_n w_{nj}F_n}$	BDD	$b_i = 1/N, d_{ij} = \dfrac{w_{ij}F_j^{-1}}{\sum_n w_{in}F_n^{-1}}$
LB	$\tau_{ij} = \dfrac{w_{ij}F_i}{\sum_{n,k} w_{nk}F_n}$	LD	$\tau_{ij} = \dfrac{w_{ij}F_j^{-1}}{\sum_{n,k} w_{nk}F_k^{-1}}$

Table 3.2: Definition of birth probabilities ($b_{i(j)}$) and death probabilities ($d_{(i)j}$), or of final replacement probability (τ_{ij}), for six distinct evolutionary dynamics. The indices denote the individuals I_i giving birth and I_j dying. In instances where the replacement probability is not explicitly stated, it can be derived by multiplying the respective birth and death probabilities.

We consider both the fitness and replacement weights of individuals to be computed based on a weighted average of their interactions within their environment, as has been widely done both in pairwise games (Ohtsuki et al. 2006, Santos & Pacheco 2005, Santos, Rodrigues & Pacheco 2006, Santos, Pacheco & Lenaerts 2006, Allen et al. 2017), and multiplayer games (Santos et al. 2008, Pattni et al. 2015, 2017). Alternatively, these could have been calculated using different sampling assumptions, such as considering those two quantities to be obtained from two independent single interaction samples (Schimit et al. 2019, 2022). In those cases, there might be other effects emerging if the sampling used to calculate both quantities is correlated, as was shown in Hauert & Miekisz (2018).

The probability of fixation for a single mutant cooperator (defector) in a population with the opposing strategy is defined as ρ^C (ρ^D). Selection is said to favour the fixation of cooperation if $\rho^C > \rho^{neutral}$. The neutral fixation probability is equal to $\rho^{neutral} = 1/N = 1/(MQ)$. Moreover, cooperation is said to evolve if $\rho^C > \rho^{neutral} > \rho^D$, which is equivalent to stating that overall selection favours cooperation, as elaborated on chapter 1. Fixation probabilities can be calculated under the general fully independent movement models resorting to the proceeding explained in Broom et al. (2015) and Pattni et al. (2017). However, in the results section, we will focus on limits where fixation probabilities assume closed-form ex-

pressions.

3.2.4 Summary of parameters used in the territorial raider model

The general model introduced has several free parameters, which we present in table 3.3. Note that some of the other parameters considered are not free, since they depend on the parameters presented here, e.g. $N = M \times Q$. The results obtained in this chapter consider different limits of the free parameters. The limit of large home fidelity was considered throughout the whole set of results. In particular, the results presented in section 3.3, substantiated by section B.1 of the appendix, are valid under large home fidelity for arbitrary values of the remaining parameters. In section 3.4, we analyse the expansion of fixation probabilities within the additional limit of weak selection, the results of which are complemented by section B.2 of the appendix. In sections 3.5 and 3.6, three successive limits are considered: high home fidelity, weak selection and large networks of communities. In section B.3 of the appendix, we analyse the extent to which these rules are valid outside of the limits of large networks and weak selection.

Overall, we note that some of the limits are interdependent, and that therefore the limit of large home fidelity should be interpreted as being $h/M \to \infty$ and the limit of weak selection as $w \cdot (MQ) \to 0$. The results presented are obtained for general values of community size Q, and general payoff parameters V, K, L and ω.

Notation	Meaning
M	Number of communities
Q	Community size
h	Home fidelity
w	Intensity of selection
V	Social dilemma reward
K	Social dilemma cost
L	Threshold of cooperation
ω	Reward factor used in the PDV

Table 3.3: Free parameters of the territorial raider model.

3.3 Evolutionary dynamics under high home fidelity

Let us consider the previously introduced model in the limit of high home fidelity $h \to \infty$. In this section, we describe the evolutionary process arising from this limit

across the six introduced dynamics and derive exact expressions for single mutant fixation probabilities under any network of communities. The analysis in this section is substantiated by the work in section B.1 of appendix.

3.3.1 Fitness approximation

Consider a connected network comprising M places and an arbitrary topology. Each place is home to a community of size Q with movement following the territorial raider model (see figure 3.1). In the asymptotic limit of high home fidelity $h \to \infty$, individuals interact mostly within their community. The fitness of each individual depends mainly on the rewards $R_{c,d}^C$ and $R_{c,d}^D$ received within each community of c cooperators and d defectors, higher-order terms on h^{-1} dependent on the composition of the remaining communities. We define the asymptotic value of the fitness of a focal cooperator and defector as respectively the following:

$$f_{c,d}^C = 1 - w + wR_{c,d}^C, \tag{3.6}$$

$$f_{c,d}^D = 1 - w + wR_{c,d}^D. \tag{3.7}$$

In this limit, it is possible to obtain a closed-form expression for the fixation probability of a single mutant. The fixation process under each of the six introduced dynamics corresponds to a nested Moran process involving the fixation of a single mutant on its community and the fixation of that community in the population. A part of this process is represented in figure 3.2. The probabilities obtained are presented in the next subsections (see section B.1 of appendix for formal derivations).

3.3.2 Fixation probabilities under BDB, DBD, LB and LD dynamics

In the context of high home fidelity, replacement events within the same community happen at an asymptotically larger rate than events between different communities. As such, fixation probabilities ρ^C and ρ^D are obtained by multiplying the probability of the original mutant fixating within its community, denoted as r^C or r^D, by the probability of the community achieving fixation in the whole population. We note that these probabilities are identical under the BDB, DBD, LB and LD dynamics because the transition probability ratios that characterise the process are identical
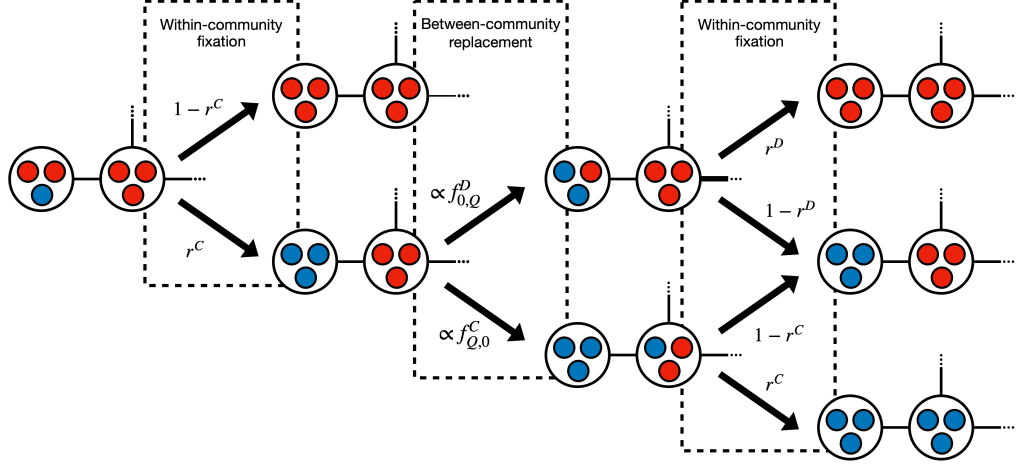
Figure 3.2: Fixation process in a population of connected communities under the asymptotic limit of high home fidelity. For simplicity, let us consider the scenario where one mutant cooperator emerges in a population of defectors. The new strategy will fixate within the community where it originated with a probability of r^C. The state attained has homogeneous communities and may change only through the occurrence of a between-community replacement. This involves either a cooperator replacing a defector from an adjacent community or the reverse, with probabilities proportional to their respective communal fitness $f_{Q,0}^C$ and $f_{0,Q}^D$. Each of those events may be followed by the within-community fixation of the new type, with respective probabilities r^C and r^D. If within-community fixation is unsuccessful, it will result in the restoration of the previous number of homogeneous communities of cooperators. However, if within-community fixation is successful, it will respectively increase or decrease by one the number of communities of cooperators in the network. The transition probability ratio Γ (see equation 3.10) between these two possible state transitions is constant and can be obtained from this diagram. The represented probabilities are the same under BDB, DBD, LB and LD dynamics. Under DBB and BDD dynamics, within-community fixation probabilities are computed from equations 3.18 and 3.19, and the transition probability ratio is obtained from equation 3.20.

at any given state of the population.

Within-community fixation is equivalent to a frequency-dependent Moran process where the fitness of individuals corresponds to its asymptotic value in isolated communities as defined in equations 3.6 and 3.7. Fixation probabilities for cooperators and defectors are determined as follows:

$$r^C = \frac{1}{1 + \sum_{j=1}^{Q-1} \prod_{c=1}^{j} \frac{f_{c,Q-c}^D}{f_{c,Q-c}^C}}, \tag{3.8}$$

$$r^D = \frac{1}{1 + \sum_{j=1}^{Q-1} \prod_{d=1}^{j} \frac{f_{Q-d,d}^C}{f_{Q-d,d}^D}}. \tag{3.9}$$

Upon reaching a state with homogeneous communities, one of two state-changing events may unfold. In one scenario, a cooperator replaces a defector from an adjacent community, with probability proportional to its communal fitness $f_{Q,0}^C$. Subse-

quently, the new cooperator may fixate within that community with a probability of r^C. Alternatively, a defector may replace a cooperator from a different community, proportionally to $f_{0,Q}^D$, and the new defector may fixate within the new community with a probability of r^D. The fixation process of one community on the entire population is equivalent to a fixed fitness Moran process, where the transition probability ratio is as follows (see a visual representation in figure 3.2 and a formal derivation in section B.1.1 of appendix):

$$\Gamma = \frac{f_{0,Q}^D \cdot r^D}{f_{Q,0}^C \cdot r^C}. \tag{3.10}$$

Please note that the ratio between the two within-community fixation probabilities can be considered in its following simplified form (Nowak et al. 2004, Sample & Allen 2017):

$$\frac{r^D}{r^C} = \prod_{c=1}^{Q-1} \frac{f_{c,Q-c}^D}{f_{c,Q-c}^C}. \tag{3.11}$$

The fixation probability of a single mutant cooperator or defector in a population of the opposing type is respectively the following:

$$\lim_{h \to \infty} \rho^C = r^C \cdot P_{Moran}\left(\Gamma^{-1}\right) = r^C \cdot \frac{1 - \Gamma}{1 - \Gamma^M}, \tag{3.12}$$

$$\lim_{h \to \infty} \rho^D = r^D \cdot P_{Moran}\left(\Gamma\right) = r^D \cdot \frac{1 - \Gamma^{-1}}{1 - \Gamma^{-M}}. \tag{3.13}$$

when $\Gamma \neq 1$. Otherwise, $\lim_{h \to \infty} \rho^C = r^C/M$ and $\lim_{h \to \infty} \rho^D = r^D/M$.

The high home fidelity limit reveals this nested Moran process characterised by frequency-dependent fitness at the lower level and an equivalent fixed fitness of communities at the higher level. This emerges naturally from a simple individual selection process which operates within communities and between individuals of distinct communities with the frequency of replacements coupled with how often individuals interact in the same group. We note that fixation probabilities are independent of the topology of the network, i.e. the set of edges linking the homes of different communities. The number of communities M, their size Q, and the multiplayer game played by individuals are enough to determine the evolutionary outcome of the process. The same results could be obtained from alternative movement models under the limit of isolated communities of the same size, as discussed in the appendix. Given the general nature of equations 3.12 and 3.13, they can be used to assess the viability of cooperation under social dilemmas in any network of

communities.

Social dilemmas are characterised by the conflict between cooperation as a socially optimal strategy and defection as an individually optimal strategy (Peña et al. 2016, Broom et al. 2019). Given this definition, we should expect the first to excel in between-community replacements and the second at within-community fixation. The balance between these two factors is present at each step of the higher level (community) fixation process, as is represented in figure 3.2. Condition $\rho^C > \rho^D$ is met in the following circumstances:

$$\frac{f_{Q,0}^C}{f_{0,Q}^D} > \left(\frac{r^D}{r^C}\right)^{1+\frac{1}{M-1}}. \tag{3.14}$$

This condition is more easily met when the size of the network is increased. Under $M \to \infty$, it becomes equivalent to $\Gamma < 1$, further implying that $\rho^C > 1/N > \rho^D$ and that there is one and only one stable strategy. This shows that the definition of Γ encapsulates the balance between the socially and individually optimal strategies, and is enough to determine the outcome of the evolutionary process under large networks.

Failure of cooperation in the CPD under BDB, DBD, LB and LD dynamics

Under the CPD with BDB, the effective fitness Γ of the between-community process can be obtained using equation 3.10. Replacing r^D/r^C with the simplified ratio between the two probabilities from equation 3.11, we obtain the following explicit expression for Γ:

$$\Gamma = \frac{f_{0,Q}^D}{f_{Q,0}^C} \cdot \prod_{c=1}^{Q-1} \frac{f_{c,Q-c}^D}{f_{c,Q-c}^C}. \tag{3.15}$$

We split the denominator and numerator of the previous product into two products and apply the definition of rewards under the CPD (see table 3.1), thus obtaining the following:

$$\Gamma = \frac{1-w}{1-w+w(V-K)} \frac{\prod_{c=1}^{Q-1} 1-w+w\frac{c}{Q-1}V}{\prod_{c'=1}^{Q-1} 1-w+w\left(\frac{c'-1}{Q-1}V-K\right)}. \tag{3.16}$$

We note that an extension of the products in the numerator and denominator to

$c = 0$ and $c' = Q$ respectively, would include the extra terms multiplied by each of the products. Doing that, together with the change of variable $c = c' - 1$, we obtain the following:

$$\Gamma = \frac{\prod_{c=0}^{Q-1} 1 - w + w\dfrac{c}{Q-1}V}{\prod_{c'=1}^{Q} 1 - w + w\left(\dfrac{c'-1}{Q-1}V - K\right)} = \frac{\prod_{c=0}^{Q-1} 1 - w + w\dfrac{c}{Q-1}V}{\prod_{c=0}^{Q-1} 1 - w + w\left(\dfrac{c}{Q-1}V - K\right)} =$$

$$= \prod_{c=0}^{Q-1} \frac{1 - w + w\dfrac{c}{Q-1}V}{1 - w + w\left(\dfrac{c}{Q-1}V - K\right)}.$$

(3.17)

We have that $\Gamma > 1$ for any choice of payoff parameters, intensity of selection, and community size. This means that the fixed fitness Moran probability will always be lower than $1/M$. At the same time, we note that $r^C < 1/Q$ because under the CPD, cooperators have strictly lower rewards than defectors in the same group. Therefore, when we consider the BDB or equivalent dynamics under the CPD with high home fidelity, cooperators never fixate above the neutral probability $1/(MQ)$ for any community number and size, network topology, and payoff parameter choices.

3.3.3 Fixation probabilities under DBB and BDD dynamics

The DBB and BDD dynamics lead to different quantitative results as transition probability ratios in the resulting Markov chain are different from the previous four dynamics. Fixation probabilities are obtained in a parallel way to the ones presented in 3.12 and 3.13, using the following corrected values of within-community fixation probabilities r^C and r^D, and transition probability ratios Γ:

$$r^C_{DBB/BDD} = \frac{1}{1 + \sum_{j=1}^{Q-1} \prod_{c=1}^{j} \dfrac{f^D_{c,Q-c}}{f^C_{c,Q-c}} \cdot \left(1 + \dfrac{f^C_{c,Q-c} - f^D_{c,Q-c}}{T_{DBB/BDD}(c, Q-c) - f^C_{c,Q-c}}\right)},$$

(3.18)

$$r^D_{DBB/BDD} = \frac{1}{1 + \sum_{j=1}^{Q-1} \prod_{d=1}^{j} \dfrac{f^C_{Q-d,d}}{f^D_{Q-d,d}} \cdot \left(1 + \dfrac{f^D_{Q-d,d} - f^C_{Q-d,d}}{T_{DBB/BDD}(Q-d, d) - f^D_{Q-d,d}}\right)},$$

(3.19)

$$\Gamma_{DBB/BDD} = \left(\frac{f^D_{0,Q}}{f^C_{Q,0}}\right)^2 \cdot \frac{r^D_{DBB/BDD}}{r^C_{DBB/BDD}},$$

(3.20)

with $T_{DBB/BDD}$ denoting the total weight-fitness correction factors under those two dynamics, which are positive as evident in their definition:

$$T_{DBB}(c, d) = c \cdot f_{c,d}^C + d \cdot f_{c,d}^D, \tag{3.21}$$

$$T_{BDD}(c, d) = d \cdot f_{c,d}^C + c \cdot f_{c,d}^D. \tag{3.22}$$

There are two main distinctions between these equations and those derived in the previous section for the remaining dynamics. On one side, both DBB and BDD amplify between-community replacement events, owing to the squaring of the communal fitness ratio in 3.20. At the same time, they suppress within-community selection, as can be concluded from the additional coefficients multiplied by the fitness ratio in equations 3.18 and 3.19. The condition $\rho^C > \rho^D$ leads to

$$\frac{f_{Q,0}^C}{f_{0,Q}^D} > \left(\frac{r_{DBB/BDD}^D}{r_{DBB/BDD}^C} \right)^{\frac{1}{2}\left(1 + \frac{1}{M-1}\right)}, \tag{3.23}$$

where the right-hand side is closer to 1 than that of equation 3.14, thus benefiting cooperation.

3.4 The limit of weak selection

In this section, we analyse the expansion of fixation probabilities within the additional limit of weak selection, which unveils simple contributions of within-community fixation processes and between-community replacement events. We further analyse these contributions under the general social dilemma section. These findings are complemented by the content in section B.2 of the appendix.

3.4.1 Fixation probabilities under weak selection

Further considering the weak selection limit $w \to 0$, the fixation probabilities presented in section 3.3 can be expanded, leading to the following equations (see section B.2 of the appendix for more details):

$$\rho^C \approx \frac{1}{MQ} + \frac{w}{2} \left[\frac{1}{Q} \left(1 - \frac{1}{M} \right) \Delta^{CD} + \left(1 + \frac{1}{M} \right) \delta^C - \left(1 - \frac{1}{M} \right) \delta^D \right], \tag{3.24}$$

where

$$\Delta^{CD} = R^C_{Q,0} - R^D_{0,Q} = -\Delta^{DC}, \tag{3.25}$$

$$\delta^C = \left. \frac{\partial r^C}{\partial w} \right|_{w \to 0} = \frac{1}{Q^2} \sum_{c=1}^{Q-1} (Q-c) \left[R^C_{c,Q-c} - R^D_{c,Q-c} \right], \tag{3.26}$$

$$\delta^D = \left. \frac{\partial r^D}{\partial w} \right|_{w \to 0} = \frac{1}{Q^2} \sum_{d=1}^{Q-1} (Q-d) \left[R^D_{Q-d,d} - R^C_{Q-d,d} \right]. \tag{3.27}$$

Equation 3.24 comprises three terms which are defined in equations 3.25–3.27. The term Δ^{CD} embodies the contribution of between-community events and corresponds to the difference between payoffs of communal cooperators and communal defectors. The sign of this term is determined by which of the two strategies is socially optimal. The terms δ^C and δ^D represent the contributions originating from the within-community fixation process of cooperators and defectors, respectively. Considering ρ^D leads to the swapping of superscripts C and D on these three terms.

The expansion assumes a different form under the DBB and BDD dynamics, both of which result in the following equation:

$$\rho^C_{DBB/BDD} \approx \frac{1}{MQ} + \frac{w}{2} \left[2\frac{1}{Q}\left(1 - \frac{1}{M}\right)\Delta^{CD} + \left(1 - \frac{1}{Q-1}\right)\left(1 + \frac{1}{M}\right)\delta^C + \right. $$
$$\left. - \left(1 - \frac{1}{Q-1}\right)\left(1 - \frac{1}{M}\right)\delta^D \right]. \tag{3.28}$$

This reflects the aspects highlighted in the previous section about the impact of these dynamics. We observe the amplification of between-community selection by a factor of 2, and the suppression of within-community selection by a factor of $1 - 1/(Q-1)$.

Each of the three contributing terms present in equations 3.24 and 3.28 shows a correction coefficient related to the finiteness of the network, which naturally vanishes under $M \to \infty$. Increasing the network size magnifies the relative impact of between-community replacement events on the fixation probability. At the same time, it increases the impact of the within-community fixation of residents but makes the within-community fixation of mutants relatively less significant than it is in smaller networks. In the limiting case where there are only two communities ($M = 2$), this last term exhibits a finite network correction coefficient three times larger than that of the within-community fixation of residents. This is so because the fixation of the original mutant in its community takes an increased importance in

the overall process.

Increasing the size of communities decreases the impact of between-community contributions under both dynamics. Simultaneously, it amplifies the impact of within-community contributions under DBB and BDD dynamics. From equation 3.28, we conclude that under the smallest communities ($Q = 2$), the expansion of fixation probabilities under DBB and BDD dynamics is reduced to a single term depending on Δ^{CD}, and within-community fixation terms vanish. In a mixed sub-population of one cooperator and one defector, both types have the same probability of being chosen first and the resulting replacement event is then certain to occur. Therefore, within-community fixation probabilities are equal to $1/2$ for both types, regardless of the payoffs received by individuals. This remains true under stronger selection as was noted in Pattni et al. (2017).

3.4.2 General social dilemmas under weak selection

Consider the general social dilemmas defined in table 3.1. We calculate the values of each of the three contributions Δ^{CD}, δ^C and δ^D under all of the dilemmas introduced there, and present them in table 3.4.

Multiplayer Game	Δ^{CD}	δ^C	δ^D
CPD	$V - K$	$-\frac{Q-1}{2Q}\left(K + \frac{V}{Q-1}\right)$	$\frac{Q-1}{2Q}\left(K + \frac{V}{Q-1}\right)$
PD, VD	$V - K$	$-\frac{Q-1}{2Q}K$	$\frac{Q-1}{2Q}K$
PDV	$\frac{V}{Q}\frac{1-\omega^Q}{1-\omega} - K$	$-\frac{Q-1}{2Q}K$	$\frac{Q-1}{2Q}K$
S	$V - K/Q$	$-\frac{1}{Q}(H_Q - 1)K$	$\frac{Q-1}{Q^2}K$
TVD, SH	$\begin{cases} V - K & Q \geq L \\ -K & Q < L \end{cases}$	$-\frac{Q-1}{2Q}K$	$\frac{Q-1}{2Q}K$
FSH	$\begin{cases} \frac{V}{Q} - K & Q \geq L \\ -K & Q < L \end{cases}$	$-\frac{Q-1}{2Q}K$	$\frac{Q-1}{2Q}K$
TS	$\begin{cases} V - K/Q & Q \geq L \\ -K/L & Q < L \end{cases}$	$\begin{cases} -\frac{K}{Q^2}\left(Q(H_{Q-1} - H_L) + \frac{L+1}{2}\right) & Q \geq L \\ -\frac{Q-1}{2Q}\frac{K}{L} & Q < L \end{cases}$	$\begin{cases} \frac{1}{Q^2}\frac{K}{2}(2Q - L - 1) & Q \geq L \\ \frac{Q-1}{2Q}\frac{K}{L} & Q < L \end{cases}$
HD	$\frac{Q-1}{Q}K$	$\frac{Q-1}{Q^2}\left(\left(\frac{Q}{2} - 1\right)K - V\right)$	$\frac{1}{Q}\left(\left(H_Q - 1\right)V - \left(\frac{Q+1}{2} - H_Q\right)K\right)$

Table 3.4: Value of fixation probability expansion terms under weak selection for each social dilemma. The terms denote the contributions of between-community events (Δ^{CD}), within-community fixation of cooperators (δ^C) and defectors (δ^D). Their definitions can be found in equations 3.25, 3.26, and 3.27.

The values of Δ^{CD} can be trivially obtained based on the calculation of the rewards among communal cooperators and communal defectors. The values of δ^C and δ^D are often simple to calculate because payoff differences between cooperators and defectors in mixed communities are constant under most social dilemmas. The only dilemmas under which this is not as trivial are the S, the TS and the HD dilemmas,

under which we had to include the harmonic series defined as the following:

$$H_Q = \sum_{i=1}^{Q} \frac{1}{i}. \tag{3.29}$$

Under all public goods dilemmas, the term Δ^{CD} is positive when cooperation is the socially optimal strategy. This happens when the reward for cooperating is sufficiently high, provided communities have a size capable of producing the reward. In the same dilemmas, the terms δ^C and δ^D exhibit negative and positive signs, respectively, due to defection being a dominant strategy.

Under the HD dilemma, the contribution Δ^{CD} remains positive regardless of reward value. The contributions δ^C and δ^D can be negative and positive for high V/K, positive and negative for low V/K, and both positive for intermediate V/K when $Q > 2$. These patterns reflect that cooperation is always socially optimal in this dilemma, while within a fixed group it maintains anti-coordination properties.

We will observe that cooperation can evolve under sufficiently large V/K, irrespective of the number of communities M, their size Q (provided it allows them to produce a reward), and how they are connected. This is true even in the limiting case of two arbitrarily large communities. For all public goods games apart from the CPD, this can be concluded based on the fact that the contribution of between-community events can be made arbitrarily large by increasing V, while the remaining contributions remain constant. We cannot conclude the same for the CPD at this point, as the remaining contributions (δ^C and δ^D) hold negative dependences on V. However, a more detailed analysis in the following sections will reveal that those conclusions remain true under the DBB/BDD dynamics. In parallel, under the HD dilemma, cooperation can evolve under sufficiently low V/K irrespective of the number and size of communities, and their connections. This comes from the positive linear dependence that all three contributions have on the value of K.

Moreover, based on equations 3.24 and 3.28 and the particular values their terms hold under each public goods dilemma, we conclude in section B.3.1 of the appendix that decreasing the size of the network has a detrimental effect to cooperation under all public goods dilemmas. Smaller networks systematically lead to stricter conditions for the evolution of cooperation in public goods dilemmas. Conversely, no consistent trend emerges in the HD dilemma.

Summing the expansions obtained for the fixation probabilities of cooperators

and defectors, we arrive at the following equation:

$$\rho^C + \rho^D \approx \frac{2}{MQ} + \frac{w}{M}(\delta^C + \delta^D), \qquad (3.30)$$

where, under the DBB/BDD dynamics, an additional coefficient $1 - 1/(Q-1)$ is included in the second term on the right-hand side. It is worth noting that when the difference between the payoffs of cooperators and defectors in the same group is constant, the contributions of the within-community fixation processes of cooperators and defectors to equations 3.24 and 3.28 are symmetric, i.e. $\delta^C = -\delta^D$. For such dilemmas, there is always one and only one stable strategy under weak selection. This is true for all social dilemmas discussed here, except for the S and the TS with $Q > L + 1$, where bi-stability is possible ($\delta^C + \delta^D < 0$), and the HD dilemma, which allows for mutual fixation and therefore instability of both strategies ($\delta^C + \delta^D > 0$). As established in section 3.3, under $M \to \infty$ there is one and only one stable strategy, determined by the value of Γ. This is in agreement with the fact that, for the remaining dilemmas, the second term on the right-hand side of equation 3.30 vanishes under large networks. We conclude that both weak selection and a large number of communities often lead to simple dominance cases. Based on these findings, we emphasise that in all public goods dilemmas, if the fixation of cooperators is favoured under weak selection or large networks, then the fixation of defectors won't be (and vice versa). In the next section, we will extend our analysis, systematically presenting the conditions under which cooperation evolves for all social dilemmas.

3.5 The rules of cooperation under general multiplayer social dilemmas

In this section, we further extend our analysis of general multiplayer social dilemmas. Cooperation evolves successfully, i.e. $\rho^C > \rho^{neutral} > \rho^D$, for larger numbers of communities if

$$\Delta^{CD} > Q(\delta^D - \delta^C). \qquad (3.31)$$

This rule is obtained considering that the first-order term of the weak selection expansion in equation 3.24 has to be positive. The equation above is valid under the BDB/DBD/LB/LD dynamics, whereas for the DBB/BDD dynamics, a multiplying

| Multiplayer Game | Evolution of cooperation under | |
	BDB/DBD/LB/LD	DBB/BDD
CPD	$\emptyset$	$V/K > (Q-1)$
PD, VD	$V/K > Q$	$V/K > \dfrac{Q}{2}$
PDV	$V/K > \dfrac{1-\omega}{1-\omega^Q}Q^2$	$V/K > \dfrac{1-\omega}{1-\omega^Q}\dfrac{Q^2}{2}$
S	$V/K > H_Q$	$V/K > \left(H_Q - \dfrac{1}{2}\dfrac{Q}{Q-1}H_{Q-1}\right)$
TVD, SH	$\begin{cases} V/K > Q & Q \geq L \\ \emptyset & Q < L \end{cases}$	$\begin{cases} V/K > \dfrac{Q}{2} & Q \geq L \\ \emptyset & Q < L \end{cases}$
FSH	$\begin{cases} V/K > Q^2 & Q \geq L \\ \emptyset & Q < L \end{cases}$	$\begin{cases} V/K > \dfrac{Q^2}{2} & Q \geq L \\ \emptyset & Q < L \end{cases}$
TS	$\begin{cases} V/K > H_Q - H_L + 1 & Q \geq L \\ \emptyset & Q < L \end{cases}$	$\begin{cases} V/K > 1/2\left[1 + \left(1 - \dfrac{1}{Q-1}\right)(H_Q - H_L)\right] & Q \geq L \\ \emptyset & Q < L \end{cases}$
HD	$V/K < \dfrac{Q - 1/Q - H_{Q-1}}{H_{Q-1}}$	$V/K < \dfrac{\dfrac{Q-1}{Q-2}(Q - 2/Q) - H_{Q-1}}{H_{Q-1}}$

Table 3.5: Rules for the evolution of multiplayer cooperation under networks of communities. We assume a large number M of communities and that they are composed of at least two individuals ($Q \geq 2$). These conditions guarantee that $\rho^C > \rho^{neutral} > \rho^D$. We denote the harmonic series as $H_Q = \sum_{i=1}^{Q} i^{-1}$. Under $Q = 1$, the derived conditions are the following: cooperation never evolves under the CPD, TVD, SH, FSH, and TS (assuming that $L \geq 2$), cooperation evolves for $V/K > 1$ under the PD, PDV, VD and S, and both strategies are neutral under the HD. These results are valid under arbitrary values of w and M, and they are the same under all six dynamics.

factor $(1/2)(1 - 1/(Q - 1))$ is added to the right-hand side of the equation.

We systematically computed the terms Δ^{CD}, δ^C and δ^D under each of the general social dilemmas approached, which were summarised in table 3.4. Applying their values to condition 3.31 and its DBB/BDD-corrected version, we obtain the conditions under which cooperation evolves for each of the social dilemmas studied here, for all community sizes Q and the six evolutionary dynamics, and present them in table 3.5. Cooperation can evolve under all of the social dilemmas approached for at least some of the explored dynamics. We opted to show the rules obtained under a high number of communities to allow a systematic analysis of the dilemmas, as obtaining them for arbitrary values of M was attainable but often intricate. These limits were considered in a particular order: first $h \to \infty$, then $w \to 0$, and finally $M \to \infty$. The order of these limits is relevant, given that different orders can lead to distinct fixation probability expansions and conditions for the evolution of cooperation (Sample & Allen 2017), as well as generate or erase surprising finite population effects as it was seen in chapter 2. In section B.3 of the appendix, we analyse the validity of the simple rules presented here when these limits are relaxed.

The results presented in this table suggest that social dilemmas split into distinct groups. Non-threshold public goods dilemmas such as the PD, the VD, the S, and the PDV allow cooperators to evolve under any community size if the reward-to-cost ratio V/K surpasses a critical value dependent on Q. This value is the same under the PD and the VD, but lower under the S and the convex PDV ($w > 1$), and higher under the concave PDV ($w < 1$). The CPD presents a distinct landscape, where cooperation only evolves under the DBB and BDD dynamics. The critical value of the reward-to-cost ratio in this dilemma is the highest of all non-threshold public goods games. We will analyse this dilemma in the following section.

Threshold dilemmas such as the TVD, the SH, the FSH, and the TS have a critical value of the reward-to-cost ratio, above which cooperation evolves, only if the size of communities is at least of the same size as the public goods production threshold ($Q \geq L$). Otherwise, cooperation can never evolve regardless of the value of V/K. The TVD and the SH lead to the same conditions, which coincide with the PD and the VD when $Q \geq L$. The TS leads to lower critical values of the reward-to-cost ratio, and the FSH leads to higher values. We further note that the critical values obtained under the FSH when $Q \geq L$ are simply the ones obtained under the PDV with $\omega \to 0$. Critical values under threshold games generally don't depend on L, although their existence does. The exception to this is the TS dilemma, under which a larger production threshold decreases the critical value of the reward-to-cost ratio when communities are large enough to produce rewards.

The HD dilemma, which unlike the others is a commons dilemma, behaves distinctively from all of the remaining dilemmas. The reward-to-cost ratio has to be lower than a critical value for cooperation to evolve. It is clear that in this case, high rewards are detrimental to the evolution of cooperation.

We note that the critical value of the reward-to-cost ratio under public goods dilemmas always increases with the size of communities and regardless of the used evolutionary dynamics. This allows us to provide the visual representation from figure 3.3 with the areas under which cooperation evolves for community sizes up to a given value. Additionally, as mentioned in section 3.4, considering lower values of M always leads to stricter conditions for the evolution of cooperation. This reinforces the conclusion that populations organised into large networks of small communities lead to a larger region of the parameter space under which cooperation evolves. This is so because cooperators hold an advantage in between-community reproduction

events (intensified under large M), but they are disadvantaged in within-community fixation processes (minimised under small Q).
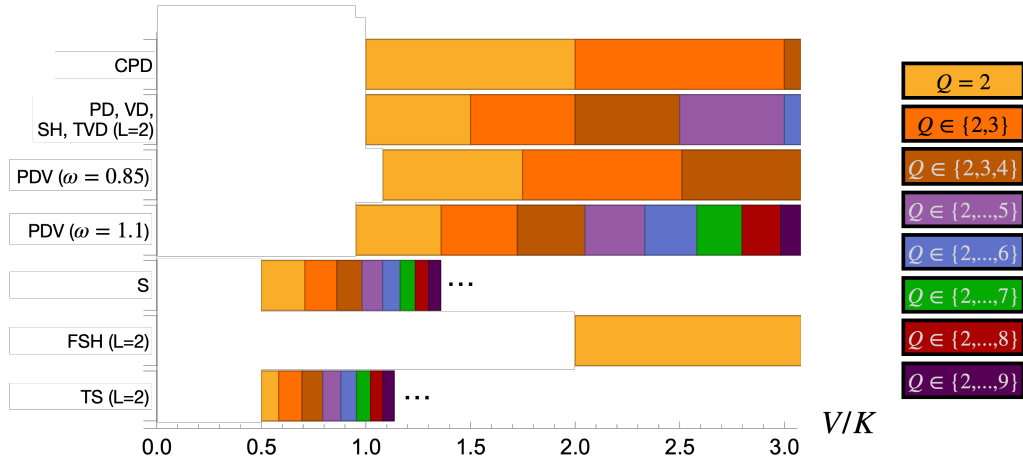
Figure 3.3: Regions under which cooperation evolves for each public goods dilemma under networks of communities. Each coloured region covers the values of the reward-to-cost ratio, i.e. V/K, under which cooperation evolves for a given set of community size values which are stated in the legend. These regions are obtained from the rules for the evolution of cooperation presented in table 3.5. Under low enough values of V/K, all dilemmas have uncoloured regions, as no community size allows the evolution of cooperation. We opted for not showing the areas of the S and the TS dilemmas with higher values of V/K (starting from the ellipsis), as coloured regions quickly decreased in size: at $V/K = 3$, cooperation evolves for any $Q \leq 231$ under the S and $Q \leq 377$ under the TS when $L = 2$.

In this context, the HD dilemma has key differences compared with the public goods dilemmas. Under this game, cooperators hold an advantage in between-community reproduction events for any payoff parameters. Regarding within-community fixation processes, defectors hold an advantage in small communities, but cooperators are the ones doing so in larger communities. However, there is a second overlapping effect which is described in section 3.4: increasing the size of communities decreases the impact of between-community reproduction and increases the impact of within-community fixation. Under the BDB dynamics, the second effect is not strong enough and the first effect dominates: communities with larger size always lead to higher critical values below which cooperators fixate, therefore benefiting them. However, under the DBB/BDD dynamics, both effects interplay and each dominates at a different scale of community sizes. Cooperators always evolve when $Q = 2$ because fixation depends only on between-community reproduction. When increasing the community size to $Q = 3, 4$, the emerging critical values below which cooperation evolves decrease with community size because of the increased importance of within-community fixation beneficial to defectors in those community sizes. However, for larger values of $Q \geq 5$, cooperation evolves for larger regions of V/K

when increasing Q because within-community fixation starts benefiting cooperators.

Comparing the critical values obtained between the different evolutionary dynamics, we note that the DBB and BDD dynamics always extend the values of V/K for which cooperation successfully fixates when compared to the remaining dynamics. They therefore have lower critical values in all public goods dilemmas and higher critical values in the HD dilemma. We note the extreme case of the CPD, under which cooperators never evolve under the BDB and equivalent dynamics, but find an evolutionary way under the DBB and BDD dynamics. These results can be explained by the fact that these dynamics when compared to the remaining, amplify the impact of between-community replacement terms (where cooperators succeed relative to defectors), and suppress within-community selection terms (where defectors succeed).

3.6 The Charitable Prisoner's Dilemma and pairwise cooperation

The CPD is a particular game of interest among public goods dilemmas. Under the CPD, cooperators do not benefit from their own contributions to public goods. This assures not only that individuals have equal gains from switching, but also that the gains are the same for all group sizes. In other words, the cost K is the effective cost that a cooperator pays for not defecting, regardless of group composition and size. This game is thus a social dilemma regardless of how large the reward is and the size of the interacting group (Broom et al. 2019). Other games have equal gains from switching, but the gains vary with group size. One such game is the PD, which was introduced in Hamburger (1973), under which the cost of cooperating is $K - V/Q$, and therefore may not even present a social dilemma under some payoff choices and group sizes (Broom et al. 2019).

Table 3.5 shows that cooperation evolves in the CPD when $V/K > (Q - 1)$. Given our particular interest in it, we present here the condition for the evolution of cooperation obtained under the CPD when a finite number of communities M is considered:

$$V/K > (Q - 1) \cdot \frac{1 - \frac{2}{MQ}}{1 - \frac{2(Q-1)}{MQ}}. \tag{3.32}$$

This rule quantifies the detrimental effect that considering a lower number of larger

communities (lower M and higher Q) has on the evolution of cooperation. At the same time, it materialises a fundamental result: cooperation can evolve provided rewards are high enough, for any given community size and number, and regardless of the connections between them. This was already concluded for the remaining public goods dilemmas. This is a remarkably general result that works for the smallest networks of two communities under which cooperation evolves if $V/K > (Q-1)^2$.

A parallel result was attained in Allen et al. (2017) by considering the pairwise donation game in an evolutionary graph which is split into M cliques of Q individuals each. Individuals within the same clique are considered to have unit-weighted edges and there is an arbitrary set of infinitesimal edges between individuals of different cliques. The vanishing edges act to isolate the individuals within each clique, guaranteeing that cooperation can always evolve in the pairwise donation game if V/K is high enough.

The rules obtained under the CPD are parallel not only to the clique structures explored in Allen et al. (2017) but also to the results obtained in Ohtsuki et al. (2006) for large regular networks. They showed that cooperation can evolve under the DBB dynamics if the reward-to-cost ratio is larger than the average number of neighbours each individual has on an interaction network. We note that in our model and the particular limit of large home fidelity, each individual regularly interacts with $Q-1$ others and that this is exactly the critical value of the reward-to-cost ratio under the DBB dynamics. However, the results obtained here for networked communities allow cooperation to evolve under the smallest networks when the corrected rule presented in equation 3.32 is met, thus going beyond the large network assumption.

At the same time, when interacting via the CPD, cooperators can never evolve if the evolutionary dynamics considered are the BDB/DBD/LB/LD dynamics, as shown in section 3.3.2 for arbitrary values of intensity of selection and number of communities. This had been already hypothesised in Pattni et al. (2017) for the general formulation of the territorial raider movement model, similar to what was observed in previous evolutionary pairwise games on graphs models (Ohtsuki et al. 2006). However, we note that this feature of the BDB dynamics is a singular case when stochastic combinations of different types of dynamics are considered, as was shown in Zukewich et al. (2013).

The CPD can be seen as a multiplayer extension of the pairwise donation game and as such, the two games may lead to analogous results. More generally, the

exploration of higher-order interactions leads to different interacting structures and evolutionary outcomes (Perc et al. 2013), even in other cases where the multiplayer game considered is a natural extension of its pairwise version. However, in the particular limit studied here, individuals always interact within their own communities which are all of the same size. Therefore, the average payoffs obtained in a well-mixed community playing the pairwise donation game are the same as the payoffs obtained in a group of fixed size repeatedly playing the CPD. This is no longer the case when lower home fidelity values are considered, and new higher-order differences are expected to arise in that context.

3.7   Discussion

In the present chapter, we use the territorial raider model previously approached (Broom et al. 2015, Pattni et al. 2017, Schimit et al. 2019, 2022), a fully independent movement model which is described by one single parameter, the home fidelity of individuals. The general framework originally proposed in Broom & Rychtář (2012) can be thought of as a natural extension of evolutionary games on graphs to multiplayer interactions, under which replacement events between individuals in the population occur proportionally to how often they interact. We focus on the limit of high home fidelity, under which individuals interact mostly within their community with the rare occurrence of cross-community group interactions. We derive the evolutionary dynamics in this limit, which is revealed to be a nested Moran process resembling metapopulation models where migration is coupled with selection (these are classified in Yagoobi et al. (2023)) but asymptotically rare as it is considered in Hauert & Imhof (2012). Therefore, we show that metapopulation dynamics of multiplayer interactions can be derived from the basic assumptions dating back to evolutionary graph theory. This derivation is achieved without considering between-community events to be of a different nature through the introduction of migration (Hauert & Imhof 2012, Yagoobi et al. 2023), group splitting and replacement (Traulsen & Nowak 2006, Traulsen et al. 2008, Akdeniz & van Veelen 2020), or two or more levels of intensity of selection (Wang et al. 2011, Hauert & Imhof 2012). The same results could be obtained from alternative movement models under the limit of isolated communities of the same size, as discussed in the appendix.

In this context, we show that whether a strategy evolves or not depends on the

advantage it holds against other strategies in two contexts: when in homogeneous groups and when in within-community fixation processes. Multiplayer social dilemmas involve the existence of a conflict between cooperating as a socially optimal strategy and defecting as an individually optimal strategy (Peña et al. 2016, Broom et al. 2019). Therefore, we obtain a general condition for the evolution of cooperation which translates into a simple balance between its advantages in homogeneous communities and its disadvantages over within-community fixation processes.

Applying this balance to the multiplayer social dilemmas explored in Broom et al. (2019), we obtain simple rules for the evolution of multiplayer cooperation in community-structured populations. These depend on the reward-to-cost ratio, and the number and size of communities. Cooperation evolves under all social dilemmas for any given number of communities, as long as there are at least two, that they are large enough to produce rewards (when applicable), and that the rewards are high enough in public goods dilemmas or low enough in the HD dilemma (a commons dilemma focused on the fair consumption of pre-existing resources). In public goods dilemmas, cooperation evolves more easily when the costs of production are shared (the S and the TS dilemmas – see Santos et al. (2008) and Archetti & Scheuring (2012) for an account of this), when the reward production function is supralinear (the PDV), and when individuals benefit from their own production (all public goods dilemmas, except for the CPD). However, finding that cooperation can evolve under the CPD in any community-structured population was remarkable by itself, given that this dilemma does not have any of the above characteristics and extends some of the strictest properties of the pairwise donation game to larger group sizes. Other characteristics of public goods dilemmas could be assessed in the future by considering asymmetric reward contributions and productivities (quantified as each individual's reward-to-cost ratio) (Wang et al. 2023), or even different mobility distributions and costs (Bara et al. 2024).

Moreover, the general results derived are not restricted to public goods dilemmas. The multiplayer HD game revealed an entirely different landscape when compared to its pairwise equivalent, the S dilemma. The differences between the two types of multiplayer dilemmas highlight that the considerations taken when extending pairwise games to higher-order interactions may reveal fundamental differences between them. These differences materialise here in the distinction between dilemmas focused on production (public goods dilemmas) and fair consumption of a pre-existing

resource (commons dilemmas). Furthermore, the use of the general rule obtained for the evolution of cooperation can be extended to the study of systems where evolutionary games have been employed, such as in AI monitoring (Alalawi et al. 2024), disease evolution and spread (Morison et al. 2024), environmental governance (Couto et al. 2020), and healthcare investment (Alalawi et al. 2020).

Remarkably, the derived dynamics did not depend on how communities were connected, with the community effects overwriting other potentially overlapping structural effects. It was observed in Broom et al. (2015) that high home fidelity led to a simple fixed fitness Moran process independent of topology in the territorial raider model with $Q = 1$, which is simply a particular case of the more general nested Moran process we derived in this chapter. For general home fidelity values, it was shown in Schimit et al. (2019, 2022) that temperature and average group size can be good predictors of fixation probabilities in the HD dilemma and the CPD, for a wide selection of topologies. Interpreted in that light, our results show that when strict subpopulation temperature (defined in Pattni et al. (2017) as the sum of all replacement weights of an individual outside their community) is asymptotically zero (i.e., no interactions outside the community) and the size of the network of places is fixed, the success of the fixation process is determined by the size of communities and independent of other topological features. This is in contrast with the models under which network topology plays a key role, such as evolutionary games on static pairwise graphs (Santos & Pacheco 2005, Ohtsuki et al. 2006, Allen et al. 2017) and satisfaction-dependent movement models (Erovenko et al. 2019, Pires et al. 2023) explored in chapter 5.

Public goods dilemmas consistently lead to the evolution of cooperation down to lower values of the reward-to-cost ratio when a larger number of smaller communities is considered. This is in line with what is observed in alternative community and deme models (Hauert & Imhof 2012, Hauert et al. 2014, Pattni et al. 2017), and multilevel selection models (Traulsen & Nowak 2006, Traulsen et al. 2008, Akdeniz & van Veelen 2020). The only exception to this is presented by multilevel public goods games when punishment is introduced, in which case larger communities are beneficial for cooperation (Wang et al. 2011). It was shown in Allen et al. (2017) that networks of isolated clusters interacting via the pairwise donation game also favour cooperation more frequently under smaller clusters and larger networks. Furthermore, strong isolated pairs were shown to be a strong predictor of coopera-

tion in any evolutionary graphs (Allen et al. 2017). Therefore, fragmentation into smaller social communities or groups might be one of several key mechanisms at the origin of cooperative behaviour observed around us. This is further supported by experimental studies which show that, in smaller groups, altruistic interventions occur more often (Fischer et al. 2011), and free riding is less common (Steven J. Karau & Kipling D. Williams 1993). Perhaps this helps explain why interactions in smaller groups, particularly in groups of two individuals, are consistently observed to be more prevalent in a wide range of human social interactions (Peperkoorn et al. 2020).

The results presented in this chapter were obtained within the limit of high home fidelity, under which communities become asymptotically bounded interacting groups. A relaxation of this limit is expected to lead to several key differences. Firstly, we would expect an increase in the rate at which between-community events happen, tied to the occurrence of group interactions between individuals of different communities, and therefore to the blurring of the interacting boundaries between them. In the pairwise donation game, considering less isolated clusters leads to stricter conditions for the evolution of cooperation (Allen et al. 2017). Even though a similar trend has been observed in the CPD in some small networks (Broom et al. 2015, Pattni et al. 2017), this should not be extrapolated to larger networks and all topologies as interacting groups have variable size and the dilemma no longer has an equivalent pairwise representation. In that case, the group structure underlying the multiplayer interactions depends not only on the size and number of communities but also on how the home nodes of each community are connected. Accounting for interacting groups in a different way may therefore lead to fundamentally different results, even when the underlying social structure remains very similar or the same (Gómez-Gardeñes, Romance, Criado, Vilone & Sánchez 2011, Gómez-Gardeñes, Vilone & Sánchez 2011). Parallel approaches to higher-order interactions show surprisingly high cooperative states under a class of multiplayer extensions of the Prisoner's Dilemma (Civilini et al. 2024). Similar effects may emerge under communities with blurred boundaries, namely when considering dilemmas with non-rivalrous public goods and/or shared costs, such as the Snowdrift dilemma, given their propensity to evolve cooperation under high group size variance (Archetti & Scheuring 2012, Santos et al. 2008, Gómez-Gardeñes, Vilone & Sánchez 2011). A preliminary study of these effects will be done towards the end of chapter 4.

Chapter 4

Multiplayer social dilemmas in completely mixed populations and networks of mixing communities[1]

4.1 Introduction

Models of evolutionary pairwise games often assume well-mixed populations, in the sense that interactions between individuals are equally likely, due to the tractability this confers to them. Two examples of this are the replicator equation introduced in chapter 1, and the frequency-dependent Moran process introduced in chapter 1 and later studied in chapter 2. The results obtained in those contexts can be used as a term of comparison for the analysis of evolutionary outcomes on structured populations. Well-mixed populations are a well defined concept in evolutionary games when only pairwise games are considered. However, under multiplayer interactions, there is a wide range of populations where individuals may be indistinguishable. It is thus useful to have a clear understanding of the appropriate population against which we can compare the results obtained in structured populations with multiplayer interactions, namely those of chapter 3.

A generalisation of a well-mixed population for multiplayer interactions is one where in a group of a given size, all possible group compositions have the same

---

[1]This chapter is based on a working paper done in collaboration with Professor Mark Broom.

probability of occurring (Broom & Rychtář 2012). This assures that individuals are indistinguishable apart from their strategy. Under independent movement models such as the one studied in chapter 3, one way to guarantee this is by considering that all players have the same probability distribution over the places of the network (Broom & Rychtář 2012). This additionally means that all individuals have the same replacement weights apart perhaps from the self-replacement weights, as stated in Schimit et al. (2019). However, the broad definition can be fulfilled under an arbitrary group size distribution. Particularly, it can be fulfilled under several different modelling assumptions in the territorial raider model. One of them is a complete network where each node is home to exactly one individual and the home fidelity (h) is arbitrary. Another example would be a network with any set of links between the nodes, where the whole population is based in the same home node, again with arbitrary home fidelity. These models lead to well-mixed populations with different group size distributions. Alternative independent movement models can be easily conceptualised, and general group size distributions can also be introduced ad hoc (Broom et al. 2019), as long as group compositions are random.

A stricter concept of a completely mixed population is introduced in Broom & Rychtář (2012). A population following an independent movement model is said to be completely mixed, if not only individuals but also all places in the network are indistinguishable. This means that all individuals have the same uniform probability distribution over the places of the network. This will lead to a unique population with a particular group size distribution.

In this chapter, we will explore the concept of completely mixed population and show that it can be obtained in the territorial raider model by considering complete networks with $h = 1$. In section 4.2, we will start by deriving this and some of the characteristics of the population, such as group size distribution. In section 4.3, we will obtain expressions for the fixation probability of a single mutant in general well-mixed populations with multiplayer interactions under the six different evolutionary dynamics explored so far. We will further consider the expansion of the fixation probabilities in the limit of weak selection. In section 4.4, we will apply the results obtained to five multiplayer social dilemmas previously analysed in chapter 3, and obtain conditions for the evolution of cooperation in completely mixed populations. These results will then be used as a benchmark to which the rules obtained in chapter 3 will be compared. In section 4.5, we extend our analysis

of the five multiplayer social dilemmas for broader home fidelity values and network topologies in the territorial raider model. Finally, in section 4.6, we summarise these results and discuss them in light of the remaining literature on multiplayer social dilemmas.

4.2 Completely mixed populations

Consider a population with N individuals distributed over a complete network with M places following the territorial raider model introduced in chapter 3. In the next sections we will focus on the emerging dynamics when home fidelity is $h = 1$ under the territorial raider model in complete networks. In this context, all individuals have the same probability $p_{nm} = p = 1/M$ of being in any place in the network. Each individual spends as much time in their home node as in any of the remaining nodes of the networks. As such, this leads to a completely mixed population. In this context, the fitness and replacement weights will be the same regardless of whether we have individuals split equally between communities with the same size, or one community with N individuals and the remaining ones empty. We will thus treat Q not as the community size, but instead more generally as the *density* of individuals over the connected places of the complete network $Q = N/M$.
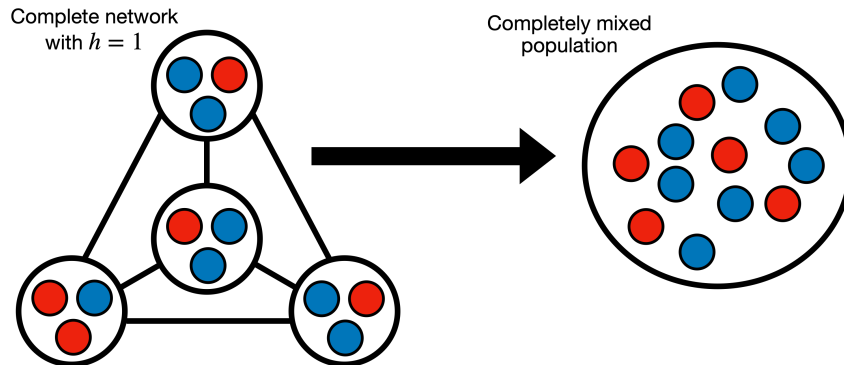
Figure 4.1: Equivalence between territorial raider model on complete network with $h = 1$ and completely mixed population. On the left, the territorial raider model in a complete networks with 4 places and communities of size 3. Under $h = 1$, this model is equivalent to a completely mixed population, i.e. a well-mixed population where individuals assemble in random groups of size following a binomial distribution with parameters $N = M \times Q = 12$ and $p = 1/M = 1/4$.

4.2.1 Group size distribution, replacement weights and temperature

In this context, the size of the groups formed in any of the nodes of the network follows a binomial distribution with parameters N and $1/M$, i.e. $B(N, 1/M)$. This way, if at a given moment, a node of the network is chosen at random, the observed group has a mean size of $N/M = Q$. However, from the point of view of each individual, the number of other individuals in their current group will follow a binomial distribution with parameters $N-1$ and $1/M$, i.e. $B(N-1, 1/M)$. This way, the experienced group size of individuals will have a mean of $1 + (N-1)/M = Q + 1 - 1/M$.

We call w_1 the replacement weights between the different individuals in a well-mixed population, and w_0 the self-replacement weights. In particular, in a completely mixed population, the self-replacement weights correspond to the probability of being alone:

$$w_0 = \left(1 - \frac{1}{M}\right)^{N-1}, \tag{4.1}$$

which in the limit of large populations and networks with asymptotic density $Q = \lim_{N \to \infty} \lim_{M \to \infty} (N/M)$ becomes:

$$w_0 \to \exp(-Q). \tag{4.2}$$

Therefore replacement weights between different individuals simply correspond to the probability of not being alone divided by the remaining individuals:

$$w_1 = \frac{1 - w_0}{N - 1} = \frac{1}{N - 1} \left(1 - \left(1 - \frac{1}{M}\right)^{N-1}\right) \tag{4.3}$$

Temperature is defined in Lieberman et al. (2005) as the sum of all replacement weights of a vertex. Under the current model, as pointed out in Broom et al. (2015), this can be interpreted as excluding self-replacement weights, therefore depending on the graph structure and the parameter h. In completely mixed populations, this is equal to the following:

$$T = 1 - w_0 = 1 - \left(1 - \frac{1}{M}\right)^{N-1} \tag{4.4}$$

4.2.2 Fitness under completely mixed populations

As reported in the previous sections, when $h = 1$ in complete networks, each individual has an equal probability $p = 1/M$ of being in any place P_m of the network. We denote $F^C_{N_c,N_d}$ and $F^D_{N_c,N_d}$ as the fitness of cooperators and defectors in populations with N_c cooperators and N_d defectors. These can be defined the following way:

$$F^C_{N_c,N_d} = 1 - w + w \cdot \pi^C_{N_c,N_d}, \tag{4.5}$$

$$F^D_{N_c,N_d} = 1 - w + w \cdot \pi^D_{N_c,N_d}. \tag{4.6}$$

depending on the average payoffs received by cooperators $\pi^C_{N_c,N_d}$ and defectors $\pi^D_{N_c,N_d}$ in such populations, which can be obtained by calculating the probability of any other cooperator and defector being in the same place as the focal individual. The number of other cooperators c and defectors d in the focal individual's group follow two binomial distributions. This way, the fitness can simply be calculated in the following way:

$$\pi^C_{N_c,N-N_c} = \sum_{c=0}^{N_c-1} \binom{N_c-1}{c} p^c (1-p)^{N_c-1-c} \sum_{d=0}^{N-N_c} \binom{N-N_c}{d} p^d (1-p)^{N-N_c-d} R^C_{c+1,d},$$
$$\tag{4.7}$$
$$\pi^D_{N-N_d,N_d} = \sum_{c=0}^{N-N_d} \binom{N-N_d}{c} p^c (1-p)^{N-N_d-c} \sum_{d=0}^{N_d-1} \binom{N_d-1}{d} p^d (1-p)^{N_d-1-d} R^D_{c,d+1}.$$
$$\tag{4.8}$$

4.3 Fixation probabilities under well- and completely mixed populations

4.3.1 Fixation probabilities

Individuals of the same type in a well mixed population are indistinguishable and therefore hold the same replacement weights and fitness values in the population. Therefore, the state of the population can be described by the number of individuals using each strategy, all states with the same number of individuals using each type will lead to the same transition probabilities. We can thus describe the fixation process of a single mutant on a population of residents based on a biased random walk. This allows us to use the closed form equation given in Karlin & Taylor (1975)

for the fixation probability of one mutant cooperator in a population of defectors
and the reverse as respectively the following:

$$\rho^C = \frac{1}{1 + \sum_{j=1}^{N-1} \prod_{N_c=1}^{j} \frac{F_{N_c,N-N_c}^D}{F_{N_c,N-N_c}^C}}, \tag{4.9}$$

$$\rho^D = \frac{1}{1 + \sum_{j=1}^{N-1} \prod_{N_d=1}^{j} \frac{F_{N-N_d,N_d}^C}{F_{N-N_d,N_d}^D}}. \tag{4.10}$$

We note that these probabilities are identical under the BDB, DBD, LB and LD
dynamics because the transition probability ratios that characterise the process are
identical at any given state of the population.

The DBB and BDD dynamics lead to different quantitative results as transition
probability ratios in the resulting Markov chain are different from the previous four
dynamics. Fixation probabilities are obtained in a parallel way to the ones presented
in 4.9 and 4.10, using the following corrected expressions:

$$\rho_{DBB/BDD}^C =$$

$$= \frac{1}{1 + \sum_{j=1}^{N-1} \prod_{N_c=1}^{j} \frac{F_{N_c,N-N_c}^D}{F_{N_c,N-N_c}^C} \cdot \left(1 + \frac{(w_0-w_1)\left(F_{N_c,N-N_c}^D - F_{N_c,N-N_c}^C\right)}{w_1 T_{DBB/BDD}(N_c,N-N_c)+(w_0-w_1)F_{N_c,N-N_c}^C}\right)},$$

$$\tag{4.11}$$

$$\rho_{DBB/BDD}^D =$$

$$= \frac{1}{1 + \sum_{j=1}^{N-1} \prod_{N_d=1}^{j} \frac{F_{N-N_d,N_d}^C}{F_{N-N_d,N_d}^D} \cdot \left(1 + \frac{(w_0-w_1)\left(F_{N-N_d,N_d}^C - F_{N-N_d,N_d}^D\right)}{w_1 T_{DBB/BDD}(N-N_d,N_d)+(w_0-w_1)F_{N-N_d,N_d}^D}\right)},$$

$$\tag{4.12}$$

with $T_{DBB/BDD}$ denoting the total weight-fitness correction factors under those two
dynamics, which are positive as evident in their definition:

$$T_{DBB}(N_c, N_d) = N_c \cdot F_{N_c,N_d}^C + N_d \cdot F_{N_c,N_d}^D, \tag{4.13}$$

$$T_{BDD}(N_c, N_d) = N_d \cdot F_{N_c,N_d}^C + N_c \cdot F_{N_c,N_d}^D. \tag{4.14}$$

The DBB and BDD dynamics introduce a correction term into the fixation probability as it can be seen by comparing equations 4.11 and 4.12 with equations 4.9 and 4.10. As the denominator in the correction coefficient is always positive, the correction coefficient amplifies differences between transition probability ratios if $w_0 > w_1$, or suppresses them if $w_1 > w_0$.

In the particular case of a completely mixed population, the condition $w_0 > w_1$ is met if:

$$\left(1 - \frac{1}{M}\right)^{N-1} > \frac{1}{N}, \tag{4.15}$$

which under large populations and networks simply corresponds to:

$$N > \exp(Q). \tag{4.16}$$

This means that for any given density $Q = \lim_{N \to \infty} \lim_{M \to \infty}(N/M)$, there is always a population size above which $w_0 > w_1$. Lower densities lead more easily to $w_0 > w_1$, and higher densities, typically require exponentially larger populations to do so. In those cases, individuals spend more time with themselves than with any other particular individual thus leading to the amplification of differences between transition probabilities in completely mixed populations.

In another example, namely well-mixed populations where individuals have pairwise interactions, the DBB and BDD dynamics lead to the same fixation probabilities as the other dynamics if self-replacements are considered to occur at the same rate as other replacements under neutral selection, i.e. $w_0 = w_1$. If self-replacements are not possible, i.e. $w_0 = 0$, then the DBB and BDD dynamics suppress the differences between transition probabilities.

Finally, the limit of large home fidelity was considered in the territorial raider model for communities of the same size in chapter 3. In that limit, even though the overall population is deeply structured, its communities are asymptotically isolated, and become well-mixed, interacting repeatedly within the same group of size Q. In that case, individuals are never alone, thus leading to $w_0 = 0$ and $w_1 = 1/(Q - 1)$. That is the reason why it is reported that selection is suppressed in within-community events under the DBB and BDD dynamics under $h \to \infty$, a key point in explaining why cooperation evolves under all dilemmas in those dynamics, but not in the remaining dynamics.

4.3.2 Fixation probabilities under weak selection

We consider the expansion of the equations obtained from fixation probabilities under weak selection. In order to do so, we consider that $w \cdot N \to 0$ and therefore we can represent fixation probabilities in the following form:

$$\rho^C \approx \frac{1}{N} + \left.\frac{\partial \rho^C}{\partial w}\right|_{w \to 0} \cdot w, \tag{4.17}$$

$$\rho^D \approx \frac{1}{N} + \left.\frac{\partial \rho^D}{\partial w}\right|_{w \to 0} \cdot w, \tag{4.18}$$

where the zeroth order term is the fixation probability under neutral selection, which can also be denoted as $\rho^{neutral} = 1/N$.

The first-order expansion terms are obtained by deriving the fitness in relation to w and simplifying those expressions to get the following:

$$\left.\frac{\partial \rho^C}{\partial w}\right|_{w \to 0} = \frac{1}{N^2} \sum_{N_c=1}^{N-1} (N - N_c) \left[\pi^C_{N_c, N-N_c} - \pi^D_{N_c, N-N_c} \right], \tag{4.19}$$

$$\begin{aligned}
\left.\frac{\partial \rho^D}{\partial w}\right|_{w \to 0} &= \frac{1}{N^2} \sum_{N_d=1}^{N-1} (N - N_d) \left[\pi^D_{N-N_d, N_d} - \pi^C_{N-N_d, N_d} \right] = \\
&= \frac{1}{N^2} \sum_{N_c=1}^{N-1} N_c \left[\pi^D_{N_c, N-N_c} - \pi^C_{N_c, N-N_c} \right].
\end{aligned} \tag{4.20}$$

Performing the same expansion for the DBB and BDD dynamics, we observe that the first-order term would simply have a correction coefficient added to it:

$$\left.\frac{\partial \rho^*_{DBB/BDD}}{\partial w}\right|_{w \to 0} = \left(1 + \frac{w_0 - w_1}{w_1 N + (w_0 - w_1)} \right) \cdot \left.\frac{\partial \rho^*}{\partial w}\right|_{w \to 0}, \tag{4.21}$$

which under large completely mixed populations simply becomes $1 + \exp(-Q)$.

The correction coefficient only impacts the evolutionary dynamics by amplifying/suppressing fixation. It does not affect the sign of the first-order term of the expansion, and thus the DBB and BDD dynamics have no impact on the conditions for cooperation to evolve explored in the following section.

4.4 Cooperation and social dilemmas in completely mixed populations

4.4.1 General social dilemmas in completely mixed populations

We consider a selection of the social dilemmas studied in Broom et al. (2019). These multiplayer games represent different dilemmas regarding the production of public goods with different characteristics or even the consumption of pre-existing commons. We apply the equations 4.7 and 4.8 obtained for completely mixed populations to five different social dilemmas, and obtain the results presented in table 4.1. The derivation of these equations is done in appendix C.1.

Game	$\pi^C_{N_c, N-N_c}$	$\pi^D_{N_c, N-N_c}$
CPD	$\frac{N_c - 1}{N - 1}\left[1 - \left(1 - \frac{1}{M}\right)^{N-1}\right]V - K$	$\frac{N_c}{N - 1}\left[1 - \left(1 - \frac{1}{M}\right)^{N-1}\right]V$
PD	$\frac{M}{N}\left[1 - \left(1 - \frac{1}{M}\right)^N\right]V + \frac{N_c - 1}{N - 1}\left[1 - \frac{M}{N}\left(1 - \left(1 - \frac{1}{M}\right)^N\right)\right]V - K$	$\frac{N_c}{N - 1}\left[1 - \frac{M}{N}\left(1 - \left(1 - \frac{1}{M}\right)^N\right)\right]V$
VD	$V - K$	$\left[1 - \left(1 - \frac{1}{M}\right)^{N_c}\right]V$
S	$V - \frac{M}{N_c}\left[1 - \left(1 - \frac{1}{M}\right)^{N_c}\right]K$	$\left[1 - \left(1 - \frac{1}{M}\right)^{N_c}\right]V$
HD	$\frac{M}{N_c}\left(1 - \frac{1}{M}\right)^{N - N_c} \cdot \left[1 - \left(1 - \frac{1}{M}\right)^{N_c}\right]V$	$\frac{M}{N - N_c}\left[1 - \left(1 - \frac{1}{M}\right)^{N - N_c}\right](V + K) - K$

Table 4.1: Exact average payoff obtained under multiplayer social dilemmas in completely mixed populations.

The fitness of both cooperators and defectors under the CPD and the PD depends linearly on the frequency of the types in the population. This means that both multiplayer games in completely mixed populations have equivalent pairwise games in well-mixed populations. In the CPD, the fitness of defectors is larger than that of cooperators for any positive values of V and K. In the PD, defectors have larger fitness if V/K is larger than a critical value. Even though both games are motivated as extensions of the pairwise Prisoner's Dilemma to multiplayer interactions, they hold significantly different results. This comes directly from the fact that cooperators benefit from their own contributions in the PD, contrary to what happens in the CPD.

The VD, S and HD hold different results, as the type with larger fitness depends not only on the payoff parameters V and K, but also on the state of the population, i.e. the number of cooperators N_c. Therefore, they may allow for mutual invasion of

the two types or no invasion from either type. We compare the invasion scenarios as they are defined in Taylor et al. (2004), considering $V > 0$ and $K > 0$, and obtain the following results, simplified for large N:

- CPD - Defectors are always dominant;

- PD - Defectors are dominant when $V/K < \dfrac{1}{1 - \exp(-Q)}$, and Cooperators are dominant when $V/K > \dfrac{1}{1 - \exp(-Q)}$

- VD - Defectors are dominant when $V/K < 1$, mutual invasion occurs when $1 < V/K < \exp(Q)$, and Cooperators are dominant when $V/K > \exp(Q)$;

- S - Defectors are dominant when $V/K < 1$, mutual invasion occurs when $1 < V/K < \dfrac{\exp(Q) - 1}{Q}$, and Cooperators are dominant when $V/K > \dfrac{\exp(Q) - 1}{Q}$;

- HD - Mutual invasion occurs when $V/K < \dfrac{Q - 1 + \exp(-Q)}{1 - (Q + 1)\exp(-Q)}$, and Defectors are dominant when $V/K > \dfrac{Q - 1 + \exp(-Q)}{1 - (Q + 1)\exp(-Q)}$;

In Public Goods Games apart from the CPD, low enough rewards lead to the dominance of defectors, whereas high enough rewards lead to the dominance of cooperators. Under the VD and the S there is an additional regime of mutual invasion for intermediate reward values, thus potentially leading to mutual fixation and the instability of both strategies. Under the HD, cooperators are never dominant, with mutual invasion occurring for low rewards, and defectors becoming dominant for large enough rewards.

The CPD and PD are games of dominance, where therefore the evolutionary dynamics considered don't change the evolutionary outcomes and the dominant strategy is always the one which fixates with probability higher than the neutral one. However, under the VD, the S and the HD, we observe values of parameters for which mutual invasion occurs. In those cases, it is not trivial which of the strategies fixates on the other, as it is stated in Taylor et al. (2004) for pairwise games in well-mixed populations. In these cases, choosing the DBB or BDD dynamics might also move the boundaries under which each strategy fixates successfully. To further study these boundaries, we take into consideration the weak selection limit.

4.4.2 Rules of cooperation under large completely mixed populations

We apply the average payoff functions obtained in section 4.4.1 for five social dilemmas onto the fixation probability equations presented in section 4.3.2. We further consider the limit of large populations ($N \to \infty$) in large networks ($M \to \infty$), denoting the asymptotic density of individuals as $Q = \lim_{N\to\infty} \lim_{M\to\infty}(N/M)$ and the weak selection limit valid $w \cdot N \to 0$. This simplifies the first-order terms in the expansion of fixation probabilities. Namely under the VD, S and HD, under which mutual invasion occurs, it allows us to obtain the conditions for ρ^C and ρ^D to be larger than the neutral value fixation probability $\rho^{neutral}$. These conditions are summarised in table 4.2, as well as the evolutionary scenarios they may lead to. The derivation of these conditions is done in appendix C.2. We recall the classification of the evolutionary outcomes introduced in chapter 1:

- Selection favours cooperation if $\rho^C > \rho^{neutral} > \rho^D$;

- Selection favours defection if $\rho^D > \rho^{neutral} > \rho^C$;

- Selection favours instability if $\rho^C > \rho^{neutral}$ and $\rho^D > \rho^{neutral}$;

- Selection favours bi-stability if $\rho^C < \rho^{neutral}$ and $\rho^D < \rho^{neutral}$.

Game	$\rho^C > \rho^{neutral}$	$\rho^D > \rho^{neutral}$	Selection favours
CPD	Never	Always	Defection
PD	$V/K > \dfrac{Q}{1-\exp(-Q)}$	$V/K < \dfrac{Q}{1-\exp(-Q)}$	Defection, Cooperation
VD	$V/K > \dfrac{Q/2}{1-\dfrac{1-\exp(-Q)}{Q}}$	$V/K < \dfrac{Q^2/2}{1-\exp(-Q)(Q+1)}$	Defection, Instability, Cooperation
S	$V/K > \dfrac{L_1(Q)-1+\dfrac{1-\exp(-Q)}{Q}}{1-\dfrac{1-\exp(-Q)}{Q}}$	$V/K < \dfrac{Q-1+\exp(-Q)}{1-\exp(-Q)(Q+1)}$	Defection, Instability, Cooperation
HD	$V/K < \dfrac{\dfrac{Q}{2}-1+\dfrac{1-\exp(-Q)}{Q}}{1-\exp(-Q)\cdot(L_2(Q)+1)}$	$V/K > \dfrac{\dfrac{Q}{2}+1-L_1(Q)-\dfrac{1-\exp(-Q)}{Q}}{L_1(Q)-(1-\exp(-Q))}$	Cooperation, Instability, Defection

Table 4.2: Conditions for the evolution of multiplayer cooperation under large completely mixed populations with asymptotic density Q.

In some of these conditions, the functions $L_1(Q)$ and $L_2(Q)$ were used, which are defined based on the limit of the difference between the harmonic series, i.e.

$H_{N-1} = \sum_{i=1}^{N-1} 1/i$, and two other geometric-harmonic series:

$$L_1(Q) = \lim_{M \to \infty} \left[H_{M \times Q - 1} - \sum_{i=1}^{M \times Q - 1} \frac{\left(1 - \frac{1}{M}\right)^i}{i} \right], \qquad (4.22)$$

$$L_2(Q) = \lim_{M \to \infty} \left[\sum_{i=1}^{M \times Q - 1} \frac{\left(1 - \frac{1}{M}\right)^{-i}}{i} - H_{M \times Q - 1} \right]. \qquad (4.23)$$

These two functions are both zero for asymptotically low density Q, i.e. $L_1(0) = L_2(0) = 0$, and both increase with Q, thus being positive functions. $L_1(Q)$ increases
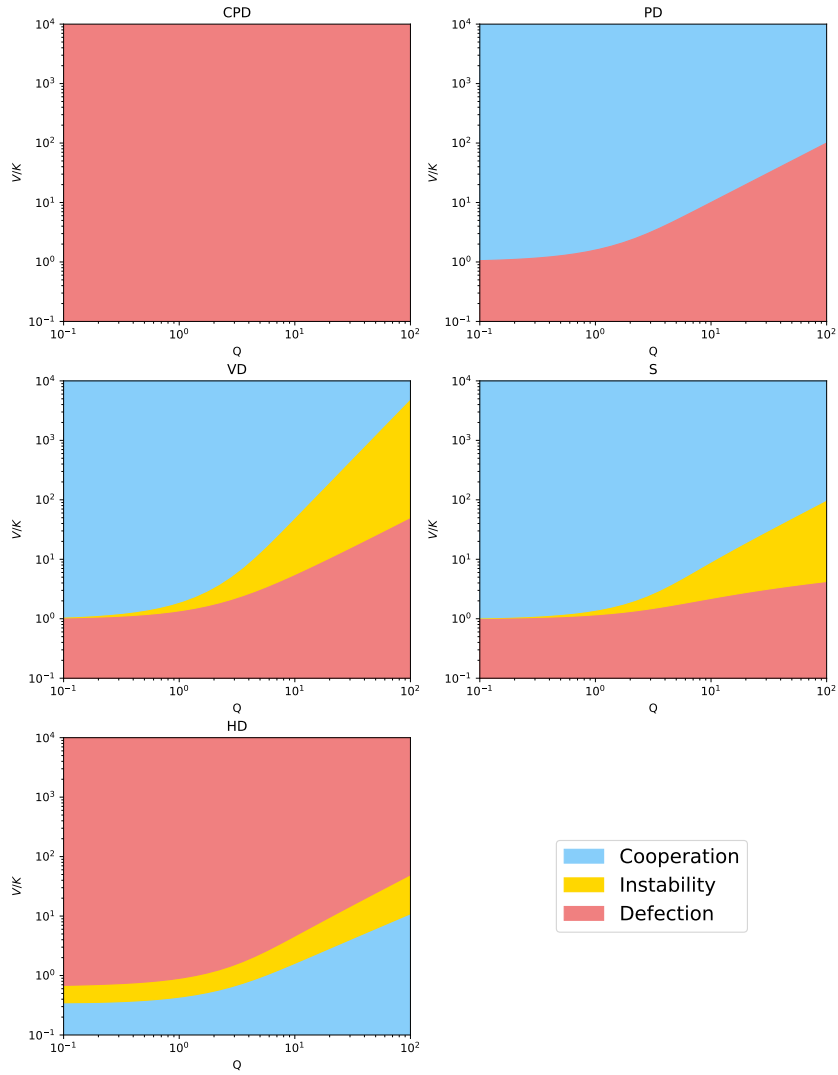
Figure 4.2: Evolutionary outcomes obtained for different values of the reward-to-cost ratio V/K in large completely mixed populations with asymptotic density Q. The figure was built based on the critical values from the conditions in table 4.2.

sublinearly with Q, and takes, for example, values $L_1(1) \approx 0.80$, $L_1(2) \approx 1.32$, $L_1(3) \approx 1.69$, and $L_1(20) \approx 3.57$. $L_2(Q)$ increases supralinearly with Q, and takes, for example, $L_2(1) \approx 1.32$, $L_2(2) \approx 3.68$, $L_2(3) \approx 8.26$, and $L_2(20) \approx 2.56 \times 10^7$. However, the result of $\exp(-Q) \cdot (L_2(Q) + 1)$ is 1 for $Q = 0$ and decreases monotonically to zero as Q increases. The geometric-harmonic series used here also come up in Haq et al. (2024) when the HD game is explored in complete territorial networks with arbitrary h for the particular case where each node hosts one individual ($Q = 1$).

The rules for the evolution of cooperation in table 4.2 can be intricate, so we use them to represent the areas under which selection favours cooperation, instability, or defection in figure 4.2, for different values of the density Q and the reward-to-cost ratio. We do not represent cases of bi-stability as these were not found. Under large populations and networks, the conditions depend only on the asymptotic value of the ratio $Q = N/M$, which we named the density of the population, corresponding to the community size under large home fidelity used in chapter 3, or the subpopulation size used in other approaches (Pattni et al. 2017).

Cooperation can never evolve under the CPD in completely mixed populations. However, in the remaining PGGs, i.e. the PD, the VD, and the S, it always has a chance of evolving if the value of the reward-to-cost ratio is larger than a critical value determined by the density of the population. In the HD, it does so if the reward-to-cost ratio is lower than a critical value. The critical values of V/K increases in the four PGGs and in the HD game. This assures that higher density of individuals hinders the chances of cooperation evolving under PGGs, but affects them positively under the HD.

In figure 4.2, the critical value of V/K under the Prisoner's Dilemma starts at 1 for asymptotically low density $Q \to 0$ and increases approaching from above the value of Q for larger densities. In this game, $V/K > Q$ means that in groups of up to size Q, the share of the reward reaped by a cooperator is larger than the cost paid by them. Since cooperators benefit from their contributions to the public good, cooperation thus evolves only when a large share of the interactions in which individuals partake do not represent a dilemma.

In the Volunteer's Dilemma, the critical values start at 1 as well, but a gap opens between successful fixation of cooperators and the failed fixation of defectors. Even though cooperators fixate successfully for rewards of approximately $Q/2$ for larger

densities, defectors only fail to fixate for rewards of approximately above $Q^2/2$. The region of instability increases its size quadratically. Defection becomes unstable more easily, but cooperation very rarely becomes stable. This is so because under high density of individuals, 1) a small number of cooperators are advantageous in populations of defectors because they always get a full reward contrary to defectors; and 2) a small number of defectors are advantageous in populations of cooperators because they often get the rewards from cooperators without paying a cost.

In the Snowdrift game, the critical values start at 1 once more, and there is a gap opened which is narrower than under the VD. For large densities, cooperators fixate successfully for rewards growing sublinearly on Q and defectors become unstable for rewards close to Q. This results are better than those obtained under all previous dilemmas. This is due cooperators always benefiting from the full reward, which increases their chances of fixating on defectors, as seen in the VD. However, here they pay a lower cost if other cooperators are present in the group as well, therefore making their own populations much more resistant to invading defectors, when compared to the VD.

Finally, in the Hawk-Dove game, defectors try to monopolise the rewards by resorting to costly aggression. Therefore, if the reward-to-cost ratio is high enough, defectors hold an advantage because their aggressive behaviour pays off. The critical values of the rewards increase with Q, because in larger groups, it is more likely that several defectors will be present in the same group, thus leading to higher costs of fighting and lower chances of monopolising the reward, improving the chances of cooperators evolving.

4.4.3 Comparison between community-structured and completely mixed populations

The results obtained in this context can be used as a benchmark to which we can compare the results from structured populations. The completely mixed population emerges naturally from considering the territorial raider model in complete networks with $h = 1$. Another interesting limit of this model is the one obtained for any network when $h \to \infty$, which has been explored extensively in chapter 3. In that work, the emerging dynamics are shown to be a nested Moran process, where individuals first fixate at within-community level, after which communities may fixate in the whole population. Furthermore, conditions for the evolution of cooperation were

obtained there for 10 different social dilemmas, including the 5 multiplayer dilemmas studied here. This makes it natural for us to explore the results obtained under community structure in comparison to those under completely mixed populations. We restrict our comparison to integer values of density $Q \leq 2$, where the community structure results are valid.

First of all, cooperation evolves under the CPD in community-structured populations when the DBB and BDD dynamics are considered, whereas it never does in completely mixed populations. This highlights that community structure can indeed be a powerful promoter of cooperation, allowing for cooperation to evolve in dilemmas which are particularly challenging and have no chance of evolving cooperation in mixed populations. In the remaining games, cooperation may evolve in completely mixed populations. However, there are gaps between the parameter regions for which cooperation evolves under completely mixed and community-structured populations.

Under the PD, only one strategy fixates successfully at a time. The critical reward-to-cost ratio V/K above which cooperators fixate successfully under completely mixed populations is larger than Q but approaches that value for larger densities. This can be compared to Q and $Q/2$ obtained under community-structured populations for different dynamics. Community structure always leads to a wider parameter region where cooperation fixates successfully. When communities become larger, the critical values obtained in the BDB, DBD, LB, and LD dynamics under the two organisations of populations converge to the same value Q. In those dynamics, cooperation can only evolve if cooperators have a direct individual benefit in cooperating. However, comparing the two structures under the DBB and BDD dynamics, the gap between the two critical values is considerable and maintained for large Q (values become Q and $Q/2$). This is explained by the fact these dynamics are sensitive to the viscosity of evolutionary processes on structured populations, as originally seen in Ohtsuki et al. (2006) and further analysed in chapter 3 for this multiplayer game framework.

In the remaining games VD, S, and HD, it's possible to observe both cooperators and defectors fixating successfully on populations of the opposing type–see instability regions on figure 4.2. In comparison, under weak selection and large networks of community-structured populations, there is always one single strategy fixating successfully on the other.

Under the VD, community-structured populations allow for the evolution of co-operation if $V/K > Q$ for the BDB and equivalent dynamics. This value is therefore in the instability region of completely mixed populations, between $Q/2$ and $Q^2/2$ under large densities. Under these dynamics, community structure widely stabilises cooperation when $Q < V/K < Q^2/2$, but it might instead stabilise defection when $Q/2 < V/K < Q$. However, under the DBB and BDD dynamics, community structure guarantees the evolution and stability of cooperation if $V/K > Q/2$, which covers the whole region of evolution of cooperation and instability, and part of the region of defection under completely mixed populations (see for example $Q = 2$ and $V/K = 1.5$).

Under the Snowdrift game in community-structured populations with the BDB and equivalent dynamics, the critical value of the reward-to-cost ratio is the sum of the harmonic series with Q terms. Similar to the VD, this value falls on the instability region of completely mixed populations, meaning that community structure sometimes stabilises cooperation but other times defection in comparison to completely mixed populations. However, under the DBB and BDD dynamics, the critical value obtained under community-structured populations always falls on the region of evolution of defection of completely mixed populations, thus having a parallel effect to that noted under the VD.

Overall, these results follow the general trend under public goods dilemmas that the DBB and BDD dynamics are much more sensitive to the viscosity of evolutionary processes on structured populations than the remaining dynamics studied. Community structure under the latest set of dynamics always reduced the areas under which defectors fixated successfully, but sometimes at the expense of decreasing the areas under which cooperators fixated successfully. However, community structure under DBB and BDD dynamics always extended the areas under which cooperators fixated successfully together with reducing those under which defectors did.

Under the Hawk-Dove game, the relation between critical values is not entirely consistent. Under the BDB and equivalent dynamics, community structure starts by reducing the size of the region of V/K where cooperation evolves when $Q = 2$, and moves on to fall on the instability region for $Q \geq 3$. Under the DBB and BDD dynamics, community structure starts by assuring that cooperators evolve regardless of V/K under $Q = 2$. For $Q = 3$, the critical reward-to-cost ratio falls on a finite value on the defection area of completely mixed populations, and finally for $Q \geq 4$

it falls on the instability area.

4.4.4 Fair comparisons

In Broom & Rychtář (2012), a comparison between the results under a well-mixed and a structured population model is defined as a fair comparison if the mean group size under both is the same. This proposed way of evaluating evolutionary outcomes in structured populations mainly aims at eliminating the potential overlapping effects of emerging differences in experienced group size which might be affecting fixation probabilities, thus isolating the effects of population structure.

As elaborated on section 4.2, the average group size experienced by each individual in the completely mixed population is $1 + (N - 1)/M$. In the limit of large populations in large networks, this simply becomes $Q + 1$. This says that in a large population, the experienced mean group size of individuals is one unit larger than the mean number of individuals per place. To perform a fair comparison of the results obtained under large home fidelity, where mean experienced group size would simply be equal to the density Q' due to no variance, we compare them instead with completely mixed populations with lower density $Q = Q' - 1$, which would have mean experienced group size Q'. The two populations of same size $N = N'$ will be embedded on networks of different sizes M and M', both large but holding the relation $M = M' \left(1 + \frac{1}{Q}\right)$.

This means that the gains obtained by cooperators in community structure described in the previous section would be slightly attenuated under the PD, VD and S, as lower $Q = Q' - 1$ instead of $Q = Q'$ would lead to broader regions of the evolution of cooperation. Due to this, under fair comparisons, the impact of the structure itself was quite low, with the change in experienced average group size doing most of the work. In some fair comparisons, community structure was even detrimental to the evolution of cooperation, namely when the BDB dynamics are considered. This is true for the PD for all values of Q, and for the VD and S under $Q = 2$. The CPD never evolves under the BDB dynamics in both structures, so no fair comparison between the rules is performed in that context. Under the DBB dynamics, community structure always represents an improvement for all PGGs, CPD included. In the HD game, lower Q decreases the chances of cooperation evolving in completely mixed populations, which therefore accentuates the positive results obtained in community structure when a fair comparison is considered.

4.5 Evolution of cooperation on networks of mixing communities

In this section, we evaluate the results of fixation processes for wider values of home fidelity and different network topologies. In figure 4.3, you can observe the fixation probabilities of cooperators (left) and defectors (right) for different social dilemmas (rows).

As noted in chapter 3, under large home fidelity all topologies converge to the same asymptotic fixation probability, even though the rate of convergence can be particularly slow under the CPD in complete networks. Overall, we observe that structure becomes relevant under lower values of h, therefore leading to the divergence of fixation curves in different topologies. Lower home fidelity hurts cooperation under the CPD, dropping its fixation probability to zero under all topologies, but not for the remaining dilemmas. In the VD and S games, even completely mixed populations ($h = 1$ in complete networks) allow cooperators to fixate successfully.

We observe that in the four PGGs, cooperators do better in star and circle networks than in complete ones for values $h > 1$. The star and circle networks have lower average degree, i.e. $2 \times (1 - 1/M)$ and 2 respectively, than the complete, i.e. $M - 1$, thus leading to a rescaling of the probabilities of staying within their community. Therefore, scenarios with higher subpopulation temperature (Pattni et al. 2017), i.e. probability of interacting with individuals outside their community, might be overall detrimental to the communal cooperation effects noted in chapter 3. This is also what happens when no subpopulations are considered ($Q = 1$), in that case because lower temperatures translate into individuals being mainly alone and cooperators doing better (still never evolving) because defectors cannot take advantage of them (Schimit et al. 2022).

Under all PGGs apart from the CPD in star networks with lower home fidelity, cooperators do worse, associated with the fact that under $h < 1$, groups tend to assemble in the centre and thus increase the average experienced group size. Low average group size has been shown as another good determinant of cooperation under PGGs (Schimit et al. 2019, 2022), similar to what we observe here accounting for communities. This effect is particularly present in spatial networks with high node degree variance where large groups assemble in the hubs of the network (Schimit et al. 2019, 2022) and there is a general loss of the beneficial effects of highly local
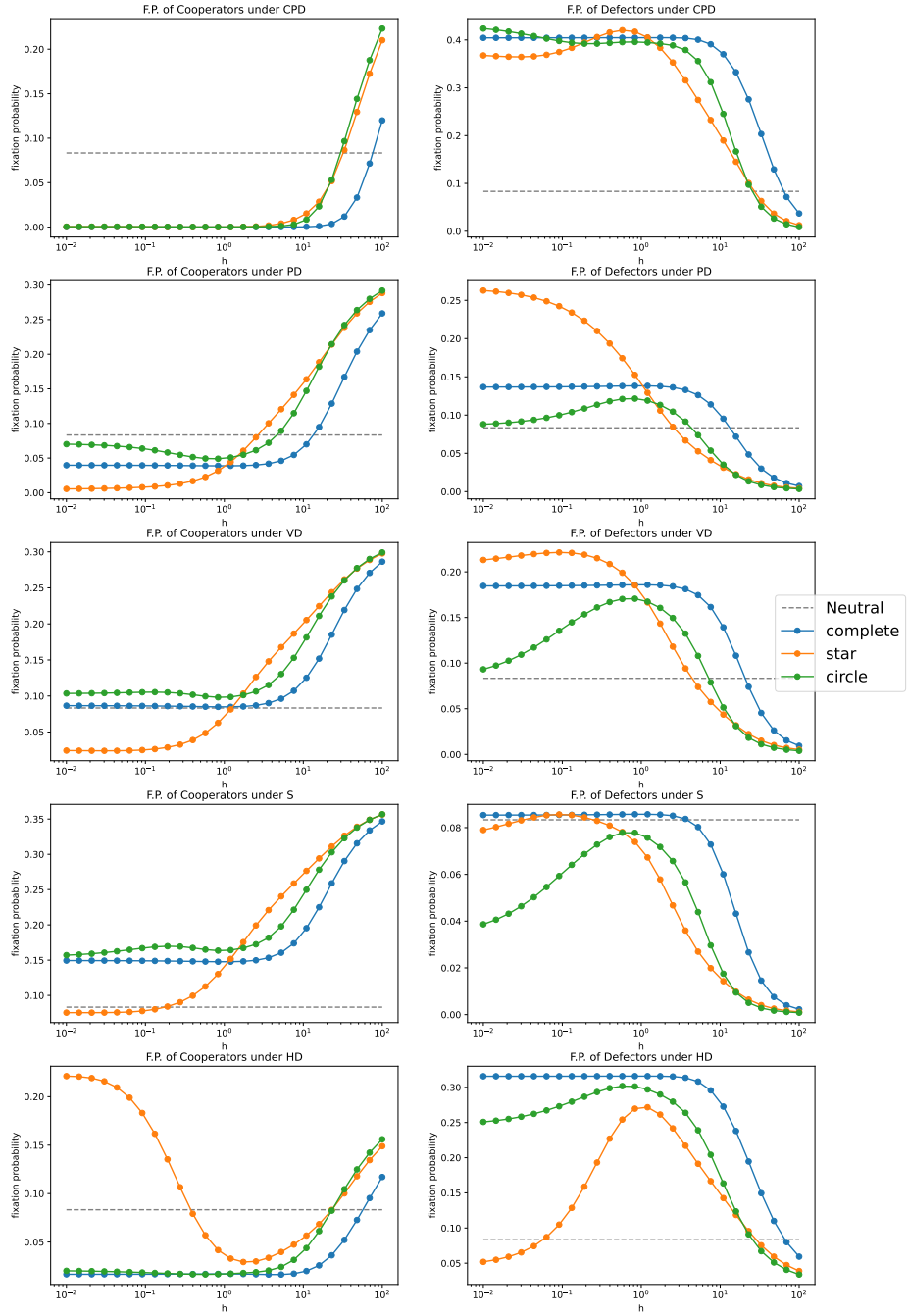
Figure 4.3: Fixation probabilities of cooperators (left) and defectors (right) under five different social dilemmas (rows) for different values of home fidelity h. Each coloured line represents a different topology of a network of size $M = 6$, and communities of size $Q = 2$. The process used was the DBB dynamics, and payoff parameters are $w = 0.4$, $V = 2$, and $K = 1$. Two cases of interest are the 1) completely mixed populations, i.e. complete network $h = 1$, and 2) community-structured population, i.e. all topologies under $h \to \infty$.

populations seen in chapter 3.

The results obtained under Hawk-Dove game show that low mixing of groups is beneficial to cooperators. This occurs both when $h \to \infty$ in all networks and $h \to 0$ in the star network. Moreover, in chapter 3, we reported that cooperators benefit from being in larger communities when there is no mixing, which might explain why they thrive the most under extreme low fidelity in star networks. In all networks when $h \approx 1$ there is high mixing of individuals and those benefits are lost.

Figure 4.4 shows the results obtained in different possible organisations of populations of size 12 under this framework. This includes communities of size 2 distributed over 6 nodes and communities of size 3 distributed over 4 nodes of complete, star and circle networks.

It is clear that under PGGs, cooperators fixate successfully for wider values of h in larger networks ($M = 6$) of smaller communities ($Q = 2$). This was already noted for the limit of large home fidelity explored in chapter 3. In the particular case of the CPD, cooperators never get to evolve when $M = 4$ and $Q = 3$ for this choice of parameters. Under large home fidelity, cooperation evolves if the reward-to-cost ratio respects the following condition: $V/K > (Q-1) \cdot (1 - \frac{2}{MQ})/(1 - \frac{2(Q-1)}{MQ})$. Under $Q = 2$ and $M = 6$ this is equivalent to $V/K > 1$. Under $Q = 3$ and $M = 4$, this is equivalent to $V/K > 2.5$. This explains why under $V = 2$ and $K = 1$ we observe cooperation succeeding in one of the community-organised populations, but not on the other. Here, we further observe that the beneficial effect of organising into smaller communities is generally maintained for lower home fidelity values.

Moreover, it can be observed in figure 4.4 that both cooperators and defectors fixate on each other for the same values of the parameters under wide intervals of h. This is generally not observed in the CPD and the PD, but is overall present in the VD, the S, and HD games. These results agree with the previous mathematical analysis of completely mixed populations under weak selection, where such cases were possible only in these three games.

4.6 Discussion

In our work we have started by elaborating on the concept of completely mixed populations and associating it to the territorial raider model in a complete network with home fidelity set as $h = 1$. We derive some of the characteristics of these
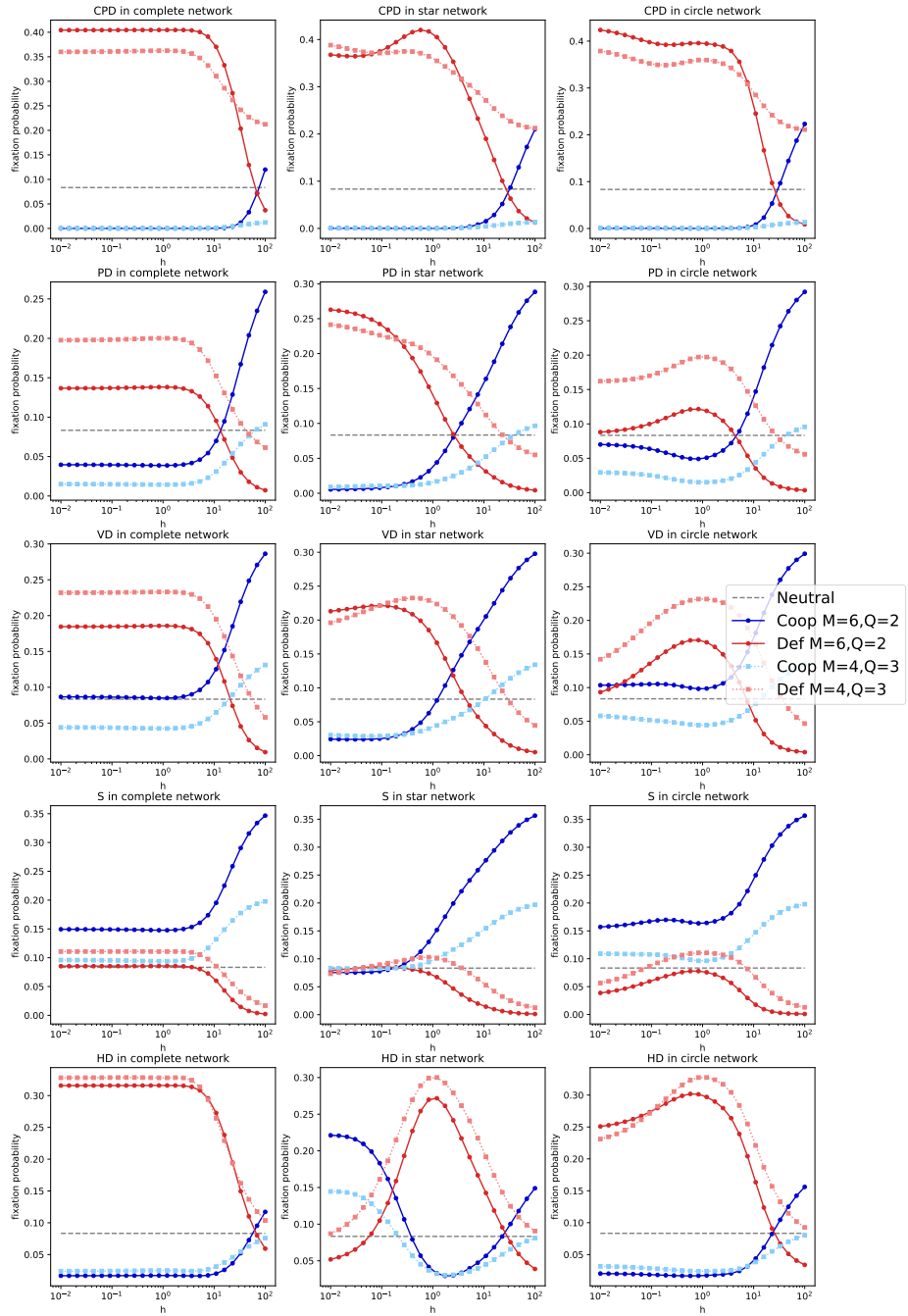
Figure 4.4: Fixation probabilities under complete (left), star (centre), and circle (right) networks for five different social dilemmas (rows). Fixation probabilities of cooperators (blue lines) and defectors (red lines) are shown in the same plots for different values of home fidelity h and two cases with equal population size: one with network size $M = 6$ and community size $Q = 2$ (circle markers), and another one with network size $M = 4$ and community size $Q = 3$ (triangle markers). The process used was the DBB dynamics, and payoff parameters are $w = 0.4$, $V = 2$, and $K = 1$.

populations for general values of population size and number of places and asymptotic density $Q = N/M$, which relates to community size under large home fidelity used in chapter 3, or the subpopulation size used in other approaches (Pattni et al. 2017). Our analysis of such populations culminates in the derivation of the fixation probability of a new type on them, and its application to analyse the evolution of cooperation under five different social dilemmas.

We conclude that cooperation does not evolve under the Charitable Prisoner's Dilemma in completely mixed populations. However, it does so under certain conditions in the remaining dilemmas. This is typically formalised based on the critical value of the reward-to-cost ratio above which cooperators evolve under PGGs, and the one below which they evolve under the HD game. This critical value increases with the value of the density of the population, thus meaning that cooperators are favoured by lower densities in PGGs and higher densities under the HD. Completely mixed populations allow scenarios of evolutionary instability of the two strategies in three different games, with special prevalence under the Volunteer's Dilemma.

We compare the general rules of cooperation under community structure obtained in chapter 3 to the ones obtained here, and note that it overall benefits the evolution of cooperation under all dilemmas. However, we observe that this effect is often limited under the BDB, DBD, LB, and LD dynamics, especially when the effect of different average group sizes is removed by performing a fair comparison. In exceptional cases, this leads to the evolution of cooperation being more limited under a community-structured population than in its fair comparison equivalent completely mixed population. Similar differences between dynamics have been noted under other approaches to population structure models (Ohtsuki et al. 2006, Pattni et al. 2017, Pires & Broom 2024), including the one explored in chapter 3, thus suggesting that these dynamics are not sensitive to the viscosity of evolutionary processes in structured populations. At the same time, this does not happen for alternative proposed mechanisms for the evolution of multiplayer cooperation, such as the co-evolution of assortative behaviour amongst cooperators through conditional movement, as it will be seen in chapter 5.

The evolution of cooperation under PGGs benefits from the organisation of populations into lower density systems. This is observed both by looking at the rules from table 4.2, obtained under completely mixed populations, but also for different network topologies and for general values of home fidelity in figure 4.4. Low subpop-

ulation temperature, i.e. low mixing between communities and low average group size are good indicators of the evolution of cooperation, similarly to what has been noted in Schimit et al. (2019) where communities are not considered (instead considering only $Q = 1$ in the territorial model). However, we are left with the question whether there is a good unique measure that accounts for both these factors. In the future, we would like assess this question in further depth by considering a wider range of network structures with various community sizes $Q > 2$ and home fidelity values.

Chapter 5

Co-evolution of cooperation and conditional movement on networks[1]

5.1 Introduction

The fundamental framework of multiplayer games on networks introduced in chapter 1 and used as a basis for the territorial raider model explored in chapters 3 and 4 is highly flexible. In its context, several types of movement models have been studied, a review of which is provided in Broom et al. (2021) together with an analysis of their robustness and applicability. In this chapter, we will focus on a Markov movement model, i.e. a model under which the next positions of individuals depend only on the current population distribution. We use the conditional movement strategy introduced in Pattni et al. (2018), under which individuals move with higher probability if they are not satisfied with their group composition.

This rule is similar to the principle behind the Win-Stay, Lose-Shift strategy introduced in chapter 1, which was shown to be evolutionarily successful in iterated pairwise games (Nowak & Sigmund 1993, Kraines & Kraines 2000). In Aktipis (2004), the principle was shown to be successful in pairwise interactions under which individuals have the possibility to move. This was coined the "walk-away" strategy, under which individuals always cooperate but move if their interactive partner defects, also successful in groups playing public goods games (Aktipis 2011). Still in

---

[1]This chapter is based on the work published in Pires et al. (2023), which results from a collaboration with Professor Igor Erovenko and Professor Mark Broom.

the context of cooperation between individuals, the co-evolution of conditional movement rules has been shown to be successful (Hamilton & Taborsky 2005, Le Galliard et al. 2005).

Therefore, we propose the use of the Broom-Rychtář framework and, in particular, the stochastic conditional rule introduced in Pattni et al. (2018) to explore the evolution of multiplayer cooperation in mobile and structured populations. As introduced in chapter 1, it is shown in Pattni et al. (2018) that complete networks sustain the co-evolution of cooperation and assortative behaviour, allowing cooperators to find and stay with each other in groups until they are found by defectors. Exploring circle and star networks, it is shown in Erovenko et al. (2019) that non-complete topologies can be detrimental to the evolution of cooperation under movement, potentially due to the negative impact of a lower clustering coefficient and a higher degree centralisation, i.e. high variance in degree centrality, on the assortative behaviour described above. Alternative evolutionary dynamics such as the ones adapted to this framework in Pattni et al. (2017) and formally defined in chapter 3 haven't been explored in this context. However, the results from both evolutionary pairwise games on graphs (Ohtsuki et al. 2006) and multiplayer games under independent movement explored in chapters 3 and 4 show that the chosen evolutionary dynamics can be determinant of the evolution of cooperation.

In this chapter, we propose to assess the influence of choosing different evolutionary dynamics on the interdependence between multiplayer cooperation, network topology, and assortative behaviour. In section 5.2, we provide a formal definition of the model used. In section 5.3, we develop a systematic analysis of the results obtained under complete, circle and star networks for all six evolutionary dynamics presented in Pattni et al. (2017). This is done for both rare and non-rare interactive mutations, respectively in subsections 5.3.1 and 5.3.2. Overall, we show that the evolution of cooperation is primarily dependent on network topology and that qualitative evolutionary outcomes are generally robust to the choice of evolutionary dynamics. In section 5.3.3, we discuss the new topological effects which haven't been previously observed in Erovenko et al. (2019). Finally, in section 5.4, we summarise and analyse the main distinction between these results and those of evolutionary games on graphs (Ohtsuki et al. 2006) and multiplayer games under independent movement observed in chapters 3 and 4. We further explore the quantitative similarities and differences between the results obtained under each evolutionary dynamics.

5.2 The Markov movement model

The work accomplished in this chapter is based on the modelling framework proposed in Broom & Rychtář (2012). In this section, we will focus primarily on the relevant aspects to the Markov model considered. Some of these aspects will be similar to those introduced for the territorial raider model in chapter 3. Similarly, the framework comprises three main features which we will expand on in the following subsections: (1) network structure and Markov movement; (2) the multiplayer game; and (3) the evolutionary dynamics.

5.2.1 Network structure and Markov movement

We start from the same basic framework as in chapters 3 and 4. Let us consider a population composed of N individuals, with the nth individual labelled I_n. Each individual is positioned in a network with M places, the mth place being labelled P_m. The network has a set of edges between its nodes, which in this model will be relevant to define the possible moves individuals can make on it. Here, we will consider the three topologies analysed in Erovenko et al. (2019): complete, star, and circle networks of different sizes. These three types of structures exhibit high degrees of symmetry, resulting in extreme clustering coefficients and degree centralisation values, both of which are critical measures in network analysis.

Although the terms "graph" and "network" are often used interchangeably in the literature, we will adopt the terminology used in Schimit et al. (2019) and in the previous chapters. Specifically, we will use the first to refer to the evolutionary graph that emerges from the replacement weights between *individuals*. On the other hand, the second will be used to refer to the network of *places* described above.

Contrary to what we considered in the previous chapters, each node in the network is home to exactly one individual, which leads to the equality $M = N$. Let $p_{n,t}(m)$ be the probability that an individual I_n is at place P_m at time t. In the context of general history-dependent movement, this probability distribution is conditional on the past positions of all individuals in the network (Broom & Rychtář 2012), denoted as $\mathbf{M}_{t'} = [M_{n,t'}]_{n=1,\dots,N}$, at all values of time $t' < t$. However, we are considering a Markov movement model, under which the probability is dependent only on the positions at which individuals were in the previous discrete time step, i.e. $t' = t - 1$. To make this dependence explicit, we define the probability distribution

introduced above as the following:

$$p_{n,t}(m|\boldsymbol{m}_{t-1}) = \mathbb{P}(M_{n,t} = m|\mathbf{M}_{t-1} = \boldsymbol{m}_{t-1}). \tag{5.1}$$

We follow the same movement model used in previous studies (Pattni et al. 2018, Erovenko et al. 2019). Each individual begins the exploration phase at their home node, from which they will go through T time steps, which we call the exploration time, before going back to their home nodes. At each time step t, individual I_n evaluates the group G_n in which they were at time $t - 1$. Groups are defined as functions of the positions at the previous time step $\boldsymbol{m}_{t-1}$ and denoted as $G_n(\boldsymbol{m}_{t-1}) = \{i : m_{i,t-1} = m_{n,t-1}\}$. The probability that individual I_n remains in the same place depends on their group's composition, as described by the following equation:

$$h_n(G_n(\boldsymbol{m}_{t-1})) = \frac{\alpha_n}{\alpha_n + (1 - \alpha_n)S^{\beta_{G_n(\boldsymbol{m}_{t-1})\backslash\{n\}}}}, \tag{5.2}$$

where S is a sensitivity parameter, α_n is the staying propensity of individual I_n and β is the attractiveness of the group. The staying probability increases with the staying propensity which may hold a value between 0 and 1. Decreasing S results in a greater impact of the group-dependent term on the staying probability. The attractiveness of the group with whom individual I_n has interacted is obtained from the sum of the attractiveness of all other individuals in that group:

$$\beta_{G_n(\boldsymbol{m}_{t-1})\backslash\{n\}} = \sum_{i \in G_n(\boldsymbol{m}_{t-1})\backslash\{n\}} \beta_i, \tag{5.3}$$

where $\beta_C = 1$ and $\beta_D = -1$ are the attractiveness of cooperators and defectors respectively.

Based on this definition, the probability $p_{n,t}(m)$ that individual I_n is at place P_m at time t depends only on the place where the individual was in the previous step $m_{n,t-1}$, and the group they were interacting with at that time $G_n(\boldsymbol{m}_{t-1})$. This probability assumes the following form:

$$p_{n,t}(m|m_{n,t-1}, G_n(\boldsymbol{m}_{t-1})) = \begin{cases} h_n(G_n(\boldsymbol{m}_{t-1})) & m = m_{n,t-1}, \\ \dfrac{1 - h_n(G_n(\boldsymbol{m}_{t-1}))}{d(m_{n,t-1})} & m \neq m_{n,t-1} \wedge l(m, m_{t-1}) = 1, \\ 0 & l(m, m_{t-1}) > 1, \end{cases}$$
$$\tag{5.4}$$

where $d(m_{n,t-1})$ represents the degree of the node where I_n was located at time $t-1$, and $l(m, m_{t-1})$ represents the shortest path between the two positions in the network.

We note that in this model, if an individual decides to move, then it moves to a neighbouring location randomly with uniform probability. In other words, the only decision an individual makes is whether to stay at the current location. See Erovenko & Rychtář (2016), Erovenko (2019), Weishaar & Erovenko (2022) for a different approach, where individuals sample all potential future locations and move strategically based on the expected payoff in each such location.

5.2.2 Multiplayer game

At every time step of the exploration phase, individuals participate in a multiplayer game with the group present in the same node of the network. This interaction results in the reward $R_{n,t}$ received by individual I_n at time t. We use the public goods game described in Pattni et al. (2018) and Erovenko et al. (2019), which is also known as the Charitable Prisoner's Dilemma (Broom et al. 2019). This multiplayer social dilemma is introduced and explored in the previous chapters 3 and 4. In this game, cooperators in a group pay a cost of K to contribute V to a public good, which is then equally split among all other members of the group, including defectors.

In this chapter, we consider all individuals to receive a background reward of R. Since a rescaling of the fitness of individuals will lead to the same stochastic process, we rescale all payoffs by R, using the scaled variables of the reward $v = V/R$ and the cost $k = K/R$. In terms of representation, this is the same as considering $R = 1$, $v = V$ and $k = K$. As previously noted in chapter 3, this is equivalent to using intensity of selection of $w = 0.5$. The payoff received by the individual in the group G_n is thus defined as follows:

$$
R_{n,t}(G_n(\boldsymbol{m}_t)) = \begin{cases} 1 - k + \dfrac{|G_n(\boldsymbol{m}_t)|_C - 1}{|G_n(\boldsymbol{m}_t)| - 1}v & \text{if } I_n \text{ is a cooperator and } |G_n(\boldsymbol{m}_t)| > 1, \\[3mm] 1 - k & \text{if } I_n \text{ is a cooperator and } |G_n(\boldsymbol{m}_t)| = 1, \\[3mm] 1 + \dfrac{|G_n(\boldsymbol{m}_t)|_C}{|G_n(\boldsymbol{m}_t)| - 1}v & \text{if } I_n \text{ is a defector and } |G_n(\boldsymbol{m}_t)| > 1, \\[3mm] 1 & \text{if } I_n \text{ is a defector and } |G_n(\boldsymbol{m}_t)| = 1, \end{cases}
$$
$$(5.5)$$

where $|G_n|$ is the total number of individuals and $|G_n|_C$ the number of cooperators

in the group. In the simpler independent movement model of chapters 3 and 4, the group composition was described in simpler terms by the number of cooperators c and defectors d (see CPD in table 3.1). This would lead to the same payoffs represented above. A distinctive feature of this public goods game is that cooperators do not benefit from their own contributions (Broom et al. 2019), which reduces the likelihood of cooperation evolving, similar to what is observed in the original pairwise Prisoner's Dilemma. Amongst all the public goods dilemmas explored in chapters 3 and 4, this one held the strictest conditions for the evolution of cooperation.

At the beginning of the exploration phase ($t = 0$), all individuals start with null fitness, and the payoffs $R_{n,t}$ received at each time step t will accumulate over time. The fitness contribution $f_{n,t}$ to an individual's fitness at time t is calculated as follows:

$$f_{n,t}(m, G_n(\boldsymbol{m}_t)|m_{n,t-1}) = \begin{cases} R_{n,t}(G_n(\boldsymbol{m}_t)) - \lambda & m \neq m_{n,t-1}, \\ R_{n,t}(G_n(\boldsymbol{m}_t)) & m = m_{n,t-1}, \end{cases} \tag{5.6}$$

where λ denotes the movement cost, rescaled by the background payoff R.

Fitness contributions are evaluated at each time step during the exploration phase until the time T is reached. Consequently, the total fitness $F_{n,t}(\boldsymbol{m}_t)$ of each individual at time t can be computed by summing the T most recent contributions up to that time:

$$F_{n,t}(\boldsymbol{m}_t) = \sum_{t'=t-T+1}^{t} f_{n,t'}(\boldsymbol{m}_k|\boldsymbol{m}_{k-1}). \tag{5.7}$$

Upon completion of the exploration phase, the fitness of individuals is calculated and they are considered to go back to their respective home nodes. Thereafter, we consider an update of the population state, based on the evolutionary process described in the following subsection.

5.2.3 Evolutionary dynamics

We consider the state of the population to be updated after individuals complete an exploration phase, accumulate their fitness, and return to their home nodes. During an update, one individual reproduces and another one is replaced by the first. We adopt the approach initially proposed in Lieberman et al. (2005) for populations in pairwise interaction networks, and later extended in Pattni et al. (2017) for general evolutionary games on networks. We recall the definition of an evolutionary graph,

where each node represents an individual, and the adjacency matrix represents the replacement weights that determine the possible replacement events.

We calculate the replacement weights based on the time individuals spend together one exploration time step after being at home (Pattni et al. 2018, Erovenko et al. 2019). We assume that individuals spend equal fractions of time with members of the same group, and only spend time with themselves when they are alone. The time spent between two individuals I_i and I_j under the set of positions of the population $\boldsymbol{M} = \boldsymbol{m}$ is denoted $u_{i,j}$, and depends only the group $G_i(\boldsymbol{m})$ meeting with I_i under those positions:

$$u_{i,j}(G_i(\boldsymbol{m})) = \begin{cases} \dfrac{1}{|G_i(\boldsymbol{m}) \setminus \{i\}|} & i \neq j \wedge j \in G_i(\boldsymbol{m}), \\ 0 & i \neq j \wedge j \notin G_i(\boldsymbol{m}), \\ 1 & i = j \wedge |G_i| = 1, \\ 0 & i = j \wedge |G_i| > 1. \end{cases} \tag{5.8}$$

The replacement weights are denoted as $w_{i,j,t}$ and are considered at a time t that is multiple of T. The positions of individuals at home are defined as $\boldsymbol{m}_{t-T}$. Replacement weights correspond to the average time spent between individuals I_i and I_j when they are one movement time step away from home. Thus, their values can be obtained using the following equation:

$$w_{i,j,t} = \sum_{\boldsymbol{m}} u_{i,j}(G_i(\boldsymbol{m})) p(\boldsymbol{m}|\boldsymbol{m}_{t-T}). \tag{5.9}$$

After defining the underlying evolutionary graph, we are now in a position to consider the stochastic update rules of the evolutionary dynamics. At each time step of the evolutionary process, an individual I_i will reproduce and replace an individual I_j with probability of replacement τ_{ij}. The probability of selecting any set of individuals for reproduction and replacement will depend on both the fitness and the replacement weights of all individuals in the population. Previous approaches to Markov movement models have focused on the birth-death process with selection acting during birth (BDB). In the present chapter, we use the set of six dynamics defined in chapter 3. These are referred to as the BDB, DBD, DBB, BDD, LB, and LD dynamics. See section 3.2.3 of that chapter for more details on how the probability of replacement depends on the fitness and replacements for each of the

101

six evolutionary dynamics. In particular, table 3.2 shows the probabilities of birth $(b_{i(j)})$ and death $(d_{(i)j})$, or the final probability of replacement (τ_{ij}) for any pair of individuals I_i and I_j for each of the evolutionary dynamics.

Consider a population consisting of individuals with complex strategies that include both an interactive and a movement component. The interactive component determines whether an individual cooperates (C) or defects (D) during interactions in the public goods game presented. The movement component is defined by their staying propensity denoted as α_n, which takes one of the values $\{0.01, 0.1, 0.2, ..., 0.8, 0.9, 0.99\}$, similarly to what was considered in previous works (Pattni et al. 2018, Erovenko et al. 2019). This leads to a total of 22 possible complex strategies.

We assume the timescale in which mutations occur to be much larger than that of replacement events. Under this assumption, the evolutionary processes described above lead to dynamics of fixation, where at most two strategies are present in the population at any given time. Thus, it becomes essential to analyse fixation probability values, i.e. the probability that one individual using a mutant strategy will fixate in a population with a distinct resident strategy. We will consider two mutation scenarios. In the first scenario, mutations of the interactive component of strategies are much rarer than those of the movement component. In the second scenario, mutations of both strategy components occur at the same rate.

Rare interactive strategy mutations

In this scenario, mutations in movement strategies occur at a higher rate than those in interactive strategies. For each interactive strategy, there exists an optimal staying propensity towards which the population evolves. The optimal staying propensity of defectors is always the maximum value of α, which is 0.99 since there is no benefit in moving when everyone defects. As for cooperators, its value can be determined by computing fixation probabilities between all cooperator strategies. The strategy with the optimal staying propensity cannot be invaded by any other strategy with a probability higher than the neutral fixation rate of $1/N$. Fixation probabilities can be obtained by running simulations starting with one single mutant individual subject to the evolutionary dynamics described above. The simulation ends either in a successful fixation, where all individuals use the mutant's strategy, or an unsuccessful one, where all individuals use the resident's strategy. By running this

simulation for n_t trials, the fixation probability can be computed from the fraction of those trials ending in successful fixations.

We assume that populations evolve towards the optimal staying propensity of their interactive strategy, after which interactive strategy mutations become relevant. We calculate the fixation probabilities of mutant cooperators against resident defectors using their optimal propensity, and consider the mutant cooperator strategy with the highest fixation probability, denoted ρ^C, as the fittest mutant. Similarly, we obtain the fixation probability of the fittest mutant defector against resident cooperators, denoted ρ^D, by performing parallel computations. We then compare these two probabilities against the neutral fixation probability of $1/N$. We classify the evolutionary outcome based on the principle elaborated in chapter 1 and already used in the previous chapters, restated here:

- Selection favours cooperation if $\rho^C > 1/N > \rho^D$;

- Selection favours defection if $\rho^D > 1/N > \rho^C$;

- Selection favours instability if $\rho^C > 1/N$ and $\rho^D > 1/N$;

- Selection favours bi-stability if $\rho^C < 1/N$ and $\rho^D < 1/N$.

Non-rare interactive strategy mutations

When mutations of both the interactive and movement components of strategies occur at the same timescale, a successful strategy will face individuals of both types of interactive strategies throughout the evolutionary process. Thus, the optimal staying propensities of cooperators and defectors are determined by comparing their fixation probabilities on mixed populations. We consider a mixed population of $N/2$ cooperators and $N/2$ defectors for simplicity. Cooperators will have one optimal movement strategy for each of the possible defector complex strategies, and vice versa. We define the mutually-optimal propensities as those where none of the interactive types increases their probability of fixation in the mixed population by unilaterally changing their movement strategy.

To find the pair of mutually-optimal strategies, we calculate the fixation probabilities of cooperators and defectors starting from the mixed population for all combinations of staying propensities. We find the equilibrium pair by starting with any strategy, and iterating over the fittest mutant of the opposing interactive type,

until we find a fixed point of the mutually-optimal pair. We classify the evolutionary outcome of the process based on the fixation probabilities, denoted $\rho^C_{N/2}$ and $\rho^D_{N/2}$, of the two equilibria strategies starting from the mixed population:

- Selection favours cooperation if $\rho^C_{N/2} > 1/2 > \rho^D_{N/2}$;

- Selection favours defection if $\rho^D_{N/2} > 1/2 > \rho^C_{N/2}$;

- Selection is neutral if $\rho^C_{N/2} \approx 1/2$ and $\rho^D_{N/2} \approx 1/2$,.

5.3   Results

In this section, we analyse the outcomes of comprehensive systematic simulations of the Markov movement model outlined earlier. Our focus is on identifying the variations caused by different evolutionary dynamics. For this purpose, we use two types of plots. The first type illustrates the evolutionary outcomes for different value combinations of population size (N) and movement cost (λ). The second displays the numerical value of the fixation probabilities for cooperators and defectors as the movement cost varies.

For the plots that depict the regions where each evolutionary outcome prevails, we will employ the following colour-coding scheme:

- Blue indicates that selection favours cooperation;

- Orange indicates that selection favours defection;

- Grey indicates that selection favours bi-stability or is neutral;

- Yellow indicates that selection favours instability.

It is important to note that the colour-coding scheme is used for both mutation scenarios, even though the non-rare interactive mutation scenario does not feature the yellow colour.

The plots with evolutionary outcomes presented here differ slightly from those in Erovenko et al. (2019) for the same dynamics. In the work done in this chapter, we have implemented a 2σ rule to manage stochastic uncertainty, which has been applied to both mutation scenarios. We assume that the mutant fixation probability exceeds the neutral one only if the simulated fixation probability exceeds the neutral fixation probability by at least two standard deviations. This means that for

the rare interactive strategy mutations scenario the threshold is $1/N + 2\sigma$, and for the non-rare interactive mutations scenario the threshold is $1/2 + 2\sigma$. This mostly impacted the complete network as the region where selection favours defectors became slightly smaller. The estimations of the standard deviation in each case are provided in Erovenko et al. (2019). They are based on 100,000 simulation trials for each combination of parameters in the rare interactive mutations case and 10,000 simulation trials in the non-rare interactive mutations case. The thick grey lines around the neutral fixation probability value on the fixation probability plots show the $\pm 2\sigma$ area of stochastic uncertainty.

We present these plots in sections 5.3.1 and 5.3.2, for the two mutation scenarios, under complete, circle, and star networks. We use the following parameter values: $S = 0.03$, $k = 0.04$, $v = 0.4$, $T = 10$. A summary of the newly observed topological effects is provided in section 5.3.3. We identify the patterns observed on the figures throughout section 5.3. However, it is only in section 5.4 that we do a cross-scenario analysis and provide explanations for the similarities and differences observed between the evolutionary dynamics.

5.3.1   Rare interactive strategy mutations

Complete Network

The evolutionary outcomes obtained under complete networks are similar for different evolutionary dynamics, as evidenced by the region plots in figure 5.1. Selection promotes stability for most of the parameter space. Cooperators are favoured for lower values of the movement cost regardless of population size, while defectors do better for large movement costs and small networks.

Despite the similarities, there are still a few clear emerging differences. The region where defectors dominate is larger under dynamics where selection acts on the death event. Under the DBD and LD dynamics, selection favours defectors regardless of population size when movement costs are high enough ($\lambda \geq 0.8$), and it does so for much lower movement costs under small enough populations. The regions under which cooperation dominates are the largest under the BDB and LB dynamics. Finally, bi-stability is favoured more often under the BDD and DBB dynamics than under the remaining dynamics.

An important aspect to highlight is that there is a small region where selection
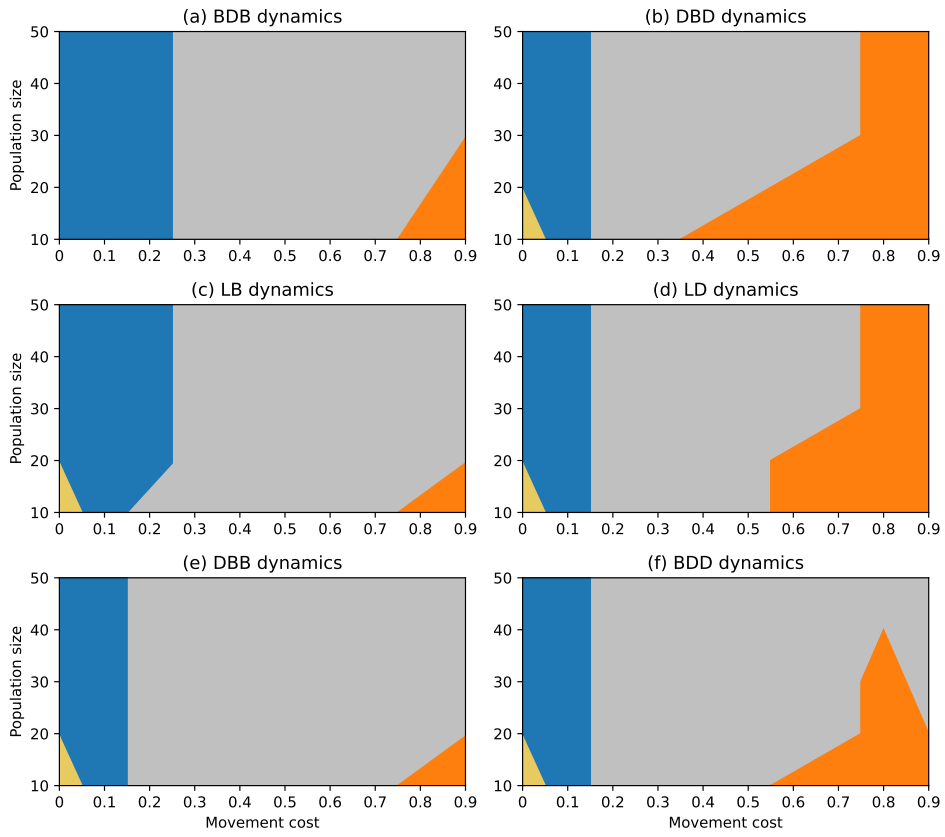
Figure 5.1: Evolutionary outcomes under complete networks and rare interactive mutations for different choices of evolutionary dynamics, population size and movement cost.
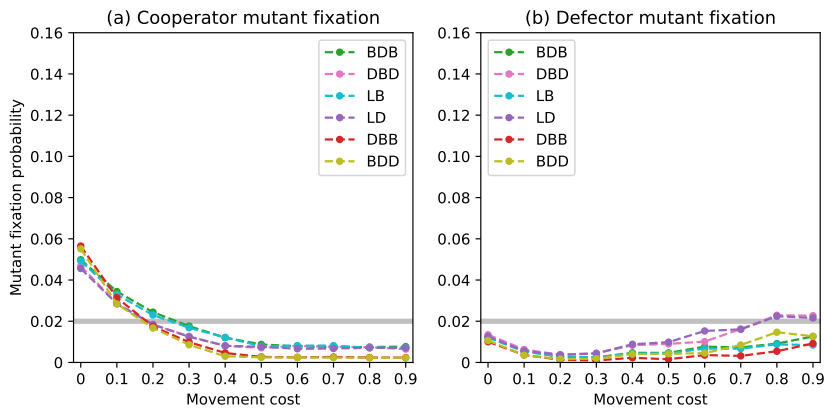
Figure 5.2: Fixation probabilities of fittest mutant cooperators and defectors under a complete network with $N = 50$ and rare interactive mutations for different evolutionary dynamics.
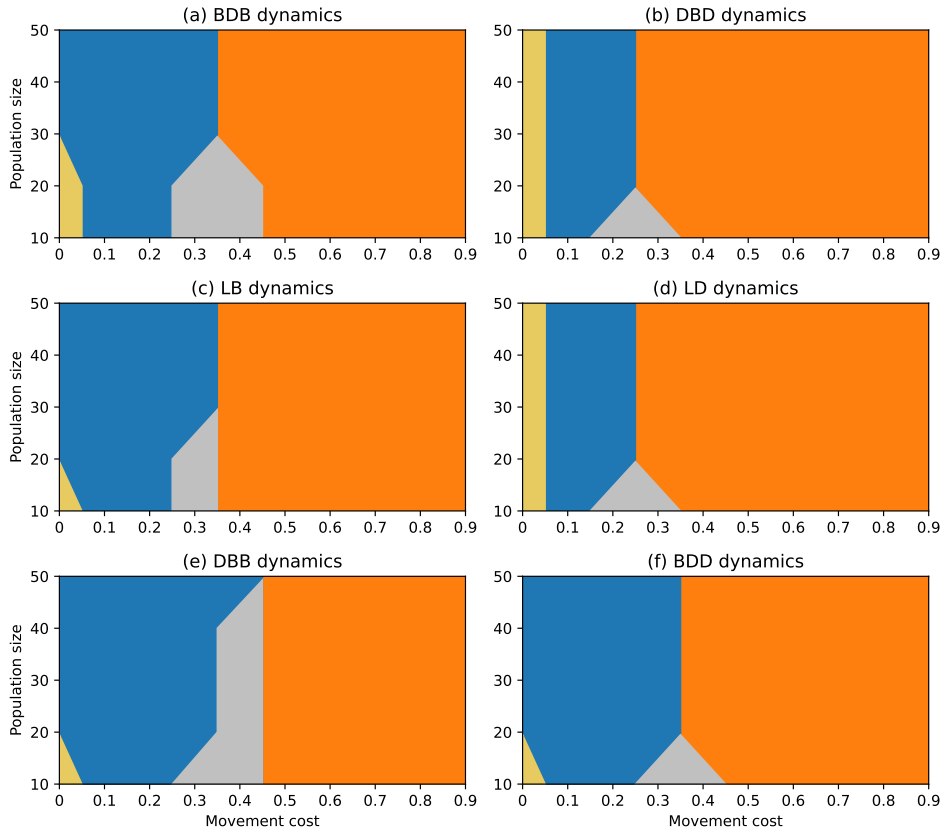
Figure 5.3: Evolutionary outcomes under circle networks and rare interactive mutations for different choices of evolutionary dynamics, population size and movement cost.
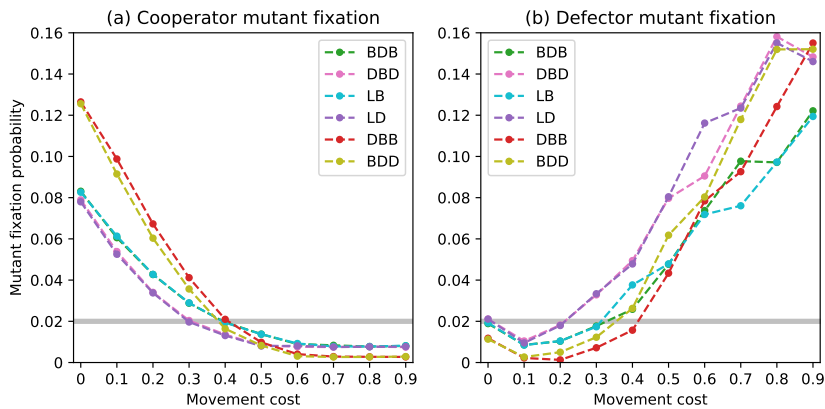
Figure 5.4: Fixation probabilities of fittest mutant cooperators and defectors under a circle network with $N = 50$ and rare interactive mutations for different evolutionary dynamics.

favours instability of both strategies under null movement costs and the smallest populations which is present under almost all dynamics. This was not documented in the analysis of the BDB dynamics on the complete network in Erovenko et al. (2019), but it was observed then under the circle network.

The fixation probabilities for $N = 50$ are displayed in figure 5.2. All six evolu-
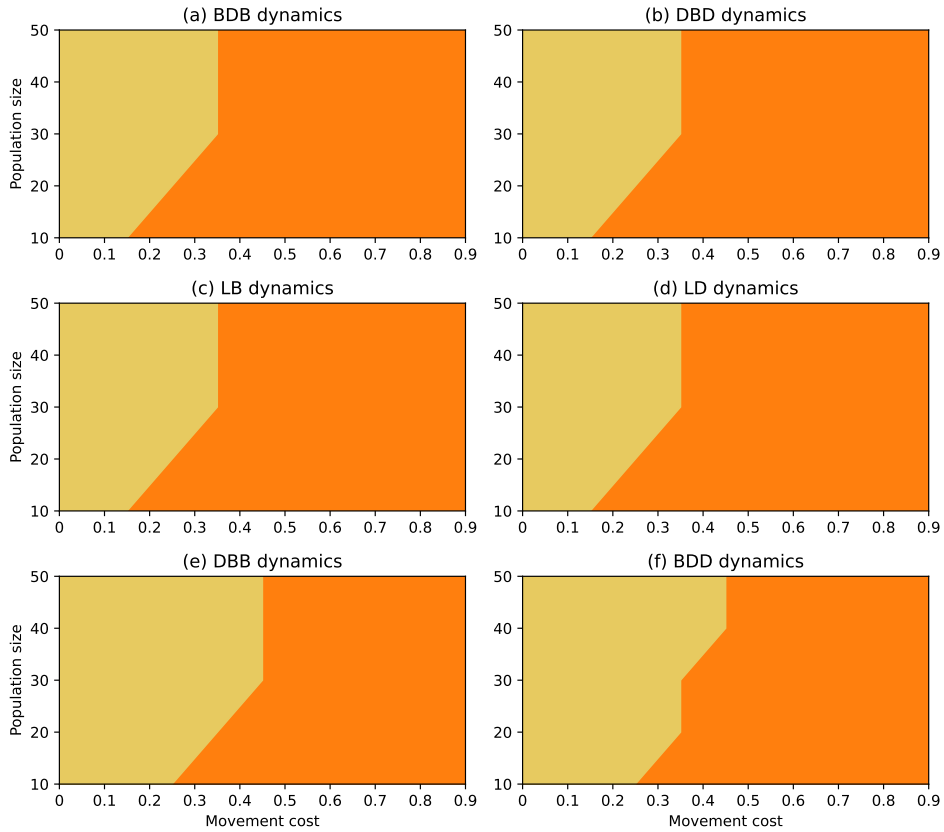
Figure 5.5: Evolutionary outcomes under star networks and rare interactive mutations for different choices of evolutionary dynamics, population size and movement cost.
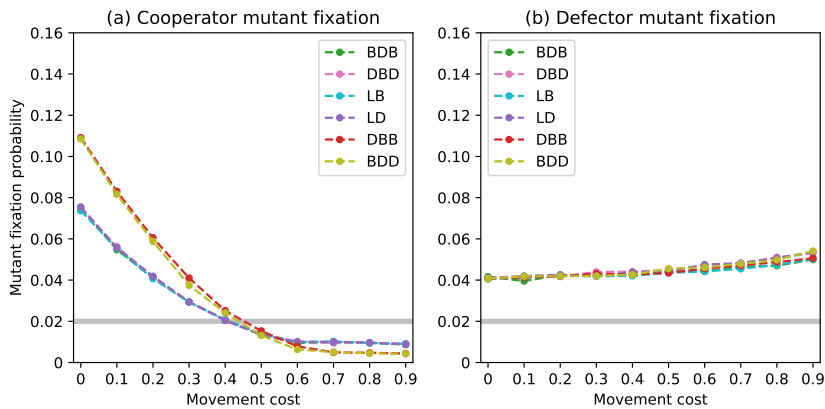
Figure 5.6: Fixation probabilities of fittest mutant cooperators and defectors under a star network with $N = 50$ and rare interactive mutations for different evolutionary dynamics.

tionary dynamics exhibit similar trends in fixation probabilities, which align with the results presented in Erovenko et al. (2019), particularly for the fixation of co-operators. It is worth noting, however, that dynamics DBD and LD give defectors a chance to fixate above neutrality in populations of size 50, resulting in fixation probabilities that are twice as high as those of the other dynamics. This will be

further discussed in section 5.4.

Our analysis revealed the formation of pairs of dynamics leading to similar results. Specifically, the pairs BDB/LB and DBD/LD had overlapping curves and the pair DBB/BDD similarly led to quite close values. This pattern emerged for both the fixation of cooperators and defectors. There are punctual deviations observed in the first two pairs, which can be attributed to considering different discrete values for the optimal staying propensities of resident cooperators. Furthermore, we observed the overlap of the curves referring to the four dynamics BDB, LB, DBD and LD for the fixation of mutant cooperators in the presence of large movement costs, and the fixation of defectors under low movement costs. In these situations, the DBB and BDD dynamics also exhibit overlapping curves. However, differences can be observed within these pairs of dynamics for the remaining movement cost values. This result was surprising and it is discussed in section 5.4, as previous work (Pattni et al. 2017, Schimit et al. 2022) suggests that complete networks should lead the BDB/DBD and BDD/DBB pairs of dynamics to yield the same outcomes.

Circle Network

The circle network leads to results presented in figure 5.3. These exhibit a general pattern of single strategy stability, with cooperators dominating in regions of lower movement costs (excluding the minimal value of $\lambda = 0$) and defectors dominating in higher cost regions.

There are two exceptions to this trend: selection favours bi-stability for intermediate values of movement costs and favours instability for minimal values. The first typically occurs for small populations as observed in Erovenko et al. (2019), which suggests it might be associated with the finiteness of populations, stabilising when these are larger. However, the second remains present regardless of population size under DBD/LD dynamics because, contrary to what happens under other dynamics, defectors fixate above $1/N$ for $\lambda = 0$ under all population sizes.

The DBD and LD dynamics exhibit unique characteristics. Compared to other dynamics, they facilitate the evolution of defection at lower values of movement costs and favour instability of both strategies for null movement costs regardless of population size. These observations suggest that these dynamics promote the fixation of defectors and hinder that of cooperators, as was seen under the complete network.

Examining the fixation probabilities displayed in figure 5.4, we can easily draw the conclusion that various evolutionary dynamics follow similar patterns. The DBD/LD dynamics present smaller regions where cooperators fixate above neutrality and larger regions where defectors do so, leading to the result already displayed in figure 5.3.

Similar to the complete network, the fixation probabilities of cooperators have overlapping curves within the pairs of dynamics BDB/LB and DBD/LD. The same holds true for the fixation of defectors, especially for low movement costs. However, larger costs lead to increased noise in the values, which may be linked to the fact that only discrete values of the strategic staying propensity of resident cooperators are considered. This can result in choosing either side of the scale when the optimal staying propensities fall between two discrete values. The high sensitivity of fixation probabilities to the staying propensity of residents contributes to the sudden spikes seen for $\lambda = 0.4, 0.7$ in the BDB/LB and $\lambda = 0.6$ in the DBD/LD pair of dynamics, in otherwise overlapping curves.

In the circle network, the BDD and DBB dynamics result in much larger deviations from neutral selection, both for the overall fixation of cooperators and for the fixation of defectors at low movement costs. The numerical difference is remarkable, with values lower than neutral achieving near-zero fixation in certain cases, and values higher than neutral being more than 50% higher than under any other dynamics.

Star Network

The mapping of evolutionary outcomes under star networks is displayed in figure 5.5. These plots exhibit minimal differences. The conclusion drawn in Erovenko et al. (2019) that cooperators are consistently unstable under this topology remains valid, which is the most pronounced instance of topological effects dominating over the evolutionary dynamics.

The region plots for the four dynamics BDB, LB, DBD, and LD are identical. The high similarity within pairs BDB/LB and DBD/LD was already observed in the previous sections. However, it is surprising that the two pairs are equivalent to each other, considering the large differences observed between them in other topologies, including complete networks.

Although the differences with the two remaining dynamics DBB and BDD are

minor, it is noteworthy that they appear to be more similar to each other than to the previously mentioned four other dynamics.

The fixation probabilities obtained for $N = 50$, as displayed in figure 5.6, suggest a greater level of similarity among the dynamics than under other topologies. The dynamics BDB/LB and DBD/LD result in nearly identical outcomes between them for the fixation of both cooperators and defectors. For the fixation of cooperators, the DBB and BDD dynamics produce results that are essentially the same between them but are systematically farther from neutrality when compared to the other four dynamics. However, for the fixation of defectors, the numerical results of all six dynamics coincide.

5.3.2 Non-Rare interactive strategy mutations

Complete Network

The scenario with non-rare interactive mutations results in a significantly different landscape of evolutionary outcomes under complete networks, as depicted in figure 5.7. Cooperators are favoured by selection for wide regions of low and intermediate movement costs under all dynamics. Regions where selection does not favour either strategy are narrow and transitional, both for large movement costs and for limiting null costs. It is worth mentioning that the complete network once again appears to promote the evolution of cooperation across a broad range of parameter values.

A comparison of the results obtained under each dynamics reveals that the DBD and LD dynamics result in larger regions where defection is stable when compared to the other dynamics. Defection remains consistently stable down to $\lambda = 0.6$ regardless of population size, and for null movement costs of $\lambda = 0$ (sometimes together with cooperation) for most population sizes. In contrast, the BDB and LB dynamics remain the dynamics under which cooperation is selected across the widest regions, whereas defectors have very limited values for which they are stable.

The DBB and BDD dynamics show sets of regions somehow between the previous two pairs of dynamics. However, comparing these two dynamics, it is clear that the first is slightly more favourable towards cooperation than the second. This is akin to the previous comparison between the pairs BDB/LB and DBD/LD, suggesting the presence of a systematic difference which was not expected to be present under the complete network, which we discuss in section 5.4.
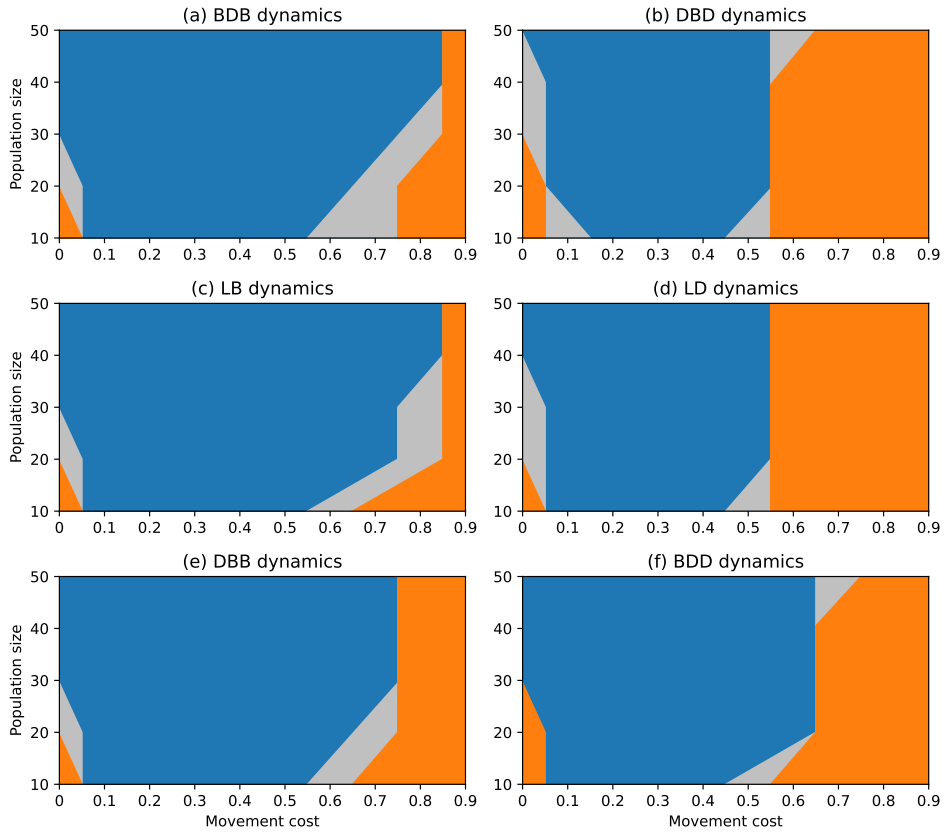
Figure 5.7: Evolutionary outcomes under complete networks and non-rare interactive mutations for different choices of evolutionary dynamics, population size and movement cost.
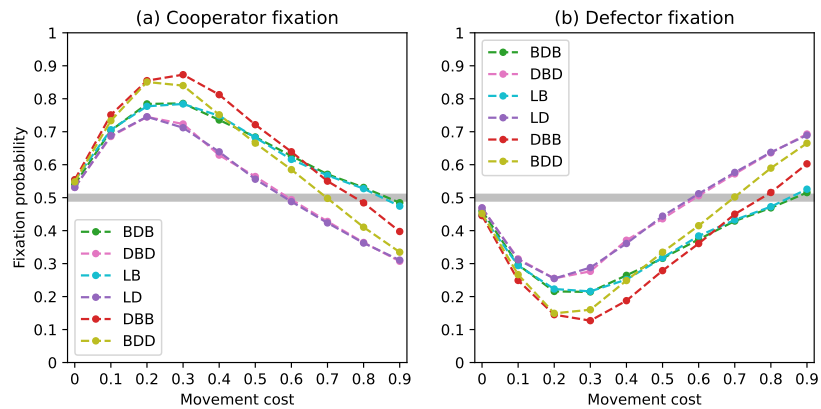
Figure 5.8: Fixation probabilities of fittest mutant cooperators and defectors under a complete network with $N = 50$ and non-rare interactive mutations for different evolutionary dynamics.
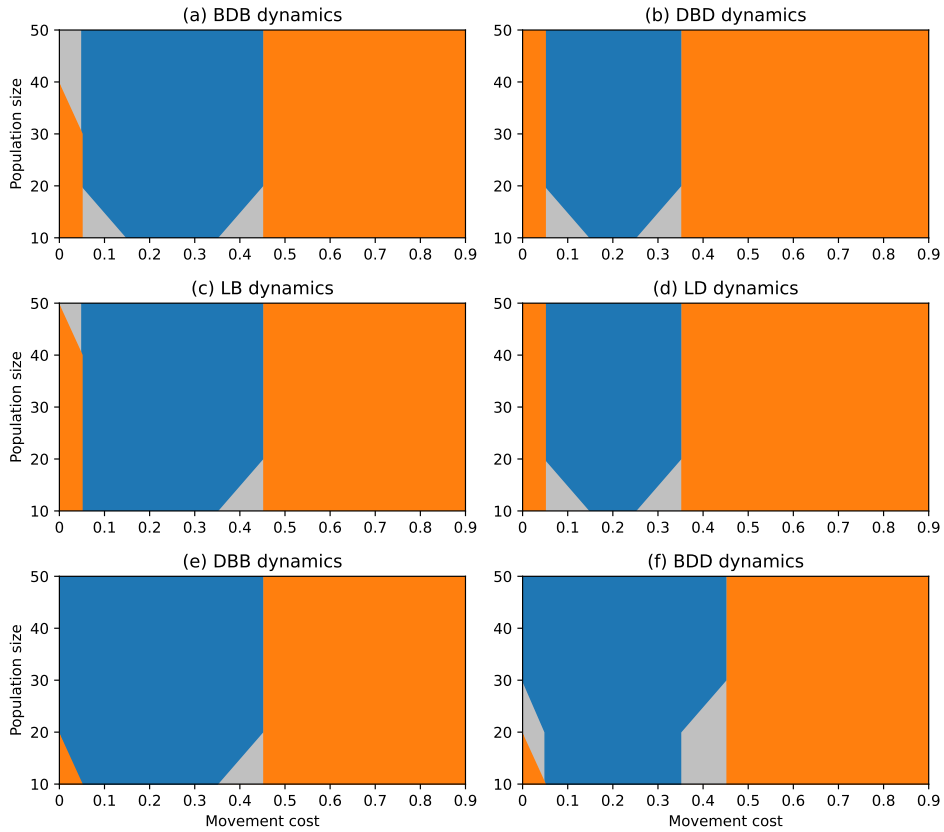
Figure 5.9: Evolutionary outcomes under circle networks and non-rare interactive mutations for different choices of evolutionary dynamics, population size and movement cost.
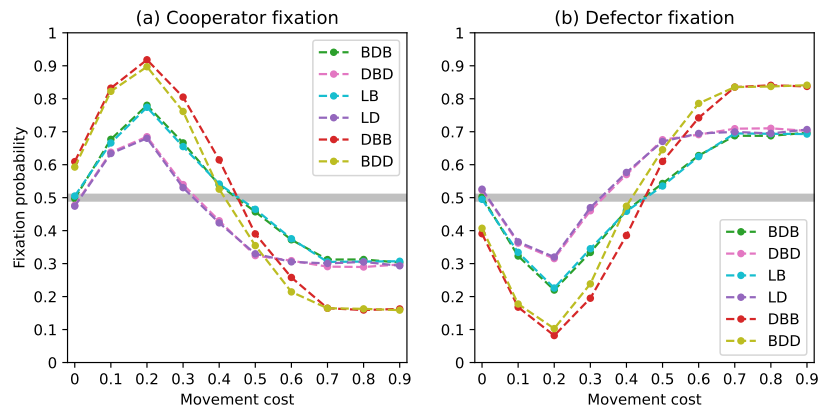
Figure 5.10: Fixation probabilities of fittest mutant cooperators and defectors under a circle network with $N = 50$ and rare interactive mutations for different evolutionary dynamics.

In this scenario, we examined the fixation probabilities starting from a mixed state with an equal number of cooperators and defectors with mutually-optimal staying propensities. As a result, the fixation probabilities of both types displayed in figure 5.8 are symmetrical and sum up to one for each choice of movement cost.

Once again, the trends among the different dynamics are highly similar. The
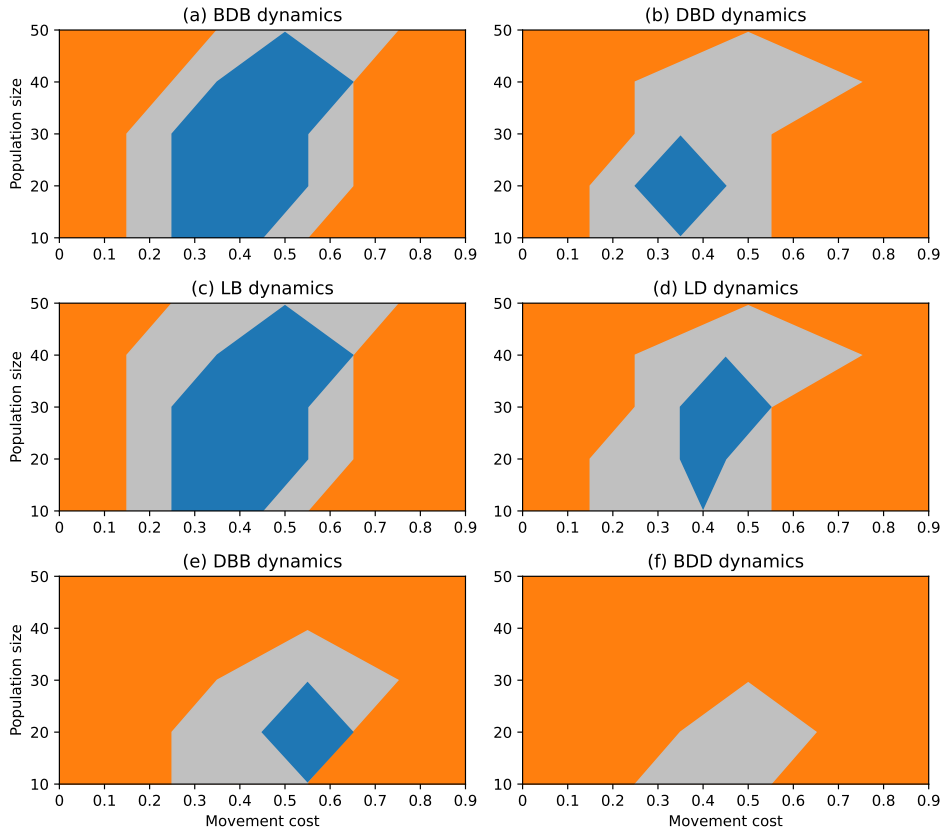
Figure 5.11: Evolutionary outcomes under star networks and non-rare interactive mutations for different choices of evolutionary dynamics, population size and movement cost.
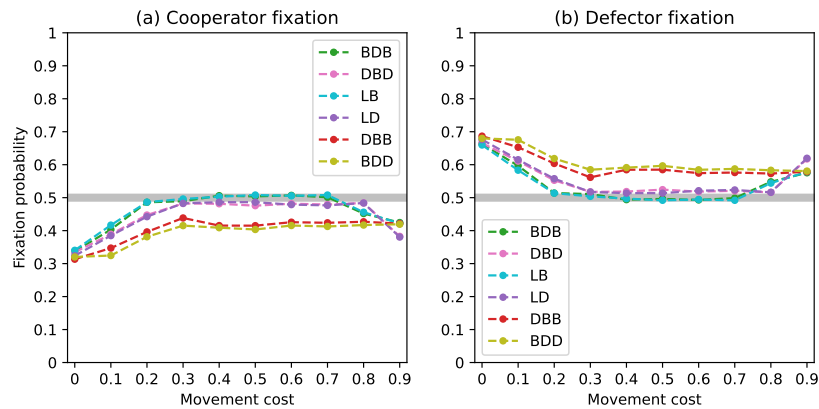
Figure 5.12: Fixation probabilities of fittest mutant cooperators and defectors under a star network with $N = 50$ and rare interactive mutations for different evolutionary dynamics.

fixation probability of cooperators is at near-neutral level for null movement costs, rising above it for intermediate costs before falling below it for higher values. Fixation probabilities are coincident within pairs BDB/LB and DBD/LD, with the first consistently leading to better outcomes for the evolution of cooperation. The DBB dynamics lead to the fixation of cooperators with higher probabilities than the BDD.

These quantitative findings support the observations made from the region plots.

Circle Network

The evolutionary outcomes obtained under circle networks with non-rare interactive mutations are exhibited in figure 5.9. This figure shows that, similarly to the complete network, defectors are favoured for both null and larger values of the movement cost, while cooperators are favoured from low to intermediate values of this. The transitions between cooperators to defectors showed narrow regions where selection favoured neither of the two strategies in particular. Defectors were stable down to lower values of movement costs than under the complete network, thus assuring that, in comparison, this topology favoured them slightly more often.

The results obtained under this setting show small differences when compared to the ones obtained under rare interactive mutations for the same topology. This might be associated with the scarcity of regions where selection favours bi-stability or instability of the two strategies under the previous mutation setting. This is a feature particular to the circle network, which is not present under the other studied topologies.

While the differences between evolutionary dynamics are not as striking as under other settings, we still observe that the DBD and LD dynamics assure the largest regions of selection of defection, for movement costs of $\lambda = 0$ and $\lambda \geq 0.4$ regardless of the size of the population.

The fixation probabilities for populations of size $N = 50$, as depicted in figure 5.10, reveal certain features more clearly. The pairs of dynamics BDB/LB and DBD/LD continue to exhibit close alignment within them. The two pairs additionally converge to similar values both for low and high movement costs, values under which the DBB and BDD dynamics similarly converge to each other. For the remaining values, the BDB/LB dynamics systematically lead to higher fixation probabilities of cooperators than the DBD/LD, just like the DBB shows an improvement (even if quite small) when compared to the BDD dynamics.

Finally, the DBB and BDD dynamics exhibit a clear pattern of amplified selection, with values above neutrality being the highest and values below neutrality being the lowest among all dynamics.

Star Network

The results obtained for the evolutionary process in star networks under non-rare interactive mutations are shown in figure 5.11. Unlike the results obtained in the same topology with rare interactive mutations, the different dynamics in this case result in substantial differences. Across all dynamics, defectors are favoured by selection at both low and high movement costs. However, there are intermediate regions where either cooperation or no strategy is favoured, and these regions are highly variable and dependent on the particular dynamics being considered.

This case presented a unique challenge that was discussed in Erovenko et al. (2019). It was usually impossible to find a mutually-optimal pair of staying propensities for cooperators and defectors. This was caused by the fact that the optimal staying propensity of defectors had a jump discontinuity as a function of the staying propensity of cooperators. We circumvented this issue as it was done in Erovenko et al. (2019) by assuming that the staying propensities may change only to the nearest values. This could lead to either local equilibria or local loops; in the latter case it is assumed that the optimal staying propensities corresponded to the "middle" values in the loops. We employed the same approach in this work. This might have been the driver of the wider variation of the outcomes between different dynamics compared to the complete or circle networks.

Despite the wide variations, the BDB and LB dynamics lead to equivalent maps of evolutionary regions, under which cooperation is solidly favoured for intermediate values. Conversely, the DBD and LD dynamics exhibit larger regions of favoured defection and smaller regions of favoured cooperation, which may differ from each other due to a higher susceptibility to stochastic fluctuations. The DBB and BDD dynamics show the widest regions of favoured defection, particularly for large populations where defection is favoured regardless of the movement cost value. When comparing these two dynamics, the BDD continues to exhibit a stronger tendency to promote defectors, failing to sustain cooperation across all population sizes and movement cost values explored.

These results differ greatly from those obtained through rare interactive mutations, as this scenario does not permit selection to favour instability. In the previous mutation scenario, not only did we observe little to no differences between dynamics, but we also observed cooperation to be unstable for all explored values. Therefore,

this mutation scenario presents an opportunity for cooperators to evolve within star networks.

Figure 5.12 displays the fixation probabilities of cooperators and defectors when $N = 50$. Fixation probability values obtained under different dynamics are quite similar quantitatively. However, the proximity to the neutral selection fixation probability of 1/2 allows for small differences between the dynamics to potentiate distinct qualitative evolutionary outcomes.

It is still clear that the BDD and DBB dynamics hold fixation probabilities the furthest away from neutrality, in this case promoting more often than other dynamics the evolution of defection. Selection happening on the birth event still seems to benefit the fixation of cooperators and oppose that of defectors slightly, which can be seen by comparing the BDB/LB dynamics against the DBD/LD and the DBB dynamics against the BDD.

5.3.3 Comparative analysis

The two mutation scenarios resulted in distinct evolutionary outcomes, partially due to their different nature. In the first, i.e. when interactive mutations are rare, selection favouring instability was consistently observed in the complete and circle networks under null movement costs, and in the star network under null-to-intermediate movement costs. The presence of these regions was brought to light through the examination of alternative evolutionary dynamics to the BDB used in Erovenko et al. (2019), since these uncovered the region in the complete network and extended it for larger populations in the circle network.

In that context, mutant cooperators systematically fixate above neutrality for low enough movement costs and for all topologies and evolutionary dynamics. Selection favouring instability of both strategies for $\lambda = 0$ is thus associated with mutant defectors doing so as well in that limit. The stability of resident cooperators relies on the extra steps that defectors have to do before finding groups of cooperators to exploit. Even though defectors benefit from moving (shown by their fittest mutant's staying propensity not being 0.99), they still earn less than cooperators because of the higher movement cost they pay and the limited time they spend amongst them. When $\lambda = 0$, the absence of movement costs gives defectors an evolutionary advantage, leading to a fixation above neutrality. This occurs regardless of population size in the circle network for some dynamics, possibly due its locality being

preserved under larger populations, enabling defectors to quickly encounter groups of cooperators.

Additionally, the first mutation scenario led to significantly noisier fixation probabilities of mutant defectors and less distinguishable patterns. This was due to optimal staying propensities of resident cooperators being dependent on the movement cost – contrary to the constant staying propensity of 0.99 achieved by resident defectors – which had to be calculated from a discrete set of values. This computation added an uncertainty to the resulting fixation probabilities which made the distinction of patterns comparatively more difficult, especially for larger movement costs.

Upon examination of the results obtained from the non-rare interactive mutation scenario and comparison with the previous, it becomes evident that different topologies result in distinct relationships. We observe that regions where selection favours one single strategy (i.e. cooperators or defectors) in the first mutation scenario typically carry over into the second scenario. However, regions where selection favours bi-stability or instability of both strategies can fall onto any of the possible evolutionary outcomes in the second scenario. These shifts are especially prominent in topologies such as the complete network where selection favouring bi-stability is a prevalent outcome, or the star network where selection often favours instability.

The distinctive nature of the star network is once again evident in the substantial variability of evolutionary outcomes observed in the non-rare interactive mutation scenario. This is attributed to the proximity of fixation probabilities to the neutral fixation value of $1/2$, which results in small quantitative changes having a significant impact on the qualitative outcomes. This phenomenon may be linked to the jump discontinuity reported in Erovenko et al. (2019) and mentioned in section 5.3.2, which occurs in the mutually-optimal staying propensities potentially leading to the dynamics taking on a decisive role as it is observed in figures 5.11 and 5.12. We see instances where cooperation evolves in regions where defectors consistently dominated under rare interactive mutations.

Furthermore, we have observed both surprising similarities and novel differences between the outcomes produced by different evolutionary dynamics, some of which emerged systematically across various topologies and mutation scenarios. We summarise and analyse them in the final section of this chapter in comparison to what the previous literature has suggested to us. We anticipate their influence to extend

beyond the scope of the specific population structure and mobility model utilised in this study.

5.4 Discussion

We present a comprehensive analysis of the variations obtained between six distinct evolutionary dynamics on the evolution of cooperation within structured populations following Markov movement. These dynamics were originally expanded in Pattni et al. (2017) to allow their application to a broader range of structured populations models, such as the ones introduced in Broom & Rychtář (2012). Our examination of these results under the three extreme network topologies studied in Erovenko et al. (2019) brought to light several key features of these evolutionary dynamics.

The most striking of these features is that the set of evolutionary dynamics analysed yields overall qualitatively similar results, indicating that network topology has a greater influence than the particular dynamics considered. The features that characterise evolutionary outcomes under each topology, some of which were already pointed out in Erovenko et al. (2019), are shown to hold across evolutionary dynamics. A deviation from this pattern was observed in the star network with non-rare interactive mutations, a scenario that was highlighted in both this study and in Erovenko et al. (2019) for its unique properties.

We observed the formation of two pairs of dynamics BDB/LB and DBD/LD equivalent within them. Their equivalence stems from the general underlying framework of multiplayer games in networks (Broom & Rychtář 2012), under which the evolutionary graph is calculated from the time any two individuals spend together, with time spent alone included as a self-replacement weight. The total time passed is the same for each individual, thus resulting in an isothermal graph and the reported equivalent pairs of dynamics (Pattni et al. 2015, 2017).

Moreover, the DBB and BDD pair of dynamics, and to a lesser extent the BDB/LB and DBD/LD pairs, sometimes showed similar values. The statistical study performed in Schimit et al. (2022) concluded that the dynamics within each of these pairs may result in equivalent fixation probability distributions under independent movement. While both pairs passed this test, the first pair exhibited a closer affinity than the second, a characteristic that appears to have been carried over into the results we obtained under a more complex Markov movement model.

However, the pervasive similarity of qualitative outcomes obtained under *all* dynamics came out as a surprising result, considering the substantial differences that some dynamics have shown in promoting cooperative behaviour in the past. In the original paper (Ohtsuki et al. 2006), the DBB dynamics (and BDD, by extension) showed that the viscosity of the evolutionary process on networks can lead to the evolution of cooperation without the need for other overlapping mechanisms to be present. This was in stark contrast to the results obtained under the BDB dynamics (and DBD, by extension), in which network structure alone was not sufficient for cooperation to evolve. This was later observed under the territorial raider model where individuals played a multiplayer Charitable Prisoner's Dilemma in a network (Pattni et al. 2017). In both of these models, replacement events and the interactions between individuals are characterised by their locality. The first assures that, compared to defectors, cooperators are more often surrounded by other cooperators, while the second guarantees that this generates an evolutionary advantage to cooperate if rewards are high enough.

The present Markov model presents a distinct picture from previous models, including the territorial raider model studied in chapters 3 and 4. Although replacement events maintain their locality (see section 5.2), the exploration time of $T = 10$ enables individuals to navigate the network contingent on whom they meet. On one hand, this partially suppresses the impact of structural viscosity on the fitness of individuals. On the other hand, the assortative behaviour that emerges under certain network topologies proves to be much more powerful in promoting cooperation, surpassing the impact of viscosity. These two factors suppress the exceptional significance of the DBB (and BDD) dynamics in ensuring the successful evolution of cooperation.

Instead, the small differences that persisted in the evolutionary outcomes under the six dynamics show another picture. The BDB/LB dynamics were found to promote the evolution of cooperation over a wider range of parameter values, while the DBD/LD dynamics did the same for the evolution of defection. A systematic comparison between the two pairs of dynamics revealed that cooperators had higher fixation probabilities in the first pair, while defectors had higher fixation probabilities in the second. This pattern held across all topologies and mutation scenarios, with only rare and isolated exceptions.

Although the difference was more pronounced when comparing those pairs of

dynamics, it was also present between the DBB and BDD dynamics. Together with the previous observation, this suggests that cooperation is overall favoured by selection when this acts during birth rather than death, regardless of whether this is the first or the second, or indeed referring to simultaneous events. According to previous results (Pattni et al. 2017), the replacement structure being symmetric and doubly stochastic should result in equivalent pairs of dynamics. However, this is only true when choosing a different replacement pair between the same types does not change the future fitness of individuals (Schimit et al. 2022), such as under complete networks or fixed fitness. In our results, fitness being highly variable surprisingly leads to the consistent reported differences within pairs of dynamics BDB/DBD, DBB/BDD and LB/LD, even under complete networks, indicating an effect which could be explored more extensively in future studies.

Another distinction between the dynamics is that in the second mutation case and for the fixation of cooperators in the first mutation case, the DBB and BDD consistently amplify selection compared to the other dynamics across topologies. This effect has been observed under the territorial raider model and is analysed in chapters 3 and 4. When selection acts during the second event, fitness and replacement weights become intertwined in the same probability. The replacement structure is often biased towards individuals of the same type, for example, when individuals spend a disproportionate fraction of time alone. In those cases, the DBB and BDD dynamics systematically favour the replacement of individuals with lower fitness by ones with higher fitness, thus acting as amplifiers of selection, when compared to dynamics where fitness and replacement structure are considered separately.

The only setting where the amplification effect was less pervasive was the fixation of defectors in the rare interactive mutation case. This is potentially associated with both mutants and residents having low staying propensities, leading to lower self-replacement weights and, therefore, a lesser bias towards same-type replacement. The star network serves as a notable limiting case, where both the mutant defector's and resident cooperator's staying propensity is 0.01, and under which defector fixation probabilities are the same for all dynamics, thus showing no amplification by these dynamics.

Further investigations on evolutionary models of finite structured populations could focus on the interplay between structure and assortative behaviour in promoting cooperation. The results obtained using this particular model highlight broader

121

features of models incorporating these aspects and should be taken into account accordingly. Nevertheless, the model of population structure and mobility introduced in Broom & Rychtář (2012) shows once again its flexibility. It offers the ability to create new theoretical tools and study specific evolutionary systems. The model is well-suited for analysing aggressive behaviour in territorial patches of biological populations. Additionally, it has potential in social sciences, such as in the study of labour market dynamics where employer networks could be viewed as territorial networks through which individuals move. It is our hope that this original modelling framework and all the advancements made thus far will provide valuable insights into real-world systems like these.

Chapter 6

Self-organisation of common goods usage in populations with Win-Stay, Lose-Shift-Good strategy[1]

6.1 Introduction

Common goods are resources that are available to multiple individuals but are susceptible to depletion because one individual's use reduces the amount available to others (Ostrom 1990). These typically include natural resources such as groundwater basins, grazing land, forests, air quality, and fisheries. However, their challenges are sometimes parallel to those of human-built resources which are available for collective use, such as roads, public transport systems and Internet services. Shared usage of such resources is pervasive in social systems making their study central to economics, social and life sciences. Given the finite nature of commons, several challenges arise from their usage, which under uncoordinated action may lead to the "tragedy of the commons" as described by Hardin (1968). As a result, the governance of these shared resources has become a crucial issue, extensively studied by Elinor Ostrom, in, for example Ostrom (1990), whose work in this area earned her the Nobel Memorial Prize in Economic Sciences.

---

[1]This chapter is based on a working paper done in collaboration with Dr Paolo Castagno, Professor Marco Ajmone Marsan, and Professor Vincenzo Mancuso.

Individuals wanting a given resource often have several options of commons available to them that may fulfil the same need. This raises new questions on how such systems can attain a sustainable distributed consumption and avoid scenarios of disproportionate usage, over-consumption and depletion of one of the commons while others remain available. In the context of grazing, foraging, and hunting, both animals and humans must decide whether to remain in a partially exploited land or move in search of new resources. These dynamics have contributed to the evolution of nomadic patterns, both in hunter-gatherer and pastoralist societies. Moreover, parallel problems emerge in industrialised societies. For instance, individuals have to choose daily which form of public transport to take or which road to drive on; institutions managing water distribution may need to choose which water resources to use; fishing companies have to decide the areas at which they will fish; and devices connected to mobile networks, such as mobile phones, have to choose to which computing facilities they will send their requests. The quality and/or availability of each of those resources decreases with the number of individuals simultaneously using them, thus conferring them some common properties.

The ideal free distribution (IFD) theory was originally developed by Fretwell & Lucas (1969) in the context of animal territorial behaviour, as briefly introduced in chapter 1. It predicts that individuals will distribute themselves across different resource patches to maximise their own benefit, assuming perfect knowledge and no movement costs. As a result, individuals spread in a way that equalises availability or quality across all used resources. The fact that the IFD strategy constitutes an evolutionarily stable strategy was later proven by Cressman & Křivan (2006). However, when individuals have minimal information about the current state of the system and in the absence of governing institutions, attaining a distributed usage over the available commons may be impossible to coordinate. In the systems above mentioned, coordination would require either a governing institution directing individuals on which option to use, constant communication between individuals, or free movement of individuals allowing for direct observation, all of which are sometimes impossible or, at the very least, costly.

In this chapter, we propose the extension of Win-Stay, Lose-Shift (WSLS) strategy to systems of usage and consumption of common goods. The original strategy is introduced in chapter 1 in the context of iterated social dilemmas, and its principle is similar to the one used in chapter 5 when exploring conditional movement

on networks. Individuals using WSLS strategy will consume a particular common good until they are unsuccessful or their experienced quality falls below a threshold, at which point they shift to a different good at random. In section 6.2, we show that the dynamics obtained in a population using this strategy lead to the self-organisation of distributed usage of commons. The equilibrium obtained leads to an overall high average experienced quality in the population without individuals nor central institutions storing, transmitting or processing any information. In section 6.3, we focus on the application of these results to Internet services and formalise the problem associated with server selection in mobile networks. In section 6.4, we formalise some of the theory on how individuals may act selectively towards different commons. In section 6.5, we consider hybrid systems where individuals adapt their patience to failure based on information, showing that significant improvements can be attained, achieving in some cases the optimal distribution of usage, something which is then confirmed in section 6.6, by the evaluation of the evolution of the system with adaptive individuals. The usage of the Win-Stay, Lose-Shift-Good strategy and the validity of the developed concepts can be extended to understand other distributed systems such as population distribution on grazing or foraging land, or to inform solutions to the governing of complex social systems such as usage of public transport or other technological common goods.

6.2 Win-Stay, Lose-Shift-Good

We consider a population of N_u users with an available set of N_g common goods which are denoted G_i, with $i = 1, 2, \cdots, N_g$. This system is represented in figure 6.1. We denote as Q_i the quality of common good G_i. The quality may relate to a quantifiable probability of having a failed or unsatisfactory attempt to use the good $Q_i = 1 - P_i^{(F)}$, where $P_i^{(F)}$ is the failure probability of good G_i, holding a value between 0 and 1. We consider the cases where probability of failure increases, and therefore quality decreases, with the number of current simultaneous users n_i of G_i. Note that $\sum_{i=1}^{N_g} n_i = N_u$. A failed attempt might happen due to reduced availability, overcrowding, general lower quality of experience, or active competition with other users. As mentioned in the introduction, some examples of these goods can be land for grazing or foraging, fishing or hunting areas, water supply systems, means of transportation, technological goods, or Internet services such as those offered by

mobile network operators.
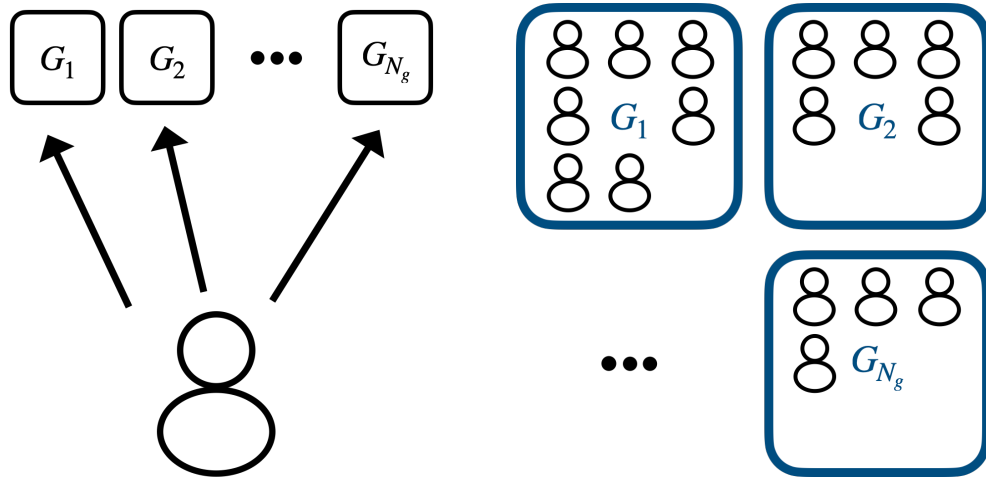
Figure 6.1: Representation of a system of common goods usage. On the left, individuals can choose which of the N_g goods they will use without any information besides their individual experience. On the right, the distribution of the population of individuals over the available goods.

Let us consider that the population is fully distributed and individuals have minimal information. They get no information about the characteristics of the common goods from neither one another nor central institutions, e.g. operators. They are only informed by the direct perception of the quality of the used good, also lacking information about the current number of users of the good.

In this context, we introduce an extension of WSLS to common goods usage, which we refer to by the same WSLS. Individuals do not interact directly with each other, but only with the good they have chosen to use. Under WSLS, individuals initially choose one of the available goods at random and stay there until they have a failed or unsatisfactory attempt of use. When the failed event occurs, they shift to one of the other goods at random. If in the particular system considered, individuals can't fail to use the commons, and instead they just have a lower experienced quality, then consider that they may set their own probability of shifting proportional to the experienced quality of the good.

Consider a large enough population of individuals using the described WSLS strategy. Each individual attempts to use the good of their choice at an average frequency of λ_u attempts per unit time. Let us assume that the quality of the good they are using changes slowly, and that their usage may have only an infinitesimal relative effect on the current number of users n_i of each good, given the large size of the population. This system can be modelled through the differential equations

determining changes in the number of users on each good:

$$\dot{n}_i = -\lambda_u \cdot n_i \cdot P_i^{(F)}(n_i) + \frac{1}{N_g - 1} \sum_{j \neq i} \lambda_u \cdot n_j \cdot P_j^{(F)}(n_j), \qquad (6.1)$$

where n_i is approximated to a continuous variable.

The first term on the right hand-side corresponds to the rate at which individuals have failed usage attempts and leave the common good G_i. The second term corresponds to the rate at which individuals have failed attempts at using other common goods and switch to G_i. This leads to the following equilibrium equations:

$$n_1 \cdot P_1^{(F)}(n_1) = n_2 \cdot P_2^{(F)}(n_2) = \ldots = n_{N_g} \cdot P_{N_g}^{(F)}(n_{N_g}). \qquad (6.2)$$

6.3 Application to Internet services

Mobile networks are wireless communication systems that enable users to connect and exchange data, such as voice, text, and Internet services through interconnected base stations. Connecting to such systems allows users to perform computations on in-network computing facilities, i.e. servers, which are essential to the implementation and use of Internet services. In those cases, active mobile users submit frequent requests to the network, which are then processed in the base stations and the associated network backhaul, and are then routed to a server for computing. The user can often choose the server where the request will be processed, however, with very limited information on them. Active mobile users form a population of individuals who have to choose between N_g options, only knowing their past experienced success with them. This makes this system suitable to test out the use of WSLS strategies. Figure 6.2 shows a schematic representation of this system.

6.3.1 Server quality and probability of failure

Servers have different characteristics, such as their computing power and their distance from the end user, that translates in service latency. Latency is defined as the delay between sending a service request and getting the corresponding response. The main components of latency are the time d_i for the request to arrive at the server, the processing delay at the server and the time d_i for the response to go from the server back to the user. Computing power refers to the ability of a server to
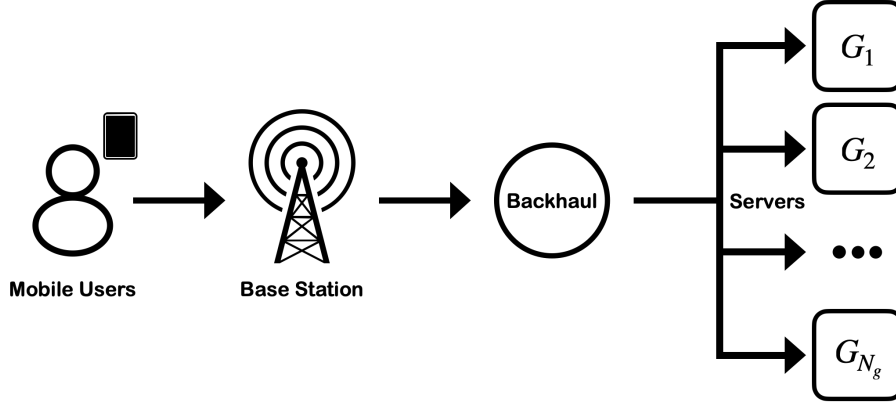
Figure 6.2: Server selection problem in Internet access as a system of common goods usage. A population is constituted of active mobile users who connect to the network through a base station. They have their connection attributed through the backhaul to their chosen server G_i out of N_g available options.

process tasks quickly and handle large amounts of data, which can be quantified by the number of requests per unit time they have the capacity μ_i to serve. We further denote the total system capacity as $\mu = \sum_i \mu_i$, representing the total number of requests it can serve per unit time. The system load is denoted as $\rho = N_u \cdot \lambda_u / \mu$ and represents the fraction of total requests per second over the system capacity.

The characteristics of servers determine how the probability of success of the submitted service requests, and therefore the quality of experience on that server, depends on the number of current users. Each server immediately processes requests that arrive to find it idle, and queues requests that arrive when the server is busy. Due to a finite buffer size, some requests can be lost because they arrive when the server's buffer is full (this is called a loss event and has probability $P_i^{(L)}(n_i)$ at server i when n_i users are accessing it), and others are discarded by the users when the results of the computation are returned to the requesting user too late to be useful (this is called an excessive delay event and has probability $P_i^{(D)}(n_i)$ at server i). Both cases lead to failed attempts at using the server. Based on the characteristics of each server, both the loss probability and the time delay distribution can be calculated analytically using standard queuing theory results as in Mancuso et al. (2022), which are partially described in section 6.3.2.

The outcomes of any two submitted requests are assumed to be independent and have failure probability that change slowly, like the number of users. The failure probability is obtained as $P_i^{(F)}(n_i) = P_i^{(L)}(n_i) + (1 - P_i^{(L)}(n_i)) \cdot P_i^{(D)}(n_i)$. This allows us to describe the system through equations 6.1 with equilibrium condition 6.2.

To validate these results, we present simulation results for WSLS strategies gen-

erated with a realistic simulator akin to the one used in Mancuso et al. (2022, 2023), which is further explained in the following section. The resulting evolution of the population distribution and server-specific probabilities of failure are presented together with the differential equation results in figure 6.3. These are obtained for values of the system load ρ ranging from 0.5 to 1.25. The results obtained through the simulator align with what predicted by the analysis of the dynamical system originally proposed.

(a) Population distribution evolution under $\rho = 0.5$. **(b)** Evolution of failure probability under $\rho = 0.5$.

(c) Population distribution evolution under $\rho = 1$. **(d)** Evolution of failure probability under $\rho = 1$.

(e) Population distribution evolution under $\rho = 1.25$. **(f)** Evolution of failure probability under $\rho = 1.25$.
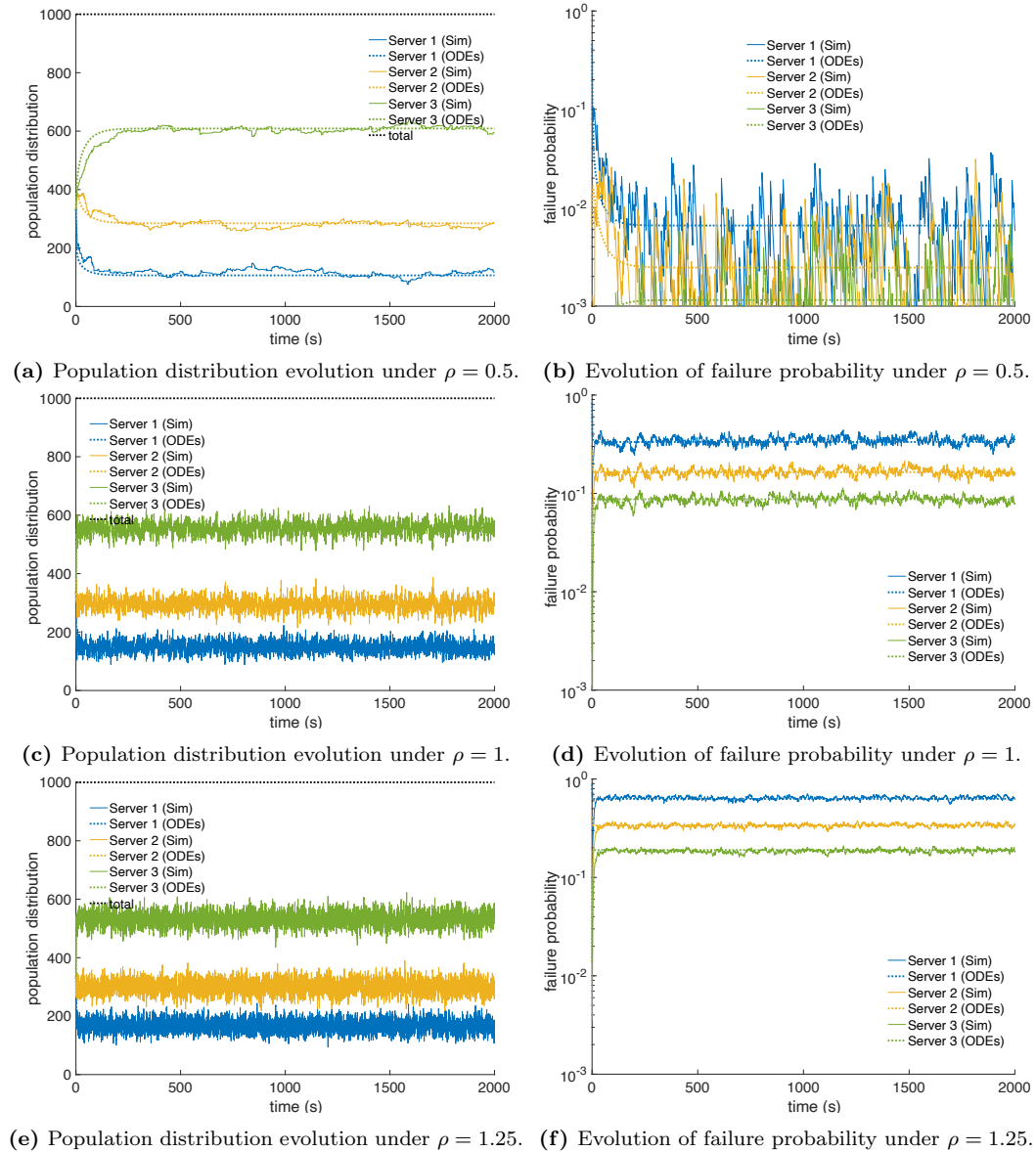
Figure 6.3: Simulation of a population of 1000 users using WSLS strategies on three available M/M/1 servers $G_i, i \in \{1, 2, 3\}$. We show the evolution of population distribution and server-specific average probability of failure for three different load values $\rho = 0.5, 1, 1.25$. Each server has the capacity to serve $\mu_i = \{100, 200, 400\}$ requests per second (reqs/s). The time between user and server is set as $d_i = \{10, 20, 30\}$ ms, and individuals' timeout $\tau = 100$ ms.

In particular, we observe that under all three load values, the result of the

evaluation shows the population distribution evolving to the theoretical value given by equation 6.2. In this equilibrium, a server with higher capacity holds more users and exhibits lower average probability of failure, whereas a server with lower capacity has fewer users and higher average failure probability. This suggests that the equilibrium slightly overflows servers with lower capacity, but because their usage rate is overall lower, this might have a low impact on the overall system probability of failure.

The stochastic oscillations around this equilibrium value are higher under higher system load, whereas convergence to this value and alignment with the ODE result (derived from equation 6.1) is slower under lower system load. Server-specific probability of failure shows lower noise under higher load, and a striking alignment with the long-term behaviour of the probability of failure in the computed ODE. However, low load leads to higher noise of the server-specific probability of failure, often leading to an overlap between the values.

6.3.2 Simulator

The model presented above is validated by comparing its results with a discrete-event simulator developed in Matlab. The simulator reproduces the arrival of requests from independent individuals to chosen servers, and tracks how individuals change server over time as a response to the observed performance of the server they use. In table 6.1, we have set the used parameters in the overall model and the values considered in the simulator.

We consider a population of N_u mobile users, in the literature described as "user equipment" (UE). Each UE connects to the same base station (BS), which is attached to the backhaul (BH) through which a set of N_g servers can be reached. As previously described, each individual issues on average λ_u requests per second (reqs/s) to their server of choice and at each time there are n_i individuals submitting requests on server G_i.

The time delay between a request being sent and its arrival at the chosen server G_i is denoted as d_i. These are considered to be the same for all individuals as they connect to the same base station. Each server G_i is modelled as a Markovian queuing system of the general form $M/M/c_i/k_i$. In such systems, requests from each user arrive independently following a Poisson process with average rate given by λ_u, so that the aggregate process of arrivals at server G_i is a Poisson process as well

Notation	Parameter	Values
N_u	Number of users	1000
N_g	Number of servers available	3
G_i	Servers	$\{G_1, G_2, G_3\}$
μ_i	Service capacity of server G_i	$\{100, 200, 400\}$ (servs/s)
μ	System service capacity	$\sum_i \mu_i = 700$ (servs/s)
ρ	System workload	$0.25; 0.5; 0.75; 1; 1.25$
λ_u	User service request rate	$\rho \cdot \mu / N_u$ (reqs/s)
c_i	Number of processors of sever G_i	1
k_i	Buffer size of server G_i	10 reqs
d_i	Time between individuals and server G_i	$\{10, 20, 30\}$ ms
τ	Service timeout	100 ms
$T_i^{(k)}$	Tolerance of type k on server G_i	$1; 5;$ adaptive
T_0	Initialised adaptive tolerance	$5; 10$
x_0	Initialised estimated failure probability	0
β	Learning rate	0.10

Table 6.1: Parameters used in the simulator of Internet access. For free parameters, we display the values used in the evaluations, whereas for dependent parameters we denote their dependence.

with an average arrival rate at server of $n_i \lambda_u$. Requests are queued and processed in first come, first served order (FCFS), according to the availability of processors, and the server eventually sends a message back to the individual that generated the request. The service time of arriving requests at server G_i follows an exponential distribution with average value μ_i^{-1}, where μ_i denotes the capacity of the server, i.e. the average number of requests they serve per second (servs/s). The number of available processors in the server is given by c_i, each of which can take one request at a time. We denote k_i as the buffer size, with $k_i - c_i$ being the maximum number of requests waiting to be served.

The value of the system load ρ is defined as the ratio between the total population request rate $N_u \lambda_u$ divided by the total service capacity of the system $\mu = \sum_i \mu_i$. Since the capacity of servers and population size is constant in the simulations, the system load is varied by changing the user service request rate λ_u. For example, when the system load is set as $\rho = 1$, the user service request rate is adjusted to 0.7 reqs/s.

At the beginning of the simulation, individuals select one server each, uniformly at random. Each individual starts to send a Markovian process of requests to the chosen server as described above. The simulator tracks individual failures, i.e., requests which are lost because they arrive when the buffer size is full or those whose

return delay (counted as the sum of the delay between individual and server and back and the service time at the server) exceeds the set timeout τ. The results shown in section 6.3 were obtained by considering that, after experiencing a single failed request, an individual switches to another server at random. However, in sections 6.4 to 6.6, each individual k will be assigned a set of tolerance values, $T_i^{(k)}, i = 1, \cdots, N_g$, one for each of the available servers. In those cases, the simulator counts individual failures. When the failure count of an individual k sending requests to server G_i hits the tolerance value $T_i^{(k)}$, the individual shifts to another server, and the failure counter is reset. The next server to be used is selected uniformly at random.

With the above, we can track the size of populations attached to each of the available servers, and observe how the failure probability of individuals and servers changes over time. In the case of adaptive adjustment of tolerance values, the simulator allows to track such adjustments and derive the average behaviour.

6.4 Introducing selective tolerance to common goods failure

We further consider a heterogeneous population with N_t types of individuals with subpopulations of size $N_u^{(1)}, N_u^{(2)}, \ldots, N_u^{(N_t)}$, with $\sum_k N_u^{(k)} = N_u$. Each type of individual k has a set of tolerance (or threshold) values $T_i^{(k)}$, which dictate how many failures they accept at each common good G_i before shifting to another one. We make the simplifying assumptions that the outcomes of any two usage attempts are independent and have the same failing probability $P_i^{(F)}(n_i)$, and that this value changes slowly with time. In this case, the number of attempts an individual makes until the number of failures achieves their tolerance value should follow a negative binomial distribution with average value $T_i^{(k)}/P_i^{(F)}(n_i)$. Therefore, the probability that a randomly chosen attempt of usage by an individual of a type k leads to shifting is equal to $P_i^{(F)}(n_i)/T_i^{(k)}$. Considering large subpopulations of types, we again describe the approximately continuous changes in the distribution of the types n_{ik}, i.e. the number of users of type k using each common good i, in differential terms:

$$\dot{n_{ik}} = -\lambda_u \cdot n_{ik} \cdot \frac{P_i^{(F)}(n_i)}{T_i^{(k)}} + \frac{1}{N_g - 1} \sum_{j \neq i} \lambda_u \cdot n_{jk} \cdot \frac{P_j^{(F)}(n_j)}{T_j^{(k)}}. \qquad (6.3)$$

The population will be at equilibrium when the following conditions are met for

all types k:

$$\frac{n_{1k} \cdot P_1^{(F)}(n_1)}{T_1^{(k)}} = \frac{n_{2k} \cdot P_2^{(F)}(n_2)}{T_2^{(k)}} = \ldots = \frac{n_{N_g k} \cdot P_{N_g}^{(F)}(n_{N_g})}{T_{N_g}^{(k)}}. \qquad (6.4)$$

Under a state of equilibrium, the different types of individuals will be distributed between the set of available commons depending not only on the probability of failure functions and the population size, but also on the values of tolerance to failure of the individuals in the population.

However, similarly to the original dynamical equilibrium given by equation 6.2, this might be a sub-optimal case. We introduce definition 1 of a distribution with optimal equalised quality, inspired by the ideal free distribution (Fretwell & Lucas 1969, Cressman & Křivan 2006), as an ideal organised distribution of common goods usage.

Definition 1. For a given population size N_u, we denote $\mathbf{n}^* = [n_i^*]$ respecting $\sum_i n_i^* = N_u$ as the optimal equalised quality distribution between used common goods. This can be defined as the distribution where the subset of used commons $\{G_i : n_i^* > 0\}$ respects

$$P_i^{(F)}(n_i^*) = y(N_u), \qquad (6.5)$$

where $y(N_u)$ is an increasing function of the population size and depends on the set of available common goods. The complementary subset of unused common goods $\{G_i : n_i^* = 0\}$ respects

$$\lim_{n_i^* \to 0} P_i^{(F)}(n_i^*) > y(N_u). \qquad (6.6)$$

A self-interested individual looking to maximise the success of its usage of commons would avoid those with higher failure probabilities. In strategic terms, under WSLS strategies with selective tolerance, they would increase their tolerance to failure for commons with lower failure probabilities and decrease their tolerance for higher probability ones. Due to the competing nature of the use of commons, lower usage of one of them decreases the failure probability at it. Therefore, self-interested individuals would have a positive impact on the overall system and push in the direction of optimal equalised quality and failure probabilities between different commons, even if the impact of a single individual is negligible. This will be further elaborated in section 6.6 by considering adaptive tolerance to failure. For now, let us start by noting that a population with one or more types of individuals

can achieve optimal equalised quality between common goods if individuals tune in their tolerance values accordingly. Theorem 4 describes this result.

Theorem 4. *The population distribution n_i^* corresponding to equalised quality between used common goods is attainable by any population using WSLS strategies if and only if they hold a set of tolerance vectors $T_i^{(k)}$ that respects*

$$\sum_{k=1}^{N_t} N_u^{(k)} \cdot \left(\frac{T_i^{(k)}}{\sum_j T_j^{(k)}} \right) = n_i^*. \tag{6.7}$$

Proof. The system of equations defined by equation 6.4 characterises the equilibrium conditions of a heterogeneous population. This means that the presence of a type k at any good can be written as a function of n_{1k}:

$$n_{jk} = n_{1k} \cdot \frac{P_1^{(F)}(n_1)}{T_1^{(k)}} \cdot \frac{T_j^{(k)}}{P_j^{(F)}(n_j)} \tag{6.8}$$

Therefore, the total number of individuals $N_u^{(k)}$ of type k is equal to the following at equilibrium:

$$N_u^{(k)} = \sum_j n_{jk} = n_{1k} \frac{P_1^{(F)}(n_1)}{T_1^{(k)}} \sum_j \frac{T_j^{(k)}}{P_j^{(F)}(n_j)}, \tag{6.9}$$

which can be rearranged as:

$$n_{1k} = N_u^{(k)} \cdot \frac{T_1^{(k)}/P_1^{(F)}(n_1)}{\sum_j T_j^{(k)}/P_j^{(F)}(n_j)}. \tag{6.10}$$

This relation is not valid just for $i = 1$ but for any i. Therefore, we can represent n_{ik} at equilibrium the following way:

$$n_{ik} = N_u^{(k)} \cdot \frac{T_i^{(k)}/P_i^{(F)}(n_i)}{\sum_j T_j^{(k)}/P_j^{(F)}(n_j)}. \tag{6.11}$$

We now hypothesise that there is a combination of vectors of strategic tolerance for which the population achieves the optimal distribution with equalised quality n_i^* (see definition 1). In that case, the tolerance vector of each type will relate to their

134

distribution in the following way:

$$n_{ik} = N_u^{(k)} \cdot \frac{T_i^{(k)}}{\sum_j T_j^{(k)}}. \tag{6.12}$$

However, n_i^* can be attained by different distributions of types over the goods. We thus sum over all types k to relate the population distribution and the tolerance vectors in the equalised quality state:

$$n_i^* = \sum_{k=1}^{N_t} N_u^{(k)} \cdot \frac{T_i^{(k)}}{\sum_j T_j^{(k)}}. \tag{6.13}$$

Therefore, any combination of types with tolerance vectors $T_i^{(k)}$ and size $N_u^{(k)}$ that respects the equation above will lead to an equalised equilibrium n_i^*.

$\square$

A population using WSLS strategies can always achieve the state with optimal equalised quality between common goods if they accordingly choose their selective tolerance to failure. Even though central coordination between individuals could lead to equalised quality, fully distributed populations composed of self-interested individuals might achieve the same by trying to minimise the failure probabilities of individual requests. We will explore this hypothesis by resorting to adaptive tolerance to failure in section 6.6.

Note that for any set of common goods, there might exist population sizes N_u for which the equal performance between used common goods will exclude completely a subset of the commons. In this case, for optimal equalised quality to be achieved, all types of individuals will necessarily have no tolerance to failure in that good $T_i^{(k)} = 0$, meaning that they will move from it without submitting requests. However, if there are no such common goods, hybrid populations with both selective and non-selective individuals might be enough to achieve the optimal equalised quality distribution.

6.5 Hybrid systems of selective common goods usage

Let us consider a system with only two types of individuals $k = 1, 2$. Individuals of type $k = 1$ do not distinguish between common goods, thus being non-selective individuals with constant $T_i^{(1)} = T, \forall i$. Individuals of type $k = 2$ have selective

tolerance values towards common goods $T_i^{(2)}$. We denote the fraction of selective individuals as $\gamma = N_u^{(2)}/N_u$.

Applying theorem 4 to the population defined by these parameters, we conclude that the equilibrium with optimal equalised quality is attained if selective individuals choose their tolerance to failure as to respect the following equations:

$$(1 - \gamma)N_u \cdot \frac{1}{N_g} + \gamma N_u \cdot \frac{T_i^{(2)}}{\sum_j T_j^{(2)}} = n_i^*. \tag{6.14}$$

Under conditions of equalised quality, certain common goods exhibit lower usage (n_i^*) compared to others. However, the original non-selective equilibrium, as expressed in equation 6.2 and recovered here under $\gamma = 0$, results in a suboptimal intermediate state: even though those commons have lower usage rates than others, the difference is insufficient to reach the ideal distribution, leading to higher failure probabilities on them. Consequently, selective individuals respecting equation 6.14 will correct this by avoiding commons which ideally would have lower usage and flock to the remaining ones.

However, the condition of equilibrium with equalised quality of equation 6.14 may only be fulfilled if γ is large enough. We denote the lowest usage of any of
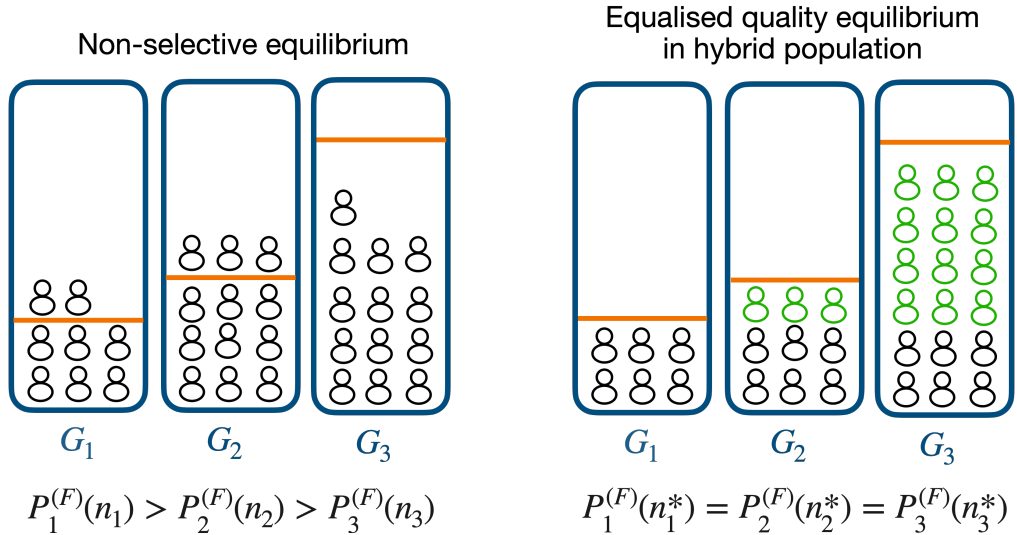
Figure 6.4: Distribution of a population over three common goods where $n_1^* < n_2^* < n_3^*$. On the left, we see this makes G_1 and G_2 overused and G_3 underused at the non-selective equilibrium given by equation 6.2. On the right, selective individuals are shown in green. Only non-selective individuals use G_1 in the hybrid system, which means that this was considered at $\gamma = \gamma^c$, i.e. the minimum proportion of selective individuals that allows the population to achieve equalised quality. At the equalised quality equilibrium, non-selective individuals use the three goods at the same rate. This is achieved through selective individuals avoiding G_1 and distributing over G_2 and G_3 respecting equation 6.16.

the common good at equalised quality as $n^*_{min} = \min_i(n^*_i)$, which could be zero. The critical value γ^c above which equalised quality can be attained is the one where selective individuals don't spend any time on the common good(s) corresponding to that minimum, i.e. $T^{(2)}_{\arg\min(n^*_i)} = 0$. Applying this to equation 6.14 replacing i by $\arg\min_i(n^*_i)$, we obtain the following expression for γ^c:

$$\gamma^c = \frac{N_u - N_g \cdot n^*_{min}}{N_u}. \tag{6.15}$$

An illustration of what happens under $\gamma = \gamma_c$ is given in figure 6.4. If $\gamma < \gamma^c$, that (those) good(s) will necessarily have a usage larger than n^*_{min}, thus never achieving equalised quality. To obtain equalised quality under $\gamma = \gamma^c$, selective individuals will have to distribute themselves among the remaining common goods by choosing the following values of tolerance to failure:

$$\frac{T^{(2)}_i}{\sum_j T^{(2)}_j} = \frac{n^*_i - n^*_{min}}{N_u - N_g \cdot n^*_{min}}, \tag{6.16}$$

thus forcing the remaining $(1 - \gamma^c)N_u$ non-selective individuals to distribute equally between common goods.

6.6 Adaptive tolerance to common goods failure

Let us consider self-interested individuals with selective tolerance values who are averse to the usage of common goods with lower quality and higher probability of failure. These individuals may adapt their tolerance to common goods failure to minimise reliance on such goods. We hypothesise that a population of such individuals will attain the equalised quality distribution n^*_i in an uncoordinated manner.

To test this hypothesis, we propose a learning method in the following subsection, allowing individuals to dynamically adjust their tolerance to failure of each common good. We then evaluate the results in the subsequent sections.

6.6.1 Adaptive tolerance method

We propose an adaptive tolerance method relying only on one's previous experiences with usage of the common goods, thus avoiding considering communication or direct

coordination between different individuals. Individuals perform an assessment of their own success rates and adapt their tolerance values accordingly.

For each focal individual k with adaptive tolerance:

- Define a vector for the estimated usage failure probability under each common good $x^{(k)} = \left(x_1^{(k)}, ..., x_{N_g}^{(k)}\right)$. Initialise it with values x_0 for all common goods.

- Define a vector for the strategic tolerance to failure under each common good $T^{(k)} = \left(T_1^{(k)}, ..., T_{N_g}^{(k)}\right)$. Initialise it with values T_0 for all common goods.

- The individual will choose a common good G_i at random and attempt to use it repeatedly until $T_i^{(k)}$ failures are achieved. We denote R as the number of usage attempts until the $T_i^{(k)}$ failures are achieved.

- The individual will update the estimated usage failure probability under that common good $x_i^{(k)}$ considering both the previous estimation and the new experienced average $T_i^{(k)}/R$:

$$x_i^{(k)} \longleftarrow (1 - \beta) \cdot x_i^{(k)} + \beta \cdot T_i^{(k)}/R,$$

where β is the learning rate.

- The individual will update the vector of strategic tolerance $T^{(k)}$ based on the information on vector $x^{(k)}$. Considering $l = \arg\min_j x_j^{(k)}$, if $x_l^{(k)} < x_i^{(k)}$ and $T_i^{(k)} > 1$, then they will update:

$$T_i^{(k)} \longleftarrow T_i^{(k)} - 1$$

$$T_l^{(k)} \longleftarrow T_l^{(k)} + 1.$$

- The individual will shift to one of the other common goods randomly and restart the usage phase.

6.6.2   Evaluation of adaptive tolerance in Internet Services

Resorting to the protocol described in the previous section, we evaluate the performance of populations composed of individuals with adaptive tolerance to common goods failure, whose results we present in figure 6.5. In the first panel, we observe that the population quickly reaches a distribution which has clear quick stochastic

138
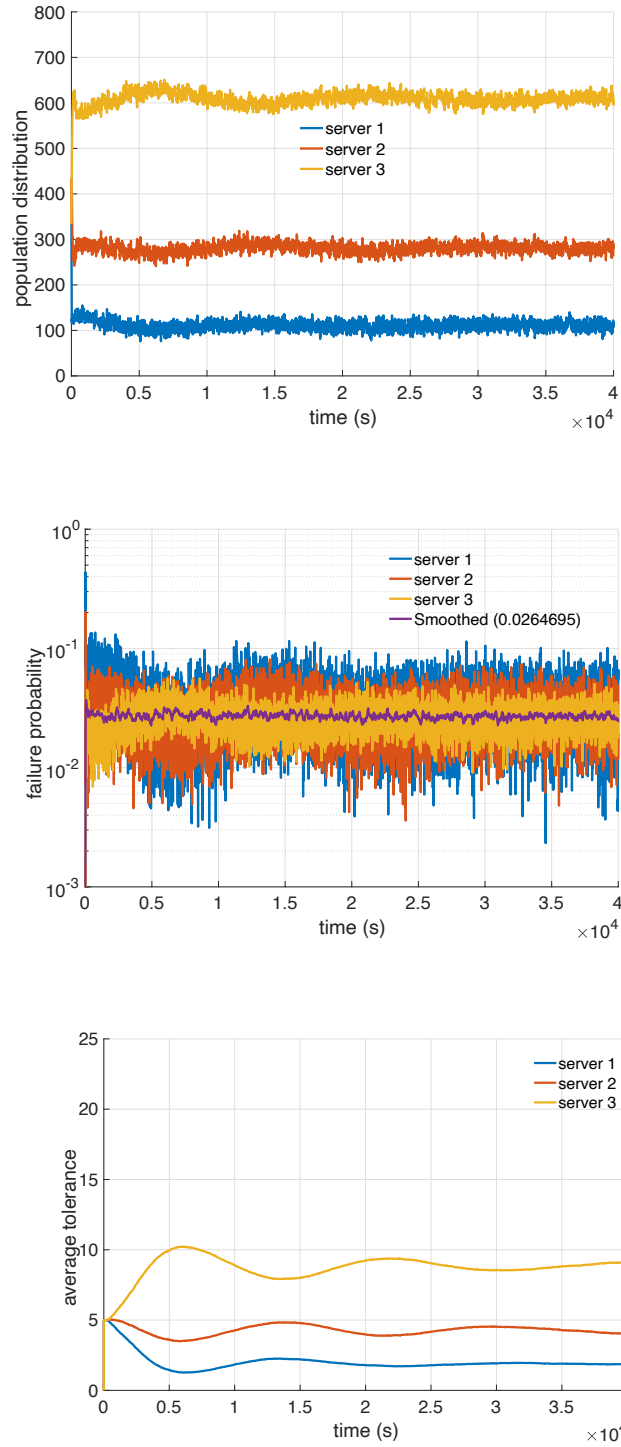
Figure 6.5: Simulation of a population of 1000 users using WSLS strategies with adaptive tolerance to common good failure on three available M/M/1 servers $G_i, i \in \{1, 2, 3\}$. We show the evolution of the population distribution, and of server-specific average probability of failure and average tolerance. Each server has the capacity to serve $\mu_i = \{100, 200, 400\}$ requests per second (reqs/s) and the system load was set at $\rho = 0.75$. The time between user and server is set as $d_i = \{10, 20, 30\}$ ms, and individuals' timeout $\tau = 100$ ms. Tolerance values are learned by each user independently. The value reported next to "Smoothed" in the plot with average probabilities of failure reports the average of the low-pass-filtered system-level failure probability, taken over the last 10% of samples.
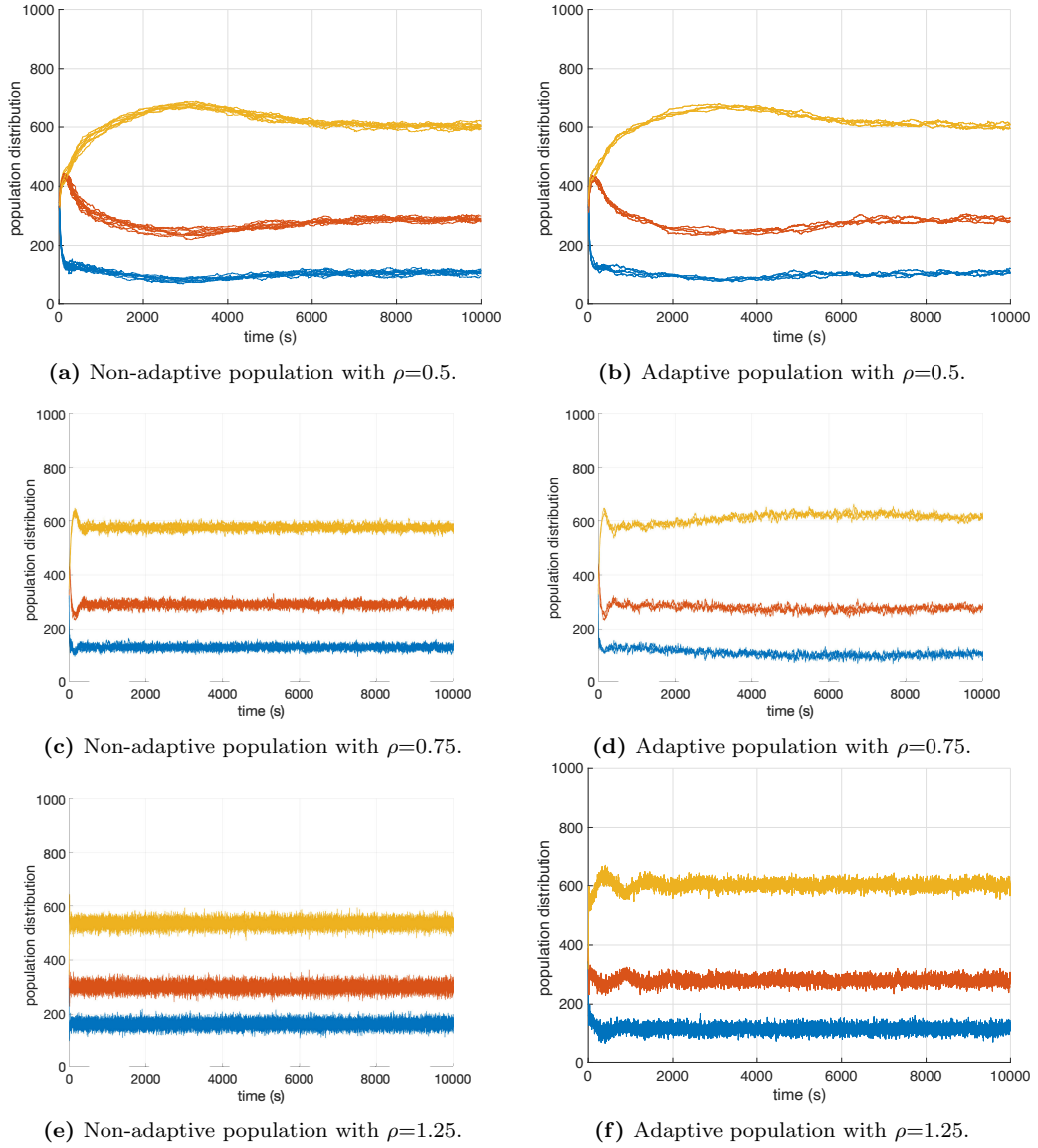
Figure 6.6: Superposition of multiple simulations of the evolution of non-adaptive (left) and adaptive (right) populations using WSLS strategies. The population of 1000 individuals is initially distributed at random over the three available M/M/1 servers $G_i, i \in \{1, 2, 3\}$. Non-adaptive individuals have a set tolerance to 5 failures, whereas adaptive individuals start from that and learn the tolerance values. We consider three different values (rows) of the system load $\rho = \{0.5, 0.75, 1.25\}$. Each server has the capacity to serve $\mu_i = \{100, 200, 400\}$ requests per second (reqs/s). The time between user and server is set as $d_i = \{10, 20, 30\}$ ms, and individuals' timeout $\tau = 100$ ms.

fluctuations and subtle long-term oscillations, but which is close to an equilibrium state. The oscillations are smooth and seem to dampen over time, suggesting that a stable population distribution equilibrium might be reached.

The second panel in figure 6.5 shows that the average probability of failure is reached quickly and doesn't vary much over time. Server-specific probabilities of failure have wider oscillations. Servers with lower capacity (1 and 2) tend to be overcrowded in the early stages of the evolution, likely due to the initialised val-

ues of individual tolerances being the same, thus initially leading to overall better performance at higher capacity server (3). This is corrected over time by the individual's independent learning process, which eventually overshoots the tolerance at the highest-capacity server 3, thus leading to small self-correcting oscillations – this can be seen in the third panel in figure 6.5. Through this whole process the overall system average performance is positive and the overlap of the curves shows that the system attains equalised quality.

Furthermore, in figure 6.6, we present an overlap of several evolution curves of the population starting randomly distributed. Each plot shows a different system load (rows) and the non-adaptive (left) and adaptive (right) systems compared. In those curves it is clearly observed that there isn't much of difference between the curves obtained at each scenario. Even if the population starts at different distributions, its evolution quickly moves into a determined distribution state. This distribution evolves with time, depending on two aspects shown before for the $\rho = 0.75$ adaptive case: the server-specific probability distributions and the individuals' independently learned tolerance values. These two aspects change slower with time, thus leading to slower average changes of the population distribution curve.

Finally, figure 6.6 additionally shows that the differences between the equilibrium population distributions in populations of individuals with non-adaptive and adaptive tolerances is quite small for lower loads than under overloading–in this case $\rho = 1.25$. This is so because failure probabilities are more sensitive to changes in usage rates under lower loads. After capacity is reached at $\rho = 1$, the probability distribution is often dominated by the limitations of the system to failure. The probability of failure will likely be larger than $1 - 1/\rho$, which is 20% under $\rho = 1.25$. Therefore, probabilities of failure become less sensitive to changes, which are maintained at the same order of magnitude, and we observe higher differences between the population distribution at equilibrium when individuals are non-adaptive and the equalised quality equilibrium attained by populations of adaptive individuals.

6.6.3 Evaluation for changing load

We evaluate the evolution of the population distribution and server-specific probabilities of failure when the load of the system changes with time. For this, we have simulated that the load is changed every hour to a value between $\rho = 0.25$ and $\rho = 1.25$, as reported in figure 6.7. The distribution over the servers and probabil-

(a) Distribution of non-adapting population.

(b) Failure probability in non-adapting population.

(c) Distribution of adapting population.

(d) Failure probability in adapting population.
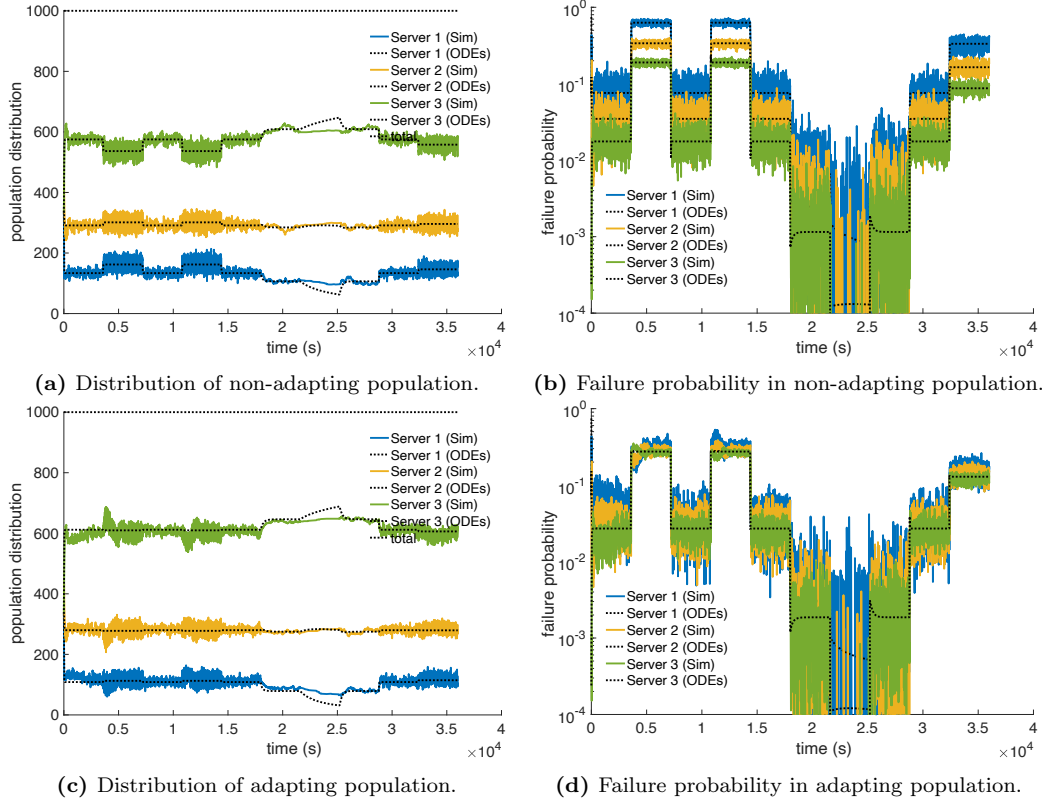
Figure 6.7: Simulation of a population of 1000 users using WSLS strategies with non-adaptive (top) and adaptive (bottom) tolerance values to common good failure on three available M/M/1 servers $G_i, i \in \{1, 2, 3\}$. The system load ρ is set to switch every hour according to the following sequence: 0.75, 1.25, 0.75, 1.25, 0.75, 0.5, 0.25, 0.5, 0.75. We show the evolution of population distribution (left) and server-specific average probability of failure $P^{(F)}$ (right). Non-adaptive individuals have a set tolerance of 5 failures, whereas adaptive individuals start from that and learn the tolerance values independently. The ODE results are obtained applying the set of equations 6.3. For adaptive populations, the ODEs were ideally altered by setting the ratio between the tolerance in different servers equal to the current ratio of server usage, guaranteeing that the system always heads towards equalised probability of failure. Each server has the capacity to serve $\mu_i = \{100, 200, 400\}$ requests per second (reqs/s). The time between user and server is set as $d_i = \{10, 20, 30\}$ ms, and individuals' timeout $\tau = 100$ ms.

ities of failure quickly change after load values are switched. In the non-adapting populations, server-specific failure probabilities stabilise at different values. These values can be well differentiated, especially for larger load values $\rho = 1.25$ where, as mentioned before, the general overuse effect of the system is present and average failure probabilities hit values close to 20%.

In comparison, the adapting population reaches remarkably identical failure probabilities between servers, with only small differences emerging from them. The small differences are likely to be coming from the fact that we have initialised tolerance values at 5, thus meaning that their learned values are limited between 1 and 13, with the sum of them being fixed at $5 \times 3 = 15$. This is a limit to the maximum difference between the learned tolerance values at each of the three servers, which

are slightly visible for large load values. Nonetheless, as noted before, the results obtained are remarkably close to equalised probability of failure between servers, and valid under a wide range of system load values and quick dynamic changes.

The theoretical ODE results typically match the average behaviour of the simulation results, apart from the intervals of extremely low system load $\rho = 0.25$. In such cases, the simulation statistics move much slower than the ODE predictions. This is likely associated with the fact that the ODE statistics themselves change slowly, instead of so abruptly as for all remaining load values.

6.7   Discussion

In this chapter, we have proposed an extension of the Win-Stay, Lose-Shift strategy to common good usage. As noted before, this has been studied in the context of other strategic settings, such as iterated, mobile, and spatial dilemmas. In the simplest form of the Win-Stay, Lose-Shift-Good strategy, individuals have no memory nor information about the system beyond the perceived outcome of their current usage of a common good. The emerging dynamics in a population of individuals using such strategies leads to stable equilibria where there is already a considerable improvement when compared to the outcome of random usage of common goods.

However, the introduction of selective tolerance to common goods failure allows populations to self-organise into an optimised usage distribution over the common goods. This state should be attained by a population of self-interested individuals acting to maximise the average perceived quality of the goods they use. This is confirmed by considering a relatively simple learning method used by individuals independently adapting their selective tolerances to failure. This multiagent reinforcement learning setting consistently led to the self-organisation of the population into the optimised usage distribution.

Furthermore, it has been shown with behavioural experiments and theoretically explained that the introduction of a small fraction of hardwired agents can lead to an overall improvement of observed prosocial behaviour in hybrid populations (Santos et al. 2019). More generally, hybrid social systems can trigger large-scale prosocial behaviour of humans and virtual agents (Oliveira et al. 2021). These ideas are relevant to the context of common good usage, where the introduction of selective adaptive individuals in hybrid systems with non-selective individuals

shows general improvements in the overall experienced quality. In this case, the interests of individual users are not at conflict, but instead represent a coordination problem. Selective adaptive individuals avoid overcrowding servers thus improving the experienced quality for everyone, both selective and non-selective individuals. Hybrid systems have the potential to reach the optimal scenario of equalised quality, or probability of failure, if their existence overcomes a critical value.

In the context of grazing and foraging, positive results have been observed in supporting the attainment of the IFD. Some examples are the size of spider cooperative colonies which grow and develop webs that allow them to maximise the total food intake per capita for the particular environment where they are (Yip et al. 2008). Another example is that of bumblebees, which frequent different patches of land selectively, depending on their flower density and nectar levels (Dreisig 1995, Abraham 2005). Our results highlight one of the possible strategies individuals in a population may have available to them when accessing different common goods under minimal communication and strong limitations on what they can observe at a given time. The results obtained under adaptive tolerance to failure show that indeed the ideal free distribution may be achieved, even under such limitations, as long as individuals are able to store information about previously used resources.

We considered the above framework in light of the server selection problem faced by mobile users accessing Internet services. This system is inherently dynamic and subject to heavy stochastic fluctuations. However, the results we obtained through a realistic simulation of this complex system verify our theoretical predictions of the equilibria achieved by individuals using WSLS strategies, with both non-selective and selective tolerance to failure. We further applied the simple individual adaptive method for selective tolerance to failure mentioned above, showing that populations of such individuals can reach the optimised usage distribution even when the usage rates are changed dynamically. The general WSLS strategy and the adaptive tolerance method can thus be applied to network usage protocols with the potential to improve overall general network accessibility, even in hybrid populations where users use a variety of protocols. As shown, in some cases, a critical mass of individuals with adaptive tolerance to failure can guarantee the optimisation of the experienced quality of the service for all individuals using the network.

The theoretical principles developed within this framework can be further considered in light of other multiagent systems of common good usage. In particular,

recent research of individual behavioural patterns in public transport services shows that people typically stick to the same commuting route on a regular basis (Costa et al. 2023), even when facing small disruptions (Marra & Corman 2023). If disruptions come from overcrowding, they can be locally regulated, for instance through collective rerouting strategies (Luan et al. 2024). However, upon experiencing successive failures with their typical route, they might switch to a different option on a daily basis. This makes this topic one of potential interest, where a better understanding of individual behaviour and their adaptive strategies may help developing better public transport usage regulating mechanisms.

Parallel approaches using population dynamics have been used in the context of water supply management in urban areas. These are complex interconnected systems, where controlling mechanisms guarantee the continuous access to water resources, which are available in different water storage units (Ramírez-Llanos & Quijano 2010a). This problem has been approached using population dynamics and, in particular, the IFD in order to find solutions that guarantee constant access to a water supply of dense urban areas (Ramirez-Llanos & Quijano 2010b).

In all these systems, if the distribution of usage changes quickly enough, the system might be temporarily malfunctional, as it was shown for internet services under abruptly variable loads. However, over time, a population of adaptive individuals are able to attain the adequate balanced equilibrium. We haven't considered more complex scenarios, where, for instance, the different options available to individuals have dynamically changing properties, or where new options become available or previous options become unavailable. This could be further explored in the future. However, the results just mentioned obtained for adaptive populations could indicate that the new equilibria would be reached over time. It is often the case that there are individual costs associated with shifting from the previously chosen common good, or even associated with storing information about usage history and adapting one's tolerance to failure accordingly. These possibilities could be explored in the future.

Chapter 7

Skill interaction-transmission dynamics and the evolution of new skills[1]

7.1 Introduction

Human societies are complex and highly cooperative structures built around the production of material goods, services, knowledge, culture, institutions, and more. For these to manifest, they require material resources and infrastructure, as well as the skills to apply them effectively. For example, the best equipped barber shop is nothing without a skilled barber and an atomic power station does not run safely without the people who are trained to operate it. Specialisation emerges from the division of labour in society, whose association with socio-economic success can be first attributed to Émile Durkheim in Durkheim (1984/1893). Some human skills, such as tool manufacturing, working of hard metals, agricultural production, or animal domestication, date back to pre-historic times. However, the complex nature of modern day societies generates new challenges.

Similarly to knowledge, skills can be seen as a cultural good (Derex & Morgan 2023) and, as such, they are typically transmitted through social learning in a process that can be analysed through the lens of cultural evolution (Cavalli-Sforza & Feldman 1981, Boyd & Richerson 1988). For example, crows learn to identify people who did them ill (Marzluff et al. 2010) and pass on their animosity to their mob

---

[1]This chapter is based on a working paper done in collaboration with Professor Rudolf Hanel.

and their offspring if the opportunity arises (Cornell et al. 2012). This is equally true for skills. In humans, early skill transmission typically occurs in the family or school context through repetition of actions (parent to child or educator to student). When moving to the labour market, skills are often learned by direct contact with peers who know how to perform certain tasks. Even though centuries apart, in pre-modern societies, the same peer skill transmission through joint labour was frequent, as artisans and farmers would typically join forces with unskilled individuals in order to produce something, while the unskilled would learn in the process.

In recent years, the fields of economic complexity and evolutionary economic geography have made striking advances in understanding the impact of having a skilled and knowledgeable workforce on industrial development and its geographic organisation. In particular, the presence of industrial skills and knowledge can be determinants of future economic growth (Hidalgo et al. 2007). The concept of industry relatedness (see a review in Hidalgo et al. (2018)) is used to explain why innovation is often geographically concentrated, as the skills and knowledge used in one industry can be transferable to others (Neffke et al. 2011). Leveraging higher-order effects on the inter-industry labour flow network reveals clusters of industries where there is a strong skill overlap that generates fertile ground for innovation (O'Clery & Kinsella 2022). Furthermore, in countries with high rates of migration, a high transfer of new skills happens often by contact with the specialised returning workforce (Hagan & Wassink 2016). In this context, the value of what a person knows depends on whom that person works with, and having co-workers with complementary qualifications is beneficial (Neffke 2019). These approaches highlight the positive impact that skill development and diversification can have on guaranteeing the success of local economies.

However, the adoption of new skills by individuals in these complex social systems should be itself dependent on the possibility that these may provide them with an individual benefit. If a set of skills is not attractive enough for newcomers to learn them, it will die out. New skills will similarly require a sufficient attractiveness in the environment where they appear, in order to be socially adopted and become a part of it. It is often the case that the evolution and survival of a new skill is dependent on the pre-existing presence of other skills and resources that make it evolutionarily possible. Therefore, in order to understand the evolution and extinction of skills which determines the course of human history, we need to consider the incentives

driving individuals to adopt them, as well as how these skills interact synergistically within the system.

In this chapter, we will explore the role of interactions between skilled and unskilled individuals in skill transmission in social systems, focusing on the characteristics that skills need to fulfil to successfully evolve. We will do so by developing a model of population dynamics, where individuals with different skills interact with each other and the outcome of their interactions determines their social fitness. In turn, this affects which skills are more likely to be adopted by unskilled individuals in their interactions with skilled individuals. We consider the outcome of an interaction between a set of skills to be fixed over time. This thus describes a static regime happening at a relatively fine time-scale where the (market) environment has not yet reacted by adapting the incentives to the adoption of skills.

In section 7.2, we formally define this framework for a population with an arbitrary number of distinct skills. Section 7.3 examines the properties required for a single skill to evolve within an otherwise unskilled environment, categorising them as sustainable, tentative, or unsustainable, according to the observed outcome. In section 7.4, we show that the evolution of a second skill in a population where another skill is already established is only possible if the second skill is sustainable or if there are synergistic properties between the two skills. In section 7.5, we explore the introduction of an Nth skill, by considering the previously stable equilibrium as a mean-field skill, against which the new Nth skill will compete for the existing unskilled individuals to enter the market. This allows us to leverage the insights from the 2-skill model and determine the success of any new skill as a function of its synergy with the previous equilibrium and the availability of unskilled individuals. In section 7.6, we explore the stable co-existence of skills and note that this is only possible due to the frequency-dependent nature of their success generated by the synergistic interaction between skills.

7.2   The skill interaction-transmission model

To study the evolution of new skills in social contexts, we have developed a model of skill transmission dynamics within interacting populations. To construct such a model, we have used elements of both epidemiological and game-theoretic modelling.

Let us consider a population of individuals, each of which has an associated

skill type S_i, where $i = 0, 1, ..., N$. We consider S_0 to define unskilled individuals. Individuals in the population interact with each other. After an individual with a skill S_i interacts with one with skill S_j, they will respectively receive a_{ij} and a_{ji}. This establishes their interaction as a matrix game with $N + 1$ types, with a general payoff matrix which is given by the following general matrix in table 7.1.

	S_0	S_1	S_2	$\dots$	S_N
S_0	a_{00}	a_{01}	a_{02}	$\dots$	a_{0N}
S_1	a_{10}	a_{11}	a_{12}	$\dots$	a_{1N}
S_2	a_{20}	a_{21}	a_{22}	$\dots$	a_{2N}
$\vdots$	$\vdots$	$\vdots$	$\vdots$	$\ddots$	$\vdots$
S_N	a_{N0}	a_{N1}	a_{N2}	$\dots$	a_{NN}

Table 7.1: Payoff matrix of a general N-skill game.

We make the assumption that the population is well-mixed and that, therefore, individuals interact with each other with equal frequency. In this case, we can use the mean field approximation to determine the fitness F_i of the individuals of each strategy type S_i. This is akin to the fitness considered in evolutionary games (Maynard Smith 1974, Broom & Rychtář 2013) and it depends on the density of each strategy S_i in the population, denoted s_i, which holds a value between 0 and 1. We thus calculate the fitness through an average of the payoffs received weighted by the density of each type they may interact with:

$$F_i(s_0, s_1, ..., s_N) = \sum_{j=0}^{N} a_{ij} s_j. \tag{7.1}$$

We consider the following dynamics ruling the distribution of types in the population. Unskilled individuals learn from skilled individuals of type S_i proportionally to how frequently they may interact with them (calculated from the density of that skill s_i) and to the potential fitness gain $(F_i - F_0)$ serving as their motivation to learn. The learning rate ϵ_i determines the time rate at which interaction of unskilled individuals with skilled ones S_i would lead to learning, for each unit of wealth gain. The frequency-dependent transmission rate couples the interactions between individuals to the dynamics. We further consider skilled individuals to leave the population at a rate γ_i. Therefore, the dynamics can be described by a set of N differential equations:

$$\frac{ds_i}{dt} = \epsilon_i \left[F_i(s_0, s_1, ..., s_N) - F_0(s_0, s_1, ..., s_N) \right] s_0 s_i - \gamma_i s_i. \tag{7.2}$$

Note that $\sum_i s_i = 1$, because variables s_i are densities as mentioned before, and therefore the above equation can be rewritten considering $s_0 = 1 - \sum_{i=1}^{N} s_i$.

This model can generate complex dynamics, incorporating elements of both epidemic and evolutionary game-theoretic models, which we will untangle in the following sections. In the 1-skill model, considering $\gamma = 0$ recovers the replicator equation presented in chapter 1. Even though some of the characteristics of the model are parallel to evolutionary game theory when more than one skill is considered and $\gamma_i = 0$ for all skills, the equivalence is no longer true. On the other hand, considering constant fitness differences between the skills eliminates the frequency-dependent character of transmission rates, leading to an N-strain SIS model.

We note that there are a set of natural scaled parameters which will be useful to treat this system, which are defined in table 7.2. The parameter x_i represents the loss rate of skill S_i, when everyone is unskilled ($s_0 = 1$). It will thus reflect the skill's potential to evolve in an unskilled population. Parameter σ_{ij} represents the synergy coefficient between two skills S_i and S_j. It encapsulates how much better (relative to unskilled individuals) it is for an individual with skill S_i to interact with another with skill S_j instead of interacting with an unskilled individual. This serves as a clear measure of supra-linear productive complementarity between different or the same skills. If $i = j$, then this is the intra-skill synergy (intraspecific skill synergy), whereas if $i \neq j$, then it represents the cross-skill synergy (interspecific skill synergy).

Parameter	Definition
Loss rate	$x_i = \dfrac{\gamma_i/\epsilon_i}{a_{i0} - a_{00}}$
Synergy coefficient	$\sigma_{ij} = \dfrac{a_{ij} - a_{0j}}{a_{i0} - a_{00}}$

Table 7.2: Natural scaled parameters of skill interaction-transmission model. The loss rate of a skill describes the rate at which this skill is lost from the population when it appears (and thus almost everyone else is unskilled). The synergy coefficient describes the potential payoff gain that a skill S_i has by interacting with another skill S_j, thus serving as a measure of their productive complementarity. Note that the synergy coefficient corresponds to the intra-skill synergy of S_i if $i = j$, and the cross-skill synergy between S_i and S_j if $i \neq j$. These intrinsic skill characteristics reflect their potential to evolve.

7.3 Interaction-transmission of one skill

Let us start by looking at the 1-skill version of this model. In this version, we consider individuals to be either unskilled S_0, or to possess a skill S_1. Individuals

interact with each other and receive the payoffs from table 7.3, depending on their own skill status and on that of the individual with whom they are interacting. This establishes their interaction as a 2×2 game.

	S_0	S_1
S_0	a_{00}	a_{01}
S_1	a_{10}	a_{11}

Table 7.3: Payoff matrix of a general 1-skill 2×2 game.

The fitness F_0 and F_1 can be calculated through the following, where we have used the fact that $s_0 + s_1 = 1$:

$$
\begin{aligned}
F_0(s_0, s_1) &= a_{00}s_0 + a_{01}s_1 = a_{00} + (a_{01} - a_{00})s_1, \\
F_1(s_0, s_1) &= a_{10}s_0 + a_{11}s_1 = a_{10} + (a_{11} - a_{10})s_1.
\end{aligned}
\tag{7.3}
$$

The dynamics can be described by a single differential equation (note that $s_1 = 1 - s_0$):

$$
\frac{ds_1}{dt} = \epsilon_1 [F_1(s_1) - F_0(s_1)]s_0 s_1 - \gamma_1 s_1
\tag{7.4}
$$

This can be simplified by considering the naturally scaled parameters of table 7.2 and the normalising constant $C_1 = \epsilon_1(a_{10} - a_{00})$. This leads to the following equation:

$$
\frac{ds_1}{dt} = C_1 s_1 \left[(1 - \sigma_{11})s_1^2 + (\sigma_{11} - 2)s_1 + (1 - x_1) \right].
\tag{7.5}
$$

7.3.1 Existence and stability of equilibria in 1-skill model

The fixed points of the dynamical system described by equation 7.5 are found by solving for

$$
\frac{ds_1}{dt} = 0.
\tag{7.6}
$$

There are three possible fixed points s_1^* to equation 7.5. We denote the trivial solution as $s_1^0 = 0$ and the non-trivial solutions as $s_1^{\pm}$, which take the form of

$$
s_1^{\pm} = \frac{(\sigma_{11} - 2) \pm \sqrt{(\sigma_{11} - 2)^2 - 4(\sigma_{11} - 1)(x_1 - 1)}}{2(\sigma_{11} - 1)}.
\tag{7.7}
$$

Let us assume $x_1 > 0$ and $\sigma_{11} > 0$. Whereas the trivial solution is always within the appropriate region of the parameter space ($0 \le s_1 \le 1$), the non-trivial solutions might not be depending on the values of x_1 and σ_{11}.

First of all, from equation 7.7, it can be shown that $s_1^{\pm}$ hold real values if the radicand in the square root is non-negative and therefore:

- $\sigma_{11} < 1$ or

- $x_1 < \dfrac{\sigma_{11}^2}{4(\sigma_{11} - 1)}.$

Then, focusing on the solution s_1^+, it can be shown that $s_1^+ \leq 1$ is always true and $s_1^+ > 0$ is true if $x_1 < 1$ or $\sigma_{11} > 2$.

Combining conditions above, s_1^+ is real and meets $0 < s_1^+ \leq 1$ if:

- $0 \leq \sigma_{11} < 2$ and $0 \leq x_1 \leq 1$, or

- $\sigma_{11} \geq 2$ and $0 \leq x_1 \leq \dfrac{\sigma_{11}^2}{4(\sigma_{11} - 1)}.$

Focusing now on the solution s_1^-, we derive that $s_1^- \leq 1$ if $\sigma_{11} > 1$. Moreover, it respects $s_1^- > 0$ if $\sigma_{11} < 1$ or if $\sigma_{11} > 2$ and $x_1 > 1$.

Combining the conditions, s_1^- is real and meets $0 < s_1^- \leq 1$ if:

- $\sigma_{11} \geq 2$ and $1 \leq x_1 \leq \dfrac{\sigma_{11}^2}{4(\sigma_{11} - 1)}.$

The second non-trivial fixed point s_1^- exists in the appropriate domain if s_1^+ does so as well. In those cases, it is clear that both the numerator and the first summing term in their solution values (equation 7.7) are positive. This means that for all existing solutions in the appropriate domain, we will have $s_1^- < s_1^+$.

Finally, each of these equilibria is stable if

$$\left. \frac{d^2 s_1}{dt^2} \right|_{s_1 = s_1^*} < 0. \tag{7.8}$$

We thus calculate the second derivative of s_1, which leads to the function below:

$$\frac{d^2 s_1}{dt^2} = C_1 \left[A(s_1) + s_1 \left(2(1 - \sigma_{11})s_1 + (\sigma_{11} - 2) \right) \right], \tag{7.9}$$

where $A(s_1)$ is the second order polynomial of s_1 inside the brackets of equation 7.5:

$$A_1(s_1) = \left[(1 - \sigma_{11})s_1^2 + (\sigma_{11} - 2)s_1 + (1 - x_1) \right], \tag{7.10}$$

which by definition respects $A(s_1^{\pm}) = 0$.

Regarding the trivial solution, it is clear that

$$\left. \frac{d^2 s_1}{dt^2} \right|_{s_1 = s_1^0} = C_1 A_1(s_1^0) = C_1 (1 - x_1), \tag{7.11}$$

152

meaning that s_1^0 is stable when $x_1 > 1$.

Furthermore, we show that

$$\left.\frac{d^2 s_1}{dt^2}\right|_{s_1 = s_1^{\pm}} = -C_1 s_1^{\pm}\left(2(\sigma_{11} - 1)s_1^{\pm} - (\sigma_{11} - 2)\right) = -C_1 s_1^{\pm}\left(\pm\sqrt{(\sigma_{11} - 2)^2 - 4(\sigma_{11} - 1)(x_1 - 1)}\right).$$

(7.12)

This means that when real and in the appropriate domain, the solution s_1^+ is always stable and s_1^- never.

7.3.2 Evolution of one skill

The analysis of existence and stability of equilibria in the 1-skill model shows that there are three solution scenarios. These solution scenarios are represented in figure 7.1 and correspond to three types of skills summarised as the following:

- Sustainable skill – leads to endemic equilibrium s_1^+. Occurs when skill loss rate is low enough ($0 \le x_1 \le 1$) regardless of the intra-skill synergy value σ_{11};

- Tentative skill – leads to bi-stability of endemic s_1^+ and unskilled s_1^0 equilibria. The point that splits the two basins of attraction is given by s_1^-. Occurs when skill loss rate is high but compensated by a high enough intra-skill synergy value ($1 \le x_1 \le \dfrac{\sigma_{11}^2}{4(\sigma_{11} - 1)}$ and $\sigma_{11} \ge 2$);

- Unsustainable skill - leads to unskilled equilibrium $s_1^0 = 0$. Occurs otherwise.

The dependence of the occurrence of each of three solutions on the values of x_1 and σ_{11} is shown in figure 7.2.

Since sustainable and unsustainable skills lead to scenarios with a single stable equilibrium, no temporary alterations of the payoff matrix in table 7.3 can change the final outcome of the system after alterations are lifted. However, when facing a tentative skill, the system can be pushed into the basin of attraction of the endemic state by moving the value of s_1 from below to above s_1^-, after which it naturally evolves to the endemic state s_1^+, even after alterations are lifted. A temporary reduction of the value of x_1 to one would achieve this. The payoff a_{10} could be increased until $a_{10}' = a_{00} + \epsilon_1/\gamma_1$ – an incentive to skilled individuals interacting with unskilled individuals. The minimum effort incentive would be one starting at a_{10}' such that would lead to $s_1^+ = s_1(t = 0)$.
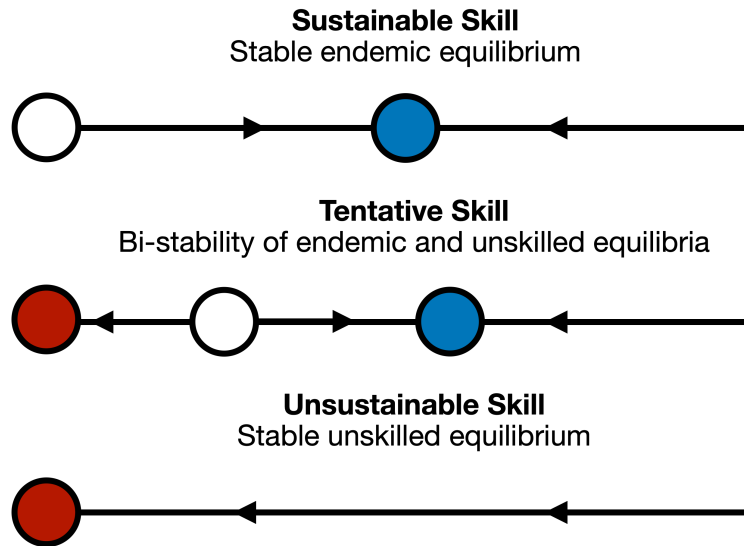
Figure 7.1: Equilibrium scenarios in 1-skill systems. The three horizontal axes represent the skill prevalence s_1, ranging from 0 to 1 (from left to right). Blue circles are used to denote stable endemic equilibria (s_1^+), red circles for stable unskilled equilibria (s_1^0), and white circles for unstable fixed points (s_1^-).
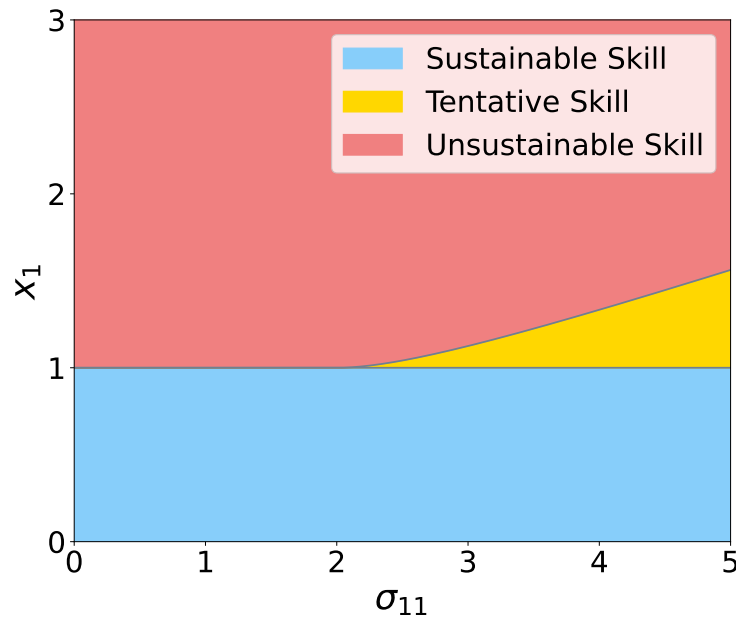
Figure 7.2: Equilibrium scenarios for values of skill loss rate (x_1) and intra-skill synergy (σ_{11}) in 1-skill systems.

7.4   Interaction-transmission of two skills

We take this question further and ask whether adding a new skill S_2 to the system would lead the system to collapse back into the previous equilibrium. Let us focus on the game matrix of interactions between the previous types and the type with the new skill:

	S_0	S_1	S_2
S_0	a_{00}	a_{01}	a_{02}
S_1	a_{10}	a_{11}	a_{12}
S_2	a_{20}	a_{21}	a_{22}

Table 7.4: Payoff matrix of a general 2-skill 3×3 game.

We adapt the previous 1-skill dynamics to two skills, by considering that individuals can only have one of the two skills, which can be taught to unskilled individuals and vanish as explained in the 1-skill model. This leads to the following equations for fitness and differential equations:

$$
\begin{aligned}
F_i(s_1, s_2) &= a_{i0}s_0 + a_{i1}s_1 + a_{i2}s_2 = \\
&= a_{i0} + (a_{i1} - a_{i0})s_1 + (a_{i2} - a_{i0})s_2
\end{aligned}
\tag{7.13}
$$

$$
\begin{aligned}
\frac{ds_1}{dt} &= \epsilon_1 s_1 \left[(F_1(s_1, s_2) - F_0(s_1, s_2))s_0 - \frac{\gamma_1}{\epsilon_1} \right] \\
\frac{ds_2}{dt} &= \epsilon_2 s_2 \left[(F_2(s_1, s_2) - F_0(s_1, s_2))s_0 - \frac{\gamma_2}{\epsilon_2} \right]
\end{aligned}
\tag{7.14}
$$

Working on these equations as done in the 1-skill case, we obtain differential equations 7.15. In these equations, we use the natural scaled parameters x_i and σ_{ij}, $i, j = 1, 2$ as defined in table 7.2. Parameters x_1 and x_2 are the scaled loss rates of skills S_1 and S_2. Parameters σ_{11} and σ_{22} represent the scaled intra-skill synergy coefficient and σ_{12} and σ_{21} the scaled cross-skill synergy coefficients.

$$
\begin{aligned}
\frac{ds_1}{dt} = C_1 s_1 \quad & [(1 - x_1) + s_1(\sigma_{11} - 2) + s_2(\sigma_{12} - 2) + \\
& + s_1 s_2(2 - \sigma_{12} - \sigma_{11}) + s_1^2(1 - \sigma_{11}) + s_2^2(1 - \sigma_{12})] \\
\frac{ds_2}{dt} = C_2 s_2 \quad & [(1 - x_2) + s_2(\sigma_{22} - 2) + s_1(\sigma_{21} - 2) + \\
& + s_1 s_2(2 - \sigma_{21} - \sigma_{22}) + s_2^2(1 - \sigma_{22}) + s_1^2(1 - \sigma_{21})] .
\end{aligned}
\tag{7.15}
$$

7.4.1 Existence and stability of trivial and single skill equilibria in 2-skill model

Position of equilibria

The trivial state of the system $(s_1^*, s_2^*) = (0, 0)$ is a always a fixed point to the set of equations 7.15. Besides this one, there are either 0, 1, or 2 equilibria on each of the edges (defined by $s_2 = 0$ and $s_1 = 0$). These equilibria are given by the following

equations.

$$s_2^* = 0 \text{ and } s_1^* = s_1^\pm = \frac{(\sigma_{11} - 2) \pm \sqrt{(\sigma_{11} - 2)^2 - 4(\sigma_{11} - 1)(x_1 - 1)}}{2(\sigma_{11} - 1)}. \tag{7.16}$$

$$s_1^* = 0 \text{ and } s_2^* = s_2^\pm = \frac{(\sigma_{22} - 2) \pm \sqrt{(\sigma_{22} - 2)^2 - 4(\sigma_{22} - 1)(x_2 - 1)}}{2(\sigma_{22} - 1)} \tag{7.17}$$

Intuitively, the value of s_1^* when $s_2^* = 0$ shown in equation 7.16, is the same as the one obtained in the single skill equilibrium in equation 7.7. In parallel, the value of s_2^* when $s_1^* = 0$, assumes the same form, apart from the swapped indices.

Conditions of existence of single skill equilibria

The conditions of existence of such equilibria are similar to the ones obtained under the 1-skill model. As such, we simply reproduce here some of the results already derived.

Single skill equilibrium with $s_2^* = 0$

There is one and only one equilibrium s_1^+ in the appropriate domain (between 0 and 1) in the $s_2 = 0$ edge apart from the trivial one, if the following condition holds:

$$0 \leq x_1 \leq 1 \tag{7.18}$$

The two equilibria from eq. 7.16 exist if the following condition holds:

$$\sigma_{11} \geq 2 \text{ and } 1 \leq x_1 \leq \frac{\sigma_{11}^2}{4(\sigma_{11} - 1)} \tag{7.19}$$

Therefore, there are no equilibria in that edge if the following condition holds:

$$(\sigma_{11} < 2 \text{ and } x_1 > 1) \text{ or } \left(\sigma_{11} \geq 2 \text{ and } x_1 > \frac{\sigma_{11}^2}{4(\sigma_{11} - 1)}\right) \tag{7.20}$$

Single skill equilibrium with $s_1^* = 0$

In a parallel way, there is one and only one equilibrium s_2^+ in the appropriate domain (between 0 and 1) in the $s_1 = 0$ edge (apart from the trivial one) if the following conditions holds:

$$0 \leq x_2 \leq 1 \tag{7.21}$$

The two equilibria from eq. 7.17 exist if the following condition holds:

$$\sigma_{22} \geq 2 \text{ and } 1 \leq x_2 \leq \frac{\sigma_{22}^2}{4(\sigma_{22} - 1)} \tag{7.22}$$

Therefore, there are no equilibria in that edge if the following condition holds:

$$(\sigma_{22} < 2 \text{ and } x_2 > 1) \text{ or } \left(\sigma_{22} \geq 2 \text{ and } x_2 > \frac{\sigma_{22}^2}{4(\sigma_{22} - 1)} \right) \tag{7.23}$$

Stability of equilibria

The Jacobian evaluated at a general point (s_1, s_2) of the parameter space is the following:

$$J(s_1, s_2) = \begin{bmatrix} J_{11}(s_1, s_2) & J_{12}(s_1, s_2) \\ J_{21}(s_1, s_2) & J_{22}(s_1, s_2) \end{bmatrix}, \tag{7.24}$$

where

$$
\begin{aligned}
J_{11}(s_1, s_2) &= C_1 \left(B_1(s_1, s_2) + s_1 \left[(\sigma_{11} - 2) + 2s_1(1 - \sigma_{11}) + s_2(2 - \sigma_{12} - \sigma_{11}) \right] \right) \\
J_{12}(s_1, s_2) &= C_1 s_1 \left[(\sigma_{12} - 2) + s_1(2 - \sigma_{12} - \sigma_{11}) + 2s_2(1 - \sigma_{12}) \right] \\
J_{21}(s_1, s_2) &= C_2 s_2 \left[(\sigma_{21} - 2) + 2s_1(1 - \sigma_{21}) + s_2(2 - \sigma_{21} - \sigma_{22}) \right] \\
J_{22}(s_1, s_2) &= C_2 \left(B_2(s_1, s_2) + s_2 \left[(\sigma_{22} - 2) + s_1(2 - \sigma_{21} - \sigma_{22}) + 2s_2(1 - \sigma_{22}) \right] \right)
\end{aligned}
\tag{7.25}
$$

where $B_1(s_1, s_2)$ and $B_2(s_1, s_2)$ are functions defined as the factors delimited by the brackets multiplying in the set of differential equations 7.15:

$$
\begin{aligned}
B_1(s_1, s_2) &= (1 - x_1) + s_1(\sigma_{11} - 2) + s_2(\sigma_{12} - 2) + \\
&\quad + s_1 s_2 (2 - \sigma_{12} - \sigma_{11}) + s_1^2(1 - \sigma_{11}) + s_2^2(1 - \sigma_{12}) \\
B_2(s_1, s_2) &= (1 - x_2) + s_2(\sigma_{22} - 2) + s_1(\sigma_{21} - 2) + \\
&\quad + s_1 s_2 (2 - \sigma_{21} - \sigma_{22}) + s_2^2(1 - \sigma_{22}) + s_1^2(1 - \sigma_{21})
\end{aligned}
\tag{7.26}
$$

It is useful to note that $B_1(s_1^* \neq 0, s_2^*) = 0$ and $B_2(s_1^*, s_2^* \neq 0) = 0$.

For a fixed point (s_1^*, s_2^*) to be stable, the Jacobian has to meet the following conditions: $Tr(J(s_1^*, s_2^*)) < 0$ and $\det(J(s_1^*, s_2^*)) > 0$. Based on the previous definition of the Jacobian matrix entries, this translates to the following:

$$J_{11}(s_1^*, s_2^*) + J_{22}(s_1^*, s_2^*) < 0 \text{ and } J_{11}(s_1^*, s_2^*)J_{22}(s_1^*, s_2^*) - J_{12}(s_1^*, s_2^*)J_{21}(s_1^*, s_2^*) > 0 \tag{7.27}$$

The trivial equilibria is described by $(s_1^*, s_2^*) = (0, 0)$. In that case, the entries of

157

the Jacobian are simplified and $J_{12}(0,0) = J_{21}(0,0) = 0$, which means that stability is guaranteed by $J_{11}(0,0) < 0$ and $J_{22}(0,0) < 0$, translating into:

$$x_1 > 1 \text{ and } x_2 > 1. \tag{7.28}$$

Edge equilibria also have one of the entries of the Jacobian equal to zero, namely $J_{12}(s_1^* = 0, s_2^*) = 0$ and $J_{21}(s_1^*, s_2^* = 0) = 0$. This assures that for edge equilibria, it is always true that $J_{12}(s_1^*, s_2^*)J_{21}(s_1^*, s_2^*) = 0$. This simplifies the conditions of stability from equation 7.27 to $J_{11}(s_1^*, s_2^*) < 0$ and $J_{22}(s_1^*, s_2^*) < 0$ if either $s_1^* = 0$ or $s_2^* = 0$.

Assuming that there is a single skill equilibrium $(s_1^*, s_2^* = 0)$ is in the appropriate domain, i.e., $0 < s_1^* \leq 1$, we study the conditions under which this equilibrium is stable.

The first condition $J_{11}(s_1^*, 0) < 0$ is met under $\sigma_{11} < 2$ for all solutions in the appropriate domain and under $\sigma_{11} > 2$ for solutions in the appropriate domain that respect $s_1^* > 1 - \dfrac{\sigma_{11}}{2(\sigma_{11} - 1)}$. Together, these conditions mean that the solution s_1^+ in the appropriate domain always meets $J_{11}(s_1^*, 0) < 0$, and s_1^- in the appropriate domain never does. Therefore, s_1^+ is potentially stable, depending on the sign of $J_{22}(s_1^+, 0)$ alone and s_1^- is always unstable.

Thus, it can be concluded that focusing on the edge with $s_2^* = 0$, if there is only one solution, this might be stable depending on the sign of one of the entries of the Jacobian. When there are two solutions on the that edge, the lowest one (corresponding to s_1^-) is never stable, while the largest one (corresponding to s_1^+) might be, depending on the sign of the same entry of the Jacobian.

Condition $J_{22}(s_1^+, 0) < 0$ is met and thus s_1^+ is stable under $\sigma_{21} < 2$ for the following cases:

- $0 < x_2 < 1$ for solutions in the appropriate domain that respect $s_1^+ > s_{1d}^+$;

- $1 < x_2$ for all solutions s_1^+ in the appropriate domain.

Condition $J_{22}(s_1^+, 0) < 0$ is met and thus s_1^+ is stable under $\sigma_{21} > 2$ for the following cases:

- $0 < x_2 < 1$ for solutions in the appropriate domain that respect $s_1^+ > s_{1d}^+$;

- $1 < x_2 < \dfrac{\sigma_{21}^2}{4(\sigma_{21} - 1)}$ for solutions in the appropriate domain that respect $s_1^+ > s_{1d}^+$ or $s_1^+ < s_{1d}^-$;

- $\dfrac{\sigma_{21}^2}{4(\sigma_{21}-1)} < x_2$ for all solutions s_1^+ in the appropriate domain.

We have used the following definition:

$$s_{1d}^{\pm} = \frac{(\sigma_{21}-2) \pm \sqrt{(\sigma_{21}-2)^2 - 4(\sigma_{21}-2)(x_2-2)}}{2(\sigma_{21}-1)} \tag{7.29}$$

The same analysis extends to the other edge with $s_1^* = 0$, where s_2^+ is stable if $J_{11}(0, s_2^-) < 0$ and s_2^- is never stable. The conditions obtained are the same as the ones above, with the simple switch of indices 1 and 2. This is also true for the definition of $s_{2d}^{\pm}$.

If we choose $\sigma_{21} = \sigma_{22}$, then $s_{1d}^+ = s_2^+$ (in parallel, if we chose $\sigma_{12} = \sigma_{11}$, then $s_{2d}^+ = s_1^+$). In those cases, the conditions of stability of the equilibrium on one edge become the exact conditions of existence of the equilibrium on the opposing edge, with an extra condition comparing the positions of the two. If there is only one equilibrium on the opposing edge, the equilibrium will be stable only if its position is larger than that of the other edge. If there are two equilibria on the other edge, then the equilibrium will be stable if larger than the largest one of the other edge, or lower than the smaller. If there are no equilibria on the other edge, then the equilibrium will be stable. However, if both conditions $\sigma_{11} = \sigma_{12}$ and $\sigma_{21} = \sigma_{22}$ are met, we recover the constant transmission rate model, which is analysed further in section 7.6.1.

7.4.2 Evolution of a second skill

Let us assume we start from the case with one skill S_1, and that its endemic equilibrium s_1^+ was reached – this can either correspond to the cases of a single skill endemic equilibrium or its bi-stability together with the unskilled equilibrium. Under which circumstances would adding a new strategy S_2 not result in immediate extinction of the new strategy? We now use the stability analysis of the previous equilibrium in the 2-skill space. The only cases under which there is no immediate extinction are the following:

$$0 < x_2 < 1 \text{ and } s_1^+ < s_{1d}^+, \tag{7.30}$$

$$\sigma_{21} > 2 \text{ and } 1 < x_2 < \frac{\sigma_{21}^2}{4(\sigma_{21}-1)} \text{ and } s_{1d}^- < s_1^+ < s_{1d}^+ \tag{7.31}$$

The first case corresponds to the second skill's loss rate x_2 being low enough. The second case corresponds to its synergy coefficient σ_{21} being high enough to compensate for its less advantageous loss rate with an extra condition the previously stable single skill equilibrium needs to respect one of the relations above.

Furthermore, we note that under the bi-stability case there is an unskilled equilibrium besides the endemic one when only S_1 is considered. Adding a second strategy S_2 de-stabilises the unskilled equilibrium in the first condition above, but not in the second.

7.5 Evolution of an Nth skill

Let us consider adding an Nth skill to a complex system with $N-1$ other skills. This system will have N independent variables $s_i, i = 1, 2, ..., N$. The new skill will grow if its respective differential equation evaluated at a first-order perturbation of the previous skill equilibrium $(s_1^*, s_2^*, ..., s_N = 0)$ is positive. Based on equation 7.2, this will happen if:

$$[F_N(s_1^*, s_2^*, ..., s_N = 0) - F_0(s_1^*, s_2^*, ..., s_N = 0)] s_0^* > \gamma_N/\epsilon_N. \qquad (7.32)$$

The left hand-side of the equation above can be interpreted as the fitness difference between new skilled and unskilled individuals against a mean-field skill equilibrium. By replacing the fitness by their respective expressions given by equation 7.1, we get the following condition:

$$\left[\sum_{j=0}^{N-1} a_{Nj} s_j^* - \sum_{j=0}^{N-1} a_{0j} s_j^* \right] s_0^* > \gamma_N/\epsilon_N. \qquad (7.33)$$

We join the two sums, and isolate the term $j = 0$, getting the following equivalent condition:

$$\left[\sum_{j=1}^{N-1} (a_{Nj} - a_{0j}) s_j^* + (a_{N0} - a_{00}) s_0^* \right] s_0^* > \gamma_N/\epsilon_N. \qquad (7.34)$$

Dividing all terms by $(a_{N0} - a_{00})$ and using the definition of the scaled skill loss rate and synergy coefficient from table 7.2, we obtain the following condition:

$$\left[\sum_{j=1}^{N-1} \sigma_{Nj} s_j^* + s_0^* \right] s_0^* > x_N. \qquad (7.35)$$

To simplify the condition above, let us denote as Ω_N the scaled synergy between the Nth skill and the skills in the pre-existing equilibrium, ignoring interactions with unskilled individuals:

$$\Omega_N = \sum_{j=1}^{N-1} \sigma_{Nj} \cdot s_j^* = \sum_{j=1}^{N-1} \frac{a_{Nj} - a_{0j}}{a_{N0} - a_{00}} \cdot s_j^*. \qquad (7.36)$$

This thus means that a new skill can only de-stabilise the previous equilibrium if and only if:

$$\Omega_N > \frac{x_N - s_0^{*2}}{s_0^*} = \frac{x_N}{s_0^*} - s_0^*, \qquad (7.37)$$

where Ω_N is the synergy between the Nth skill and the pre-existing equilibrium and s_0^* is the pre-existing unskilled level. This reflects the fact that new skills may only destabilise a previous equilibrium if they do well enough when interacting with the population and if there is a large enough pool of unskilled individuals allowing them to gain traction in the population.

In the 2-skill model, the condition is equivalent to:

$$\sigma_{21} > \frac{x_2 - \left(1 - s_1^+\right)^2}{s_1^+ \left(1 - s_1^+\right)}, \qquad (7.38)$$

which leads to the conditions presented in section 7.4.2.

7.6   Stable co-existence of skills

We have explored the conditions under which new skills may evolve for three cases: when there are no pre-existing existing skills; when there is one pre-existing skill; or when there are already $N - 1$ skills present. We now focus on assessing whether the system may evolve into a stable equilibrium where different skills co-exist.

7.6.1   Systems of two skills with constant transmission rates

Let us consider for a moment the simplifying assumption that skill transmission rates are constant in an N skill model. This is obtained by setting the payoff values received by each skill as independent of who they are interacting with. In this case, we can represent the payoffs received by each skill as $a_i = a_{i0} = a_{i1} = ... = a_{iN}$, thus eliminating interaction-dependent transmission rates. The fitness of each individual is now independent of the state of the population and equal to $F_i = a_i$.

In the 2-skill model, the differential equations become:

$$\frac{ds_1}{dt} = \epsilon_1(a_1 - a_0)s_1 s_0 - \gamma_1 s_1,$$
$$\frac{ds_2}{dt} = \epsilon_2(a_2 - a_0)s_2 s_0 - \gamma_2 s_2. \tag{7.39}$$

This system has one trivial fixed point at $(s_1^*, s_2^*) = (0,0)$. This will be stable and the only equilibria if and only if $x_1 \geq 1$ and $x_2 \geq 1$. There is an equilibrium with $s_2^* = 0$ at $(1 - x_1, 0)$ if $x_1 < 1$. Similarly, there is an equilibrium with $s_1^* = 0$ at $(0, 1 - x_2)$ if $x_2 < 1$. If there is only one edge equilibrium, that will be a stable one. If there are two, the one with lowest loss rate x_i will be the stable one. The case where $x_1 = x_2 < 1$ will lead to a stable solution line between the two stable points $(1 - x_1, 0)$ and $(0, 1 - x_2)$. This means that for us to have a stable equilibrium with co-existence of skills under constant transmission rates, the skills need to be indistinguishable. This raises the question: do interaction-dependent transmission rates allow for the stable co-existence of skills?

7.6.2 Stable co-existence of two skills

To explore the evolution of stable co-existence of two skills, we assess the cases in which there are no stable unskilled or single skill equilibria. In those cases, there is necessarily a resulting stable equilibrium of co-existence or a stable cycle. Let us study the combination of conditions that leads to these cases.

As previously identified in section 7.4.1, the unskilled equilibrium is stable when both $x_1 > 1$ and $x_2 > 1$. Therefore, at least one of the skills needs to be a sustainable skill as per the definition provided in section 7.3. This necessarily excludes combinations of two tentative skills, two unsustainable skills or one tentative with one unsustainable skill, cases which will likely lead to a single unskilled equilibrium, bi-stability or tri-stability. From what was explored, no co-existence equilibrium was found in such combinations. This way, there are three possible combinations of types of skills that may lead to stable co-existence, as shown in figure 7.3. In those cases, for the fixed points on the edges (of sustainable and tentative skills) to be unstable, further conditions will be necessary.

One of the possible combinations that can lead to stable co-existence is two sustainable skills. This means that they both have low loss rates ($0 < x_1 < 1$ and $0 < x_2 < 1$). In this case, the two single skill equilibria are destabilised under an

(a) Dynamics under two sustainable skills (S_1 and S_2).

(b) Dynamics under a sustainable skill (S_1) and an tentative skill (S_2).

(c) Dynamics under a sustainable skill (S_1) and an unsustainable skill (S_2).
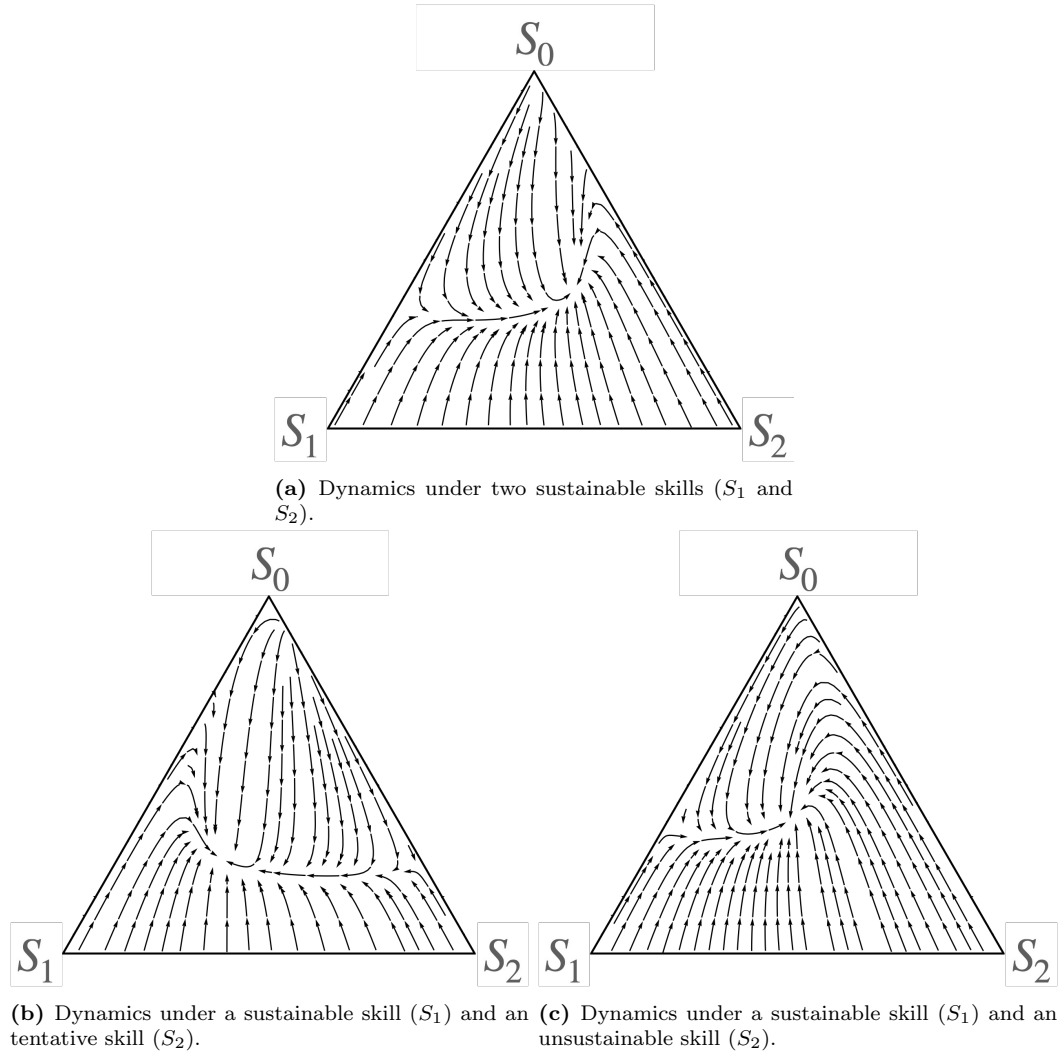
Figure 7.3: Representation of the dynamics for three different combinations of skill strength in the two skill model for which stable co-existence emerges.

additional condition ($s_1^+ < s_{1d}^+$ and $s_2^+ < s_{2d}^+$). This scenario is represented in figure 7.3a. This is a parallel case to the one mentioned under constant transmission rates, but where the skill interaction-transmission model explains the emergence of a single stable solution with co-existence of skills.

Alternatively, we may have a combination of two skills, where one is sustainable and the other is either tentative (figure 7.3b) or unsustainable (figure 7.3c). Let us say that $x_1 < 1$ and $x_2 > 1$. This means that, when alone, skill S_1 has an endemic equilibrium and S_2 either leads to bi-stability or an unskilled equilibrium depending on its intra-skill synergy value (σ_{22}). We focus on the two cases below.

If the intra-skill synergy of the second skill is high enough ($\sigma_{22} > 2$ and $\sigma_{22}^2/(4(\sigma_{22}-1)) \geq x_2$), then when alone it leads to bi-stability of S_2. Combining these two skill types destabilises the endemic equilibrium of the tentative skill S_2 under an addi-

tional condition $(s_2^+ < s_{2d}^+)$. The endemic equilibrium of the sustainable skill S_1 will be destabilised if the second skill has a high cross-skill synergy with the first $(\sigma_{21} > 2$ and $\sigma_{21}^2/(4(\sigma_{21} - 1)) > x_2)$, together with a further condition $(s_{1d}^- < s_1^+ < s_{1d}^+)$. Essentially, tentative skills combined with sustainable skills can survive in the stable co-existing equilibrium shown in figure 7.3b if and only if the tentative skill has a good cross-skill synergy.

The third dynamics represented in figure 7.3c corresponds to the combination of a sustainable skill S_1 with an unsustainable skill S_2. This case is particularly interesting as S_2 can never survive alone due to high loss rate $(x_2 > 1)$ and low intra-skill synergy $(\sigma_{22} < 2$ or $\sigma_{22}^2/(4(\sigma_{22} - 1)) < x_2)$. However, in combination with a sustainable skill S_1 with whom it has a high cross-skill synergy $(\sigma_{21} > 2$ and $\sigma_{21}^2/(4(\sigma_{21} - 1)) > x_2)$, and with a further additional condition $(s_{1d}^- < s_1^+ < s_{1d}^+)$, it can rise out of inexistence and into a stable co-existence scenario.

7.7 Discussion

In this chapter, we explored the evolution and co-existence of new skills in populations. We developed a model where the interaction and transmission of skills are interdependent. Individuals with a given skill interact with each other and produce something based on that interaction. Unskilled individuals may learn one of the skills from the individuals with whom they interact, depending on the frequency and benefits of the interactions.

Single skills were categorised as sustainable, tentative, or unsustainable, depending on the evolutionary outcome observed in the absence of other skills. Sustainable skills always lead to a stable endemic equilibrium. This occurs if a skill has a low loss rate, which can be guaranteed by a sufficiently high payoff improvement working as an incentive to learn the skill. Tentative skills are those which lead to bi-stability of endemic and unskilled equilibria, and occur when the loss rate is high but compensated by a high enough intra-skill synergy value. In these cases, temporary incentive schemes may work to assure the population is moved to the basin of attraction of the desired endemic equilibrium. Unsustainable skills are those with a single stable unskilled equilibrium, where no temporary incentives can guarantee their evolution.

A second skill introduced in a previous single skill equilibrium may destabilise it if and only if the second skill's loss rate is low enough, or if its cross-skill synergy is

high enough to compensate a higher loss rate. Some of these insights were extended to the introduction of an Nth skill into a system in an equilibrium with $N-1$ other skills. A new skill can always destabilise a pre-existing skill equilibrium if its synergy with the mean-field skill of that equilibrium is large enough. The synergy threshold is lower if the pool of unskilled individuals in the previous equilibrium is high. This is reasonable as new skills compete with the previous ones to be adopted by the same unskilled individuals. A low loss rate guarantees a lower threshold as well, even a potentially negative one, highlighting that the skill intrinsic characteristics (dependent only on their skill payoff improvement in an unskilled population) can also be enough to destabilise previous equilibria.

The stable co-existence of two skills happens for different combinations of skill types. We show that there are three different combinations which may lead to no stable single skill or unskilled equilibria, thus assuring the existence of a stable co-existence equilibrium (or potentially a limit cycle, which was never observed). We show that stable co-existence of two sustainable skills is easily observed, due to their low loss rates. Moreover, tentative and unsustainable skills, i.e. skills with high loss rates, can also evolve to co-existence if they are facing a sustainable skill with whom they have a high cross-skill synergy value. These insights highlight once again two main points. Firstly, the intrinsic value (defined by their loss rate) of a skill may be a good determinant of its evolution. However, it is not the only one, as its intra-skill synergy (in the absence of other skills) or its cross-skill synergy (when combined with sustainable skills) can make up for their high loss rates and guarantee their evolutionary success.

In this chapter, we show that skills compete for the exact same pool of resources–in this case the unskilled individuals in the population–and still reach stable co-existence. This is contrary to the common wisdom of ecological systems set out by the competitive exclusion principle as formalised by Hardin (1960). In a system with two skills, this outcome mainly relies on the existence of sustainable skills or cross-skill synergies. In systems with more than two skills, adding new skills with those characteristics guarantees the destabilisation of the previous equilibrium, but not necessarily the establishment of new higher-order equilibria with stable co-existence. It could, alternatively, lead to the collapse of previous co-existence states. This possibility would be in agreement with the idea that ecological systems become more unstable as their complexity increases (May 2019/1973), which has been further

investigated in the context of economic systems (Moran & Bouchaud 2019). Would a more complex co-existence equilibrium be more stable to the introduction of new skills or is there a maximum skill capacity that stable states can have? This could be assessed by considering the iterated introduction of random new skills on the system and observing the successive transitions between stable co-existence states and the vanishing of new and old skills. We are interested in whether we would observe the increasing complexity of the stable skill landscape increase over time or its iterated collapse and rebirth.

Throughout this chapter, we used the assumption that the outcome of the interaction between a given combination of skills is fixed, and does not change dynamically. However, in the context of interactions between productive skills, this reflects a static regime where the economical environment has not yet reacted. The value of production of a given good in society can be highly dynamic and, for example, the lack of skilled individuals in a particular trade may increase the value produced by skilled individuals in comparison to the value produced by unskilled ones. The study of these dynamics could be done considering the co-evolution of the value of the produced good in relation to the average skill level in the population, leaving behind the game-theoretic nature of our model, and associating frequency-dependence with a supply-demand function. However, the present model focused on the synergistic relation between skills and on their effects on skill evolution, for which a game-theoretic model was ideal. Our framework could be extended to include other exogenous factors which may change the payoff matrix of the interaction between skills over time, thus modifying the relative production value of acquiring a skill.

We also made the assumption that individuals interact with each other in the population with equal frequency. However, unskilled individuals might have an interest in interacting more often with those with a skill which they would benefit the most from learning. Alternatively, they might be interested in interacting with those who guarantee the highest immediate payoffs. Skilled individuals may also prefer to interact with those possessing the skills with best cross-skill synergy, and potentially form skill bubbles. Partner choice preferences such as these could be considered in the present model, namely by resorting to adaptive networks previously used in the context of evolutionary game-theoretic models (Pacheco et al. 2006b,a). These have the potential to explain the clustered way in which related skills and industries emerge in productive economies, as it has been reported in the economic

complexity literature (O'Clery & Kinsella 2022).

Chapter 8

Conclusions

In this thesis, we have leveraged a wide range of tools from evolutionary game theory to develop models of population dynamics and advance theories of social behaviour. The work presented a natural progression of complexity of social interactions. Chapter 1 introduced the relevant pre-existing models of evolutionary games. In chapter 2, we elaborated on the effects of population size in the evolution of strategies of pairwise games in well-mixed populations. The following chapters 3, 4, and 5, constitute the core of this thesis, exploring evolutionary models of cooperation in multiplayer social dilemmas, where both structure and mobility are considered in various forms. In the remaining chapters 6 and 7, we developed dynamical models of infinite populations where game-theoretic concepts were combined with other theories, namely foraging and epidemiological models. We apply such models to particular real-world problems such as systems of Internet service accessing and transmission of productive skills. In the discussion sections of each chapter of this thesis, we propose future research directions which may further advance our understanding of social behaviour and its applications.

A major part of these advances focused on understanding fixation processes of new strategic types on finite populations for broad classes of games. In chapter 2, we provide a systematic analysis of these processes under all pairwise games with two strategies in well-mixed populations. The fixation probability of a single mutant was shown to increase with population size in half of the possible games, thus making it a strikingly pervasive feature. These results are generalisable for pairwise games with more strategies as long as only a maximum of 2 strategies are present in the population at the same time. Our analysis of fixation probabilities continued

in the following chapters 3, 4, and 5, focusing on multiplayer games in structured and mobile populations. In particular, we were successful in deriving their exact analytical expressions for general multiplayer games on territorial networks. This was done for isolated communities in chapter 3 and for completely mixed populations in chapter 4. These were later applied to a large set of multiplayer games. However, there were cases where deriving expressions for fixation probabilities was not possible. In the last sections of chapter 4, we compute their values for territorial networks with mixing communities by solving systems of linear equations numerically, whereas in chapter 5, we perform agent-based simulations to obtain them. These probabilities were key in assessing the evolution of strategic behaviour, and in particular cooperation, in such systems.

In chapters 3, 4, and 5, we analyse the evolution of cooperation for a set of multiplayer social dilemmas. We explore a variety of assumptions about the structural organisation of populations and the mobility of individuals. In chapter 3, we show that cooperation in public goods dilemmas evolves successfully for populations organised onto networks of local communities. Larger networks of smaller sized communities were high promoters of cooperative behaviour under all public goods dilemmas, but the results were robust to any topology and any size of network and communities. In the limit of asymptotically isolated communities, the network structure, i.e. how communities are connected, plays no impact. In chapter 4, we show that considering a higher mixing of communities typically has a detrimental effect on cooperation, completely suppressing its evolution for the Charitable Prisoner's Dilemma, already known for its strictness. Although higher mixing also increases the impact of the topology of the network, we haven't yet observed scenarios where this topology facilitates cooperation in independent movement models.

The co-evolution of conditional movement model explored in chapter 5 showed this to be another robust mechanism for the evolution of multiplayer cooperation. In contrast to what we observed for local independent movement, the network topology played a key role on the evolution of cooperation. Similar to what was observed in Erovenko et al. (2019), networks with low degree centralisation, i.e. low variance in degree centrality (in this case, complete and circle networks) facilitated the co-evolution of cooperation and high mobility strategies under low movement costs. Those topologies allow cooperators to find each other quickly in the network, but in a decentralised way that also allows them to be missed by defectors for long enough

time before they dismantle their groups. We note that the topological features that allow them to do this may depend on the density of individuals on the network, as a higher centralisation might be useful for cooperators when casual encounters between them are rarer. This is a potentially interesting avenue to explore in the future. Nonetheless, it is clear that their success is not attributed to the locality of their interactions in the network.

These results suggest that the structural mechanisms present in the two types of movement models are different and therefore lead to distinct dependences on spatial network topology. Moreover, this is supported by the way the two mechanisms are affected by the choice of the six evolutionary dynamics explored throughout chapters 3, 4, and 5. In chapter 3, we see that the DBB and BDD dynamics consistently extend the regions of the parameter space for which cooperation evolves under community organisation. In particular, those dynamics lead to the evolution of cooperation under the CPD which does not occur under the remaining four dynamics. This is coherent with results from other models of evolutionary games on networks (Ohtsuki et al. 2006, Hauert & Imhof 2012, Allen et al. 2017, Pattni et al. 2017), as previously reviewed through this thesis. Such dynamics are sensitive to the viscosity of the evolutionary process on structured populations which allows cooperation to evolve under network reciprocity.

However, in chapters 4 and 5, we observe that the dynamics have virtually no impact on the evolutionary outcome. This is not surprising for the completely mixed populations studied in chapter 4. However, the absence of impact of the evolutionary dynamics on cooperation under the conditional movement model observed in chapter 5, further supports the idea that that mechanism is distinct from traditional network reciprocity. Conditional movement suppresses the impact of the viscosity of the evolutionary process on the fitness of individuals reported in Ohtsuki et al. (2006), but allows for a different type of mobile assortative behaviour to co-evolve under certain network topologies. The mobile assortative behaviour between cooperators is robust to choice of evolutionary dynamics, unlike network reciprocity.

These modelling methods developed in the context of evolutionary game theory provide theories of the evolution of cooperation. However, they may also offer an understanding of the adoption of broader types of behaviour in populations. In this context, evolutionary game theory has been used to model and tackle specific problems associated with AI monitoring (Alalawi et al. 2024), disease evolution

and spread (Morison et al. 2024), environmental governance (Couto et al. 2020), and healthcare investment (Alalawi et al. 2020). We propose that some of the theoretical advancements, particularly those of chapters 3 and 5, can be applied to such problems to understand how the structure and mobility of populations may affect behavioural outcomes. Moreover, in chapters 6 and 7, we focus on developing extensions of other game-theoretic concepts and apply them to understand other complex social systems.

In chapter 6, we introduce a strategy under which individuals use a particular common good until their usage fails or the experienced quality falls below a threshold, at which point they shift to a different option. This strategy was inspired by the WSLS strategy developed for iterated games (Kraines & Kraines 1989, Nowak & Sigmund 1993), and is conceptually similar to the the conditional movement rule used in chapter 5. We develop a theory of populations using such strategies, investigate their equilibria, and extend the results to hybrid populations where some individuals store information about their past experiences and adapt their tolerance to failure strategically.

We apply this theory to populations of mobile users attempting to access Internet services by submitting requests to servers in the network with minimal information about them. Overall, this strategy and its adaptive extension showed good performance results when evaluated by realistic stochastic simulations of the system. Future work will focus on extending these evaluations to realistic experimental testbeds and potentially develop platform implementations (Mancuso et al. 2022, 2023, Castagno et al. 2020). Moreover, the theory developed can be easily extended to understand other systems such as population distribution on grazing or foraging land or propose solutions to operators of systems of public transport or other technological common goods.

In chapter 7, we focus on developing a model of productive interaction and selection-transmission of skills with the aim of understanding their evolution and co-existence in complex systems. This work was motivated by the recent advances in economic complexity and evolutionary economic geography which show the key impact of a skilled and knowledgeable workforce on industrial development and its geographic organisation. To study how skills are learnt and adopted in the context of co-production and how that affects their selection in populations, we developed a dynamical model which incorporated both aspects of evolutionary game theory and

epidemiological modelling. We characterised skills as sustainable, tentative or unsustainable based on the stability of their endemic equilibria. Furthermore, we analysed their potential to destabilise previous skill equilibria when newly introduced, and their ability to co-exist with other skills. These characteristics depend on their loss rate, as well as on their intra- and inter-skill synergy coefficients. Together with the results presented throughout this thesis, we hope this work enlightens on the potential of developing the theory of game-theoretic models and extending it to find cross-disciplinary solutions to problems faced in complex social systems.

Appendix A

The effect of the weak selection limit on fixation probability functions in pairwise games

In section 2.3.2, it was observed that anti-coordination games held fixation probabilities which increased for population sizes above a turning point $N > N_{min}(w)$ (see figure 2.2). Figure A.1a suggests that turning points are inversely proportional to the intensity of selection $N_{min}(w) \sim 1/w$, which means that they would become very large under the weak selection limit. Under this limit, it could be argued that the increase in the population sizes for which fixation probabilities increase would lead to a loss of significance of fixation processes due to most of the evolutionary time being spent in transient/mixed states (Antal & Scheuring 2006, Vasconcelos et al. 2017), also called quasi-stationary states (Zhou et al. 2010, Overton et al. 2022, Nasell 1999b,a).

The average conditional fixation time is the average number of discrete steps that the population takes to go from state $i = 1$ to state $i = N$ (i.e. the fixation of a single mutant) conditional on it happening:

$$t_N = \frac{\sum_{t=0}^{\infty} t\phi_N(t)}{\sum_{t=0}^{\infty} \phi_N(t)}, \tag{A.1}$$

where $\phi_N(t)$ is the probability that the population gets from state $i = 1$ to state $i = N$ after t discrete steps. It should be clear from this definition that $\sum_{t=0}^{\infty} \phi_N(t) = \rho_N$. Following Antal & Scheuring (2006), we can obtain a recursive relation leading

173

to the following expression (see Della Rossa et al. (2017) and Huang et al. (2018) for alternative expressions):

$$t_N = \sum_{n=1}^{N-1} \frac{s_{0,n-1}s_{n,N-1}}{P_{n+}^N q_n s_{0,N-1}}, \quad s_{n,m} = \sum_{k=n}^{m} q_k, \quad q_n = \prod_{j=1}^{n} \gamma_j^N. \tag{A.2}$$

We are interested in comparing the average time obtained in the turning points $N_{min}(w)$ of figures 2.2 and A.1a with three different scenarios: the simple symmetric random walk, the neutral fixation case and the same game for maximum intensity of selection $w = 1$.

The simple symmetric random walk is obtained by considering the stochastic process under which the transition between a state i and one of its two neighbours is one-half: $P_{i+} = P_{i-} = 1/2$. The average conditional fixation time under this process is

$$t_N = \frac{1}{3}(N^2 - 1). \tag{A.3}$$

On the other hand, under the frequency-dependent Moran process the transition probabilities P_{i+} and P_{i-} do not add up to 1. This is so because at each time step there is a probability that the population will remain in the same state $P_{i=}$. Thus, when we are under neutral selection ($w = 0$), equation A.2 leads to a different equation than A.3, which is three times slower than the simple random walk

$$t_N = N(N - 1). \tag{A.4}$$

By analysing fixation processes under 2×2 games, Antal & Scheuring (2006) concluded that anti-coordination games have average conditional fixation times that grow exponentially with population size for asymptotically large populations. The base of exponential growth τ can be calculated from the payoff matrix. The average conditional fixation time thus becomes

$$t_N \sim \tau(a, b, c, d)^N, \tag{A.5}$$

where $\tau(a, b, c, d) > 1$ for any choice of $[a, b, c, d]$ leading to an anti-coordination game with $I < 0$.
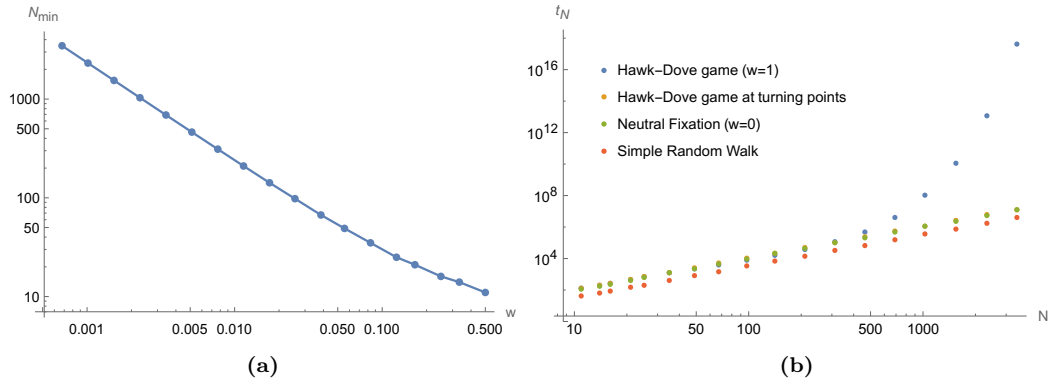
Figure A.1: Fixation process under game with payoff values $[5.5, 5, 6, 3]$, corresponding to Dove fixation in the Hawk-Dove game Figure A.1a exhibits the turning point N_{min} as a function of the intensity of selection w, showing that they have an approximately inversely proportional relation. In figure A.1b, the average conditional fixation times t_N were shown for (1) the Hawk-Dove game with the maximum intensity of selection ($w = 1$ and independent N), (2) the Hawk-Dove game at the turning points of figure A.1a ($w \in (0, 1)$ and $N = N_{min}(w)$), (3) the neutral fixation scenario ($w = 0$ and independent N), and (4) the simple random walk ($P_{i+} = P_{i-} = 1/2$).

In figure A.1b, we observe that as intensity of selection decreases $w \to 0$, and turning points increase $N_{min} \to \infty$, fixation times under this anti-coordination game keep on being of the order of the neutral ones $t_N \sim N^2$ instead of increasing exponentially with N. As noted in Sample & Allen (2017), considering limits $N \to \infty$ and $w \to 0$ in different orders may lead to different fixation outcomes. Here we present a case where it is important to clarify that relationship in order to understand what would happen asymptotically.

Appendix B

Large home fidelity in the territorial raider model

B.1 Fixation probabilities under high home fidelity

Consider a connected network with M places and an arbitrary set of edges between them. Within the extended territorial raider model, each node will be home to a community of size Q. We consider the limit of large home fidelity, where individuals interact mainly within their communities. This limit is dependent on the size of the network, and therefore when we consider $h \to \infty$, we in fact mean $h/M \to \infty$.

We denote $F_{c,d}^{C_k}$ as the fitness of cooperators C_k in a community with c cooperators and d defectors with home in place P_k. In the limit of high home fidelity, this can be represented as the following expansion:

$$F_{c,d}^{C_k} = 1 - w + w \left[\left(1 - \frac{d_k}{h + d_k}\right)^Q \cdot \prod_{i \in X(k)} \left(1 - \frac{1}{h + d_i}\right)^Q \cdot R_{c,d}^C + \mathcal{O}(h^{-1}) \right] =$$

$$= 1 - w + w R_{c,d}^C + \mathcal{O}(h^{-1}),$$

(B.1)

where $X(k)$ denotes the set of places adjacent to P_k on the network, and d_k represents the size of that set, corresponding to the degree of the node. The zeroth-order term of the expansion is dependent only on the composition of the community present in place P_k. Similarly, we have that the fitness of defectors is reduced to the following:

$$F_{c,d}^{D_k} = 1 - w + w R_{c,d}^D + \mathcal{O}(h^{-1}).$$

(B.2)

We denote $f_{c,d}^C$ and $f_{c,d}^D$ as the zeroth-order terms of the fitness expansion under high home fidelity, which are presented in equations 3.6 and 3.7 of the main text.

In the next sections, we will focus on the resulting fixation processes in the limit of high home fidelity.

B.1.1 BDB, DBD, LB and LD dynamics

Starting from the state where all individuals in the population use strategy D, we consider the occurrence of a mutation leading one of them to adopt strategy C. At each step of the BDB process, one individual is chosen for reproduction proportional to their fitness, and another one is chosen for death with probability proportional to the time spent with the first. This means that while there are mixed communities, type-changing replacement events will occur mainly within those communities as we will see below.

We denote r_h^C (r_h^D) as the within-community fixation probability of a single cooperator (defector) in a community of defectors (cooperators). We define this as the probability that starting with one mutant in a community of residents, we will observe the fixation of that mutant in the community before we observe that type vanishing. This probability is equal to the sum of the probabilities of all the paths that alter the number of mutants in that community from 1 to Q without passing by 0. We note that this can be split into the sum of the probabilities of paths under which no type-altering between-community replacements occur before within-community fixation is attained, S_1, S_2, ..., and those under which at least one type-altering between-community replacement occurs before fixation is attained, S_1', S_2', ...:

$$r_h^C = p(S_1) + p(S_2) + ... + p(S_1') + p(S_2') + ... \qquad \text{(B.3)}$$

In the limit we are considering, the sum over the first set of paths introduced before tends to the fixation probability obtained in a well-mixed community (Karlin & Taylor 1975), since individuals of the same community using the same strategy are indistinguishable. Under the BDB dynamics, the transition probabilities used in this expression can be replaced by the zeroth-order terms of the fitness expansion presented in equations B.1 and B.2, and higher-order terms are added outside the

expression:

$$p(S_1) + p(S_2) + ... = \frac{1}{1 + \sum_{j=1}^{Q-1} \prod_{c=1}^{j} \frac{f_{c,Q-c}^D}{f_{c,Q-c}^C}} + \mathcal{O}(h^{-1}). \tag{B.4}$$

The paths in the second set introduced above involve at least one between-community replacement, therefore having a probability of at least the first order in h^{-1}. This highlights the fact that they occur at a different time-scale from within-community fixation processes:

$$p(S_1') + p(S_2') + ... = \mathcal{O}(h^{-1}). \tag{B.5}$$

Therefore, the cooperator within-community fixation probability in the limit $h \to \infty$ can be represented as the following:

$$r_h^C = \frac{1}{1 + \sum_{j=1}^{Q-1} \prod_{c=1}^{j} \frac{f_{c,Q-c}^D}{f_{c,Q-c}^C}} + \mathcal{O}(h^{-1}). \tag{B.6}$$

Similar to this, we can obtain the same equation for the within-community fixation probability of a single defector by using the following expression:

$$r_h^D = \frac{1}{1 + \sum_{j=1}^{Q-1} \prod_{d=1}^{j} \frac{f_{Q-d,d}^C}{f_{Q-d,d}^D}} + \mathcal{O}(h^{-1}). \tag{B.7}$$

We denote r^C and r^D as the zeroth-order terms of the equations above, which are presented in equations 3.8 and 3.8 of the main text.

We call ρ^C the probability that a single mutant cooperator will fixate in a population of defectors. Under $h \to \infty$, populations reach the states where each community is homogeneous, i.e. $c = Q$ or $c = 0$, before any between-community replacement occurs. When the population is in one of the homogeneous community states, it will be altered only when a cooperator replaces a defector from an adjacent community, or vice versa. After a new cooperator (defector) is born, the population will move to a different homogeneous community state with one more (less) cooperator community with probability r^C (r^D), or it will return to the previous state with probability $1 - r^C$ $(1 - r^D)$.

Let us call I the set of communities composed of only cooperators, M the entire set of communities, and $M \setminus I$ the set of communities of defectors. At a homogeneous

community state denoted by I, the probability that the size of set I increases by one after a given evolutionary step is:

$$P^{|I|^+}(I) = \left(\frac{f^C_{Q,0}}{|I| \cdot f^C_{Q,0} + |M \setminus I| \cdot f^D_{0,Q}} + \mathcal{O}(h^{-1}) \right) \cdot \left(Q \cdot \sum_{i \in I, j \in M \setminus I} w_{ij} \right) \cdot \left(r^C + \mathcal{O}(h^{-1}) \right).$$
(B.8)

The expression above is the product of probabilities of three successive necessary events: 1) choosing a cooperator from a particular community for birth, 2) choosing a defector from another community to be replaced by the first cooperator, and 3) the within-community fixation of the new cooperator before another between community type-altering event occurs. Note that in the probability of choosing a cooperator for birth, we have replaced the fitness of individuals considered in the homogeneous community state by the zeroth-order terms present in equations B.1 and B.2, with higher-order terms being explicitly summed onto that probability. The replacement weights w_{ij} between individuals with homes in different places P_i and P_j are independent of their two strategies, and they are multiplied by Q to account for all the defectors present in each of the communities in $M \setminus I$. The within-community fixation probability is perturbed by higher-order terms in h^{-1} already analysed when its expression was obtained. The probability that the size of set I decreases by one is the following:

$$P^{|I|^-}(I) = \left(\frac{f^D_{0,Q}}{|I| \cdot f^C_{Q,0} + |M \setminus I| \cdot f^D_{0,Q}} + \mathcal{O}(h^{-1}) \right) \cdot \left(Q \cdot \sum_{i \in I, j \in M \setminus I} w_{ji} \right) \cdot \left(r^D + \mathcal{O}(h^{-1}) \right).$$
(B.9)

The two equations B.8 and B.9 depend on the particular set I because the sum of weights w_{ij} depends on it. These weights tend to zero as $h \to \infty$, but they can be considered at their lowest order in h^{-1}. As long as there is no disconnected component of the network of communities ($\forall i \exists j \neq i (w_{ij} \neq 0)$), this probability is low but positive, regardless of the particular set I considered. However, because replacement weights are symmetric, i.e. $w_{ij} = w_{ji}$, the terms in the two transition probabilities in the above equations are identical. Therefore, the ratio between the two probabilities, which we denote Γ, does not depend on the particular set I of communities which are composed of cooperators:

$$\Gamma = \frac{P^{|I|^-}(I)}{P^{|I|^+}(I)} = \frac{f^D_{0,Q} \cdot r^D}{f^C_{Q,0} \cdot r^C}.$$
(B.10)

Furthermore, the transition probability ratio above is constant under all homogeneous community states. After the initial within-community fixation of a cooperator, the probability that the community will fixate on the whole population thus becomes a simple fixed fitness Moran probability (Moran 1958), with equivalent relative fitness denoted by the ratio from equation B.10.

The fixation probability of one single cooperator will therefore be equal to the following:

$$\lim_{h \to \infty} \rho^C = r^C \cdot P_{Moran} \left(\Gamma^{-1} \right) = r^C \cdot \frac{1 - \Gamma}{1 - \Gamma^M}, \tag{B.11}$$

when $\Gamma \neq 1$. Otherwise, $\lim_{h \to \infty} \rho^C = r^C/M$. Similarly, we have that:

$$\lim_{h \to \infty} \rho^D = r^D \cdot P_{Moran} \left(\Gamma \right) = r^D \cdot \frac{1 - \Gamma^{-1}}{1 - \Gamma^{-M}}, \tag{B.12}$$

when $\Gamma \neq 1$. Otherwise, $\lim_{h \to \infty} \rho^D = r^D/M$.

This result is surprisingly simple and shows that the topology of the underlying network plays no role in the limit of high home fidelity, as long as there is no disconnected component of the network. The dynamics in that limit depend only on within-community fixation probabilities and on the probability ratio Γ.

The equations presented in B.6–B.12 are valid for dynamics BDB, DBD, LB, and LD. This equivalence is valid under all territorial networks in the limit $h \to \infty$. This is so because the transition probability ratios are the same under all these dynamics, both in each step of the within-community fixation processes considered to build equations B.6 and B.7, and in the community fixation process as presented in equation B.10.

Furthermore, we note that the results are robust to the use of alternative movement models when the limit of isolated communities with the same size is considered, and if the replacement weights between any two individuals are kept symmetrical, i.e. the evolutionary graph is undirected. This includes simple variations of the current movement model, e.g. all individuals could have the same probability of not being in their home node independent of its degree, in the limit where this probability tends to zero. Even though outside the limit of isolated communities, those models could lead to generally different results, in that limit the fixation probabilities would be equal to the ones obtained here. Nonetheless, these alternative movement model choices could still impact the rate at which between-community events occur.

B.1.2 DBB and BDD dynamics

A procedure analogous to the one conducted in section B.1.1 applies to the remaining two dynamics introduced in chapter 3. However, these dynamics exhibit distinct transition probability ratios compared to the four aforementioned ones, resulting in quantitatively different outcomes.

We start by noting that the sum of paths that end in fixation with no type-altering between-community replacements is obtained using different transition probabilities. Let us start with the DBB dynamics, under which the transition probability from having c cooperators to having $c + 1$ or $c - 1$ at a given evolutionary step are respectively as follows:

$$P_{DBB}^{+}(c, Q - c) = \frac{Q - c}{N} \cdot \frac{c \cdot f_{c,Q-c}^{C}}{c \cdot f_{c,Q-c}^{C} + (Q - c - 1) \cdot f_{c,Q-c}^{D}} + \mathcal{O}(h^{-1}), \quad \text{(B.13)}$$

$$P_{DBB}^{-}(c, Q - c) = \frac{c}{N} \frac{(Q - c) \cdot f_{c,Q-c}^{D}}{(c - 1) \cdot f_{c,Q-c}^{C} + (Q - c) \cdot f_{c,Q-c}^{D}} + \mathcal{O}(h^{-1}). \quad \text{(B.14)}$$

Repeating this process considering the BDD dynamics, we obtain the following transition probabilities, which were simplified by multiplying the numerator and denominator by both cooperator and defector's fitness:

$$
\begin{aligned}
P_{BDD}^{+}(c, Q - c) &= \frac{c}{N} \cdot \frac{(Q - c) \cdot \left(f_{c,Q-c}^{D}\right)^{-1}}{(Q - c) \cdot \left(f_{c,Q-c}^{D}\right)^{-1} + (c - 1) \cdot \left(f_{c,Q-c}^{C}\right)^{-1}} + \mathcal{O}(h^{-1}) = \\
&= \frac{c}{N} \cdot \frac{(Q - c) \cdot f_{c,Q-c}^{C}}{(Q - c) \cdot f_{c,Q-c}^{C} + (c - 1) \cdot f_{c,Q-c}^{D}} + \mathcal{O}(h^{-1}),
\end{aligned}
$$
$$\text{(B.15)}$$

$$
\begin{aligned}
P_{BDD}^{-}(c, Q - c) &= \frac{Q - c}{N} \cdot \frac{c \cdot \left(f_{c,Q-c}^{C}\right)^{-1}}{(Q - c - 1) \cdot \left(f_{c,Q-c}^{D}\right)^{-1} + c \cdot \left(f_{c,Q-c}^{C}\right)^{-1}} + \mathcal{O}(h^{-1}) = \\
&= \frac{Q - c}{N} \cdot \frac{c \cdot f_{c,Q-c}^{D}}{(Q - c - 1) \cdot f_{c,Q-c}^{C} + c \cdot f_{c,Q-c}^{D}} + \mathcal{O}(h^{-1}).
\end{aligned}
$$
$$\text{(B.16)}$$

The ratio $U(c, d) = P^{-}(c, d)/P^{+}(c, d)$ between transition probabilities under

both dynamics leads to the following expression:

$$U_{DBB/BDD}(c, Q-c) = \frac{P_{DBB/BDD}^-(c, Q-c)}{P_{DBB/BDD}^+(c, Q-c)} =$$
$$= \frac{f_{c,Q-c}^D}{f_{c,Q-c}^C} \cdot \left(\frac{T_{DBB/BDD}(c, Q-c) - f_{c,Q-c}^D}{T_{DBB/BDD}(c, Q-c) - f_{c,Q-c}^C} \right) = \quad \text{(B.17)}$$
$$= \frac{f_{c,Q-c}^D}{f_{c,Q-c}^C} \left(1 + \frac{f_{c,Q-c}^C - f_{c,Q-c}^D}{T_{DBB/BDD}(c, Q-c) - f_{c,Q-c}^C} \right),$$

where we have used the following definitions:

$$T_{DBB}(c, d) = c \cdot f_{c,d}^C + d \cdot f_{c,d}^D, \quad \text{(B.18)}$$

$$T_{BDD}(c, d) = d \cdot f_{c,d}^C + c \cdot f_{c,d}^D. \quad \text{(B.19)}$$

Now, we use these transition probability ratios to compute the zeroth-order term of the within-community fixation probability expansion, similar to what was done in section B.1.1, getting the following result:

$$r_{DBB/BDD}^{C,h} = \frac{1}{1 + \sum_{j=1}^{Q-1} \prod_{c=1}^{j} \frac{f_{c,Q-c}^D}{f_{c,Q-c}^C} \left(1 + \frac{f_{c,Q-c}^C - f_{c,Q-c}^D}{T_{DBB/BDD}(c,Q-c) - f_{c,Q-c}^C} \right)} + \mathcal{O}(h^{-1}).$$
$$\text{(B.20)}$$

Following the same procedure for the within-community fixation of defectors, we get the following result:

$$r_{DBB/BDD}^{D,h} = \frac{1}{1 + \sum_{j=1}^{Q-1} \prod_{d=1}^{j} \frac{f_{Q-d,d}^C}{f_{Q-d,d}^D} \cdot \left(1 + \frac{f_{Q-d,d}^D - f_{Q-d,d}^C}{T_{DBB/BDD}(Q-d,d) - f_{Q-d,d}^D} \right)} + \mathcal{O}(h^{-1}).$$
$$\text{(B.21)}$$

We denote $r_{DBB/BDD}^C$ and $r_{DBB/BDD}^D$ as the zeroth-order terms of the equations above, which are presented in equations 3.18 and 3.19 of the main text.

The difference in transition probabilities, when compared to the previous 4 dynamics, also affects the probability that the number of communities increases or decreases by one in the next evolutionary step. We start by looking at what hap-

pens under the DBB dynamics:

$$P_{DBB}^{|I|^+}(I) =$$

$$= \left(\frac{1}{M} + \mathcal{O}(h^{-1})\right) \cdot \left(Q \cdot \left(\sum_{i \in I, j \in M \setminus I} w_{ij}\right) \cdot \left(\frac{f_{Q,0}^C}{f_{0,Q}^D} + \mathcal{O}(h^{-1})\right)\right) \cdot \left(r_{DBB}^C + \mathcal{O}(h^{-1})\right).$$

$$(B.22)$$

The preceding probability encompasses: 1) the uniform random selection of a specific community for the death of one of its individuals; 2) the subsequent selection, if the first individual was a defector, of a cooperator community for birth, involving any of its Q cooperators; and 3) the fixation of the invading cooperator in the newly mixed community. The sum of fractions above includes a simplification coming from the fact that the denominator is a sum over all products of weights and fitness according to the definition from table 3.2 of the main text, which in the limit $h \to \infty$ simply tends to the fitness of communal residents $f_{0,Q}^D$ plus higher-order terms in h^{-1}. This will introduce another key difference in the results. We obtain the following transition probability in the opposing direction:

$$P_{DBB}^{|I|^-}(I) =$$

$$= \left(\frac{1}{M} + \mathcal{O}(h^{-1})\right) \cdot \left(Q \cdot \left(\sum_{i \in I, j \in M \setminus I} w_{ji}\right) \cdot \left(\frac{f_{0,Q}^D}{f_{Q,0}^C} + \mathcal{O}(h^{-1})\right)\right) \cdot \left(r_{DBB}^D + \mathcal{O}(h^{-1})\right).$$

$$(B.23)$$

Now looking at what happens under BDD dynamics, we obtain the following expressions for transition probabilities between homogeneous community states:

$$P_{BDD}^{|I|^+}(I) =$$

$$= \left(\frac{1}{M} + \mathcal{O}(h^{-1})\right) \cdot \left(Q \cdot \left(\sum_{i \in I, j \in M \setminus I} w_{ij}\right) \cdot \left(\frac{\left(f_{0,Q}^D\right)^{-1}}{\left(f_{Q,0}^C\right)^{-1}} + \mathcal{O}(h^{-1})\right)\right) \cdot \left(r_{BDD}^C + \mathcal{O}(h^{-1})\right),$$

$$(B.24)$$

$$P^{|I|^-}_{BDD}(I) =$$

$$= \left(\frac{1}{M} + \mathcal{O}(h^{-1})\right) \cdot \left(Q \cdot \left(\sum_{i \in I, j \in M \setminus I} w_{ij}\right) \cdot \left(\frac{\left(f^C_{Q,0}\right)^{-1}}{\left(f^D_{0,Q}\right)^{-1}} + \mathcal{O}(h^{-1})\right)\right) \cdot \left(r^C_{BDD} + \mathcal{O}(h^{-1})\right).$$

$$(B.25)$$

We note that, once again, the highest-order terms in these probabilities are indeed first-order in h^{-1} due to the effects of between-community replacements happening between different communities on the network. However, the particular set of edges between the nodes of the network, i.e. its topology, does not influence the ratio between probabilities, but only the time-scale at which these transitions occur. The probability ratio $\Gamma_{DBB/BDD}$ is independent of I and its size, as was under the remaining dynamics:

$$\Gamma_{DBB/BDD} = \frac{P^{|I|^-}_{DBB/BDD}(I)}{P^{|I|^+}_{DBB/BDD}(I)} = \left(\frac{f^D_{0,Q}}{f^C_{Q,0}}\right)^2 \cdot \frac{r^D_{DBB/BDD}}{r^C_{DBB/BDD}}. \qquad (B.26)$$

Therefore the resulting process under high home fidelity in these two dynamics is parallel to the one occurring under the remaining four dynamics, with two quantitative differences: within-community fixation probabilities have correction coefficients as represented in equations B.20 and B.21, and the overall population process has an altered equivalent fitness characterised in equation B.26.

The resulting fixation probabilities are therefore the following:

$$\lim_{h \to \infty} \rho^C_{DBB/BDD} = r^C_{DBB/BDD} \cdot P_{Moran}\left(\Gamma^{-1}_{DBB/BDD}\right) = r^C_{DBB/BDD} \cdot \frac{1 - \Gamma_{DBB/BDD}}{1 - \Gamma^M_{DBB/BDD}},$$

$$(B.27)$$

when $\Gamma_{DBB/BDD} \neq 1$. Otherwise, $\lim_{h \to \infty} \rho^C_{DBB/BDD} = r^C_{DBB/BDD}/M$. Similarly, we have that:

$$\lim_{h \to \infty} \rho^D_{DBB/BDD} = r^D_{DBB/BDD} \cdot P_{Moran}\left(\Gamma_{DBB/BDD}\right) = r^D_{DBB/BDD} \cdot \frac{1 - \Gamma^{-1}_{DBB/BDD}}{1 - \Gamma^{-M}_{DBB/BDD}},$$

$$(B.28)$$

when $\Gamma_{DBB/BDD} \neq 1$. Otherwise, $\lim_{h \to \infty} \rho^D_{DBB/BDD} = r^D_{DBB/BDD}/M$.

B.2 Fixation probabilities under high home fidelity and weak selection

Making the assumption of high home fidelity, we now introduce the limit of weak selection. Both limits considered depend on the number of places on the network, since large home fidelity in fact means $h/M \to \infty$ and weak selection means to $w \cdot (MQ) \to 0$. Therefore, when large networks are further considered, the values of h and w have to be chosen accordingly. We highlight the fact that the limits are considered in this order: first, we consider home fidelity to be asymptotically high, then we consider selection to be asymptotically weak, and only then may we consider large networks. It has been proved that the order in which the limits of weak selection and large population size are considered impacts the resulting asymptotic fixation probability expansions and the conditions for the evolution of a given strategy to be favoured in comparison to neutral fixation (Sample & Allen 2017).

B.2.1 BDB, DBD, LB, and LD dynamics

We start from equation B.11 and expand it around $w \to 0$. In that case, we obtain the following expression:

$$\rho^C \approx \left[r^C \cdot \frac{1 - \Gamma}{1 - \Gamma^M} \right] \Big|_{w \to 0} + w \left[\frac{\partial}{\partial w} \left(\frac{1 - \Gamma}{1 - \Gamma^M} \right) \cdot r^C + \frac{\partial r^C}{\partial w} \cdot \left(\frac{1 - \Gamma}{1 - \Gamma^M} \right) \right] \Big|_{w \to 0}.$$
(B.29)

We start to simplify this equation by noting that, under this limit, within-community fixation probabilities tend to $1/Q$. In that limit, we define their derivatives in respect to w as the following:

$$\delta^C = \frac{\partial r^C}{\partial w} \Big|_{w \to 0} = \frac{1}{Q^2} \sum_{j=1}^{Q-1} \sum_{c=1}^{j} [R_{c,Q-c}^C - R_{c,Q-c}^D],$$
(B.30)

$$\delta^D = \frac{\partial r^D}{\partial w} \Big|_{w \to 0} = \frac{1}{Q^2} \sum_{j=1}^{Q-1} \sum_{d=1}^{j} \left[R_{Q-d,d}^D - R_{Q-d,d}^C \right].$$
(B.31)

.

These equations can be simplified by taking into account that each term on the inner sum is repeated $Q - c$ and $Q - d$ times respectively in the outer sum, thus

leading to the following expressions:

$$\delta^C = \frac{1}{Q^2} \sum_{c=1}^{Q-1} (Q-c)[R_{c,Q-c}^C - R_{c,Q-c}^D], \qquad (B.32)$$

$$\delta^D = \frac{1}{Q^2} \sum_{d=1}^{Q-1} (Q-d) \left[R_{Q-d,d}^D - R_{Q-d,d}^C \right]. \qquad (B.33)$$

.

In the same limit, we observe that $\Gamma \to 1$, leading the Moran probability with effective fitness Γ to simply tend to $1/M$. We then evaluate the derivative of the Moran probability and obtain the following relation:

$$\frac{\partial}{\partial w} \left(\frac{1-\Gamma}{1-\Gamma^M} \right) \bigg|_{w \to 0} = \frac{1}{2} \left(1 - \frac{1}{M} \right) \left(-\frac{\partial \Gamma}{\partial w} \bigg|_{w \to 0} \right). \qquad (B.34)$$

The derivative of the effective fitness Γ can be obtained in the following way:

$$-\frac{\partial \Gamma}{\partial w} \bigg|_{w \to 0} = \Delta^{CD} + Q \left(\delta^C - \delta^D \right), \qquad (B.35)$$

where

$$\Delta^{CD} = R_{Q,0}^C - R_{0,Q}^D = -\Delta^{DC}. \qquad (B.36)$$

Replacing these redefined terms onto the original equation B.29 of the expanded fixation probability, we obtained the following relation:

$$\rho^C \approx \frac{1}{MQ} + \frac{w}{2} \left[\frac{1}{Q} \left(1 - \frac{1}{M} \right) \Delta^{CD} + \left(1 + \frac{1}{M} \right) \delta^C - \left(1 - \frac{1}{M} \right) \delta^D \right]. \qquad (B.37)$$

Following the same procedure for the fixation probabilities of defectors, we obtain the previous equation with swapped indexes C and D:

$$\rho^D \approx \frac{1}{MQ} + \frac{w}{2} \left[\frac{1}{Q} \left(1 - \frac{1}{M} \right) \Delta^{DC} + \left(1 + \frac{1}{M} \right) \delta^D - \left(1 - \frac{1}{M} \right) \delta^C \right]. \qquad (B.38)$$

B.2.2 DBB and BDD dynamics

The expansion is slightly different when we consider the DBB and BDD dynamics. The original expansion is parallel to the one presented in equation B.29, the only difference being that all instances of r^C, r^D, and Γ are replaced by their respective equations under the DBB and BDD dynamics. Evaluated in the limit $w \to 0$, the

three quantities lead to the same values as in the previous dynamics. Therefore, all differences come from their derivatives. Based on the definitions presented in equations B.20 and B.21, and the previously defined derivatives δ^C and δ^D, we obtain the following relations for their derivatives evaluated in the limit $w \to 0$:

$$
\left. \frac{\partial r_{DBB}^C}{\partial w} \right|_{w \to 0} = \left. \frac{\partial r_{BDD}^C}{\partial w} \right|_{w \to 0} =
$$
$$
= \frac{1}{Q^2} \sum_{j=1}^{Q-1} \sum_{c=1}^{j} \left(1 - \frac{1}{Q-1} \right) [R_{c,Q-c}^C - R_{c,Q-c}^D] = \tag{B.39}
$$
$$
= \left(1 - \frac{1}{Q-1} \right) \delta^C,
$$

$$
\left. \frac{\partial r_{DBB}^D}{\partial w} \right|_{w \to 0} = \left. \frac{\partial r_{BDD}^D}{\partial w} \right|_{w \to 0} =
$$
$$
= \frac{1}{Q^2} \sum_{j=1}^{Q-1} \sum_{d=1}^{j} \left(1 - \frac{1}{Q-1} \right) [R_{Q-d,d}^D - R_{Q-d,d}^C] = \tag{B.40}
$$
$$
= \left(1 - \frac{1}{Q-1} \right) \delta^D.
$$

The derivative of the effective fitness Γ can be obtained in the following way:

$$
\left. \frac{\partial \Gamma_{DBB/BDD}}{\partial w} \right|_{w \to 0} = 2 \left[R_{0,Q}^D - R_{Q,0}^C \right] +
$$
$$
+ Q \left[\left. \frac{\partial r_{DBB/BDD}^D}{\partial w} \right|_{w \to 0} - \left. \frac{\partial r_{DBB/BDD}^C}{\partial w} \right|_{w \to 0} \right], \tag{B.41}
$$

which, based on equations B.36, B.39 and B.40, leads to the following equation:

$$
- \left. \frac{\partial \Gamma_{DBB/BDD}}{\partial w} \right|_{w \to 0} = 2 \Delta^{CD} + Q \left(1 - \frac{1}{Q-1} \right) \left(\delta^C - \delta^D \right). \tag{B.42}
$$

Replacing these terms in the fixation probability expansion parallel to the one from equation B.29, we obtain the following resulting equations:

$$
\rho_{DBB/BDD}^C \approx \frac{1}{MQ} + \frac{w}{2} \left[2 \frac{1}{Q} \left(1 - \frac{1}{M} \right) \Delta^{CD} + \left(1 - \frac{1}{Q-1} \right) \left(1 + \frac{1}{M} \right) \delta^C + \right.
$$
$$
\left. - \left(1 - \frac{1}{Q-1} \right) \left(1 - \frac{1}{M} \right) \delta^D \right],
$$
$$
\tag{B.43}
$$

$$\rho^D_{DBB/BDD} \approx \frac{1}{MQ} + \frac{w}{2}\left[2\frac{1}{Q}\left(1-\frac{1}{M}\right)\Delta^{DC} + \left(1-\frac{1}{Q-1}\right)\left(1+\frac{1}{M}\right)\delta^D + \right.$$
$$\left. -\left(1-\frac{1}{Q-1}\right)\left(1-\frac{1}{M}\right)\delta^C\right].$$

(B.44)

B.3 Rules of cooperation under a finite number of communities and general intensity of selection

In this section, we propose to analyse the evolution and stability of cooperation when relaxing the limits of weak selection (considered in sections 3.4–3.6 of the main text) and large number of communities (considered in sections 3.5 and 3.6 of the main text). We start by considering a finite number of communities under weak selection and their impact on the simple rules previously presented. We derive an exact rule for the CPD and analyse the general impact of finiteness under the remaining social dilemmas. We then move outside the weak selection limit, analysing the impact of relaxing the two limits on the parameter regions under which cooperation evolves.

B.3.1 The effect of a finite number of communities on the evolution of cooperation

We start by analysing the particular case of the CPD under the DBB and BDD dynamics. The fixation probability of cooperators expanded under weak selection is larger than the neutral value if the following condition is true:

$$V/K > (Q-1)\cdot\frac{1-\frac{2}{MQ}}{1-\frac{2(Q-1)}{MQ}}.$$

(B.45)

The second term of the product on the right-hand side of the equation can be considered the finiteness correction coefficient. This is equal to 1 under $Q = 2$, which means that in that case, the condition obtained is the same regardless of the number of communities. However, for larger numbers of communities ($Q > 2$), the denominator is lower than the numerator in the correction coefficient above, and therefore the critical value of the reward-to-cost ratio will necessarily be larger than the one obtained under an infinite number of communities. The difference between the two should be the largest for the smallest possible network size $M = 2$, under

which the rule becomes the following:

$$V/K > (Q-1) \cdot (Q-1). \tag{B.46}$$

It was stated in section 3.4 of the main text that decreasing the number of communities increases the importance of within-community fixation against between-community replacement events in the course of a fixation process. Because of that, defectors should generally do better in smaller networks. This can be concluded based on the following rearrangement of the weak selection expansion:

$$
\begin{aligned}
\rho^C \approx \frac{1}{MQ} + \frac{w}{2} \Bigg[2\frac{1}{Q}\Delta^{CD} + \left(1 - \frac{1}{Q-1}\right)(\delta^C - \delta^D) + \\
+ \frac{1}{M}\left[-\frac{2}{Q}\Delta^{CD} + \left(1 - \frac{1}{Q-1}\right)(\delta^C + \delta^D)\right]\Bigg].
\end{aligned}
\tag{B.47}
$$

We can identify three types of terms in the equation above. The first type corresponds to the zeroth order term of the fixation probability under weak selection; the second includes the set of first-order terms in w which are independent of M; and the third (second line of the equation) represents the first-order terms in w which are dependent on M and vanish for large M, thus having a finiteness correction of the expansion. The third type does not originate on the expansion of the fixation probability under a large number of communities but instead reflects its *exact* dependence on the number of communities under weak selection. Let us analyse the effect introduced by this finiteness correction term.

Focusing on public goods dilemmas, the fixation of cooperators can only be favoured by selection for a choice of network parameters Q and M if we observe $\Delta^{CD} > 0$. This is so because the remaining contributions in equations B.37 and B.43 (involving δ^C and $-\delta^D$) are always negative (see table 3.4). Therefore, for cooperation to fixate successfully, the first contribution to the finiteness correction in equation B.47 has to be negative. The sum of the remaining correction contributions is zero in most public goods dilemmas, except for the S and the TS dilemmas, under which they are negative. This means that the M-dependent term of the weak selection expansion of the fixation probability is necessarily negative. If the fixation probability is higher than the neutral one for a given choice of network (Q and M) and payoff (V and K) parameters, it will necessarily be so for any M larger than that, whereas it might not be for choices of M lower than that. This necessarily means

that the critical reward-to-cost ratio under all public goods dilemmas (expressed in table 3.5 of the main text for a large number of communities) will increase when we decrease M. Finiteness narrows the regions of V/K for which cooperation evolves under public goods dilemmas.

Under the HD dilemma, the effect of M can be quite different because both Δ^{CD} and $\delta^C + \delta^D$ are always positive, thus leading to different signs on the two contributions to the third term in the previous equation. This complex effect of M is parallel to the effects of Q explored in section 3.4 of the main text.

Cooperation evolves under sufficiently large values of V/K when $Q \geq 2$ in non-threshold public goods and when $Q \geq L$ in threshold public goods, irrespective of the number of communities M. This conclusion arises from the linear dependency of all Δ^{CD} on V, whereas δ^C and δ^D lack such dependence except under the CPD (a game already shown to support cooperation under any number of communities through equation B.45). Consequently, there is always a critical value of V above which the first-order term of the weak selection expansion is positive. In the context of the HD dilemma, cooperation can consistently evolve under sufficiently small values of V/K when $Q \geq 2$, regardless of the network size. This stems from the linear dependence of Δ^{CD} and δ^C on K, and δ^D on $-K$, ensuring that all contributions to the fixation probability expansion are positive when K reaches a high enough value.

B.3.2 The effect of strong selection on the evolution of cooperation

In this section, we relax the weak selection limit. This limit was introduced in section 3.4 of the main text, and it was used together with the limit of large number of communities in the succeeding sections to achieve simple rules of cooperation. We focus on understanding the effect of considering larger values of intensity of selection on the critical value of the reward-to-cost ratio, denoted as $(V/K)^c$, above which cooperation fixates in public goods dilemmas and below which cooperation fixates in the HD dilemma. Figures B.1, B.2, and B.3 show the value of $(V/K)^c$ under networks with $M = 10$ communities of various sizes, such as $Q = 2, 3, 4, 6, 8$. We present results for values of w between 0 and 0.5, the interval under which all 10 social dilemmas can be considered for any possible value of V when $K = 1$, i.e. for which probabilities remain positive. More generally, this corresponds to $w \in (0, 1/(K+1))$.

The reward-to-cost ratio is affected in different ways by the increase in intensity
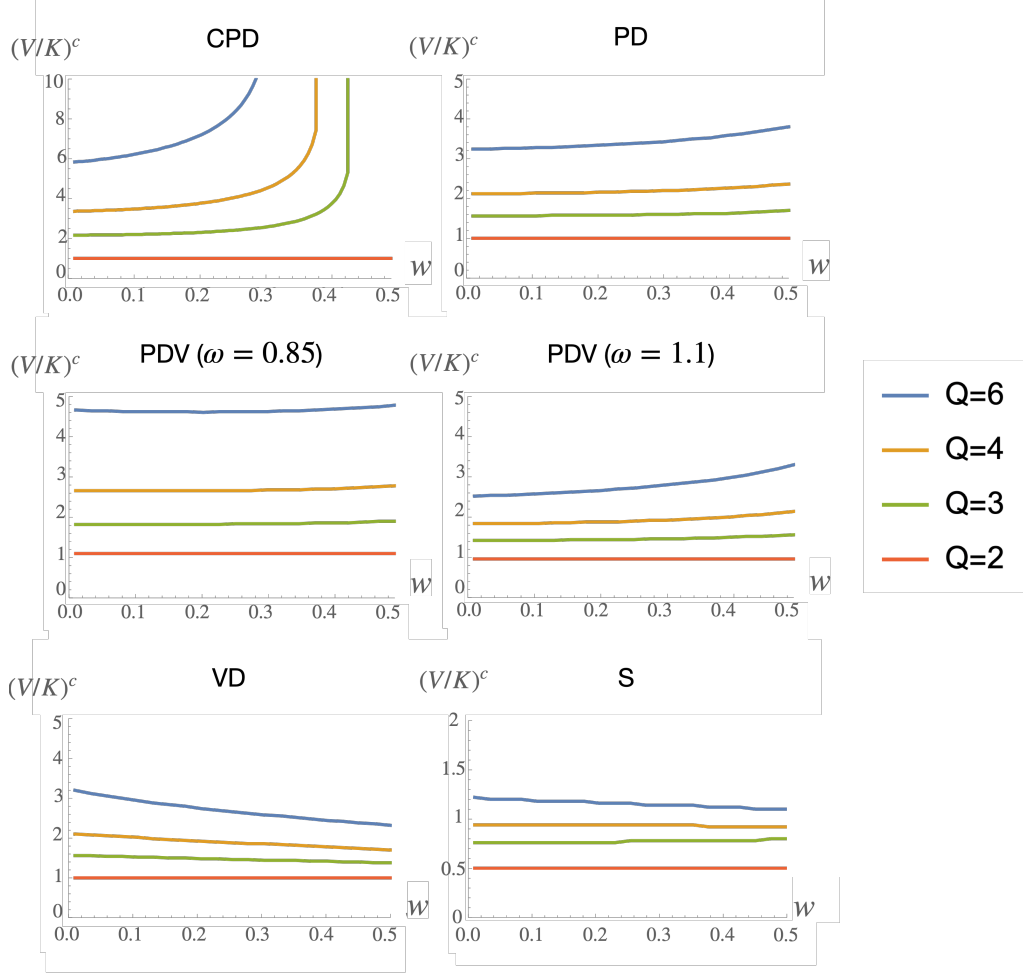
Figure B.1: Critical values of the reward-to-cost ratio for which $V/K > (V/K)^c$ leads to the successful fixation and stability of cooperation. The results are obtained for different intensities of selection under $M = 10$, $K = 1$, and different values of Q.

of selection for each of the social dilemmas, and no particular strategy is consistently favoured. We start by focusing on the CPD. Under $Q = 2$, cooperation evolves for $V/K > 1$ for all values of w and M, which is equivalent to the rule shown in table 3.5 of the main text. However, under the remaining community sizes considered, increasing the intensity of selection consistently leads to higher critical values of the reward-to-cost ratio. In those cases, weak selection has a positive effect on the evolution of cooperation. Under strong enough selection, there is no critical reward-to-cost ratio and cooperation may never evolve. We explored other values of M and observed that increasing M under strong selection extended the values of w for which there existed a critical reward-to-cost ratio.

Under other dilemmas such as the PD, the PDV, and the TS, lower intensities of selection also led to lower critical values of the reward-to-cost ratio, but the differences obtained across values of w are substantially lower. In those dilemmas,
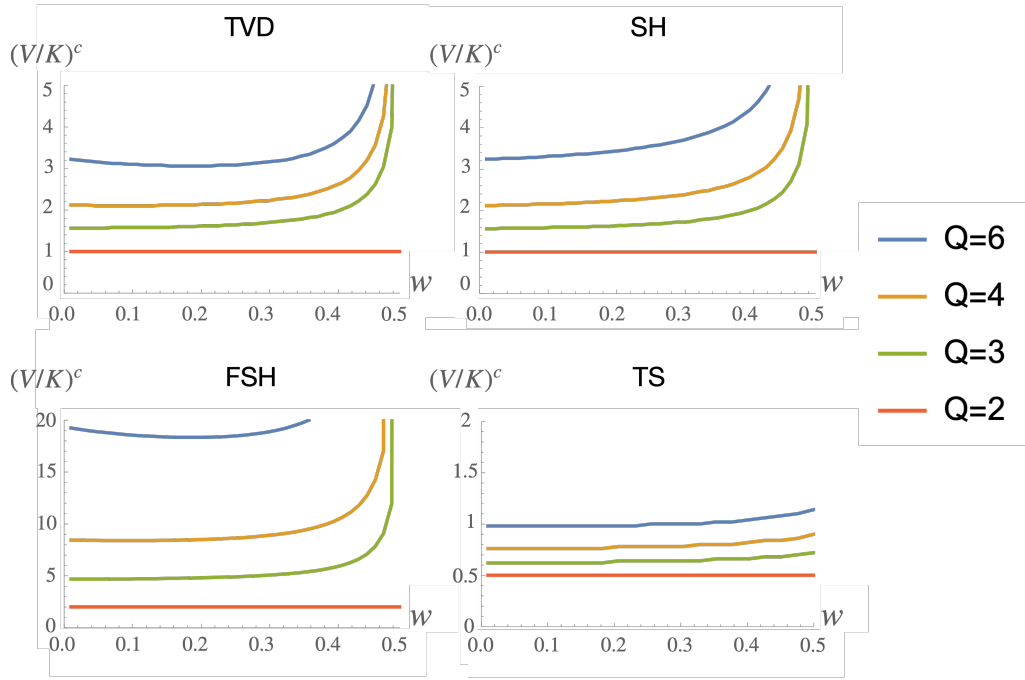
Figure B.2: Critical values of the reward-to-cost ratio for which $V/K > (V/K)^c$ leads to the successful fixation and stability of cooperation. The results are obtained for different intensities of selection under $M = 10$, $K = 1$, $L = 2$, and different values of Q.
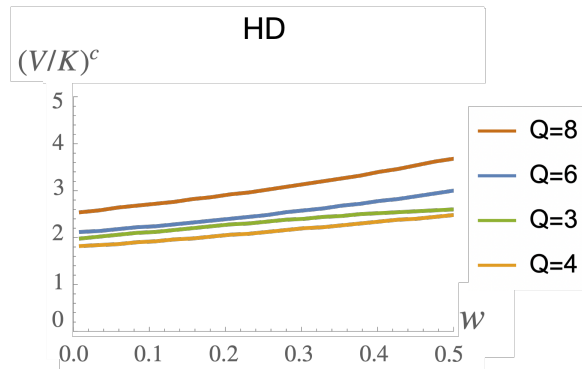
Figure B.3: Critical values of the reward-to-cost ratio for which $V/K < (V/K)^c$ leads to the successful fixation of cooperation. Cooperators fixate for all values of V/K and w when $Q = 2$. The results are obtained for different intensities of selection under $M = 10$, $K = 1$, $L = 2$, and different values of Q.

the payoff parameters we explored always led to the existence of a critical value, contrary to what was observed under the CPD and other threshold games such as the TVD, SH and the FSH, which showed otherwise similar trends. Moreover, under the PDV, the TVD, and the FSH, the minimum value of $(V/K)^c$ occurred for intermediate intensities of selection. These correspond to an optimal w for which cooperation evolves under the largest regions of the payoff parameter space.

Under the VD and the S, higher intensities of selection lead to lower critical values of the reward-to-cost ratio. Therefore, cooperation evolves for larger regions of the

payoff parameter space under stronger selection. This trend was more pronounced under the VD.

As an overall trend under public goods dilemmas, we note that larger community sizes require higher reward-to-cost ratios for cooperators to successfully fixate. This is concluded from the rules of multiplayer cooperation (section 3.5 of the main text), obtained under weak selection and a large number of communities. Here, we observe that this is still valid when those limits are relaxed.

Furthermore, we can observe some of the effects of considering a finite number of communities. The critical values obtained under $w \to 0$ and shown in figures B.1 and B.2 for public goods dilemmas are higher than the ones presented in table 3.5 of the main text, which were obtained considering a large number of communities. Larger numbers of communities were proven in section B.3.1 to decrease the values of $(V/K)^c$ above which cooperation evolves under public goods dilemmas. Naturally, the observed difference is more prominent when Q is larger and of the same order as M.

Most public goods dilemmas lead to one and only one stable strategy when one of the limits of large number of communities or weak selection is considered, as was noted in sections 3.3 and 3.4 of the main text. Under the S and the TS, the only exceptions to that rule, there are some cases of bi-stability when the system is close to neutrality, under which none of the strategies fixates on the other. Overall, this means that in either of those limits, if the fixation of cooperators is favoured by selection, we can conclude that cooperation will necessarily be a stable strategy. In settings with strong selection and a finite number of communities, such as the ones explored in this section, we have not observed any outcome where mutual fixation (and therefore instability of both strategies) occurs, thus suggesting that the previous conclusion might hold for more general regions of the parameter space.

Under the HD dilemma, the only commons dilemma studied here, cooperators fixate successfully when $V/K < (V/K)^c$. Therefore, from figure B.3, we observe that higher values of intensity of selection lead to larger regions in which cooperation fixates. As noted before, cooperation always fixates when $Q = 2$, and therefore we haven't represented in the figure the value of $(V/K)^c$ for that case. Increasing the community size to $Q = 3, 4$ lowers the critical values of V/K, thus leading to smaller regions of fixation of cooperators. However, increasing it to $Q = 5$ and above leads to a change in the opposite direction, thus increasing the regions where cooperation

fixates. This effect has been described and analysed in section 3.5 of the main text in the context of weak selection and a large number of communities, and it is valid when those limits are relaxed, as can be observed in figure B.3.

Appendix C

Multiplayer social dilemmas in completely mixed populations

C.1 Calculating fitness under completely mixed populations

C.1.1 Charitable Prisoner's Dilemma

Under the CPD, cooperators will get

$$\pi^C_{N_c, N-N_c} = E\left[\frac{c-1}{c+d-1}\right] V - K, \tag{C.1}$$

where we represented implicitly the expected value of the share of the reward received by cooperators. This can be simplified by using the fact that c and d are just the sum of random independent variables $c = \sum_{i=1}^{N_c-1} X_C^i + 1$ and $d = \sum_{j=1}^{N_d} X_j^D$, with $N_d = N - N_c$. Each random variable is 1 with probability $1/M$, i.e. its corresponding individual is in the same place as the focal one, and is 0 with probability $1 - 1/M$. We added a unit constant to c because the focal individual is a cooperators. This leads to:

$$
\begin{aligned}
E\left[\frac{c-1}{c+d-1}\right] &= E\left[\frac{\sum_{i=1}^{N_c-1} X_i^C}{\sum_{i=1}^{N_c-1} X_i^C + \sum_{i=1}^{N_d} X_j^D}\right] = \\
&= (N_c - 1) E\left[\frac{X_1^C}{X_1^C + \sum_{i=2}^{N_c-1} X_i^C + \sum_{j=1}^{N_d} X_j^D}\right],
\end{aligned}
\tag{C.2}
$$

195

where we have considered the fact that all random variables follow the same distribution. Furthermore, we can evaluate the distribution of random variable X_1^C and say that:

$$E\left[\frac{c-1}{c+d-1}\right] = (N_c - 1)pE\left[\frac{1}{1 + \sum_{i=2}^{N_c-1} X_i^C + \sum_{j=1}^{N_d} X_j^D}\right]. \qquad (C.3)$$

We now evaluate the sum of the remaining random variables n' by using the fact that it follows a binomial distribution with parameters $N - 2$ and $p = 1/M$:

$$
\begin{aligned}
E\left[\frac{1}{1 + \sum_{i=2}^{N_c-1} X_i^C + \sum_{j=1}^{N_d} X_j^D}\right] &= \\
&= \sum_{n'=0}^{N-2} \binom{N-2}{n'} p^{n'} (1-p)^{N-2-n'} \frac{1}{1+n'} = \\
&= \sum_{n'=0}^{N-2} \frac{(N-2)!}{(N-2-n')!n'!(n'+1)} p^{n'} (1-p)^{N-2-n'} = \\
&= \frac{1}{p(N-1)} \sum_{n'=0}^{N-2} \frac{(N-1)!}{(N-2-n')!(n'+1)!} p^{n'+1} (1-p)^{N-2-n'} = \\
&= \frac{1}{p(N-1)} \left(1 - (1-p)^{N-1}\right).
\end{aligned} \qquad (C.4)
$$

Joining the results obtained in equations C.3 and C.4 and introducing them back onto equation C.1, we get the following result:

$$\pi_{N_c, N-N_c}^C = \frac{N_c - 1}{N - 1}\left(1 - (1-p)^{N-1}\right)V - K. \qquad (C.5)$$

In the case of defectors in the CPD, we would follow the same procedure by replacing the values of c and d by similar the random independent variables $c =$

$\sum_{i=1}^{N_c} X_C^i$ and $d = \sum_{j=1}^{N_d-1} X_j^D = 1$, again with $N_d = N - N_c$, which would lead to:

$$
\begin{aligned}
\pi_{N_c, N-N_c}^D &= E\left[\frac{c}{c+d-1}\right] V = \\
&= E\left[\frac{\sum_{i=1}^{N_c-1} X_i^C}{\sum_{i=1}^{N_c} X_i^C + \sum_{j=1}^{N_d-1} X_j^D}\right] V = \\
&= N_c p E\left[\frac{1}{1 + \sum_{i=2}^{N_c} X_i^C + \sum_{j=1}^{N_d-1} X_j^D}\right] V = \quad\quad \text{(C.6)} \\
&= N_c p E\left[\frac{1}{1 + \sum_{i=2}^{N_c-1} X_i^C + \sum_{j=1}^{N_d} X_j^D}\right] V = \\
&= \frac{N_c}{N-1}\left(1 - (1-p)^{N-1}\right) V.
\end{aligned}
$$

C.1.2 Prisoner's Dilemma

Under the PD, cooperators get

$$
\begin{aligned}
\pi_{N_c, N-N_c}^C &= E\left[\frac{c}{c+d}\right] V - K \\
&= E\left[\frac{1 + \sum_{i=1}^{N_c-1} X_i^C}{1 + \sum_{i=1}^{N_c-1} X_i^C + \sum_{j=1}^{N_d} X_j^D}\right] V - K = \\
&= E\left[\frac{1}{1 + \sum_{i=1}^{N_c-1} X_i^C + \sum_{j=1}^{N_d} X_j^D}\right] V + \quad\quad \text{(C.7)} \\
&\quad + (N_c - 1) p E\left[\frac{1}{2 + \sum_{i=2}^{N_c-1} X_i^C + \sum_{j=1}^{N_d-1} X_j^D}\right] V - K.
\end{aligned}
$$

Let us work on the two terms separately. We use again the evaluation of the sum of independent Bernoulli trials and the fact it follows a binomial distribution.

Starting with the first term:

$$E\left[\frac{1}{1+\sum_{i=1}^{N_c-1} X_i^C + \sum_{j=1}^{N_d} X_j^D}\right] =$$

$$= \sum_{n'=0}^{N-1} \binom{N-1}{n'} p^{n'}(1-p)^{N-1-n'} \frac{1}{1+n'} =$$

$$= \sum_{n'=0}^{N-1} \frac{(N-1)!}{(N-1-n')!n'!(n'+1)} p^{n'}(1-p)^{N-1-n'} =$$

$$= \frac{1}{pN} \sum_{n'=0}^{N-1} \frac{N!}{(N-1-n')!(n'+1)!} p^{n'+1}(1-p)^{N-1-n'} =$$

$$= \frac{1}{pN} \sum_{n''=1}^{N} \frac{N!}{(N-n'')!n''!} p^{n''}(1-p)^{N-n''} =$$

$$= \frac{1}{pN} \left(1 - (1-p)^N\right). \tag{C.8}$$

Regarding the second term:

$$E\left[\frac{1}{2+\sum_{i=2}^{N_c-1} X_i^C + \sum_{j=1}^{N_d-1} X_j^D}\right] =$$

$$= \sum_{n'=0}^{N-2} \binom{N-2}{n'} p^{n'}(1-p)^{N-2-n'} \frac{1}{n'+2} =$$

$$= \sum_{n'=0}^{N-2} \frac{(N-2)!}{(N-2-n')!n'!} p^{n'}(1-p)^{N-2-n'} \frac{1}{n'+2} \frac{n'+2-1}{n'+1} =$$

$$= \sum_{n'=0}^{N-2} \frac{(N-2)!}{(N-2-n')!n'!} p^{n'}(1-p)^{N-2-n'} \left(\frac{1}{n'+1} - \frac{1}{(n'+2)(n'+1)}\right) =$$

$$= \frac{1}{p(N-1)} \sum_{n'=0}^{N-2} \frac{(N-1)!}{(N-1-(n'+1))!(n'+1)!} p^{n'+1}(1-p)^{N-1-(n'+1)} +$$

$$- \frac{1}{p^2 N(N-1)} \sum_{n'=0}^{N-2} \frac{N!}{(N-(n'+2))!(n'+2)!} p^{n'+2}(1-p)^{N-(n'+2)} =$$

$$= \frac{1}{p(N-1)} \sum_{n''=1}^{N-1} \frac{(N-1)!}{(N-1-n'')!n''!} p^{n''}(1-p)^{N-1-n''} +$$

$$- \frac{1}{p^2 N(N-1)} \sum_{n''=2}^{N} \frac{N!}{(N-n'')!n''!} p^{n''}(1-p)^{N-n''} =$$

$$= \frac{1}{p(N-1)} \left(1 - (1-p)^{N-1}\right) - \frac{1}{p^2 N(N-1)} \left(1 - Np(1-p)^{N-1} - (1-p)^N\right). \tag{C.9}$$

Finally, we take the results of these two terms and introduce them into equation

C.7 to obtain the following fitness function:

$$\pi^C_{N_c,N-N_c} =$$

$$= \frac{1}{pN} \left(1 - (1-p)^N\right) V + (N_c - 1)p \left[\frac{1}{p(N-1)} \left(1 - (1-p)^{N-1}\right) + \right.$$

$$\left. -\frac{1}{p^2 N(N-1)} \left(1 - Np(1-p)^{N-1} - (1-p)^N\right)\right] V - K =$$

$$= \frac{1}{pN} \left(1 - (1-p)^N\right) V + \frac{N_c - 1}{N - 1} \left[1 - \frac{1}{pN} \left(1 - (1-p)^N\right)\right] V - K =$$

$$= \frac{M}{N} \left[1 - \left(1 - \frac{1}{M}\right)^N\right] V + \frac{N_c - 1}{N - 1} \left[1 - \frac{M}{N} \left(1 - \left(1 - \frac{1}{M}\right)^N\right)\right] V - K.$$

$$(C.10)$$

We now perform the parallel calculations for the average payoff of defectors:

$$\pi^D_{N_c,N-N_c} = E\left[\frac{c}{c+d}\right] V =$$

$$= E\left[\frac{\sum_{i=1}^{N_c} X_i^C}{1 + \sum_{i=1}^{N_c} X_i^C + \sum_{j=1}^{N_d-1} X_j^D}\right] V =$$

$$= N_c p E\left[\frac{1}{2 + \sum_{i=2}^{N_c} X_i^C + \sum_{j=1}^{N_d-1} X_j^D}\right] V =$$

$$= N_c p \left[\frac{1}{p(N-1)} \left(1 - (1-p)^{N-1}\right) + \right. \qquad (C.11)$$

$$\left. -\frac{1}{p^2 N(N-1)} \left(1 - Np(1-p)^{N-1} - (1-p)^N\right)\right] V =$$

$$= \frac{N_c}{N-1} \left[1 - \frac{1}{pN} \left(1 - (1-p)^N\right)\right] V =$$

$$= \frac{N_c}{N-1} \left[1 - \frac{M}{N} \left(1 - \left(1 - \frac{1}{M}\right)^N\right)\right] V.$$

C.1.3 Volunteer's Dilemma

Under the VD, cooperators get the same payoff, regardless of their group composition. Therefore:

$$\pi^C_{N_c,N-N_c} = V - K. \qquad (C.12)$$

Defectors get the reward V if they have at least one cooperator on their group

and get nothing otherwise. Their average payoff is therefore:

$$\pi_{N_c, N-N_c}^D = V - \binom{N_c}{0} p^0 (1-p)^{N_c} V = \left(1 - (1-p)^{N_c}\right) V =$$

$$= \left[1 - \left(1 - \frac{1}{M}\right)^{N_c}\right] V. \tag{C.13}$$

C.1.4 Snowdrift

Under the Snowdrift game, cooperators always get the reward V and then pay a cost which depends on how many cooperators are in their group. Therefore:

$$\pi_{N_c, N-N_c}^C = V - E\left[\frac{1}{c}\right] K =$$

$$= V - E\left[\frac{1}{1 + \sum_{i=1}^{N_c-1} X_i^C}\right] K =$$

$$= V - \sum_{c'=0}^{N_c-1} \binom{N_c - 1}{c'} p^{c'} (1-p)^{N_c-1-c'} \frac{1}{1+c'} K =$$

$$= V - \sum_{c'=0}^{N_c-1} \frac{(N_c - 1)!}{(N_c - 1 - c')! c'!} p^{c'} (1-p)^{N_c-1-c'} \frac{1}{1+c'} K = \tag{C.14}$$

$$= V - \frac{1}{pN_c} \sum_{c'=0}^{N_c-1} \frac{c'+1}{(N_c - (c'+1))!(c'+1)!} p^{c'} (1-p)^{N_c-(c'+1)} K =$$

$$= V - \frac{1}{pN_c} \left(1 - (1-p)^{N_c}\right) K =$$

$$= V - \frac{M}{N_c} \left[1 - \left(1 - \frac{1}{M}\right)^{N_c}\right] K.$$

Defectors have the average payoff as under the VD, and thus they will have the same payoff:

$$\pi_{N_c, N-N_c}^D = \left[1 - \left(1 - \frac{1}{M}\right)^{N_c}\right] V. \tag{C.15}$$

C.1.5 Hawk-Dove

Under the HD game, cooperators receive nothing if there is at least one defector in their group, otherwise they receive V/c. Therefore, their average payoff is obtained by the product of the probability of having no defectors in the group by the expected value of V/c, which has been calculated for the average payoff of cooperators in the

S game:

$$\pi^C_{N_c,N-N_c} = (1-p)^{N_d} E\left[\frac{1}{c}\right] V =$$

$$= (1-p)^{N_d} \frac{1}{pN_c} \left(1 - (1-p)^{N_c}\right) V = \tag{C.16}$$

$$= \frac{M}{N_c} \left(1 - \frac{1}{M}\right)^{N-N_c} \cdot \left[1 - \left(1 - \frac{1}{M}\right)^{N_c}\right] V.$$

The expected payoff of defectors can be represented the following way:

$$\pi^D_{N_c,N-N_c} = E\left[\frac{V - (d-1)K}{d}\right] =$$

$$= E\left[\frac{1}{d}\right] (V + K) - K. \tag{C.17}$$

The calculation done for the expected value of $1/d$ from the point of view of defectors is parallel to the one done for expected value of $1/c$ from the point of view of cooperators used in the average payoff of cooperators in both the VD and the HD. Therefore, we apply that result here replacing N_c by $N - N_c$

$$\pi^D_{N_c,N-N_c} = \frac{1}{p(N-N_c)} \left(1 - (1-p)^{N-N_c}\right) (V+K) - K =$$

$$= \frac{M}{N-N_c} \left[1 - \left(1 - \frac{1}{M}\right)^{N-N_c}\right] (V+K) - K. \tag{C.18}$$

C.2 Obtaining the rules of cooperation under completely mixed populations

The rules of cooperation can be obtained by comparing the fixation probabilities of cooperators (ρ^C) and (defectors (ρ^D) to the fixation probability under neutral selection ($\rho^{neutral} = 1/N$).

C.2.1 Charitable Prisoner's Dilemma

Under the CPD, we always have that $F^D_{N_c,N-N_c} > F^C_{N_c,N-N_c}$. This means that all terms of the sum in equation 4.9 are higher than 1, and therefore $\rho^C < \rho^{neutral}$. In parallel, all the terms of the sum in equation 4.10 are lower than 1, and therefore $\rho^D > \rho^{neutral}$. This is true for any values of w, V, K, number of cooperators N_c and population size N.

C.2.2 Prisoner's Dilemma

Under the PD, we have $F_{N_c,N-N_c}^D > F_{N_c,N-N_c}^C$ for all N_c and N if

$$V/K > \frac{N-1}{\left(1-\left(1-\frac{1}{M}\right)^N\right)\frac{N}{Q}-1}, \tag{C.19}$$

which under large N and M, with a defined asymptotic value of Q, becomes:

$$V/K > \frac{Q}{1-\exp(-Q)}, \tag{C.20}$$

We have used the following well-known limit $\lim_{N\to\infty}\left(1+\frac{x}{N}\right)^N = e^x$, in which case $x = -Q$.

This is valid under any value of w and number of cooperators and population size. We can therefore use the same reasoning as before, concluding that below that threshold selection favours defection, and above it it favours cooperation.

In the remaining games, similarly to the CPD and PD, there are values of V/K for which either cooperators have higher fitness for all values of N_c of a given (large) population or defectors do. However, to obtain general rules which include the values of V/K for which cooperators are benefit under some states of the population and defectors do in others, we calculate the first-order terms of the weak selection expansion of fixation probabilities, and compute the conditions for them to be positive.

We recall the equations introduced in section 4.3.2 of the first-order terms:

$$\begin{aligned}\left.\frac{\partial\rho^C}{\partial w}\right|_{w\to0} &= \frac{1}{N^2}\sum_{j=1}^{N-1}\sum_{N_c=1}^{j}\left[F_{N_c,N-N_c}^C - F_{N_c,N-N_c}^D\right] = \\ &= \frac{1}{N^2}\sum_{N_c=1}^{N-1}(N-N_c)\left[F_{N_c,N-N_c}^C - F_{N_c,N-N_c}^D\right],\end{aligned} \tag{C.21}$$

and

$$\begin{aligned}\left.\frac{\partial\rho^D}{\partial w}\right|_{w\to0} &= \frac{1}{N^2}\sum_{N_d=1}^{N-1}(N-N_d)\left[F_{N-N_d,N_d}^D - F_{N-N_d,N_d}^C\right] = \\ &= \frac{1}{N^2}\sum_{N_c=1}^{N-1}N_c\left[F_{N_c,N-N_c}^D - F_{N_c,N-N_c}^C\right].\end{aligned} \tag{C.22}$$

C.2.3   Volunteer's Dilemma

In the case of the VD, we have that:

$$\left.\frac{\partial \rho^C}{\partial w}\right|_{w\to 0} = \frac{1}{N^2}\sum_{j=1}^{N-1}\sum_{N_c=1}^{j}\left[\left(1-\frac{1}{M}\right)^{N_c}V - K\right] =$$

$$= \frac{1}{N^2}\sum_{j=1}^{N-1}\left[\left(1-\frac{1}{M}\right)\frac{1-\left(1-\frac{1}{M}\right)^{j}}{1-\left(1-\frac{1}{M}\right)}V - jK\right], \qquad (\text{C.23})$$

where we have used the result of the geometric series. We can further simplify the expression using the result of the arithmetic and geometric series again, to get the following:

$$\left.\frac{\partial \rho^C}{\partial w}\right|_{w\to 0} = \frac{1}{N^2}\left[(M-1)\cdot\left((N-1)-(M-1)\cdot\left(1-\left(1-\frac{1}{M}\right)^{N-1}\right)\right)V +\right.$$

$$\left. -\frac{N(N-1)}{2}K\right]. $$

$$(\text{C.24})$$

Therefore, under arbitrary M and N in the weak selection limit, cooperators fixate successfully if:

$$V/K > \frac{\dfrac{N(N-1)}{2}}{(M-1)\cdot\left((N-1)-(M-1)\cdot\left(1-\left(1-\frac{1}{M}\right)^{N-1}\right)\right)}, \qquad (\text{C.25})$$

which under the limit of large networks and populations with asymptotic density $N/M = Q$, becomes:

$$V/K > \frac{Q/2}{1-\dfrac{1-\exp(-Q)}{Q}}. \qquad (\text{C.26})$$

Performing the same operation for the expansion of the fixation probability of

mutant defectors, we obtain the following:

$$\frac{\partial \rho^D}{\partial w}\bigg|_{w\to 0} = \frac{1}{N^2}\sum_{j=1}^{N-1}\sum_{N_d=1}^{j}\left[K-\left(1-\frac{1}{M}\right)^{N-N_d}V\right] =$$

$$= \frac{1}{N^2}\sum_{j=1}^{N-1}\left[jK-\left(1-\frac{1}{M}\right)^{N-j}\cdot\frac{1-\left(1-\frac{1}{M}\right)^{j}}{1-\left(1-\frac{1}{M}\right)}V\right] =$$

$$= \frac{1}{N^2}\left[\frac{N(N-1)}{2}K+\right.$$

$$\left.-M\cdot\left(\left(1-\frac{1}{M}\right)\cdot\frac{1-\left(1-\frac{1}{M}\right)^{N-1}}{1-\left(1-\frac{1}{M}\right)}-(N-1)\left(1-\frac{1}{M}\right)^{N}\right)V\right],$$

(C.27)

which after some algebra leads to the following expression:

$$\frac{\partial \rho^D}{\partial w}\bigg|_{w\to 0} = \frac{1}{N^2}\left[\frac{N(N-1)}{2}K+\right.$$

$$\left.-(M-1)M\cdot\left(1-\left(1-\frac{1}{M}\right)^{N-1}\left(Q+1-\frac{1}{M}\right)\right)V\right].$$

(C.28)

This is positive when:

$$V/K < \frac{\dfrac{N(N-1)}{2}}{(M-1)M\cdot\left(1-\left(1-\frac{1}{M}\right)^{N-1}\left(Q+1-\frac{1}{M}\right)\right)},$$

(C.29)

which in the limit of large networks and populations with a fixed asymptotic density $Q = N/M$ becomes:

$$V/K < \frac{Q^2/2}{1-\exp(-Q)\cdot(Q+1)}.$$

(C.30)

C.2.4 Snowdrift

In the case of the Snowdrift game, we obtain the following first-order term of the fixation probability of cooperators:

$$
\frac{\partial \rho^C}{\partial w}\bigg|_{w \to 0} = \frac{1}{N^2} \sum_{j=1}^{N-1} \sum_{N_c=1}^{j} \left[\left(1 - \frac{1}{M}\right)^{N_c} V - \left(1 - \left(1 - \frac{1}{M}\right)^{N_c}\right) \frac{M}{N_c} K \right]. \quad \text{(C.31)}
$$

The summations over the first term can be solved similarly to what was done in the VD, resulting on the same term multiplying by V in equation C.23. The term multiplying by K requires more work. We thus split it into the two sums and focus on them individually. The first set of summations can be simplified to the following:

$$
\sum_{j=1}^{N-1} \sum_{N_c=1}^{j} \left(-\frac{M}{N_c}\right) = \sum_{N_c=1}^{N-1} (N - N_c) \left(-\frac{M}{N_c}\right) = -M \left(N H_{N-1} - (N-1)\right), \quad \text{(C.32)}
$$

where we have used the definition of the harmonic series $H_{N-1} = \sum_{i=1}^{N-1} 1/i$.

Regarding the second term, we can simplify it to the following:

$$
\begin{aligned}
\sum_{j=1}^{N-1} \sum_{N_c=1}^{j} \left[\left(1 - \frac{1}{M}\right)^{N_c} \frac{M}{N_c} \right] &= \\
&= \sum_{N_c=1}^{N-1} (N - N_c) \left[\left(1 - \frac{1}{M}\right)^{N_c} \frac{M}{N_c} \right] = \\
&= NM \sum_{N_c=1}^{N-1} \frac{\left(1 - \frac{1}{M}\right)^{N_c}}{N_c} - M \sum_{N_c=1}^{N-1} \left(1 - \frac{1}{M}\right)^{N_c} = \\
&= NM f_1(M, N) - M(M - 1)\left(1 - \left(1 - \frac{1}{M}\right)^{N-1}\right),
\end{aligned}
\quad \text{(C.33)}
$$

where we applied the sum of the geometric series and denoted one of the geometric-harmonic series of interest as:

$$
f_1(N, M) = \sum_{i=1}^{N-1} \frac{\left(1 - \frac{1}{M}\right)^{i}}{i}. \quad \text{(C.34)}
$$

Joining all the terms, we get the following first-order term of the weak selection

expansion of the fixation probability of cooperators:

$$\left.\frac{\partial \rho^C}{\partial w}\right|_{w\to 0} = \frac{1}{N^2}\left[(M-1)\cdot\left((N-1)-(M-1)\cdot\left(1-\left(1-\frac{1}{M}\right)^{N-1}\right)\right)V+\right.$$

$$-\left(M\left(NH_{N-1}-(N-1)\right)-NMf_1(N,M)+\right.$$

$$\left.\left.+\ M(M-1)\left(1-\left(1-\frac{1}{M}\right)^{N-1}\right)\right)K\right].$$

(C.35)

This leads to the following rule for the successful fixation of cooperation:

$$V/K > \frac{M\left(NH_{N-1}-(N-1)\right)-NMf_1(N,M)+M(M-1)\left(1-\left(1-\frac{1}{M}\right)^{N-1}\right)}{(M-1)\cdot\left((N-1)-(M-1)\cdot\left(1-\left(1-\frac{1}{M}\right)^{N-1}\right)\right)}.$$

(C.36)

When the limit of large networks and populations is considered, then the condition becomes:

$$V/K > \frac{1-\exp(-Q)+Q(L_1(Q)-1)}{Q-1+\exp(-Q)}$$

(C.37)

where we used the definition of the function

$$L_1(Q) = \lim_{M\to\infty}\left(H_{M\times Q-1}-f_1(M\times Q,M)\right) =$$

$$= \lim_{M\to\infty}\sum_{i=1}^{M\times Q-1}\left[\frac{1}{i}-\frac{\left(1-\frac{1}{M}\right)^i}{i}\right] =$$

(C.38)

$$= \gamma - B_1(Q)$$

The function $L_1(Q)$ is always positive. It tends to zero for very low Q, and increases monotonically, taking, for example values $L_1(1) \approx 0.80$, $L_1(2) \approx 1.32$, $L_1(3) \approx 1.69$, and $L_1(20) \approx 3.57$.

We perform the same calculations for the expansion of the fixation probability

of defectors:

$$
\left.\frac{\partial \rho^D}{\partial w}\right|_{w\to 0} = \frac{1}{N^2} \sum_{j=1}^{N-1} \sum_{N_d=1}^{j} \left[\left(1 - \left(1 - \frac{1}{M}\right)^{N-N_d}\right) \frac{M}{N-N_d} K - \left(1 - \frac{1}{M}\right)^{N-N_d} V \right] =
$$

$$
= \frac{1}{N^2} \sum_{N_d=1}^{N-1} (N - N_d) \left[\left(1 - \left(1 - \frac{1}{M}\right)^{N-N_d}\right) \frac{M}{N-N_d} \right] K +
$$

$$
- \frac{1}{N^2} \sum_{j=1}^{N-1} \sum_{N_d=1}^{j} \left[\left(1 - \frac{1}{M}\right)^{N-N_d} V \right] =
$$

$$
= \frac{1}{N^2} \sum_{N_c=1}^{N-1} \left[\left(1 - \left(1 - \frac{1}{M}\right)^{N_c}\right) M \right] K +
$$

$$
- \frac{1}{N^2} \sum_{j=1}^{N-1} \left(1 - \frac{1}{M}\right)^{N-j} \frac{1 - \left(1 - \frac{1}{M}\right)^{j}}{1 - \left(1 - \frac{1}{M}\right)} V.
$$

$$(C.39)$$

Both summations can be easily solved by using the solution of the geometric series, thus obtaining the following expansion:

$$
\left.\frac{\partial \rho^D}{\partial w}\right|_{w\to 0} = \frac{1}{N^2} \left[(N-1)MK - (M-1)\left(1 - \left(1 - \frac{1}{M}\right)^{N-1}\right) MK - \right.
$$

$$
\left. M\left((M-1)\left(1 - \left(1 - \frac{1}{M}\right)^{N-1}\right) - (N-1)\left(1 - \frac{1}{M}\right)^{N}\right) V \right].
$$

$$(C.40)$$

Finally, based on this, defectors fixate successfully if:

$$
V/K < \frac{(N-1)M - (M-1)\left(1 - \left(1 - \frac{1}{M}\right)^{N-1}\right) M}{M\left((M-1)\left(1 - \left(1 - \frac{1}{M}\right)^{N-1}\right) - (N-1)\left(1 - \frac{1}{M}\right)^{N}\right)},
$$

$$(C.41)$$

which under large networks and populations becomes:

$$
V/K < \frac{Q - 1 + \exp(-Q)}{1 - \exp(-Q)(1 + Q)}.
$$

$$(C.42)$$

C.2.5 Hawk-Dove

In the Hawk-Dove game, we obtain the following first-order term of the fixation probability of cooperators:

$$
\left.\frac{\partial \rho^C}{\partial w}\right|_{w \to 0} = \frac{1}{N^2} \sum_{j=1}^{N-1} \sum_{N_c=1}^{j} \left[\frac{N}{QN_c} \cdot \left(1 - \frac{1}{M}\right)^{N-N_c} \cdot \left[1 - \left(1 - \frac{1}{M}\right)^{N_c}\right] V + \right.
$$

$$
\left. - \frac{N}{Q(N - N_c)} \left[1 - \left(1 - \frac{1}{M}\right)^{N-N_c}\right] (V + K) + K \right] =
$$

$$
= \frac{1}{N^2} \sum_{N_c=1}^{N-1} (N - N_c) \left[\left(1 - \frac{1}{M}\right)^{N-N_c} \cdot \left[\frac{MV}{N_c} + \frac{MV}{N - N_c} + \frac{MK}{N - N_c} \right] + \right.
$$

$$
\left. - \left(1 - \frac{1}{M}\right)^N \cdot \frac{MV}{N_c} - \frac{MV}{N - N_c} - \frac{MK}{N - N_c} + K \right] =
$$

$$
= \frac{1}{N^2} \sum_{N_c=1}^{N-1} (N - N_c) \left[\left(1 - \frac{1}{M}\right)^{N-N_c} \cdot \left[\frac{NMV}{N_c(N - N_c)} + \frac{MK}{N - N_c} \right] + \right.
$$

$$
\left. - \left(1 - \frac{1}{M}\right)^N \cdot \frac{MV}{N_c} - \frac{M}{N - N_c}(V + K) + K \right] =
$$

$$
= \frac{1}{N^2} \sum_{N_c=1}^{N-1} \left[\left(1 - \frac{1}{M}\right)^{N-N_c} \cdot \left[\frac{NMV}{N_c} + MK \right] - \left(1 - \frac{1}{M}\right)^N \cdot \frac{NMV}{N_c} + \right.
$$

$$
\left. + \left(1 - \frac{1}{M}\right)^N \cdot MV - M(V + K) + (N - N_c)K \right] =
$$

$$
= \frac{1}{N^2} \left[\left(1 - \frac{1}{M}\right)^N f_2(N, M) NMV + \right.
$$

$$
+ \left(1 - \frac{1}{M}\right) \frac{1 - \left(1 - \frac{1}{M}\right)^{N-1}}{1 - \left(1 - \frac{1}{M}\right)} MK - \left(1 - \frac{1}{M}\right)^N \cdot H_{N-1} \cdot NMV +
$$

$$
\left. + \left(1 - \frac{1}{M}\right)^N \cdot (N - 1)MV - (N - 1)M(V + K) + \frac{N(N - 1)}{2} K \right] =
$$

$$
= \frac{1}{N^2} \left[\left(1 - \frac{1}{M}\right)^N \left(f_2(N, M) - H_{N-1} + 1 - \frac{1}{N} \right) NMV - (N - 1)MV + \right.
$$

$$
\left. + \left(1 - \left(1 - \frac{1}{M}\right)^{N-1} \right) (M - 1)MK - (N - 1)MK + \frac{N(N - 1)}{2} K \right].
$$

(C.43)

We redefined the summation as the following function:

$$f_2(N, M) = \sum_{N_c=1}^{N-1} \frac{\left(1 - \frac{1}{M}\right)^{-N_c}}{N_c}. \tag{C.44}$$

Based on the equation above, we can say that cooperation evolves successfully if:

$$V/K < \frac{\left(1 - \left(1 - \frac{1}{M}\right)^{N-1}\right)(M-1)M - (N-1)M + \frac{N(N-1)}{2}}{(N-1)MV - \left(1 - \frac{1}{M}\right)^N \left(f_2(N, M) - H_{N-1} + 1 - \frac{1}{N}\right)NM}, \tag{C.45}$$

which in the limit of large populations and networks with asymptotic Q becomes:

$$V/K < \frac{(1 - \exp(-Q)) - Q + \frac{Q^2}{2}}{Q - Q \exp(-Q)\left(L_2(Q) + 1\right)}, \tag{C.46}$$

where we have redefined the limit of the difference between the series f_2 and the harmonic series:

$$L_2(Q) = \lim_{M \to \infty} \left(f_2(M \times Q, M) - H_{M \times Q - 1}\right) =$$

$$= \lim_{M \to \infty} \sum_{i=1}^{M \times Q - 1} \left[\frac{\left(1 - \frac{1}{M}\right)^{-i}}{i} - \frac{1}{i}\right] = \tag{C.47}$$

$$= B_2(Q) - \gamma.$$

Finally, the expansion of the fixation probability of defectors can be obtained

by:

$$\frac{\partial \rho^D}{\partial w}\bigg|_{w\to 0} = \frac{1}{N^2} \sum_{j=1}^{N-1} \sum_{N_d=1}^{j} \left[\frac{N}{QN_d}\left[1 - \left(1 - \frac{1}{M}\right)^{N_d}\right](V+K) - K + \right.$$

$$\left. - \frac{N}{Q(N-N_d)} \cdot \left(1 - \frac{1}{M}\right)^{N_d} \cdot \left[1 - \left(1 - \frac{1}{M}\right)^{N-N_d}\right]V\right] =$$

$$= \frac{1}{N^2} \sum_{N_d=1}^{N-1} (N-N_d)\left[\frac{M}{N_d}\left[1 - \left(1 - \frac{1}{M}\right)^{N_d}\right](V+K) - K + \right.$$

$$\left. - \frac{M}{N-N_d} \cdot \left(1 - \frac{1}{M}\right)^{N_d} \cdot \left[1 - \left(1 - \frac{1}{M}\right)^{N-N_d}\right]V\right] =$$

$$= \frac{1}{N^2} \sum_{N_d=1}^{N-1} \left[\left(\frac{MN}{N_d}\left(1 - \left(1 - \frac{1}{M}\right)^{N_d}\right) - M\left(1 - \left(1 - \frac{1}{M}\right)^{N_d}\right)\right)(V+K) + \right.$$

$$\left. -K - \left(M \cdot \left(1 - \frac{1}{M}\right)^{N_d} - M\left(1 - \frac{1}{M}\right)^{N}\right)V\right] =$$

$$= \frac{1}{N^2}\left[\left(MNH_{N-1} - MNf_1(N,M) - M(N-1) + \right.\right.$$

$$\left. +M\left(1 - \frac{1}{M}\right)\frac{1 - \left(1 - \frac{1}{M}\right)^{N-1}}{1 - \left(1 - \frac{1}{M}\right)}\right)(V+K) - \frac{N(N-1)}{2}K + $$

$$\left. - \left(M \cdot \left(1 - \frac{1}{M}\right)\frac{1 - \left(1 - \frac{1}{M}\right)^{N-1}}{1 - \left(1 - \frac{1}{M}\right)} - M(N-1)\left(1 - \frac{1}{M}\right)^{N}\right)V\right] =$$

$$= \frac{1}{N^2}\left[\left(MN(H_{N-1} - f_1(N,M)) - M(N-1)\left(1 - \left(1 - \frac{1}{M}\right)^{N}\right)\right)V + \right.$$

$$+ \left(MN(H_{N-1} - f_1(N,M)) - M(N-1) + \right.$$

$$\left.\left. + M(M-1)\left(1 - \left(1 - \frac{1}{M}\right)^{N-1}\right) - \frac{N(N-1)}{2}\right)K\right].$$

$$(C.48)$$

The term multiplied by V is always positive, and the one multiplied by K is always negative. Thus, according to the above expansion, defectors fixate successfully

if:

$$V/K > \cfrac{\cfrac{N(N-1)}{2} + M(N-1) - MN(H_{N-1} - f_1(N,M)) - M(M-1)\left(1 - \left(1 - \cfrac{1}{M}\right)^{N-1}\right)}{MN(H_{N-1} - f_1(N,M)) - M(N-1)\left(1 - \left(1 - \cfrac{1}{M}\right)^N\right)}.$$

(C.49)

In the limit of large networks and large populations with asymptotic density Q, this becomes:

$$V/K > \cfrac{\cfrac{Q}{2} + 1 - L_1(Q) - \cfrac{1 - \exp(-Q)}{Q}}{L_1(Q) - (1 - \exp(-Q))}.$$

(C.50)

Appendix D

Robustness of co-evolution of cooperation and conditional movement on networks

We extend the analysis of the evolutionary outcomes obtained under the Markov movement model outlined in chapter 5. We focus on identifying if the similarity of qualitative outcomes between different evolutionary dynamics holds when we reduce the exploration phase length to the limiting value $T = 1$. We also assess the impact of considering different values of reward c.

In this setting, assortative behaviour is suppressed because individuals do not have iterated movement decisions. The isolated evolution of interactive strategies can be considered by fixing the movement strategies of residents and mutants, in which case the model becomes similar to an independent movement model such as the territorial raider (Broom et al. 2015, Pattni et al. 2017, Schimit et al. 2019, 2022). As will be shown, similar results to the ones obtained in that model and under static interaction networks (Ohtsuki et al. 2006) are recovered.

In the following tables D.1, D.2, and D.3, we present the results obtained for the fixation probability of one cooperator on a population of defectors, under the same three topologies (complete, circle and star networks, respectively), for the two distinct dynamics BDB and DBB, and two different mobility scenarios.

Under co-evolved mobility, we consider the fixation probability of the fittest mutant cooperator on defectors with optimal staying propensities, a probability which is essential to the analysis under rare interaction mutations. Once again, the

optimal staying propensity of resident defectors is $\alpha = 0.99$. The fittest mutant cooperators have the staying propensity that maximises their fixation probability on those defectors. This is the value represented in parenthesis, together with each fixation probability under co-evolved mobility.

Under fixed mobility, we consider that both resident defectors and mutant cooperators have the same staying propensity, which, with the purpose of simplifying our search, we have considered to be the one held by the fittest mutant cooperators under co-evolved mobility.

These results were obtained based on $100,000$ simulation trials for each combination of parameters. The estimation of the standard deviation is provided in Erovenko et al. (2019). We use the following parameter values: $N = 50$, $\lambda = 0.1$, $S = 0.03$, $c = 0.04$, $T = 1$, and we considered the following different values of $v = 0.08, 0.4, 2, 8$. Note that fixation probabilities are compared to their value under neutral selection, which corresponds to $1/N = 0.02$. Probabilities higher than this value are highlighted in the tables.

For an extensive analysis of the parameter space, we refer to Erovenko et al. (2019), on whose supplementary material the impact of different values of reward-to-cost ratio and exploration time is assessed considering only the BDB dynamics.

	Co-evolved mobility		Fixed mobility	
	BDB	DBB	BDB	DBB
$v = 0.08$	0.0063 (0.99)	0.0015 (0.99)	0.0063	0.0015
$v = 0.4$	0.0065 (0.9)	0.0021 (0.8)	0.0057	0.0022
$v = 2$	0.0170 (0.8)	0.0159 (0.6)	0.0050	0.0019
$v = 8$	**0.0202** (0.9)	**0.0323** (0.4)	0.0018	0.0003

Table D.1: Fixation probabilities of cooperators under a complete network, for two distinct mobility scenarios, and different reward values and evolutionary dynamics. The value included in parenthesis together with each fixation probability value, under co-evolved mobility, corresponds to the calculated staying propensity of the fittest mutant cooperators. Resident defectors under co-evolved mobility were considered to use their optimal staying propensity of 0.99. Fixation probabilities under fixed mobility were calculated using the same staying propensity for both mutants and defectors as the obtained for the corresponding fittest mutants under co-evolved mobility. Note that fixation probabilities are compared to their value under neutral selection, which is 0.02 – probabilities higher than this value are highlighted.

In table D.1, we observe that for reward values up to $v = 2$ in the complete network, mutant cooperators do not fixate above neutrality both under the co-evolution of movement strategies and when these are fixed at the same value for resident defectors. In comparison, the main results presented in chapter 5 show that under longer exploration phases of $T = 10$ and under $v = 0.4$, cooperators fixate

under all dynamics for this movement cost $\lambda = 0.1$.

When the reward value is high enough ($v = 8$), co-evolving mobility allows for the successful fixation of cooperators. However, under fixed mobility, we observe that the fixation of cooperators decreases for the highest values of the reward. The fact that it never reaches the neutral fixation threshold is in accordance with the proposition that under $T = 1$ and fixed mobility, assortative behaviour vanishes, and only the spatial viscosity of the evolutionary process described in Ohtsuki et al. (2006), and also observed in Pattni et al. (2017), can sustain cooperation. Viscosity is not present in complete networks, as all individuals are connected, hence the lack of success of cooperators under fixed mobility.

The differences between dynamics are smaller under this topology, and are mainly related to the overall effect of amplification of selection described in chapter 5.

	Co-evolved mobility		Fixed mobility	
	BDB	DBB	BDB	DBB
$v = 0.08$	0.0062 (0.99)	0.0015 (0.99)	0.0062	0.0015
$v = 0.4$	0.0070 (0.9)	0.0034 (0.8)	0.0063	0.0040
$v = 2$	**0.0285** (0.8)	**0.0564** (0.7)	0.0062	**0.0221**
$v = 8$	**0.0622** (0.8)	**0.1040** (0.7)	0.0067	**0.0378**

Table D.2: Fixation probabilities of cooperators under a circle network. Other information as in the caption of table D.1.

Table D.2 shows the results obtained under circle networks. These are fairly similar to the ones from complete networks under co-evolved mobility, but they hold key differences under fixed mobility. In the later, we observe that fixation probabilities under the BDB dynamics are consistently below neutrality, while under the DBB they increase considerably for larger reward values, reaching values above that threshold for both $v = 2$ and $v = 8$. This shows that under $T = 1$, and in the absence of co-evolving mobility, the viscosity of the process can still allow for the fixation of cooperation. This is again in agreement with the conclusions from Ohtsuki et al. (2006), that if the average degree of a network is lower than (a function) of the reward-to-cost ratio, cooperation can evolve under some dynamics. Here we further show that the distinct nature of the BDB and DBB dynamics is recovered when there is no co-evolved assortative behaviour. This difference should be associated with the network viscosity of the process but not with the later mechanism.

Finally, the results obtained under star networks hold similarities with to the ones obtained under complete networks. Under co-evolved mobility, cooperation

	Co-evolved mobility		Fixed mobility	
	BDB	DBB	BDB	DBB
$v = 0.08$	0.0064 (0.99)	0.0022 (0.99)	0.0064	0.0022
$v = 0.4$	0.0105 (0.7)	**0.0288** (0.4)	0.0059	0.0032
$v = 2$	**0.0530** (0.5)	**0.1731** (0.01)	0.0049	0.0043
$v = 8$	**0.0760** (0.6)	**0.2551** (0.01)	0.0023	0.0027

Table D.3: Fixation probabilities of cooperators under a star network. More information included in the caption of table D.1.

fixates under both evolutionary dynamics for high enough rewards. The minimum value for which it happens is lower under the DBB dynamics, and, once again, these dynamics amplify selection and allow for cooperators to fixate with high probabilities. Under fixed mobility, this network leads to fixation probabilities as low as under complete networks. This is a highly centralised network, where all individuals can potentially meet (in the centre), therefore corresponding to a highly connected interactive structure, under which viscosity is no longer present Ohtsuki et al. (2006), and cooperation cannot evolve under $T = 1$ without co-evolved mobility.

In summary, we observed that strictly limiting exploration phases to $T = 1$, co-evolving staying propensities and network viscosity can still allow cooperation to fixate. The later is related to the mechanism analysed in the context of evolutionary games for the first time in Ohtsuki et al. (2006). Here we recover a result similar to the original rule stated there: cooperation can evolve only in networks with low enough degree, far from complete, and under particular evolutionary dynamics. These results are relevant for the analysis we perform in chapter 5, as they show that the fundamental differences between some of these dynamics come from their relation to the viscosity of evolutionary processes on networks, and are often not reflected in the presence of co-evolving assortative behaviour.

Bibliography

Abraham, J. N. (2005), 'Insect choice and floral size dimorphism: sexual selection or natural selection?', *Journal of Insect Behavior* **18**, 743–756.

Akdeniz, A. & van Veelen, M. (2020), 'The cancellation effect at the group level', *Evolution* **74**(7), 1246–1254.

Aktipis, C. A. (2004), 'Know when to walk away: contingent movement and the evolution of cooperation', *Journal of theoretical biology* **231**(2), 249–260.

Aktipis, C. A. (2011), 'Is cooperation viable in mobile organisms? simple walk away rule favors the evolution of cooperation in groups', *Evolution and Human Behavior* **32**(4), 263–276.

Alalawi, Z., Bova, P., Cimpeanu, T., Di Stefano, A., Duong, M. H., Domingos, E. F., Han, T. A., Krellner, M., Ogbo, B., Powers, S. T. et al. (2024), 'Trust ai regulation? discerning users are vital to build trust and effective ai regulation', *arXiv preprint arXiv:2403.09510* .

Alalawi, Z., Zeng, Y. et al. (2020), 'Toward understanding the interplay between public and private healthcare providers and patients: an agent-based simulation approach', *EAI Endorsed Transactions on Industrial Networks and Intelligent Systems* **7**(24), 166668.

Allen, B., Lippner, G., Chen, Y.-T., Fotouhi, B., Momeni, N., Yau, S.-T. & Nowak, M. A. (2017), 'Evolutionary dynamics on any population structure', *Nature* **544**, 227–230.

Alvarez-Rodriguez, U., Battiston, F., de Arruda, G. F., Moreno, Y., Perc, M. & Latora, V. (2021), 'Evolutionary dynamics of higher-order interactions in social networks', *Nature Human Behaviour* **5**(5), 586–595.

Amaral, L. A. N., Scala, A., Barthélémy, M. & Stanley, H. E. (2000), 'Classes of small-world networks', *Proceedings of the national academy of sciences* **97**(21), 11149–11152.
URL: *www.pnas.org*

Antal, T. & Scheuring, I. (2006), 'Fixation of strategies for an evolutionary game in finite populations', *Bulletin of Mathematical Biology* **68**(8), 1923–1944.

Archetti, M. & Scheuring, I. (2012), 'Review: Game theory of public goods in one-shot social dilemmas without assortment', *Journal of Theoretical Biology* **299**, 9–20.

Assenza, S., Gómez-Gardeñes, J. & Latora, V. (2008), 'Enhancement of cooperation in highly clustered scale-free networks', *Physical Review E* **78**, 017101.
URL: *https://link.aps.org/doi/10.1103/PhysRevE.78.017101*

Axelrod, R. (1984), *The Evolution of Cooperation*, Basic Books, New York, USA.

Axelrod, R. & Hamilton, W. D. (1981), 'The evolution of cooperation', *Science* **211**(4489), 1390–1396.

Bara, J., Santos, F. P. & Turrini, P. (2024), 'The impact of mobility costs on cooperation and welfare in spatial social dilemmas', *Scientific Reports* **14**(1), 10572.

Battiston, F., Cencetti, G., Iacopini, I., Latora, V., Lucas, M., Patania, A., Young, J.-G. & Petri, G. (2020), 'Networks beyond pairwise interactions: Structure and dynamics', *Physics Reports* **874**, 1–92. Networks beyond pairwise interactions: Structure and dynamics.
URL: *https://www.sciencedirect.com/science/article/pii/S0370157320302489*

Bomze, I. M. (1986), 'Non-cooperative two-person games in biology: A classification', *International journal of game theory* **15**, 31–57.

Boyd, R. & Richerson, P. J. (1988), *Culture and the evolutionary process*, University of Chicago press.

Broom, M., Erovenko, I. V., Rowell, J. T. & Rychtář, J. (2020), 'Models and measures of animal aggregation and dispersal', *Journal of Theoretical Biology* **484**.

Broom, M., Erovenko, I. V. & Rychtář, J. (2021), 'Modelling Evolution in Structured Populations Involving Multiplayer Interactions', *Dynamic Games and Applications* **11**(2), 270–293.

Broom, M., Hadjichrysanthou, C. & Rychtář, J. (2010), 'Evolutionary games on graphs and the speed of the evolutionary process', *Proceedings of the Royal Society A: Mathematical, Physical and Engineering Sciences* **466**(2117), 1327–1346.

Broom, M., Lafaye, C., Pattni, K. & Rychtář, J. (2015), 'A study of the dynamics of multi-player games on small networks using territorial interactions', *Journal of Mathematical Biology* **71**(6-7), 1551–1574.

Broom, M., Pattni, K. & Rychtář, J. (2019), 'Generalized Social Dilemmas: The Evolution of Cooperation in Populations with Variable Group Size', *Bulletin of Mathematical Biology* **81**(11), 4643–4674.

Broom, M. & Rychtář, J. (2012), 'A general framework for analysing multiplayer games in networks using territorial interactions as a case study', *Journal of Theoretical Biology* **302**, 70–80.

Broom, M. & Rychtář, J. (2013), *Game-Theoretical Models in Biology*, 1st edn, Chapman & Hall/ CRC Press, London, UK.

Bruni, M., Broom, M. & Rychtář, J. (2014), 'Analysing territorial models on graphs', *Involve, a Journal of Mathematics* **7**(2), 129–149.

Caporael, L. R. (1997), 'The evolution of truly social cognition: The core configurations model', *Personality and Social Psychology Review* **1**(4), 276–298.

Castagno, P., Mancuso, V., Sereno, M. & Marsan, M. A. (2020), 'A simple model of mtc flows applied to smart factories', *IEEE Transactions on Mobile Computing* **20**(10), 2906–2923.

Cavalli-Sforza, L. L. & Feldman, M. W. (1981), *Cultural transmission and evolution: A quantitative approach*, Princeton University Press.

Civilini, A., Anbarci, N. & Latora, V. (2021), 'Evolutionary game model of group choice dilemmas on hypergraphs', *Physical Review Letters* **127**(26), 268301.

Civilini, A., Sadekar, O., Battiston, F., Gómez-Gardeñes, J. & Latora, V. (2024), 'Explosive cooperation in social dilemmas on higher-order networks', *Physical Review Letters* **132**, 167401.
URL: *https://link.aps.org/doi/10.1103/PhysRevLett.132.167401*

Cornell, H. N., Marzluff, J. M. & Pecoraro, S. (2012), 'Social learning spreads knowledge about dangerous humans among american crows', *Proceedings of the Royal Society B: Biological Sciences* **279**(1728), 499–508.

Costa, M. A., Marra, A. D. & Corman, F. (2023), 'Public transport commuting analytics: A longitudinal study based on gps tracking and unsupervised learning', *Data Science for Transportation* **5**(3), 15.

Couto, M. C., Pacheco, J. M. & Santos, F. C. (2020), 'Governance of risky public goods under graduated punishment', *Journal of Theoretical Biology* **505**, 110423.

Couzin, I. D., Krause, J. et al. (2003), 'Self-organization and collective behavior in vertebrates', *Advances in the Study of Behavior* **32**(1), 10–1016.

Cressman, R. (1990), 'Strong stability and density-dependent evolutionarily stable strategies', *Journal of theoretical biology* **145**(3), 319–330.

Cressman, R. & Křivan, V. (2006), 'Migration dynamics for the ideal free distribution', *The American Naturalist* **168**(3), 384–397.

de Souza, E. P., Ferreira, E. M. & Neves, A. G. M. (2019), 'Fixation probabilities for the Moran process in evolutionary games with two strategies: graph shapes and large population asymptotics', *Journal of Mathematical Biology* **78**(4), 1033–1065.

Della Rossa, F., Dercole, F. & Vicini, C. (2017), 'Extreme Selection Unifies Evolutionary Game Dynamics in Finite and Infinite Populations', *Bulletin of Mathematical Biology* **79**(5), 1070–1099.

Derex, M. & Morgan, T. J. H. (2023), The Cultural Transmission of Technological Skills, *in* 'The Oxford Handbook of Cultural Evolution', Oxford University Press.
URL: *https://doi.org/10.1093/oxfordhb/9780198869252.013.32*

Diekmann, A. (1985), 'Volunteer's Dilemma', *Journal of Conflict Resolution* **29**(4), 605–610.

Doebeli, M. & Hauert, C. (2005), 'Models of cooperation based on the Prisoner's Dilemma and the Snowdrift game'.

Dorogovtsev, S. N. & Mendes, J. F. F. (2003), *Evolution of Networks: From Biological Nets to the Internet and WWW*, Oxford University Press, Oxford, UK.

Dreisig, H. (1995), 'Ideal free distributions of nectar foraging bumblebees', *Oikos* **72**(2), 161–172.

Durkheim, É. (1984/1893), *The Division of Labor in Society*, New York: Free Press.

Erovenko, I. (2019), 'The evolution of cooperation in one-dimensional mobile populations with deterministic dispersal', *Games* **10**(1), 2.

Erovenko, I. & Rychtář, J. (2016), 'The evolution of cooperation in 1-dimensional mobile populations', *Far East Journal of Applied Mathematics* **95**(1), 63–88.

Erovenko, I. V., Bauer, J., Broom, M., Pattni, K. & Rychtář, J. (2019), 'The effect of network topology on optimal exploration strategies and the evolution of cooperation in a mobile population', *Proceedings of the Royal Society A: Mathematical, Physical and Engineering Sciences* **475**(2230).

Erovenko, I. V. & Broom, M. (2024), 'The evolution of cooperation in a mobile population on random networks: Network topology matters only for low-degree networks', *Dynamic Games and Applications* pp. 1–23.

Fischer, P., Krueger, J. I., Greitemeyer, T., Vogrincic, C., Kastenmüller, A., Frey, D., Heene, M., Wicher, M. & Kainbacher, M. (2011), 'The Bystander-Effect: A Meta-Analytic Review on Bystander Intervention in Dangerous and Non-Dangerous Emergencies', *Psychological Bulletin* **137**(4), 517–537.

Fox, J. & Guyer, M. (1978), '"Public" Choice and Cooperation in n-Person Prisoner's Dilemma', *Journal of Conflict Resolution* **22**(3), 469–481.

Fretwell, S. D. & Lucas, H. L. (1969), 'On territorial behavior and other factors influencing habitat distribution in birds: I. theoretical development', *Acta biotheoretica* **19**(1), 16–36.

Fudenberg, D., Nowak, M. A., Taylor, C. & Imhof, L. A. (2006), 'Evolutionary game dynamics in finite populations with strong selection and weak mutation', *Theoretical Population Biology* **70**(3), 352–363.

Fundenberg, D. & Maskin, E. (1990), 'Evolution and cooperation in noisy repeated games', *The American Economic Review* **80**(2), 274–279.

Girvan, M. & Newman, M. E. J. (2002), 'Community structure in social and biological networks', *Proceedings of the National Academy of Sciences* **99**(12), 7821–7826.
URL: *https://www.pnas.org*

Gómez-Gardeñes, J., Romance, M., Criado, R., Vilone, D. & Sánchez, A. (2011), 'Evolutionary games defined at the network mesoscale: The Public Goods game', *Chaos: An Interdisciplinary Journal of Nonlinear Science* **21**(1), 016113.

Gómez-Gardeñes, J., Vilone, D. & Sánchez, A. (2011), 'Disentangling social and group heterogeneities: Public Goods games on complex networks', *Europhysics Letters* **95**(3), 68003.

Hadjichrysanthou, C., Broom, M. & Rychtář, J. (2011), 'Evolutionary Games on Star Graphs Under Various Updating Rules', *Dynamic Games and Applications* **1**(3), 386–407.

Hagan, J. M. & Wassink, J. (2016), 'New skills, new jobs: Return migration, skill transfers, and business formation in mexico', *Social Problems* **63**(4), 513–533.

Hamburger, H. (1973), 'N-person Prisoner's Dilemma', *Journal of Mathematical Sociology* **3**(1), 27–48.

Hamilton, I. M. & Taborsky, M. (2005), 'Contingent movement and cooperation evolve under generalized reciprocity', *Proceedings of the Royal Society B: Biological Sciences* **272**(1578), 2259–2267.

Hamilton, W. D. (1967), 'Extraordinary Sex Ratios', *Science* **156**, 477–488.

Hanski, I. (1998), 'Metapopulation dynamics', *Nature* **396**, 41–49.
URL: *www.nature.com*

Haq, H., Schimit, P. H. T. & Broom, M. (2024), 'The effects of herding and dispersal behaviour on the evolution of cooperation on complete networks', *Journal of Mathematical Biology* **89**(5), 49.

Hardin, G. (1960), 'The competitive exclusion principle', *Science* **131**(3409), 1292–1297.

Hardin, G. (1968), 'The Tragedy of the Commons', *Science* **162**(3859), 1243–1248.

Hauert, C., Chen, Y.-T. & Imhof, L. A. (2014), 'Fixation Times in Deme Structured, Finite Populations with Rare Migration', *Journal of Statistical Physics* **156**(4), 739–759.

Hauert, C. & Doebeli, M. (2004), 'Spatial structure often inhibits the evolution of cooperationin the snowdrift game', *Nature* **428**, 643–646.

Hauert, C. & Imhof, L. A. (2012), 'Evolutionary games in deme structured, finite populations', *Journal of Theoretical Biology* **299**, 106–112.

Hauert, C. & Miekisz, J. (2018), 'Effects of sampling interaction partners and competitors in evolutionary games', *Physical Review E* **98**(5), 052301.

Hauert, C., Traulsen, A., Brandt, H., Nowak, M. A. & Sigmund, K. (2007), 'Via Freedom to Coercion: The Emergence of Costly Punishment', *Science* **316**(5833), 1905–1907.

Helbing, D. (1992), A mathematical model for behavioral changes by pair interactions, *in* G. Haag, U. Mueller & K. G. Troitzsch, eds, 'Economic Evolution and Demographic Change: Formal Models in Social Sciences', Springer, pp. 330–348.

Hidalgo, C. A., Balland, P.-A., Boschma, R., Delgado, M., Feldman, M., Frenken, K., Glaeser, E., He, C., Kogler, D. F., Morrison, A., Neffke, F., Rigby, D., Stern, S., Zheng, S. & Zhu, S. (2018), The principle of relatedness, *in* A. J. Morales, C. Gershenson, D. Braha, A. A. Minai & Y. Bar-Yam, eds, 'Unifying Themes in Complex Systems IX', Springer International Publishing, Cham, pp. 451–457.

Hidalgo, C. A., Klinger, B., Barabási, A.-L. & Hausmann, R. (2007), 'The product space conditions the development of nations', *Science* **317**(5837), 482–487.

Hofbauer, J. & Sigmund, K. (1998), *Evolutionary Games and Population Dynamics*, Cambridge University Press.

Huang, F., Chen, X. & Wang, L. (2018), The Equivalence Induced by Unifying Fitness Mappings in Frequency-Dependent Moran Process, *in* 'Proceedings of the 2018 IEEE 7th Data Driven Control and Learning Systems Conference (DD-CLS'18)', Enshi, China, pp. 847–853.

Karlin, S. & Taylor, H. M. (1975), *A First Course in Stochastic Processes*, second edn, Academic Press, New York, USA.

Ketterson, E. & Nolan Jr, V. (1990), Site attachment and site fidelity in migratory birds: experimental evidence from the field and analogies from neurobiology, *in* 'Bird migration: physiology and ecophysiology', Springer, pp. 117–129.

Kimura, M. & Weiss, G. H. (1964), 'The stepping stone model of population structure and the decrease of genetic correlation with distance', *Genetics* **49**, 561–576.

Kraines, D. & Kraines, V. (1989), 'Pavlov and the prisoner's dilemma', *Theory and decision* **26**, 47–79.

Kraines, D. P. & Kraines, V. Y. (2000), 'Natural selection of memory-one strategies for the iterated prisoner's dilemma', *Journal of Theoretical Biology* **203**(4), 335–355.

Krause, J. & Ruxton, G. D. (2002), *Living in Groups*, Oxford Univ. Press, Oxford, UK.

Le Galliard, J.-F., Ferriere, R. & Dieckmann, U. (2005), 'Adaptive evolution of social traits: origin, trajectories, and correlations of altruism and mobility', *The American Naturalist* **165**(2), 206–224.

Levins, R. (1969), 'Some Demographic and Genetic Consequences of Environmental Heterogeneity for Biological Control', *Bulletin of the Entomological Society of America* **15**(3), 237–240.

Lieberman, E., Hauert, C. & Nowak, M. A. (2005), 'Evolutionary dynamics on graphs', *Nature* **433**(7023), 312–316.

Luan, X., Eikenbroek, O. A., Corman, F. & van Berkum, E. C. (2024), 'Passenger social rerouting strategies in capacitated public transport systems', *Transportation Research Part E: Logistics and Transportation Review* **188**, 103598.

Majhi, S., Perc, M. & Ghosh, D. (2022), 'Dynamics on higher-order networks: a review', *Journal of the Royal Society Interface* **19**(188).

Mancuso, V., Badia, L., Castagno, P., Sereno, M. & Ajmone Marsan, M. (2023), Efficiency of distributed selection of edge or cloud servers under latency constraints,

in '2023 21st Mediterranean Communication and Computer Networking Conference (MedComNet)', pp. 158–166.

Mancuso, V., Castagno, P., Sereno, M. & Ajmone Marsan, M. (2022), Stateful versus stateless selection of edge or cloud servers under latency constraints, *in* '2022 IEEE 23rd International Symposium on a World of Wireless, Mobile and Multimedia Networks (WoWMoM)', pp. 110–119.

Marra, A. D. & Corman, F. (2023), 'How different network disturbances affect route choice of public transport passengers. a descriptive study based on tracking', *Expert Systems with Applications* **213**, 119083.

Marzluff, J. M., Walls, J., Cornell, H. N., Withey, J. C. & Craig, D. P. (2010), 'Lasting recognition of threatening people by wild american crows', *Animal Behaviour* **79**(3), 699–707.

Masuda, N. (2009), 'Directionality of contact networks suppresses selection pressure in evolutionary dynamics', *Journal of Theoretical Biology* **258**(2), 323–334.

Matsui, A. (1992), 'Best response dynamics and socially stable strategies', *Journal of Economic Theory* **57**(2), 343–362.
URL: *https://www.sciencedirect.com/science/article/pii/002205319290040O*

May, R. M. (2006), 'Network structure and the biology of populations', *Trends in Ecology and Evolution* **21**(7), 394–399.

May, R. M. (2019/1973), *Stability and complexity in model ecosystems*, Princeton university press.

Maynard Smith, J. (1974), 'The theory of games and the evolution of animal conflicts', *Journal of Theoretical Biology* **47**(1), 209–221.

Maynard Smith, J. (1982), *Evolution and the Theory of Games*, Cambridge University Press.

Maynard Smith, J. (1991), 'Honest signalling: the Philip Sidney game', *Animal Behaviour* **42**(6), 1034–1035.

Maynard Smith, J. & Harper, D. (2003), *Animal signals*, Oxford University Press.

Maynard Smith, J. & Price, G. R. (1973), 'The Logic of Animal Conflict', *Nature* **246**, 15–18.

Moran, J. & Bouchaud, J.-P. (2019), 'May's instability in large economies', *Physical Review E* **100**(3), 032307.

Moran, P. A. P. (1958), 'Random processes in genetics', *Mathematical Proceedings of the Cambridge Philosophical Society* **54**(1), 60–71.

Morison, C., Fic, M., Marcou, T., Mohamadichamgavi, J., Antón, J. R., Sayyar, G., Stein, A., Bastian, F., Krakovská, H., Krishnan, N. et al. (2024), 'Public goods games in disease evolution and spread', *arXiv preprint arXiv:2402.17842* .

Nasell, I. (1999*a*), 'On the quasi-stationary distribution of the stochastic logistic epidemic', *Mathematical Biosciences* **156**, 21–40.

Nasell, I. (1999*b*), 'On the time to extinction in recurrent epidemics', *Journal of the Royal Statistical Society: Series B (Statistical Methodology)* **61**(2), 309–330.

Nash, J. (1951), 'Non-cooperative games', *Annals of Mathematics* **54**(2), 286–295.

Neffke, F., Henning, M. & Boschma, R. (2011), 'How do regions diversify over time? industry relatedness and the development of new growth paths in regions', *Economic geography* **87**(3), 237–265.

Neffke, F. M. (2019), 'The value of complementary co-workers', *Science advances* **5**(12), eaax3370.

Newman, M. E. J. (2006), 'Modularity and community structure in networks', *Proceedings of the National Academy of Sciences* **103**(23), 8577–8582.
URL: *www.pnas.orgcgidoi10.1073pnas.0601602103*

Newman, M. E. J. (2012), 'Communities, modules and large-scale structure in networks', *Nature physics* **8**(1), 25–31.

Nowak, M. A. (2006), 'Five Rules for the Evolution of Cooperation', *Science* **314**, 1560–1563.
URL: *https://www.science.org*

Nowak, M. A. & May, R. M. (1992), 'Evolutionary games and spatial chaos', *Nature* **359**, 826–829.

Nowak, M. A., Sasaki, A., Taylor, C. & Fudenberg, D. (2004), 'Emergence of cooperation and evolutionary stability in finite populations', *Nature* **428**, 646–650.

Nowak, M. A. & Sigmund, K. (1992), 'Tit for tat in heterogeneous populations', *Nature* **355**(6357), 250–253.

Nowak, M. & Sigmund, K. (1993), 'A strategy of win-stay, lose-shift that outperforms tit-for-tat in the prisoner's dilemma game', *Nature* **364**(6432), 56–58.

Ohtsuki, H., Hauert, C., Lieberman, E. & Nowak, M. A. (2006), 'A simple rule for the evolution of cooperation on graphs and social networks', *Nature* **441**(7092), 502–505.

Oliveira, R., Arriaga, P., Santos, F. P., Mascarenhas, S. & Paiva, A. (2021), 'Towards prosocial design: A scoping review of the use of robots and virtual agents to trigger prosocial behaviour', *Computers in Human Behavior* **114**, 106547.

Ostrom, E. (1990), *Governing the commons: The evolution of institutions for collective action*, Cambridge university press.

Overton, C. E., Wilkinson, R. R., Loyinmi, A., Miller, J. C. & Sharkey, K. J. (2022), 'Approximating Quasi-Stationary Behaviour in Network-Based SIS Dynamics', *Bulletin of Mathematical Biology* **84**(1).

O'Clery, N. & Kinsella, S. (2022), 'Modular structure in labour networks reveals skill basins', *Research Policy* **51**(5), 104486.

Pacheco, J. M., Santos, F. C., Souza, M. O. & Skyrms, B. (2009), 'Evolutionary dynamics of collective action in N-person stag hunt dilemmas', *Proceedings of the Royal Society B: Biological Sciences* **276**(1655), 315–321.

Pacheco, J. M., Traulsen, A. & Nowak, M. A. (2006*a*), 'Active linking in evolutionary games', *Journal of Theoretical Biology* **243**(3), 437–443.

Pacheco, J. M., Traulsen, A. & Nowak, M. A. (2006*b*), 'Coevolution of strategy and structure in complex networks with dynamical linking', *Physical Review Letters* **97**(25).

Page, K. M. & Nowak, M. A. (2002), 'Unifying evolutionary dynamics', *Journal of Theoretical Biology* **219**(1), 93–98.
  URL: *https://www.sciencedirect.com/science/article/pii/S0022519302931127*

Pattni, K., Broom, M. & Rychtář, J. (2017), 'Evolutionary dynamics and the evolution of multiplayer cooperation in a subdivided population', *Journal of Theoretical Biology* **429**, 105–115.

Pattni, K., Broom, M. & Rychtář, J. (2018), 'Evolving multiplayer networks: Modelling the evolution of cooperation in a mobile population', *Discrete and Continuous Dynamical Systems - Series B* **23**(5), 1975–2004.

Pattni, K., Broom, M., Rychtář, J. & Silvers, L. J. (2015), 'Evolutionary graph theory revisited: When is an evolutionary process equivalent to the Moran process?', *Proceedings of the Royal Society A: Mathematical, Physical and Engineering Sciences* **471**(2182).

Peña, J. & Rochat, Y. (2012), 'Bipartite graphs as models of population structures in evolutionary multiplayer games', *PLoS ONE* **7**(9).

Peña, J., Wu, B. & Traulsen, A. (2016), 'Ordering structured populations in multiplayer cooperation games', *Journal of the Royal Society Interface* **13**, 20150881.

Peperkoorn, L. S., Becker, D. V., Balliet, D., Columbus, S., Molho, C. & Van Lange, P. A. (2020), 'The prevalence of dyads in social life', *PLoS ONE* **15**(12 December).

Perc, M., Gómez-Gardeñes, J., Szolnoki, A., Floría, L. M. & Moreno, Y. (2013), 'Evolutionary dynamics of group interactions on structured populations: A review', *Journal of the Royal Society Interface* **10**(80).

Petit, O. & Bon, R. (2010), 'Decision-making processes: the case of collective movements', *Behavioural processes* **84**(3), 635–647.

Pires, D. L. & Broom, M. (2022), 'More can be better: An analysis of single-mutant fixation probability functions under 2×2 games', *Proceedings of the Royal Society A: Mathematical, Physical and Engineering Sciences* **478**, 20220577.

Pires, D. L. & Broom, M. (2024), 'The rules of multiplayer cooperation in networks of communities', *PLoS Computational Biology* **20**(8), e1012388.

Pires, D. L., Erovenko, I. V. & Broom, M. (2023), 'Network topology and movement cost, not updating mechanism, determine the evolution of cooperation in mobile structured populations', *PLoS ONE* **18**(8), e0289366.

Porter, M. A., Onnela, J.-P., Mucha, P. J. et al. (2009), 'Communities in networks', *Notices of the American Mathematical Society* **56**(9), 1082–1097.

Poundstone, W. (1992), *Prisoner's Dilemma: John von Neumann, Game Theory and the Puzzle of the Bomb*, Anchor Books, New York, USA.

Proulx, S. R., Promislow, D. E. & Phillips, P. C. (2005), 'Network thinking in ecology and evolution', *Trends in Ecology and Evolution* **20**(6), 345–353.

Ramírez-Llanos, E. & Quijano, N. (2010*a*), Analysis and control for the water distribution problem, *in* '49th IEEE Conference on Decision and Control (CDC)', IEEE, pp. 4030–4035.

Ramirez-Llanos, E. & Quijano, N. (2010*b*), 'A population dynamics approach for the water distribution problem', *International Journal of Control* **83**(9), 1947–1964.

Robbins, H. (1952), 'Some aspects of the sequential design of experiments', *Bulletin of the American Mathematical Society* **55**, 527–535.

Sample, C. & Allen, B. (2017), 'The limits of weak selection and large population size in evolutionary game theory', *Journal of Mathematical Biology* **75**(5), 1285–1317.

Santos, F. C. & Pacheco, J. M. (2005), 'Scale-free networks provide a unifying framework for the emergence of cooperation', *Physical Review Letters* **95**(9).

Santos, F. C., Pacheco, J. M. & Lenaerts, T. (2006), 'Evolutionary dynamics of social dilemmas in structured heterogeneous populations', *Proceedings of the National Academy of Sciences* **103**(9), 3490–3494.
URL: *www.pnas.orgcgidoi10.1073pnas.0508201103*

Santos, F. C., Pacheco, J. M. & Skyrms, B. (2011), 'Co-evolution of pre-play signaling and cooperation', *Journal of Theoretical Biology* **274**(1), 30–35.

Santos, F. C., Rodrigues, J. F. & Pacheco, J. M. (2006), 'Graph topology plays a determinant role in the evolution of cooperation', *Proceedings of the Royal Society B: Biological Sciences* **273**(1582), 51–55.

Santos, F. C., Santos, M. D. & Pacheco, J. M. (2008), 'Social diversity promotes the emergence of cooperation in public goods games', *Nature* **454**(7201), 213–216.

Santos, F. P., Pacheco, J. M., Paiva, A. & Santos, F. C. (2019), Evolution of Collective Fairness in Hybrid Populations of Humans and Agents, *in* 'Proceedings of the AAAI Conference on Artificial Intelligence, 33(1)', pp. 6146–6153.
  URL: *www.aaai.org*

Santos, F. P., Santos, F. C., Paiva, A. & Pacheco, J. M. (2015), 'Evolutionary dynamics of group fairness', *Journal of Theoretical Biology* **378**, 96–102.

Schaffer, M. E. (1988), 'Evolutionarily stable strategies for a finite population and a variable contest size', *Journal of Theoretical Biology* **132**(4), 469–478.

Schimit, P. H. T., Pattni, K. & Broom, M. (2019), 'Dynamics of multi-player games on complex networks using territorial interactions', *Physical Review E* **99**(3).

Schimit, P. H. T., Pereira, F. H. & Broom, M. (2022), 'Good predictors for the fixation probability on complex networks of multi-player games using territorial interactions', *Ecological Complexity* **51**, 101017.
  URL: *https://linkinghub.elsevier.com/retrieve/pii/S1476945X2200037X*

Skyrms, B. (1996), *Evolution of the Social Contract*, Cambridge University Press, Cambridge, UK.

Skyrms, B. (2001), 'The Stag Hunt', *Proceedings and Addresses of the American Philosophical Association* **75**(2), 31–41.

Skyrms, B. (2004), *The stag hunt and the evolution of social structure*, Cambridge University Press.

Skyrms, B. (2010), *Signals: Evolution, Learning, & Information*, Oxford University Press.

Souza, M. O., Pacheco, J. M. & Santos, F. C. (2009), 'Evolution of cooperation under N-person snowdrift games', *Journal of Theoretical Biology* **260**(4), 581–588.

Steven J. Karau & Kipling D. Williams (1993), 'Social Loafing: A Meta-Analytic Review and Theoretical Integration', *Journal of Personality and Social Psychology* **65**(4), 681–706.

Tarnita, C. E., Antal, T., Ohtsuki, H. & Nowak, M. A. (2009), 'Evolutionary dynamics in set structured populations', *Proceedings of the National Academy of*

Sciences **106**(21), 8601–8604.

URL: *https://www.pnas.org/doi/abs/10.1073/pnas.0903019106*

Taylor, C., Fudenberg, D., Sasaki, A. & Nowak, M. A. (2004), 'Evolutionary game dynamics in finite populations', *Bulletin of Mathematical Biology* **66**(6), 1621–1644.

Taylor, P. D. & Jonker, L. B. (1978), 'Evolutionarily Stable Strategies and Game Dynamics', *Mathematical Biosciences* **40**, 145–156.

Traulsen, A. & Hauert, C. (2009), 'Stochastic evolutionary game dynamics', *Reviews of Nonlinear Dynamics and Complexity* **2**, 25–61.

Traulsen, A. & Nowak, M. A. (2006), 'Evolution of cooperation by multilevel selection', *Proceedings of the National Academy of Sciences* **103**(29), 10952–10955.
URL: *https://www.pnas.org*

Traulsen, A., Nowak, M. A. & Pacheco, J. M. (2006), 'Stochastic dynamics of invasion and fixation', *Physical Review E - Statistical, Nonlinear, and Soft Matter Physics* **74**(1).

Traulsen, A., Pacheco, J. M. & Nowak, M. A. (2007), 'Pairwise comparison and selection temperature in evolutionary game dynamics', *Journal of Theoretical Biology* **246**(3), 522–529.

Traulsen, A., Shoresh, N. & Nowak, M. A. (2008), 'Analytical Results for Individual and Group Selection of Any Intensity', *Bulletin of Mathematical Biology* **70**, 1410–1424.

Trivers, R. L. (1971), 'The evolution of reciprocal altruism', *The Quarterly review of biology* **46**(1), 35–57.

Van Segbroeck, S., Santos, F. C., Lenaerts, T. & Pacheco, J. M. (2009), 'Reacting Differently to Adverse Ties Promotes Cooperation in Social Networks', *Physical Review Letters* **102**(5).

Vasconcelos, V. V., Santos, F. P., Santos, F. C. & Pacheco, J. M. (2017), 'Stochastic Dynamics through Hierarchically Embedded Markov Chains', *Physical Review Letters* **118**(5).

von Neumann, J. (1928), 'Zur theorie der gesellschaftsspiele', *Mathematische annalen* **100**(1), 295–320.

von Neumann, J. & Morgenstern, O. (1944), 'Theory of games and economic behavior'.

Wagner, E. O. (2020), 'Conventional Semantic Meaning in Signalling Games with Conflicting Interests', *The British Journal for the Philosophy of Science* **66**(4), 751–773.
URL: *https://www.journals.uchicago.edu/doi/10.1093/bjps/axu006*

Wang, J., Wu, B., W. C. Ho, D. & Wang, L. (2011), 'Evolution of cooperation in multilevel public goods games with community structures', *Europhysics Letters* **93**(5), 58001.

Wang, X., Couto, M. C., Wang, N., An, X., Chen, B., Dong, Y., Hilbe, C. & Zhang, B. (2023), 'Cooperation and coordination in heterogeneous populations', *Philosophical Transactions of the Royal Society B: Biological Sciences* **378**, 20210504.

Weishaar, K. & Erovenko, I. (2022), 'The evolution of cooperation in two-dimensional mobile populations with random and strategic dispersal', *Games* **13**(3), 40.

Wild, G. & Traulsen, A. (2007), 'The different limits of weak selection and the evolutionary dynamics of finite populations', *Journal of Theoretical Biology* **247**(2), 382–390.

Woodroffe, R. & Ginsberg, J. R. (1999), 'Conserving the african wild dog lycaon pictus. i. diagnosing and treating causes of decline', *Oryx* **33**(2), 132–142.

Woodroffe, R., Ginsberg, J. R. & Macdonald, D. W. (1997), *The African wild dog: status survey and conservation action plan*, IUCN, Gland, Switzerland.

Wu, B., Gokhale, C. S., Wang, L. & Traulsen, A. (2012), 'How small are small mutation rates?', *Journal of Mathematical Biology* **64**(5), 803–827.

Yagoobi, S., Sharma, N. & Traulsen, A. (2023), 'Categorizing update mechanisms for graph-structured metapopulations', *Journal of the Royal Society Interface* **20**(20220769), 20220769.

Yagoobi, S. & Traulsen, A. (2021), 'Fixation probabilities in network structured meta-populations', *Scientific Reports* **11**(1).

Yip, E. C., Powers, K. S. & Avilés, L. (2008), 'Cooperative capture of large prey solves scaling challenge faced by spider societies', *Proceedings of the National Academy of Sciences* **105**(33), 11818–11822.

Zeeman, E. C. (1980), Population dynamics from game theory, *in* Z. Nitecki & C. Robinson, eds, 'Global Theory of Dynamical Systems', Springer, pp. 471–497.

Zhou, D., Wu, B. & Ge, H. (2010), 'Evolutionary stability and quasi-stationary strategy in stochastic evolutionary game dynamics', *Journal of Theoretical Biology* **264**(3), 874–881.

Zukewich, J., Kurella, V., Doebeli, M. & Hauert, C. (2013), 'Consolidating Birth-Death and Death-Birth Processes in Structured Populations', *PLoS ONE* **8**(1).